DOCUMENT RELEASE AND CHANGE FORM

Prepared For the U.S. Department of Energy, Assistant Secretary for Environmental Management
By Washington River Protection Solutions, LLC., PO Box 850, Richland, WA 99352
Contractor For U.S. Department of Energy, Office of River Protection, under Contract DE-AC27-08RV14800

TRADEMARK DISCLAIMER: Reference herein to any specific commercial product, process, or service by trade name, trademark, manufacturer, or otherwise, does not necessarily constitute or imply its endorsement, recommendation, or favoring by the United States government or any agency thereof or its contractors or subcontractors. Printed in the United States of America.

Release Stamp

DATE: Feb 09,2021

HANFORD RELEASE

1. **Doc No:** RPP-RPT-46088 **Rev.** 02A

2. **Title:**
FLOW AND TRANSPORT IN THE NATURAL SYSTEM AT WASTE MANAGEMENT AREA C

3. **Project Number:** T2R26 ☐N/A

4. **Design Verification Required:** ☐Yes ☒No

5. **USQ Number:** ☒ N/A RPP-27195

6. **PrHA Number** **Rev.** ☒ N/A

Clearance Review Restriction Type: public

7. **Approvals**

Title	Name	Signature	Date
Clearance Review	Ayers, Lynn M	*Ayers, Lynn M*	02/09/2021
Document Control Approval	Meinecke, Kathryn R	*Meinecke, Kathryn R*	02/09/2021
Originator	Bergeron, Marcel P	*Bergeron, Marcel P*	02/04/2021
Responsible Manager	Rutland, Paul L	*Rutland, Paul L*	02/04/2021

8. **Description of Change and Justification**

This revision contains updates to address comments from NRC review of WMA C WIR Evaluation and Performance Assessment and associated internal review of this document.

9. **TBDs or Holds** ☒N/A

10. **Related Structures, Systems, and Components**

a. Related Building/Facilities ☒N/A	b. Related Systems ☒N/A	c. Related Equipment ID Nos. (EIN) ☒N/A

11. **Impacted Documents – Engineering** ☒N/A

Document Number	Rev.	Title

12. **Impacted Documents (Outside SPF):**

N/A

13. **Related Documents** ☒N/A

Document Number	Rev.	Title

14. **Distribution**

Name	Organization
Bergeron, Marcel P	CLOSURE & INTERIM MEASURES
Connelly, Michael P	
Field, Jim G	PROCESS ENGINEERING
Hasan, Nazmul	
Lee, Kearn (Pat)	CLOSURE & INTERIM MEASURES
Parker, Dan	CLOSURE & INTERIM MEASURES
Rutland, Paul L	CLOSURE & INTERIM MEASURES
Singleton, Kristin M	CLOSURE & INTERIM MEASURES
Tabor, Cindy L	CLOSURE & INTERIM MEASURES
Watson, David (Dj) J	CLOSURE & INTERIM MEASURES

INFORMATION CLEARANCE REVIEW AND RELEASE APPROVAL

Part I: Background Information

Title: Flow and Transport in the Natural System at Waste Management Area C

Information Category:
- ☐ Abstract ☐ Journal Article ☐ Summary
- ☐ Internet ☐ Visual Aid ☐ Software
- ☐ Full Paper ☑ Report ☐ Other

Publish to OSTI? ☐ Yes ☑ No

Trademark/Copyright "Right to Use" Information or Permission Documentation	Yes	NA
	☐	☑

Document Number: RPP-RPT-46088 Revision 2A Date: November 2020

Author: Bergeron, Marcel P

Part II: External/Public Presentation Information

Conference Name:

Sponsoring Organization(s): WRPS

Date of Conference: Conference Location:

Will Material be Handed Out? ☐ Yes ☑ No Will Information be Published? ☐ Yes ☑ No *(If Yes, attach copy of Conference format instructions/guidance.)*

Part III: WRPS Document Originator Checklist

Description	*Yes*	*N/A*	*Print/Sign/Date*
Information Product meets requirements in TFC-BSM-AD-C-01?	☐	☑	
Document Release Criteria in TFC-ENG-DESIGN-C-25 completed? (Attach checklist)	☐	☑	
If product contains pictures, safety review completed?	☑	☐	Roberts, Sheryl K Approved - IDMS data file att.

Part IV: WRPS Internal Review

Function	*Organization*	*Date*	*Print Name/Signature/Date*
Subject Matter Expert	WRPS	12/30/2020	Bergeron, Marcel P Approved - IDMS data file att.
Responsible Manager	WRPS	11/17/2020	Rutland, Paul L Approved - IDMS data file att.
Other:			

Part V: IRM Clearance Services Review

Description	*Yes*	*No*	*Print Name/Signature*
Document Contains Classified Information?	☐	☒	If Answer is "Yes," ADC Approval Required Print Name/Signature/Date
Document Contains Information Restricted by DOE Operational Security Guidelines?	☐	☒	Reviewer Signature: Print Name/Signature/Date
Document is Subject to Release Restrictions? *If the answer is "Yes," please mark category at right and describe limitation or responsible organization below:*	☐	☒	Document contains: ☐ Applied Technology ☐ Protected CRADA ☐ Personal/Private ☐ Export Controlled ☐ Proprietary ☐ Procurement – Sensitive ☐ Patentable Info. ☐ OUO ☐ Predecisional Info. ☐ UCNI ☐ Restricted by Operational Security Guidelines ☐ Other (Specify)
Additional Comments from Information Clearance Specialist Review?	☐	☒	Information Clearance Specialist Approval APPROVED By Sarah Harrison at 3:51 pm, Jan 28, 2021 Print Name/Signature/Date

When IRM Clearance Review is Complete – Return to WRPS Originator for Final Signature Routing (Part VI)

INFORMATION CLEARANCE REVIEW AND RELEASE APPROVAL

Part VI: Final Review and Approvals

Description	*Approved for Release*		*Print Name/Signature*	
	Yes	*N/A*		
WRPS External Affairs	☒	☐	Mc Cune, Hal C	Approved - IDMS data file att.
WRPS Office of Chief Counsel	☒	☐	Roden, Mari L	Approved - IDMS data file att.
DOE – ORP Public Affairs/Communications	☒	☐	Tyree, Geoffrey T	Approved - IDMS data file att.
Other: ORP OCC	☒	☐	King, Grace J	Approved - IDMS data file att.
Other: ORP SME	☒	☐	Lobos, Rodrigo A	Approved - IDMS data file att.

Comments Required for WRPS-Indicate Purpose of Document:

This document provides supporting information for the Natural System Working Session held on May 25 through 27, 2010. This revision contains updates to address comments from NRC review of WMA C WIR Evaluation and Performance Assessment and associated internal review of this document.

APPROVED
By Sarah Harrison at 3:51 pm, Jan 28, 2021

Approved for Public Release; Further Dissemination Unlimited

Information Release Station

Was/Is Information Product Approved for Release? ☒ Yes ☐ No

If Yes, what is the Level of Releaser? ☑ Public/Unrestricted ☐ Other (Specify) _____

Date Information Product Stamped/Marked for Release: 01/28/2021

Was/Is Information Product Transferred to OSTI? ☐ Yes ☒ No

Forward Copies of Completed Form to WRPS Originator

```
- <workflow name="(SEH) Normal - RPP-RPT-46088 Rev2A" id="280521170">
  - <task name="Clearance Process" id="0" date-initiated="20201117T1001"
      performer="SARAH E HARRISON" performer-id="252341659"
      username="h5635746">
      <comments>Due Thursday December 3rd 2020 - COB Please approve the
        Flow and Transport in the Natural System at Waste Management Area C,
        Revision 2A, submitted by Marcel Bergeron for public release. Thank you,
        Sarah Harrison Information Clearance</comments>
    </task>
    <task name="Add XML" id="1" date-done="20201117T1001" />
    <task name="Manager Approval" id="41" date-due="20201120T1001" date-
      done="20201117T1013" performer="PAUL L RUTLAND" performer-
      id="140633218" username="h4494439" disposition="Approve"
      authentication="true" />
    <task name="Document Reviewer2" id="53" date-due="20201120T1012" date-
      done="20201117T1244" performer="HAL C MC CUNE" performer-
      id="226350486" username="h7687509" disposition="Public Release"
      authentication="true" />
    <task name="Document Reviewer1" id="54" date-due="20201120T1012" date-
      done="20201119T1522" performer="SHERYL K ROBERTS" performer-
      id="171787680" username="h0081997" disposition="Public Release"
      authentication="true" />
    <task name="Document Reviewer4" id="51" date-due="20201120T1012" date-
      done="20201215T1602" performer="RODRIGO A LOBOS" performer-
      id="232334741" username="h2488419" disposition="Public Release"
      authentication="true" />
    <task name="Document Reviewer3" id="52" date-due="20201120T1012" date-
      done="20201230T1330" performer="MARI L RODEN" performer-id="262637370"
      username="h0048955" disposition="Public Release" authentication="true" />
    <task name="Doc Owner Clearance Review" id="13" date-due="20201231T1330"
      date-done="20201230T1342" performer="MARCEL P BERGERON" performer-
      id="172635544" username="h0006384" disposition="Send On"
      authentication="true" />
    <task name="Milestone 1" id="24" date-done="20201230T1342" />
    <task name="ORP Document Reviewer1" id="57" date-due="20210101T1342"
      date-done="20210111T1552" performer="GEOFFREY T TYREE" performer-
      id="6158846" username="h0068565" disposition="Public Release"
      authentication="true" />
    <task name="ORP Document Reviewer3" id="59" date-due="20210101T1342"
      date-done="20210127T1036" performer="GRACE J KING" performer-
      id="211901436" username="h9807759" disposition="Public Release"
      authentication="true" />
    <task name="Doc Owner Reviews ORP Comments" id="61" date-
      due="20210128T1036" date-done="20210127T1051" performer="MARCEL P
      BERGERON" performer-id="172635544" username="h0006384"
      disposition="Send On" authentication="true" />
    <task name="Milestone 2" id="62" date-done="20210127T1051" />
    <task name="Verify Doc Consistency" id="4" date-due="20210128T1051" date-
      done="20210128T1542" performer="SARAH E HARRISON" performer-
      id="252341659" username="h5635746" disposition="Cleared"
      authentication="true" />
  </workflow>
```

RPP-RPT-46088
Revision 2A

Flow and Transport in the Natural System at Waste Management Area C

M. P. Bergeron
Washington River Protection Solutions, LLC

M. P. Connelly
TecGeo, Inc.

S. P. Reidel
GSI Water Solutions, Inc.

Date Published
January 2021

Prepared for the U.S. Department of Energy
Office of River Protection

Contract No. DE-AC27-08RV14800

Approved for Public Release;
Further Dissemination Unlimited

This page intentionally left blank.

Version History

Version	Date	Author	Change Description
Rev. 0	23-Apr-2010	M. P. Bergeron	Initial revision
Rev. 1	26-Aug-2010	M. P. Bergeron	Updates to address comments from NRC review of WMA C WIR Evaluation and Performance Assessment. Updates include selected changes to Table 3-3.
Rev. 2	21-Nov-2016	M. P. Bergeron	This update includes the addition of Section 7.0 to reflect additional information used in the development and implementation phases of the WMA C Performance Assessment.
Rev. 2A	28-Jan-2021	M. P. Bergeron	Updates to address comments from NRC review of WMA C WIR Evaluation and Performance Assessment and associated internal review of this document. Updates include selected changes to entries in Table 3-2 to be consistent with hydrostratigraphic picks made in RPP-RPT-56356, Rev. 1, *Development of Alternative Digital Geologic Models of Waste Management Area C*.

EXECUTIVE SUMMARY

This document provides supporting information for the Natural System Working Session held on May 25 through 27, 2010. This working session is one in a series sponsored by the U.S. Department of Energy's Office of River Protection and the State of Washington Department of Ecology in fiscal years 2009 and 2010. These working sessions are being used to solicit input from the working session participants, and to obtain a common understanding concerning the scope, methods, and data to be used in the *Hanford Federal Facility Agreement and Consent Order* (Ecology et al. 1989) Appendix I Performance Assessment for Waste Management Area C.

Participating working session agency members include representatives from the U.S. Department of Energy, the U.S. Environmental Protection Agency, the U.S. Nuclear Regulatory Commission, and the State of Washington Department of Ecology as well as their contractors. Other participants in the working sessions include representatives of the tribal nations, other stakeholders groups, and members of the interested public.

The primary purpose of the Natural System Working Session was to provide a forum for detailed discussions of the important features, events, and processes related to the vadose zone and groundwater release that will need to be considered and used in the Performance Assessment for Waste Management Area C. The desired outcome for this specific working session was to obtain a common understanding among working session participants concerning key features, events, and processes of the vadose zone and groundwater that will affect local-scale flow and contaminant transport processes at the Waste Management Area C that will be considered the Post-Closure Performance Assessment Scenarios.

Topics discussed in the working session and summarized in this document include the following.

- Geologic and Hydrogeologic Framework in the Region and the Hanford Site including:
  - Geologic history and setting
  - Major structural features
  - Major stratigraphic units
  - Seismicity and other geologic hazards.

- Vadose Zone Flow and Transport System at Waste Management Area C including discussions concerning:
  - Hydrogeologic units and conditions
  - Extent of known contamination
  - Factors affecting moisture movement in vadose zone
  - Flow and transport properties of major units.

- Groundwater Flow and Transport System in the vicinity of Waste Management Area C including discussions related to:
  - Major hydrogeologic units in groundwater
  - Flow conditions

  - Contamination of groundwater at Waste Management Area C
  - Flow and transport properties at Waste Management Area C.

- Proposed reference case and sensitivity cases in the Waste Management Area C Performance Assessment for combined vadose zone and groundwater flow and transport.

The previous Section 7 References has become Section 8 (new references related to Section 7 have been added to the references) and a new Section 7, which summarizes the new data/information, has been added to this document. The updates in Section 7 include the following.

- Geologic stratigraphic information from the Potassium-Uranium-Thorium geophysical logs from the recently-obtained direct push sampling and previous Potassium-Uranium-Thorium logging in groundwater wells and drywells within and around Waste Management Area C resulted in two different geologic models; one based on geologic picks from the site contractor (Washington River Protection Solutions), and the other based on geologic picks from the Nez Perce tribe.

- Neutron probe moisture logging from the direct push resulted in
  - Updates to the vadose zone hydraulic properties used in the numerical modeling to ensure the model-predicted moisture content matched observed values in the vadose zone

  - Development of an alternative heterogeneous model of the vadose zone based on field-measured moisture contents at Waste Management Area C.

- Updated transport properties of the vadose zone sediments.

- Unconfined aquifer properties based on the calibrated Central Plateau model.

A range of sensitivity analyses identified during scoping was proposed to evaluate changes in calculated groundwater impacts that result from changes in vadose zone and groundwater input parameter estimates. Final disposition of this range of sensitivity cases during the Performance Assessment implementation phase are also presented in Section 7.

Section 1.2 has been modified by including the mention of Section 7 in Section 1.2 Scope and Content of Report.

TABLE OF CONTENTS

1.0 INTRODUCTION 1-1

1.1 OBJECTIVE 1-2

1.2 SCOPE AND CONTENT OF REPORT 1-3

2.0 BACKGROUND INFORMATION 2-1

3.0 MAJOR FEATURES OF THE NATURAL SYSTEM 3-1

3.1 REGIONAL GEOLOGIC FRAMEWORK 3-1

3.2 GEOLOGIC HISTORY OF THE PASCO BASIN 3-1

3.2.1 Structural Setting of the Hanford Site with Respect to the Pacific Northwest 3-3

3.2.2 Geologic History of the Hanford Site in the Context of the Pacific Northwest 3-4

3.3 GEOLOGIC FRAMEWORK OF THE HANFORD SITE 3-9

3.4 STRUCTURAL GEOLOGY 3-10

3.5 STRATIGRAPHY OF THE HANFORD SITE 3-11

3.5.1 Columbia River Basalt Group and Ellensburg Formation 3-11

3.5.2 Post-Columbia River Basalt Group Sediments 3-12

3.6 GEOLOGY OF THE CENTRAL PLATEAU 3-12

3.6.1 Basalt 3-12

3.6.2 Ringold Formation 3-13

3.6.3 Pliocene to Pleistocene Transition 3-15

3.6.4 Quaternary Stratigraphy of the Pasco Basin 3-16

3.6.5 Clastic Dikes 3-18

3.6.1 Volcanic Ash Deposits 3-19

3.6.2 Surface Soil 3-21

3.6.3 Perched Water 3-21

3.7 LOCAL GEOLOGY IN VICINITY OF WASTE MANAGEMENT AREA C 3-21

3.7.1 Columbia River Basalt Group 3-29

3.7.2 Undifferentiated Lower Gravel-Dominated Sediments 3-29
3.7.3 Hanford Formation Sediments 3-30
3.7.4 Clastic Dikes 3-31
3.7.5 Recent Deposits 3-31
3.8 TECTONIC DEVELOPMENT OF THE HANFORD SITE 3-31
3.9 SEISMIC ACTIVITY AND EARTHQUAKES ON THE HANFORD SITE 3-33
3.10 GEOLOGIC HAZARD ASSESSMENT 3-36
3.10.1 Volcanic Hazard Assessment 3-36
3.10.2 Seismic Hazard Assessment 3-36
4.0 VADOSE ZONE SYSTEM AT WASTE MANAGEMENT AREA C 4-1
4.1 KEY FEATURES OF THE VADOSE ZONE 4-1
4.2 FACTORS AFFECTING MOISTURE MOVEMENT IN VADOSE ZONE 4-4
4.2.1 Water Retention and Unsaturated Hydraulic Conductivity 4-5
4.2.2 Moisture Dependent Anisotropy 4-8
4.2.3 Influence of Preferential Pathways 4-10
4.3 MOISTURE CONTENT AND MATRIC POTENTIAL MEASUREMENTS AT WASTE MANAGEMENT AREA C 4-11
4.3.1 Matric Potential Data 4-11
4.3.2 Moisture Content Data 4-12
4.4 ALTERNATIVE CONCEPTUAL MODELS OF VADOSE ZONE FLOW AND TRANSPORT AT WASTE MANAGEMENT AREA C 4-17
4.5 RECOMMENDED FLOW AND TRANSPORT PROPERTIES 4-17
4.5.1 Flow Properties 4-18
4.5.2 Transport-Related Properties 4-23
4.5.3 Contaminant-Specific Distribution Coefficients 4-25
5.0 GROUNDWATER SYSTEM AT WASTE MANAGEMENT AREA C 5-1
5.1 UPPERMOST AQUIFER SYSTEM 5-2

5.2 AQUIFER PROPERTIES 5-6

5.3 CHANGES IN GROUNDWATER FLOW DIRECTION 5-10

5.4 GROUNDWATER GEOCHEMISTRY 5-19

5.4.1 Background Groundwater Chemistry on Hanford Site 5-19

5.4.2 Background Groundwater Chemistry beneath Waste Management Area C 5-26

5.4.3 Groundwater Contamination beneath Waste Management Area C 5-27

5.5 CONCEPTUAL MODEL FOR THE GROUNDWATER PATHWAY AT WASTE MANAGEMENT AREA C 5-46

5.5.1 Key Characteristics of Unconfined Aquifer System 5-46

5.5.2 Hydraulic and Water Quality Impacts from Past Operations 5-47

5.5.3 Project Future Impacts 5-49

5.6 RECOMMENDED FLOW AND TRANSPORT PROPERTIES 5-50

6.0 SUMMARY OF PROPOSED CASES FOR VADOSE ZONE AND GROUNDWATER FLOW AND TRANSPORT 6-1

6.1 LOCAL-SCALE VADOSE ZONE AND GROUNDWATER FLOW AND TRANSPORT 6-1

6.1.1 Conditions for Operational Period 6-1

6.1.2 Conditions for Post-Closure Period 6-2

6.2 REGIONAL-SCALE GROUNDWATER FLOW AND TRANSPORT 6-6

7.0 ADDITIONAL INFORMATION USED IN THE DEVELOPMENT AND IMPLEMENTATION PHASES OF THE WASTE MANAGEMENT AREA C PERFORMANCE ASSESSMENT 7-1

7.1 UPDATES TO THE VADOSE ZONE STRATIGRAPHY BASED ON THE POTASSIUM-URANIUM-THORIUM GEOPHYSICAL LOGGING 7-1

7.2 NEUTRON PROBE MOISTURE LOGGING FROM THE DIRECT PUSH DATA 7-15

7.2.1 Updated Hydraulic Properties of the Hanford H1 and H3 Gravelly Units 7-17

7.2.2 Updated Properties of the Hanford H2 Sand Unit 7-21

7.2.3 Alternative Geologic Model H2 Subunits Properties 7-25

7.2.4 Summary of Revised Hydraulic Parameters 7-26

7.2.5 Alternative Heterogenous Model 7-29

7.3 UPDATED TRANSPORT PROPERTIES FOR THE VADOSE ZONE SEDIMENTS 7-41

7.3.1 Bulk Density 7-41

7.3.2 Bulk Distribution Coefficient (K_d) 7-41

7.3.3 Updated Macrodispersivity Estimates 7-44

7.4 UPDATED UNCONFINED AQUIFER PROPERTY ESTIMATES 7-45

7.4.1 Unconfined Aquifer Hydraulic Properties 7-46

7.4.2 Updated Transport Properties for the Unconfined Aquifer 7-49

7.5 DISPOSITION OF PROPOSED SENSITIVITY ANALYSES FROM SCOPING 7-50

8.0 REFERENCES 8-1

APPENDICES

APPENDIX A – FEATURES, EVENTS AND PROCESSES FOR THE VADOSE ZONE SYSTEM AT WASTE MANAGEMENT AREA C ..... A-i

APPENDIX B – MAJOR HYDROGEOLOGIC UNITS IN VICINITY OF WASTE MANAGEMENT AREA C ..... B-i

APPENDIX C – CHARACTERIZATION OF CONTAMINATION IN VADOSE ZONE FROM PAST WASTE LEAKS AND LOSSES ..... C-i

APPENDIX D – ALTERNATIVE CONCEPTUAL MODELS ..... D-i

APPENDIX E – FEATURES, EVENTS AND PROCESSES FOR THE GROUNDWATER SYSTEM AT WASTE MANAGEMENT AREA C ..... E-i

APPENDIX F – COMPARISON OF GROUNDWATER, VADOSE ZONE PORE WATER, AND TANK LEAK CHEMICAL COMPOSITIONS ..... F-i

APPENDIX G – TECHNICAL NOTE: SCOPING CALCULATIONS THAT EVALUATE INFILTRATION RATE NEEDED TO EXPLAIN PLUME DEPTH ..... G-i

APPENDIX H – REVIEW COMMENT RECORDS ..... H-i

LIST OF FIGURES

Figure 2-1. Hanford Site and its Location in Washington State. 2-2

Figure 2-2. Facilities in the 200 Areas of Hanford's Central Plateau. 2-3

Figure 2-3. Location Map of Waste Management Area C and Surrounding Area. 2-4

Figure 3-1. Geographic Elements of the Pasco Basin Portion of the Columbia Basin, Washington. 3-2

Figure 3-2. Geologic Setting of the Pasco Basin. 3-3

Figure 3-3. Generalized Stratigraphy of the Pasco Basin and Vicinity. 3-6

Figure 3-4. Geologic and Geomorphic Map of the 200 Areas and Vicinity. 3-10

Figure 3-5. Fence Diagram of Sediment Overlying the Columbia River Basalt Group in the Central Plateau, Hanford Site. 3-13

Figure 3-6. Typical Clastic Dike in Touchet Beds of the Hanford Formation. Picture taken in the Walla Walla valley near Touchet, Washington. 3-19

Figure 3-7. Projection of a Hypothetical Network of Clastic Dikes onto Waste Management Area S-SX. 3-20

Figure 3-8. Fence Diagram of the A, AX and C Tank Farms. 3-26

Figure 3-9. Clastic Dikes in the Excavated Wall of the Integrated Disposal Facility. Arrows show the abrupt change from vertical to nearly horizontal. 3-32

Figure 3-10. Clastic Dikes to Right of Figure 3-9. 3-32

Figure 3-11. Earthquake Swarm Areas in the Vicinity of the Hanford Site. 3-35

Figure 4-1. A Cross-sectional View of Heterogeneous Sediments in 200 Areas. 4-5

Figure 4-2. Typical Moisture Retention (volumetric moisture content, Θ_v, versus decreasing pressure head, h) Curves for a Fine-textured (e.g., silt) and a Coarse-textured (e.g., coarse sand) Sediment; (the curves represent fit through the experimental data). 4-6

Figure 4-3. Typical Unsaturated Hydraulic Conductivity, K(h) versus Pressure Head, h Relation for a Fine-textured (e.g., silt) and a Coarse-textured (e.g., coarse sand) Sediment; (the circles represent the experimental data). 4-6

Figure 4-4. Schematics Illustrating Comparison of (a) an Observed Plume with Simulations using (b) an Isotropic, and (c) a Variable Moisture Dependent Anisotropy for Unsaturated Hydraulic Conductivity (K); (d) Constant and Variable Anisotropy; Kh is Horizontal Hydraulic Conductivity Parallel to Bedding and Kv is Vertical Hydraulic Conductivity Perpendicular to Bedding; ψ is Matric Potential or Pressure Head (h). 4-9

Figure 4-5. Matric Potentials Measured by Filter Paper Technique on Core Samples from Borehole 299-E27-22. 4-13

Figure 4-6. Borehole 299-E27-22 Lithology and Gravimetric Moisture Content Measurements (the shaded areas in light blue and gray are regions of increased moisture)..... 4-14

Figure 4-7. Borehole C4297 Lithology and Gravimetric Moisture Content Measurements (the shaded areas in light blue and gray are regions of increased moisture)..... 4-15

Figure 4-8. Matric Potential for Borehole C4297 Samples (measured after cores were sub-sampled). 4-16

Figure 4-9. Example Plots of Freundlich Isotherm in Terms of S versus C using Freundlich Adsorption Constant (K_f) Ranging from 1 to 10 and and Freundlich Exponent (N) of 0.6. 4-37

Figure 4-10. Example Plots of Langmuir Adsorption Isotherm in Terms of S versus C Using a Binding Energy Constant (α) Ranging from 0.001 to 1 L/mg and Maximum Amount of Solute Sorbed onto Solid (β) of 100 mg/kg. 4-38

Figure 5-1. Generalized Geologic Cross-Section through the Hanford Site. 5-3

Figure 5-2. Hanford Site and Outlying Areas Water Table Map, March 2008. 5-4

Figure 5-3. Distribution of Water-Table Elevations, March 2008..... 5-5

Figure 5-4. Comparison of Major Hydrologic Units and Geologic Stratigraphy at Hanford..... 5-7

Figure 5-5. Well Location Map for Waste Management Area C. 5-9

Figure 5-6. Discharge History for and Location of the B Pond and the Gable Mountain Pond Systems. 5-12

Figure 5-7. Hydrographs from Selected Wells in the Area of Waste Management Area C, 200 East Area. 5-13

Figure 5-8. Range of Groundwater Flow Directions in the Vicinity of 241-C Tank Farm Based on Analyses of Water-Level Measurements Made in Selected Wells between 1958 and 2003..... 5-18

Figure 5-9. Modified Stiff Diagram Depicting Major Cation and Anion Compositions for Background Groundwater, Top of the Aquifer in the Hanford Site's Unconfined Aquifer..... 5-25

Figure 5-10. Major Cation and Anion Composition of Groundwater from Upgradient Wells at Waste Management Area C. 5-28

Figure 5-11. Specific Conductance and Concentrations of Nitrate and Technetium-99 versus Depth below the Water Table in Well 299-E27-22. 5-29

Figure 5-12. Average Fiscal Year 2005 Tritium Concentration in the Area of Waste Management Area C, Top of the Aquifer. 5-32

Figure 5-13. Average Fiscal Year 2005 Iodine-129 Concentration in the Area of Waste Management Area C, Top of the Aquifer. 5-33

Figure 5-14. Average June 2005 Nitrate Concentrations in the Area of Waste Management Area C, Top of the Aquifer. 5-34

Figure 5-15. Average Fiscal Year 2006 Technetium-99 Concentrations in the Area of Waste Management Area C, Top of the Aquifer. 5-35

Figure 5-16. Nitrate, Sulfate, and Technetium-99 Concentrations in Upgradient Well 299-W27-7 at Waste Management Area C. 5-37

Figure 5-17. Selected Water Quality Showing Groundwater Impacts in Vicinity of Waste Management Area C. 5-38

Figure 5-18. Sulfate, Nitrate, and Technetium-99 Concentrations in Selected Downgradient Wells at Waste Management Area C. 5-43

Figure 5-19. Technetium-99/Nitrate and Technetium-99/Sulfate Relationships for Selected Wells at Waste Management Area C (data for C4297 from PNNL-15503; all other data from Hanford Environmental Information System 1994). 5-44

Figure 5-20. Cyanide Concentration in Wells at Waste Management Area C. 5-45

Figure 7-1(a). Cross-Sections through Waste Management Area C Alternative Geologic Model I Using Washington River Protection Solutions Interpretations. 7-4

Figure 7-1(b). Cross-Sections through Waste Management Area C Alternative Geologic Model II Using Nez Perce Interpretations. 7-4

Figure 7-2. Locations of Cross-Sections at Waste Management Area C Shown in Figures 7-4 through 7-7. 7-6

Figure 7-3. Legend for Cross-Sections 7-6

Figure 7-4. West Cross-Section A to B (gray) for Different Alternative Models. 7-7

Figure 7-5. Middle Cross-Section A to C (green) for Different Alternative Models. 7-9

Figure 7-6. East Cross-Section A to D (blue) for Different Alternative Models. 7-11

Figure 7-7. Northwest to Southeast Cross-Section E to F (red) for Different Alternative Models. 7-13

Figure 7-8. Locations and Moisture Content (% Vol) Measurements in Vadose Zone at Waste Management Area C. 7-16

Figure 7-9. Histograms Showing the Range of Volumetric Moisture Content for the Backfill, H1, and H2 Units at Waste Management Area C. 7-17

Figure 7-10. Location of Integrated Disposal Facility and Selected Boreholes in 200 Area. .. 7-18

Figure 7-11. Unsaturated Hydraulic Conductivity Measurements for Sand-dominated and Gravel-dominated Samples. 7-19

Figure 7-12. Moisture Retention Data for H1 and H3 Units (17 Samples). The composite curve is shown in red. 7-21

Figure 7-13. Unsaturated Hydraulic Conductivity Measurements for Sand-dominated and Gravel-dominated Samples. 7-22

Figure 7-14. Waste Management Area C Hanford H2 Sand-Dominated Core. 7-23

Figure 7-15. Moisture Retention Data for H2 Unit (44 Samples). The Waste Management Area C composite curve is shown in red. 7-26

Figure 7-16. Unsaturated Hydraulic Conductivity Data for H2 Unit (44 Samples). The Waste Management Area C H2 composite curve is shown in red. 7-27

Figure 7-17. Plots of Model-Calculated Aqueous Moisture Content for Three Time Periods. Upper Row of Plots Uses the van Genuchten Parameters in Table 4-1, while the Lower Row of Plots Uses the Updated van Genuchten Parameters. 7-31

Figure 7-18. Plots of Model-Calculated Vadose Zone Pore Water Velocity along with Streamlines and Time Markers for Three Time Periods along a Cross-Section of the Model going through Tanks 241-C-102, 241-C-105, 241-C-108 and 241-C-111. Upper Row of Plots Uses the van Genuchten Parameters in Table 4-1, while the Lower Row of Plots Uses the Updated van Genuchten Parameters. 7-33

Figure 7-19. Plan View of Waste Management Area C Performance Assessment Model and Moisture Content-Based Model. 7-35

Figure 7-20. Waste Management Area C Basemap with Moisture Content (vol %) Data Locations. 7-36

Figure 7-21. Cross Section B-B' with Continuous Contours for Moisture Content (vol %) Interpolation. 7-37

Figure 7-22. Cross Section C-C' with Continuous Contours for Moisture Content (vol %) Interpolation. 7-37

Figure 7-23. Location of Selected Cross Sections for the Two-Dimensional Models. 7-38

Figure 7-24. Moisture Retention Curves and Unsaturated Hydraulic Conductivity Curves for the Four New Units. 7-40

Figure 7-25a. Hind Cast Water Table Map of the Hanford Site, January 1944. 7-47

Figure 7-25b. Water Table Elevations for June 1987. 7-47

Figure 7-25c. Water Table Elevations for 2013. 7-47

LIST OF TABLES

Table 1-1. Waste Management Area C Performance Assessment Working Sessions. 1-1
Table 3-1. Stratigraphic Terminology and Unit Thickness for the A-AX and C Tank Farms. 3-23
Table 3-2. Stratigraphic Contact Elevations for Boreholes in Waste Management Areas A-AX and C. 3-27
Table 4-1. Composite van Genuchten-Mualem Parameters for Various Strata at Waste Management Area C. 4-20
Table 4-2. Statistical Mean Values of van Genuchten-Mualem Parameters for Site-Wide Samples. 4-21
Table 4-3. van Genuchten-Mualem Parameters, Saturated Hydraulic Conductivity and Bulk Density for Several Clastic Dikes. 4-22
Table 4-4. Macroscopic Anisotropy Parameters for Various Strata at Waste Management Areas C and S-SX Based on Polmann (1990) Model. 4-22
Table 4-5. Effective Bulk Density (g/cm^3) Estimates at Waste Management Area C. 4-23
Table 4-6. Nonreactive Macro-dispersivity Estimates for Various Strata at Waste Management Areas C. 4-24
Table 4-7. Results for Macro-dispersivity Enhancement that Considered Sorption Based on a K_d of 0.6 mL/g for Various Strata in Waste Management Area C. 4-25
Table 4-8. Distribution Coefficients (mL/g) for Non-Radiological Constituents that are Part of the Waste Management Area C Inventory. 4-29
Table 4-9. Distribution Coefficients (mL/g) for Radiological Constituents that are Part of the Waste Management Area C Inventory. 4-34
Table 5-1. Thickness of the Unconfined Aquifer Beneath the A-AX and C Single-Shell Tanks in 200 East Area. 5-8
Table 5-2. General Estimated Groundwater Flow Directions and Flow Rates for Single-Shell Tank Waste Management Areas A-AX and C in the 200 East Area. 5-10
Table 5-3. Results from Slug Testing of Wells at 200 East Area Single-Shell Tank Farms. 5-10
Table 5-4. Results of Pre-1997 Slug Testing at C Single-Shell Tank Waste Management Area in the 200 East Area. 5-11
Table 5-5. Historical Water Level Changes Beneath the 200 East Area Single-Shell Tank Farms. 5-14
Table 5-6. Water Levels, Groundwater Flow Directions, and Water-Table Gradients in the Area of Waste Management Area C from 1958 to 2003. 5-16
Table 5-7. Hanford Site Groundwater Background Concentrations. 5-21
Table 5-8. Average Fiscal Year 2005 Groundwater Composition in Upgradient Wells at Waste Management Area C. 5-27
Table 5-9. Depth-Discrete Water Sampling Results from Well 299-E27-22. 5-29
Table 5-10. Average Concentration of Mobile Contaminants in Groundwater in the Vicinity of Waste Management Areas C for Fiscal Year 2005. 5-31

Table 5-11. Recommended Parameter Values for Unconfined Aquifer Properties for Waste Management Area C. 5-51
Table 6-1. Proposed Simulation Cases Representing the Effects of Alternative Models on Vadose Zone Flow and Transport. 6-3
Table 6-2. Proposed Simulation Cases Representing the Effects of Varying Hydraulic Conductivities on Vadose Zone Flow and Transport. 6-4
Table 6-3. Proposed Cases for Contaminant Distribution Coefficients (mL/g) for Non-Impacted Soils. 6-5
Table 6-4. Unconfined Aquifer Properties for Waste Management Area C. 6-6
Table 7-1. Summary Statistics for Volumetric Moisture Content in the Lithologic Units Underlying Waste Management Area C. 7-15
Table 7-2. Summary Statistics for Volumetric Moisture Content in the Lithologic Units Underlying Waste Management Area C Using the Hydraulic Parameters in Table 4-1. 7-16
Table 7-3. van Genuchten Parameters, Fitted Saturated Hydraulic Conductivity, and Measured Bulk Density Data for H1/H3 Units (17 Samples). 7-20
Table 7-4. van Genuchten Parameters, Fitted Saturated Hydraulic Conductivity (44 samples), and Measured Bulk Density Data (41 samples) for Integrated Disposal Facility Borehole Samples from the H2 Sandy Sequence. 7-24
Table 7-5. Composite van Genuchten-Mualem Parameters for Various Strata at the Waste Management Area C Site Used in the Base Case Evaluations of Alternative Geologic Models I and II. 7-28
Table 7-6. Summary Statistics for Volumetric Moisture Content in the Lithologic Units Underlying Waste Management Area C Using Updated van Genuchten Parameters. 7-29
Table 7-7. Travel Time Calculations Using the Original and Updated van Genuchten Parameters. 7-35
Table 7-8. Summary of Vadose Zone Hydraulic Properties for the New Units. 7-41
Table 7-9. Updated Effective Bulk Density ($E[\rho_b]$, g/cm^3) Estimates for Various Strata at Waste Management Area C Used in the Base Case Evaluations of Alternative Geologic Models I and II. 7-42
Table 7-10. Distribution Coefficients (K_d) Values Used to Approximate the Transport of the Radionuclides in the Base Case. 7-43
Table 7-11. Macrodispersivity Estimates for Various Strata at Waste Management Area C Used in the Base Case Evaluations of Alternative Geologic Models I and II. 7-45
Table 7-12. Updated Hydraulic Properties for Aquifer Soil Type at Waste Management Area C. 7-49
Table 7-13. Summary of Disposition of Alternative Conceptual Models and Vadose Zone Related Sensitivity Analysis Proposed during Scoping. 7-51
Table 7-14. Summary of Disposition of Alternative Conceptual Models and Vadose Zone Related Sensitivity Analysis Proposed during Scoping. 7-56

LIST OF TERMS

Abbreviations and Acronyms

2D	two dimensional
3D	three-dimensional
amsl	above mean sea level
bgs	below ground surface
BP	before present
CCU	Cold Creek unit
CERCLA	*Comprehensive Environmental Response, Compensation, and Liability Act of 1980*
CPGWM	Central Plateau Groundwater Model
CRBG	Columbia River Basalt Group
DOE	U.S. Department of Energy
DOE/RL	U.S. Department of Energy, Richland Operations Office
DQO	data quality objective
Ecology	State of Washington Department of Ecology
EIS	Environmental Impact Statement
EHM	Equivalent homogeneous media
EPA	U.S. Environmental Protection Agency
ERDF	Environmental Restoration Disposal Facility
FEPs	Features, Events, and Processes
FY	fiscal year
Hf	undifferentiated Hanford (formation)
HEIS	Hanford Environmental Information System
HFFACO	*Hanford Federal Facility Agreement and Consent Order*
IDF	Integrated Disposal Facility
K-U-T	Potassium-Uranium-Thorium
LLWMA	Low-Level Waste Management Area
MCL	maximum contaminant level
MPa	matric potential
NEPA	National Environmental Policy Act of 1969
PA	performance assessment
PNNL	Pacific Northwest National Laboratory
PUREX	Plutonium Uranium Extraction (Plant)
RCRA	*Resource Conservation and Recovery Act of 1976*

RETC	RETention Curve (computer code)
SST	single-shell tank
SST PA	DOE/ORP-2005-01, *Initial Single-Shell Tank System Performance Assessment for the Hanford Site*
STOMP	Subsurface Transport Over Multiple Phases (numeric code)
TC&WM	Tank Closure and Waste Management
TEDF	Treated Effluent Disposal Facility
UPR	unplanned release
WAC	Washington Administrative Code
WMA	waste management area
WRPS	Washington River Protection Solutions
WTP	Waste Treatment Plant

Units

ft	foot
g	gram
gal	gallon
in.	inch
L	liter
m	meter
mg	milligram
mi^2	square mile
µg	microgram
pCi	picocurie

Hanford Formation Primary Geologic Units

CRBG	Columbia River Basalt Group
CCU	Cold Creek unit
CCU/R	undifferentiated CCU fine unit and/or Ringold Formation
H3/CCU/R	undifferentiated Hanford formation gravel and/or CCU gravel and/or Ringold Formation, unit A
H1 unit	upper gravel-dominated sequence
H2 unit	sand-dominated sequence
H3 unit	lower gravel-dominated sequence

1.0 INTRODUCTION

This document provides supporting information for the Natural System Working Session held on May 25 through 27, 2010. This working session is one in a series (see schedule in Table 1-1) sponsored by the U.S. Department of Energy's (DOE) Office of River Protection and the State of Washington Department of Ecology (Ecology) in fiscal years (FY) 2009 and 2010. These working sessions are being used to solicit input from the working session participants, and to obtain a common understanding concerning the scope, methods, and data to be used in the *Hanford Federal Facility Agreement and Consent Order* (HFFACO) (Ecology et al. 1989) Appendix I Performance Assessment (PA) for Waste Management Area (WMA) C.

Table 1-1. Waste Management Area C Performance Assessment Working Sessions.[a,b]

Num.	Subject	Date
0.	Goal/Process	2/24–2/25
1.	Residual Inventory	5/5–5/7
2.	Assessment Context/General Conceptual Model	9/1–9/3
3.	Soil Inventory	10/27–10/29
4.	Engineered System #1 (Detailed conceptual models, FEPs and data associated with recharge, engineered surface barriers, and waste release from tank waste residuals)	1/26–1/29/2010
5.	Review of Conceptual Models and FEPs[b] Process	3/30–4/1/2010
6.	Natural System (Detailed conceptual models, FEPs, and data associated with vadose zone, groundwater, and near surface environments including discussion of existing contamination)	5/25–5/27/2010
7.	Engineered System #2 (Detailed conceptual models, FEPs, and data associated with steel corrosion, concrete/grout degradation of tanks and related facilities)	7/27–7/29/2010
8.	Exposure Scenarios (Detailed conceptual models, information, and data associated with exposure scenarios, risk and dose assessments)	9/28–9/30/2010
9.	Numeric Codes (as well as topics not covered sufficiently above)	1/25–27/2011
10.	Results from Preliminary Model Simulations supporting the Initial WMA C PA (contents of Maintenance Plan)	8/30–9/1/2011
11.	Placeholder working session	10/25–27/2011
12.	Results from Final Model simulation supporting the Initial WMA C PA	1/24–26/2012

[a] Please note that uncertainty of models and approaches will be discussed throughout the working sessions.
[b] Altered based on discussions in last working session (Engineered System #1)

FEPs = features, events, and processes
PA = performance assessment
WMA = waste management area

Participating working session agency members include representatives of the sponsoring organizations of the working sessions from DOE, the U.S. Environmental Protection Agency (EPA), the U.S. Nuclear Regulatory Commission, and Ecology as well as their contractors. Other participants in the working sessions include representatives of the tribal nations, other stakeholders groups, and members of the interested public.

The primary purpose of the Natural System Working Session was to provide a forum for discussion of three specific aspects of the Natural System:

- **Regional and Local Hydrogeologic Framework** – Major geologic and hydrologic features, events, and processes (FEPs) within the regional framework that affect the WMA C area

- **Local Vadose Zone System at WMA C** – Flow and contaminant transport in unsaturated sediments within the vadose zone in vicinity of the WMA C

- **Regional and Local Groundwater System** – Flow and contaminant transport in underlying unconfined aquifer system in vicinity of the WMA C.

1.1 OBJECTIVE

The objective of this document is to combine published data with more recent information to provide the most current information related to flow and transport in the natural system (i.e., vadose zone and groundwater systems) beneath WMA C.

The desired outcome for this specific working session was to obtain a common understanding among working session participants concerning the following.

- Geologic and Hydrogeologic Framework in the Region and the Hanford Site including:
  - Geologic history and setting
  - Major structural features
  - Major stratigraphic units
  - Seismicity and other geologic hazards.

- Vadose Zone Flow and Transport System at WMA C including discussions concerning:
  - Major hydrogeologic units and conditions
  - Extent of known contamination
  - Factors affecting moisture movement in vadose zone
  - Flow and transport properties of major units.

- Groundwater Flow and Transport System in the vicinity of WMA C including discussions related to:
  - Major hydrogeologic units in groundwater
  - Flow conditions
  - Contamination of groundwater at WMA C
  - Flow and transport properties at WMA C.

- Proposed cases for the combined vadose zone and groundwater flow and transport that should be evaluated in the WMA C PA.

1.2 SCOPE AND CONTENT OF REPORT

General topics presented to facilitate technical discussions in the working session and summarized in this document include the following.

Section 1.0, Introduction – Describes the objectives and scope of this report.

Section 2.0, Background – Provides a brief summary of the WMA C facilities.

Section 3.0, Major Features of the Natural System – Presents a general description of the major features of the natural system relevant to the WMA C that include descriptions of the geology, history, stratigraphy, and structure framework of the Pasco basin, the Hanford Site, the Central Plateau, and the area in vicinity of the WMA C.

Section 4.0, Vadose Zone System at Waste Management Area C – Provides a discussion of conceptual models of moisture movement and contaminant transport in the vadose zone at WMA C, major FEPs important to consider in conceptual models of the vadose zone during past site operations and after site closure, a brief summary of previous work, the factors affecting moisture movement, methods used to characterize moisture movement, and flow and transport parameter estimates that are recommended for use in a proposed cases for vadose zone flow and transport that should be considered in the WMA C PA.

Section 5.0, Groundwater System at Waste Management Area C – Provides a discussion of the key features and characteristics of the groundwater system at the Hanford Site with specific emphasis on the Central Plateau and the area in and around the WMA C. Included in these descriptions are discussions of the major hydrogeologic units, and their hydraulic properties, the directions and rates of groundwater flow, and the general attributes of groundwater background chemistry and contamination by selected hazardous chemicals and radiological constituents in vicinity of the WMA C. This section also discusses the major FEPs important to consider in conceptual models of groundwater flow and transport in the past operations and after site closure, conceptual models of flow and contaminant transport in the groundwater system, and flow and transport parameter estimates that are recommended for use in proposed cases for groundwater flow and transport that should be considered in the WMA C PA.

Section 6.0, Summary of Proposed Cases For Vadose Zone and Groundwater Flow and Transport – Provides of summary of proposed cases that should be considered for local-scale and regional-scale vadose zone and groundwater simulation cases in the WMA C PA.

Section 7.0, Summary of New Data/Information Used in the Development and Implementation of Waste Management Area C Performance Assessment – Summarizes additional information that was used in the development and implementation of the numerical and system level models used in the WMA C PA that included updates to the following.

- Geologic stratigraphic information from the Potassium-Uranium-Thorium (K-U-T) geophysical logs from the recently-obtained direct push sampling and previous K-U-T logging in groundwater wells and drywells within and around WMA C resulted in two different geologic models; one based on geologic picks from the site contractor (Washington River Protection Solutions [WRPS]), and the other based on geologic picks from the Nez Perce tribe.

- Neutron probe moisture logging from the direct push resulted in

    - Updates to the vadose zone van Genuchten curves used in the numerical modeling to ensure the model-predicted moisture content matched observed values in the vadose zone

    - Development of an alternative heterogeneous model of the vadose zone based on field-measured moisture contents at WMA C.

- Updated transport properties of the vadose zone sediments.

- Unconfined aquifer properties based on the calibrated Central Plateau model.

The previous Section 7 References has become Section 8 (new references related to Section 7 have been added to Section 8).

Section 8.0, References – Lists reference documents cited in this report.

2.0 BACKGROUND INFORMATION

This Section provides an overview of the WMA C. Waste Management Area C (WMA C or the 241-C Tank Farm), part of the single-shell tank (SST) system, is located in the Central Plateau (see Figure 2-1), near the eastern edge of the 200 East Area. One of the first tank farms built, it was constructed in 1944 and 1945. The WMA C contains twelve 100-series tanks and four 200-series tanks (see Figures 2-2 and 2-3). The 100-series tanks are 23 m (75 ft) in diameter, have a 5-m (15-ft) operating depth, and have an operating capacity of 1,892,700 L (530,000 gal) each. The 200-series tanks are 6 m (20 ft) in diameter with a 7.32-m (24-ft) operating depth and an operating capacity of 208,000 L (55,000 gal) each. Only tanks 241-C-101 (C-101) through 241-C-106 (C-106) have concrete pits. The other 100-series tanks are equipped with centrally located salt well pump pits. The tanks sit below grade with at least 2 m (7 ft) of soil cover to provide shielding from radiation exposure to operating personnel. Tank pits are located on top of the tanks and provide access to the tank, pumps, and monitoring equipment.

To support the transfer and storage of waste within WMA C SSTs, there is a complex waste transfer system of pipelines (transfer lines), diversion boxes, vaults, valve pits, and other miscellaneous structures.

Fourteen unplanned releases (UPRs) have occurred within or near to WMA C. The largest ones are associated with leaks in pipelines or diversion boxes, with releases from inlet/outlet ports of the SSTs, or with leaks from the SSTs. RPP-PLAN-39114, *Phase 2 RCRA Facility Investigation/Corrective Measures Study Work Plan for Waste Management Area C* provides more detail on these UPR sites.

Five tanks (241-C-103 [C-103], 241-C-201 [C-201], 241-C-202 [C-202], 241-C-203 [C-203], and 241-C-204 [C-204]) have been retrieved to meet the requirements of HFFACO. Tank C-106 also has been retrieved, but is undergoing a HFFACO Appendix H waiver request as its residual waste volume is slightly above the HFFACO limit. Tanks 241-C-108 (C-108), 241-C-109 (C-109) and 241-C-110 (C-110) are currently undergoing waste retrieval activities (HNF-EP-0182, *Waste Tank Summary Report for Month Ending April 30, 2009*). Preparations are underway to initiate waste retrieval at tank 241-C-104 (C-104).

Figure 2-1. Hanford Site and its Location in Washington State.

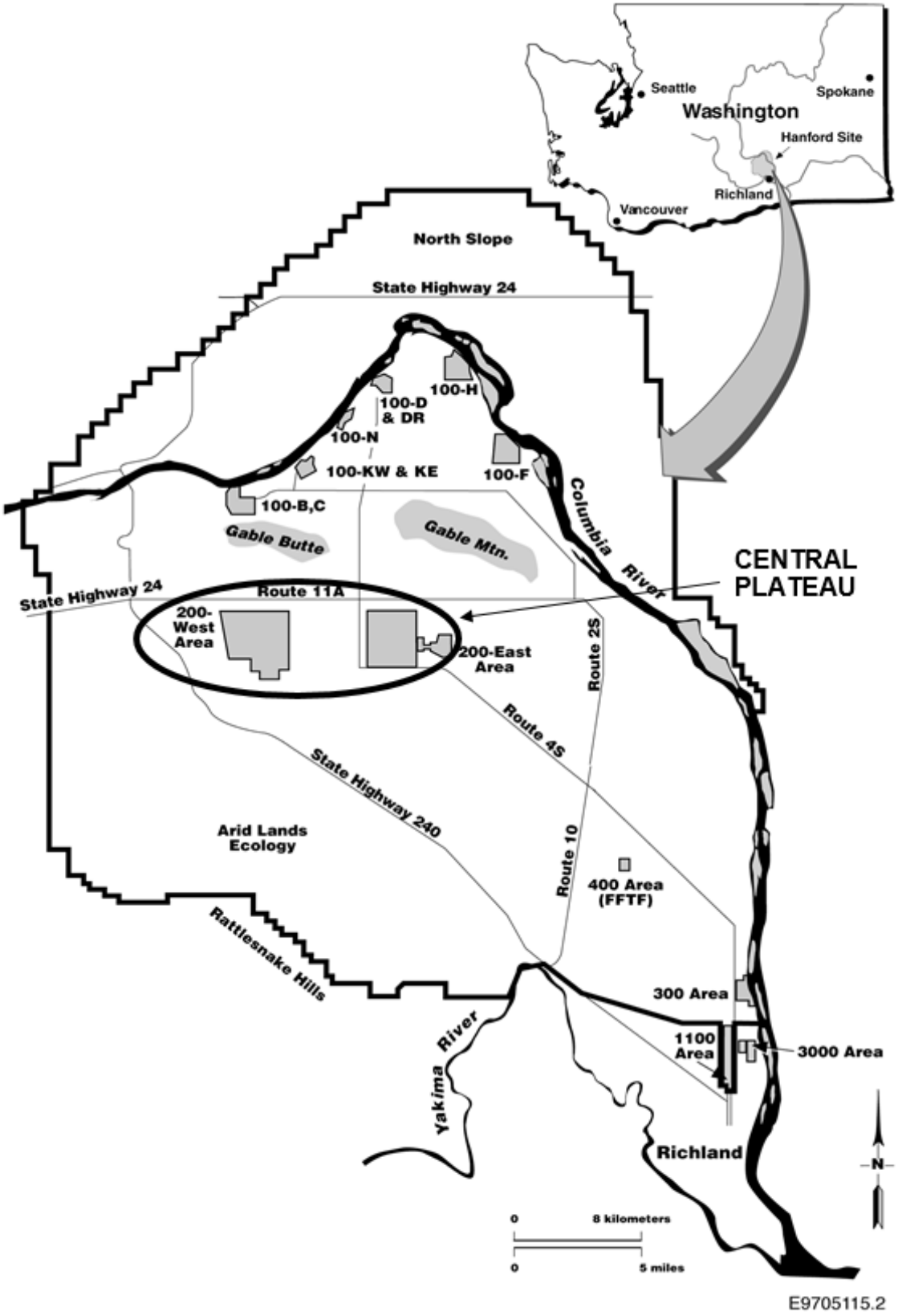

Figure 2-2. Facilities in the 200 Areas of Hanford's Central Plateau.

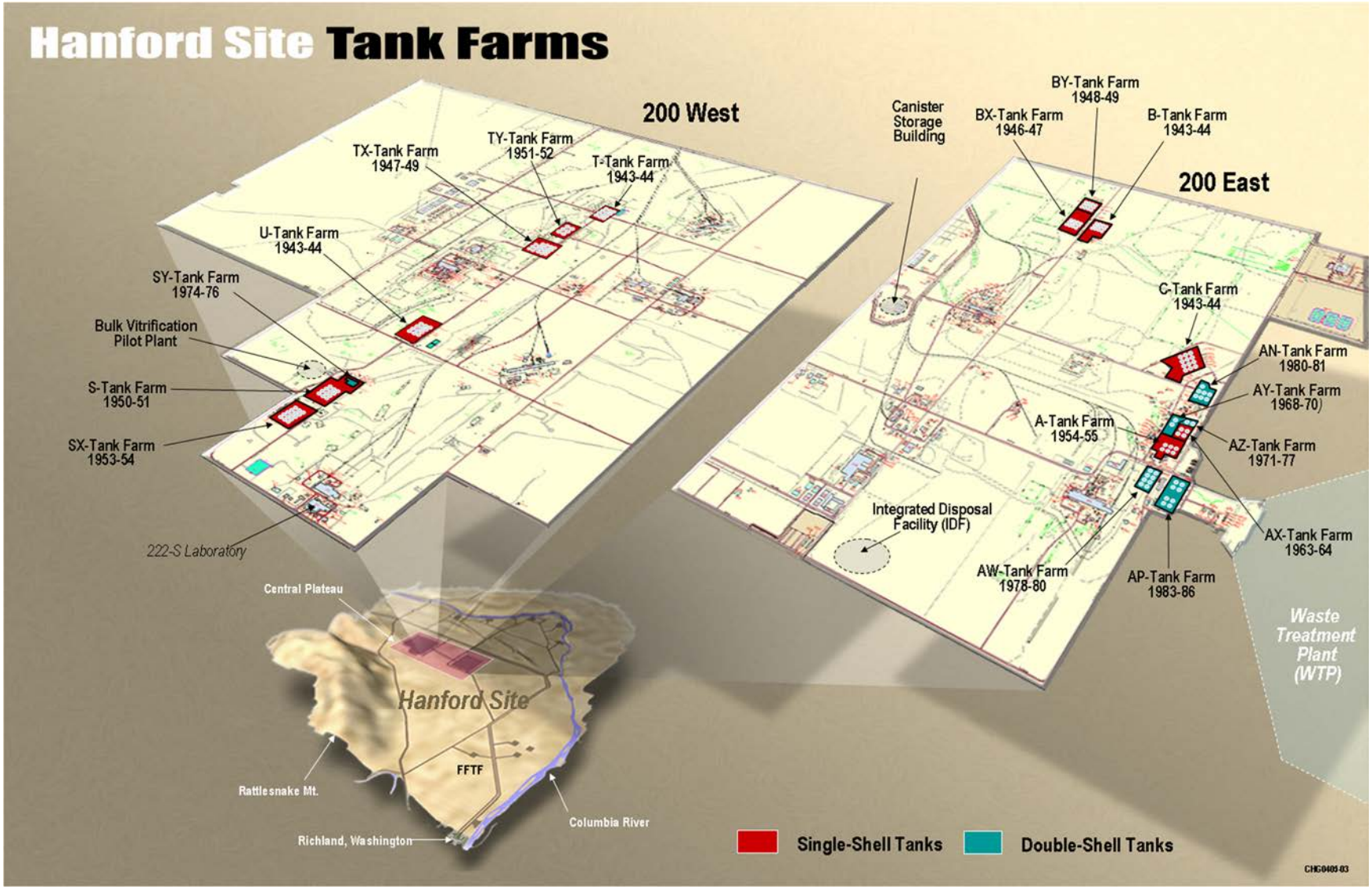

Figure 2-3. Location Map of Waste Management Area C and Surrounding Area.

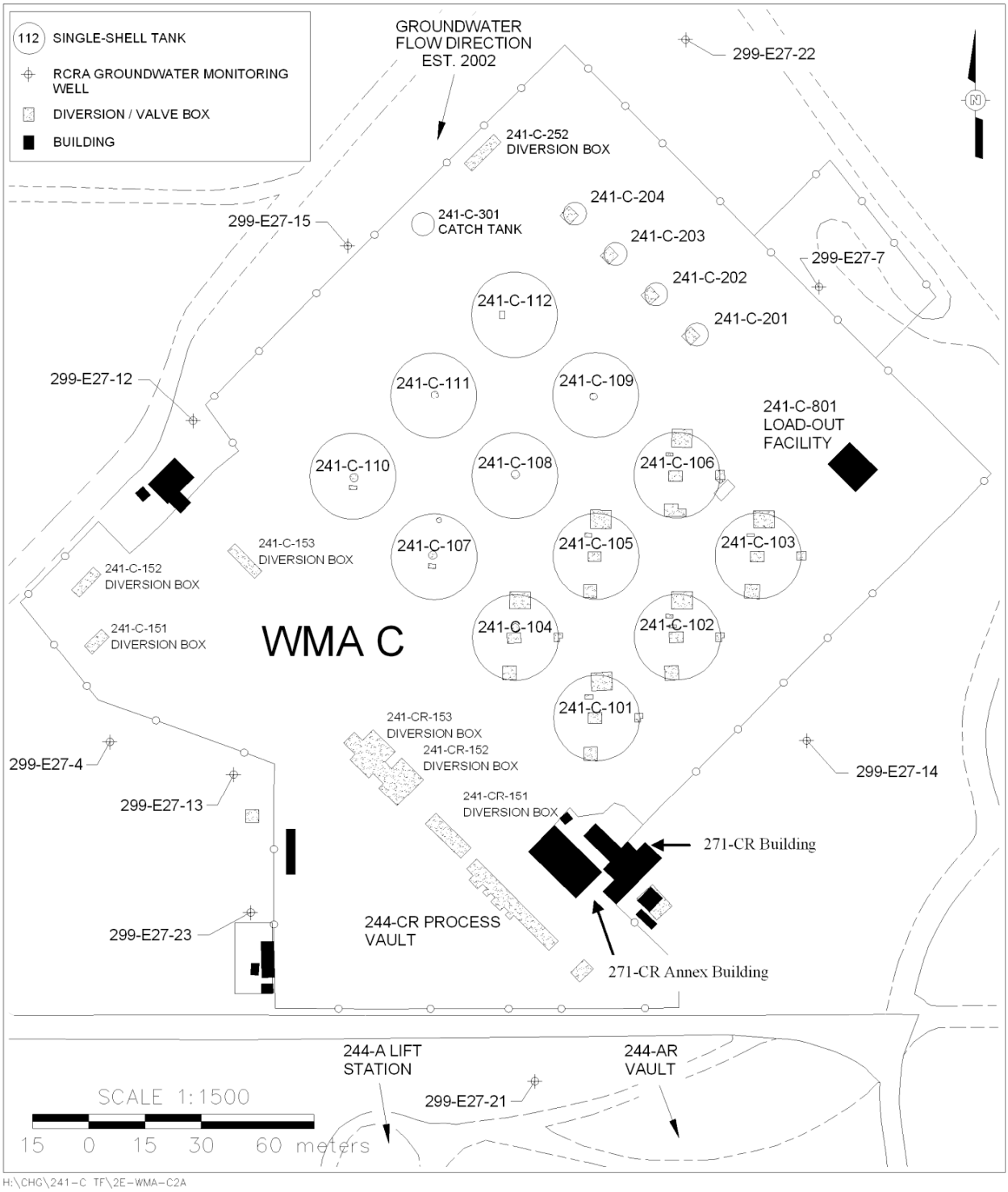

3.0 MAJOR FEATURES OF THE NATURAL SYSTEM

This section of the report provides general background information on the regional and local geologic and hydrologic framework that is relevant to the natural system at WMA C. This would include discussions of the:

- Regional geologic framework and history of the Pasco Basin
- Geologic framework, structure, and stratigraphy of the Hanford Site and the Central Plateau
- Local geologic framework in vicinity of WMA C.

Discussions of these topical areas are then followed by general summaries of historical tectonic development, seismic and earthquake activity, and a general assessment of geologic hazards that would be relevant to the Hanford Site.

3.1 REGIONAL GEOLOGIC FRAMEWORK

The Hanford Site (Figure 3-1) lies within the Columbia Plateau, a broad plain situated between the Cascade Range to the west and the Rocky Mountains to the east, and is underlain by the Miocene Columbia River Basalt Group (CRBG) (Figure 3-2). The northern Oregon and Washington portion of the Columbia Plateau is often called the Columbia Basin because it forms a lowland surrounded on all sides by mountains. The physiographic setting of the Hanford Site is dominated by the low-relief plains of the Central Plains physiographic region and anticlinal ridges of the Yakima Folds region. In the central and western parts of the Columbia Basin and Pasco Basin where the Hanford Site is located, the basalt is underlain predominantly by Tertiary continental sedimentary rocks and overlain by late Tertiary and Quaternary fluvial and glacio-fluvial deposits. All these were folded and faulted during the Cenozoic Era to form the current landscape of the region.

3.2 GEOLOGIC HISTORY OF THE PASCO BASIN

This section describes how the Hanford Site evolved within the context of the Pacific Northwest. It also forms the basis for extrapolating the detailed geology of the tank farms to the surrounding area.

Figure 3-1. Geographic Elements of the Pasco Basin Portion of the Columbia Basin, Washington.

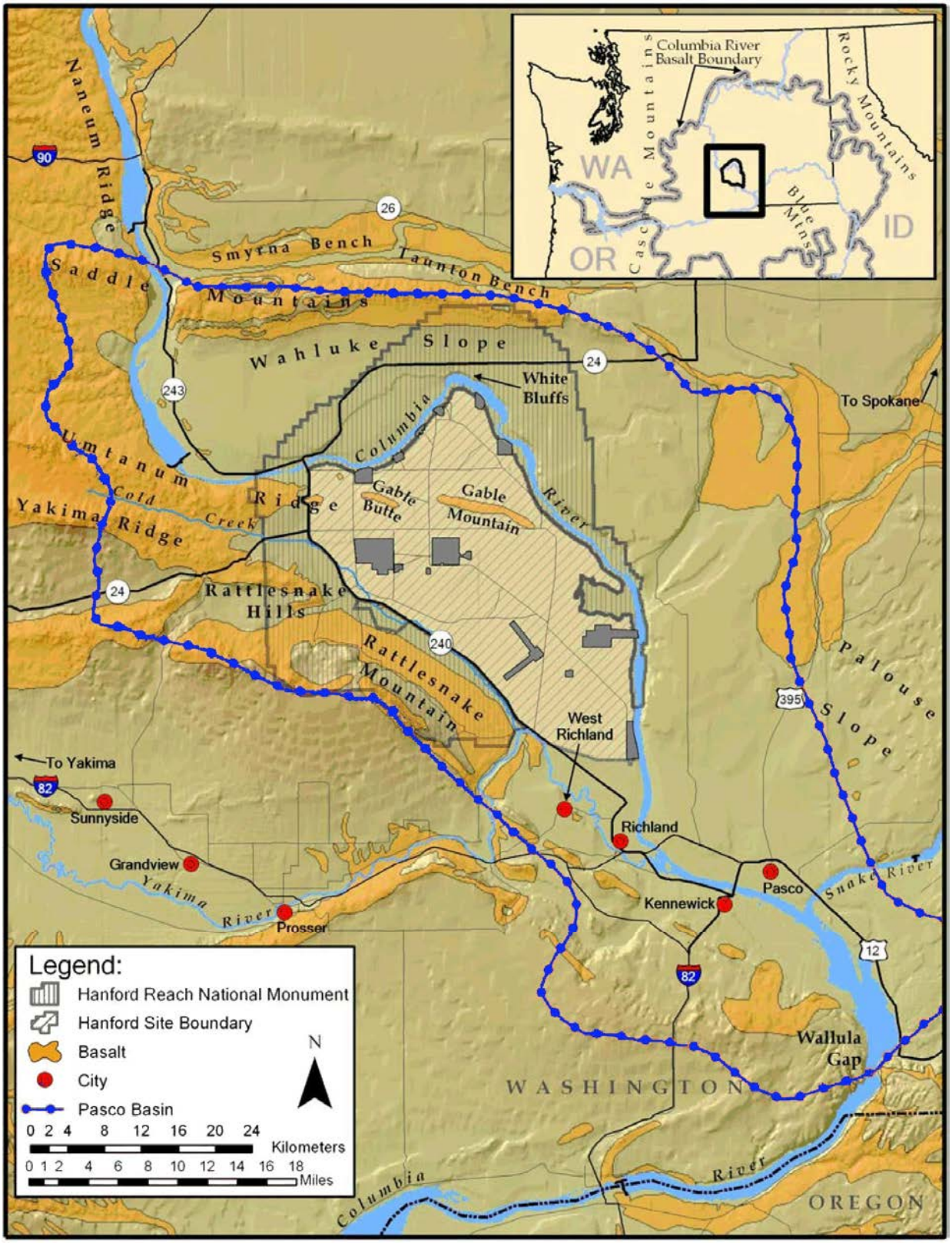

Figure 3-2. Geologic Setting of the Pasco Basin.

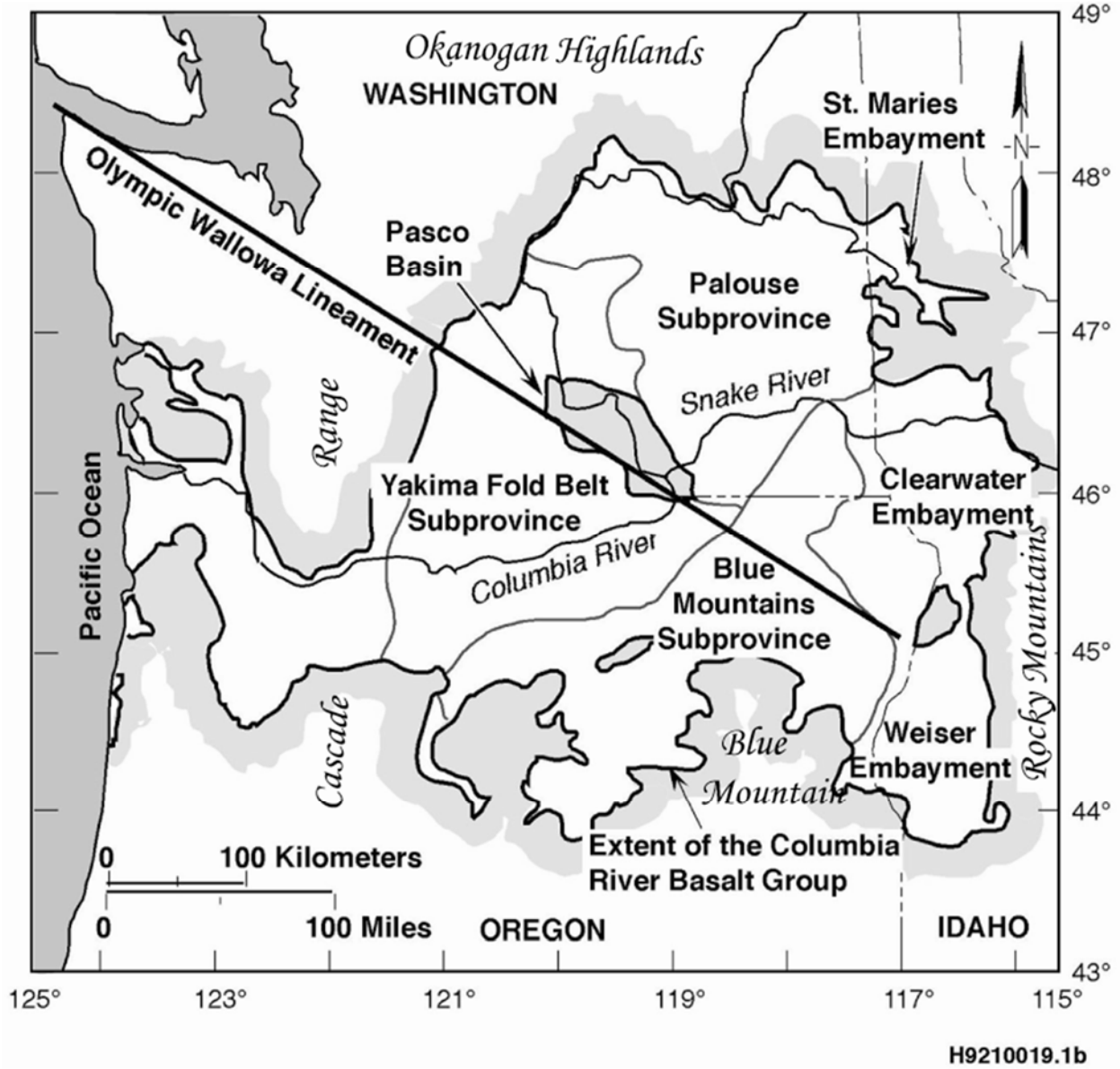

3.2.1 Structural Setting of the Hanford Site with Respect to the Pacific Northwest

The structure of the Pacific Northwest is controlled by a basement rock assemblage of accreted terranes fused onto the structurally complex North American craton by accretion during the early Mesozoic to early Cenozoic. The accreted terranes form the backbone of the Cascade Range, Okanogan Highlands, and the Blue Mountains. The terranes east of the Cascades now are mostly covered by a thick sequence of Cenozoic rocks that were folded and faulted in a north-south oriented compressive regime. North-south compression is continuing today east of the Cascades, and this pattern of Cenozoic deformation is expected to continue into the future.

The Columbia Basin is a structurally and topographically low area surrounded by mountains ranging in age from the late Mesozoic to recent (Figure 3-2). The Columbia Basin is composed of two fundamental subprovinces, the Palouse Slope and the Yakima Fold Belt (Figure 3-2). The Palouse Slope is a stable, undeformed area overlying the old continental craton that dips westward toward the Hanford Site. The Yakima Fold Belt is a series of anticlinal ridges and synclinal valleys in the western and central parts of the Columbia Basin. The edge of the old continental craton lies at the junction of these two structural subprovinces and is currently marked by the Ice Harbor dike swarm of the CRBG east of the Hanford Site.

The Blue Mountains subprovince of the Columbia River flood-basalt province is a northeast trending anticlinorium that extends 250 km from the Oregon Cascades to Idaho and forms the southern border of the Columbia Basin and the southern part of the Columbia Plateau.

3.2.2 Geologic History of the Hanford Site in the Context of the Pacific Northwest

The Hanford Site is a small portion of the Columbia Basin, but the geologic record of the Site is representative of the geologic history of the Pacific Northwest. The following discussion is designed to put the Hanford Site geology into perspective with the regional geologic setting.

3.2.2.1 Rocks Older Than the Columbia River Basalt Group. Rocks older than the CRBG are exposed mainly along the margin of the Columbia Basin. However, they are important to understanding the history of the Hanford Site because many extend under the basalt and form the foundation of the area. Stratigraphy along the margin of the CRBG is complex and varies widely in both age and lithology. The principal age, lithologies, and importance to the history of Hanford were taken from “Late Cenozoic Structure and Stratigraphy of South-Central Washington” (Reidel et al. 1994) and are summarized here.

- The oldest rocks in the Pacific Northwest are found along the northeast and east margins of the Columbia Basin near the Idaho border. These are late Precambrian and early Paleozoic metavolcanic and metasedimentary rocks (2.3 billion to 300 million years before present [BP]) interspersed with younger igneous intrusive rocks. These older rocks represent the ancient North American craton and the remnants of the 1-billion-year-old supercontinent Rodinia that broke apart 750 million years ago to form the Pacific Ocean. The boundary of that rifted margin occurs east of the Hanford Site.

- Late Paleozoic, Mesozoic, and early Cenozoic metavolcanics and metasediments are exposed along the south and western margin of the Columbia Basin. These are the rocks that were added onto the North America Plate remnant of Rodinia between 200 and 50 million years ago. Although many are of similar age to rocks along the north and east margins of the Columbia Basin, they formed as ocean islands and microcontinents far away from the Pacific Northwest. Through the process of plate tectonics, these rocks were carried along on the oceanic plate that collided with the North American Plate beginning 200 million years ago. During the collision process, these ocean islands and microcontinents were accreted onto North America and resulted in the westward growth of North America. Similar accreted terrane rocks are thought to occur deep beneath the Hanford Site.

- Along the west and northwest margin, a series of sedimentary basins formed in early Tertiary time ("Structural and Stratigraphic Interpretation of Rocks under the Yakima Fold Belt, Columbia Basin, Based on Recent Surface Mapping and Well Data" [Campbell 1989]). These basins formed in the accreted terranes and are now separated by tectonic "blocks" or uplifts exposing the accreted terranes. The Tertiary rocks extend under the Columbia Basin and Hanford Site. The rocks include the volcanic and sedimentary rocks that are 50 to 20 million years old and were derived from the erosion of highlands in the Pacific Northwest.

3.2.2.2 Columbia River Basalt Group and Ellensburg Formation. The CRBG forms the main bedrock of the Columbia Basin and Hanford Site. This consists of over 200,000 km^3 of tholeiitic flood-basalt flows that were erupted between 17 and 6 Ma and now cover approximately 200,000 km^2 of eastern Washington, eastern Oregon, and western Idaho ("An introduction to the stratigraphy, structural geology, and hydrogeology of the Columbia River Flood-Basalt Province: A primer for the GSA Columbia River Basalt Group field trips" [Tolan et al. 2009**]**). Eruptions had volumes as great as 5,000 km^3 ("The Grande Ronde Basalt, Columbia River Basalt Group; Stratigraphic Descriptions and Correlations in Washington, Oregon, and Idaho" [Reidel et al. 1989]), with the greatest amounts being erupted between 16.5 and 14.5 million years before present. Intercalated with and in some places overlying the CRBG are sedimentary rocks of the Ellensburg Formation (USGS Bulletin 1457-G, *Revisions in stratigraphic nomenclature of the Columbia River Basalt Group*).

3.2.2.3 Post-Columbia River Basalt Geologic History. Most post-CRBG sediments are confined to the synclinal valleys of the Yakima Fold Belt. Although the sedimentary record is incomplete, the sedimentation pattern is what is expected in an area with limited rainfall and significant structural development ("Paleodrainage of the Columbia River System on the Columbia Plateau of Washington State – A Summary" [Fecht et al. 1987]; "Landscape Evolution in a Flood-Basalt Province: an Example from the Pacific Northwest" [Reidel and Tolan 2009]). The dominant source of sediment between the upper Miocene to middle Pliocene (10 to 3 million years ago) is the Columbia River system. The upper Ellensburg Formation and the Ringold Formation are the main sediment packages that contain this history and record the migration of rivers and streams into their present channels (Fecht et al. 1987; Reidel and Tolan 2009). Capping the sedimentary sequence in the synclines and basins are sediments comprising the Pleistocene Hanford formation deposited during cataclysmic floods and recent eolian deposits.

Ridges of the Yakima Fold Belt were growing during the eruption of the CRBG but were usually completely buried by each new basalt eruption. After the last major basalt eruption, the ridges began to develop significant topography. Continued uplift of the Hog Ranch-Naneum Ridge anticline and the ridges of the Yakima Fold Belt forced the Columbia River and its confluence with the Salmon-Clearwater River eastward. By 10.5 million years ago, the Columbia River was flowing along the western boundary of the Hanford Site and then turning southwestward through Sunnyside Gap (Figure 3-1), the water gap through the Rattlesnake Hills to the west, and south past Goldendale, Washington. This is when the Snipes Mountain conglomerate (Figure 3-3), the last Ellensburg Formation unit in the Pasco Basin, was deposited.

Figure 3-3. Generalized Stratigraphy of the Pasco Basin and Vicinity.

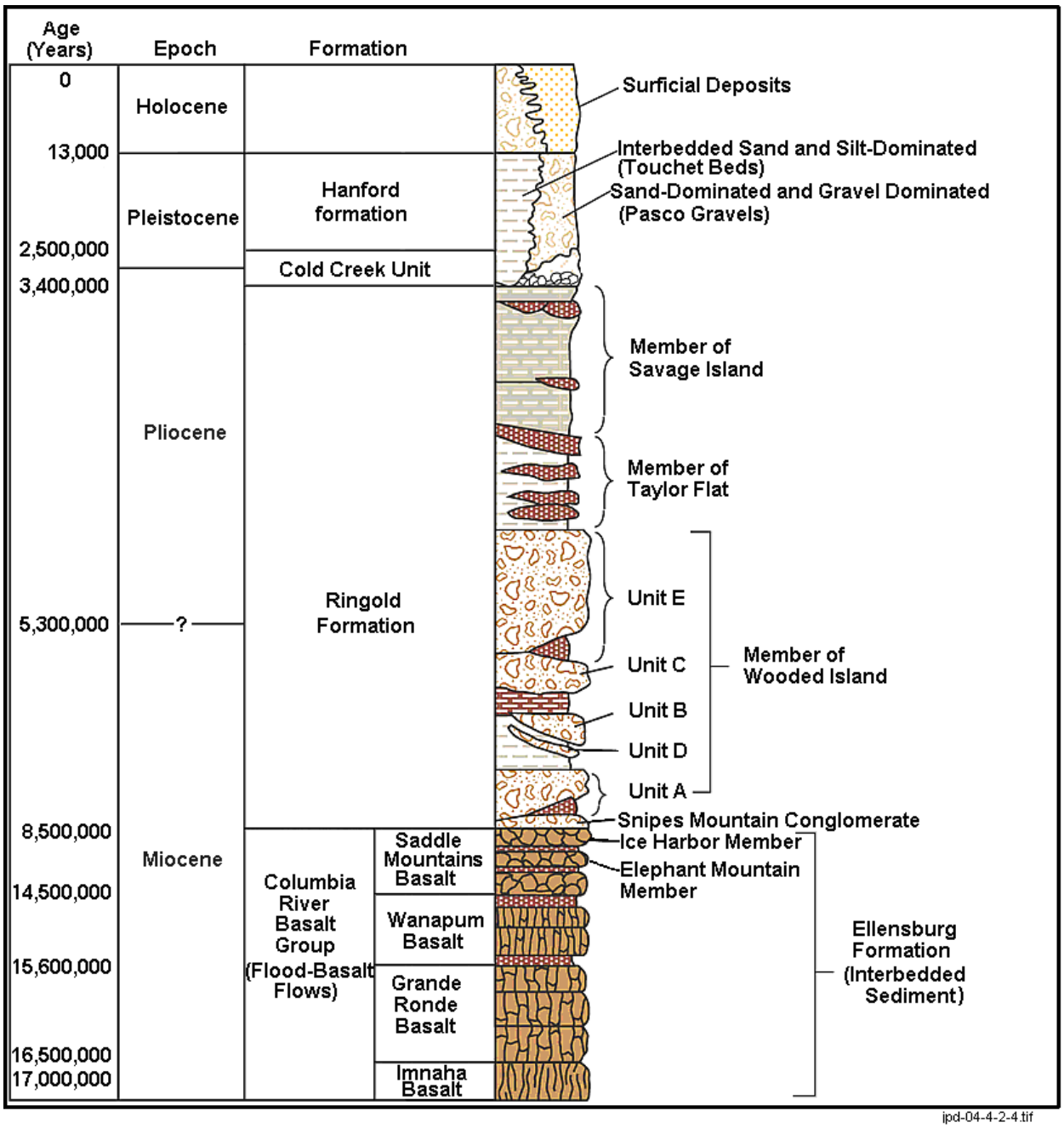

Sediment of the Ringold Formation represents evolutionary stages of the ancestral Columbia River as it was forced to change course across the Columbia Basin by the growth of the Yakima Fold Belt. Ringold Formation time began approximately 8.5 million years ago when the Columbia River abandoned Sunnyside Gap and began to flow across the Hanford Site, leaving the Pasco Basin through the present Yakima River water gap along the southwest end of the Rattlesnake Mountain anticline. The northern margin of the 8.5-million-year-old Ice Harbor basalt controls the Columbia River channel as it exits the Pasco Basin.

The first record of the Columbia River at Hanford is in the extensive gravel and interbedded sand of unit A, Ringold Formation member of Wooded Island (Figure 3-3). The Columbia River was a gravelly braid plain and widespread paleosol system that meandered across the Hanford Site (Fecht et al. 1987; Reidel and Tolan 2009; Reidel et al. 1994; BHI-00184, *Miocene- to Pliocene-Aged Suprabasalt Sediments of the Hanford Site*).

At about 6.7 million years ago, the Columbia River abandoned the Yakima River water gap along the southeast extension of Rattlesnake Mountain and began to exit the Pasco Basin through Wallula Gap (Figure 3-1). The main channel of the Columbia River in the Pasco Basin was still through Hanford and the 200 Areas. At this time, the Columbia River sediments changed to a sandy alluvial system with extensive lacustrine and overbank deposits (Fecht et al. 1987; Reidel and Tolan 2009; Reidel et al. 1994; BHI-00184). A widespread lacustrine-overbank deposit called the lower mud was deposited over some of the Hanford Site at this time and is a nearly continuous feature under the 200 West Area and much of the 200 East Area. The lower mud was then covered by another extensive sequence of fluvial gravels and sands. The most extensive of these is called unit E, Ringold Formation member of Wooded Island, but locally other sequences are recognized (e.g., units C and D). Unit E is one of the most extensive Ringold Formation gravels and appears to be mostly continuous under the 200 Areas. To the north near the 100 Areas, Ringold Formation sediments reflect mostly overbank deposition of fine-grained sediments during this time.

The Columbia River sediments became more sand-dominated about 5 million years ago when over 90 m (295 ft) of interbedded fluvial sand and overbank deposits accumulated at Hanford. These deposits are collectively called the Ringold Formation member of Taylor Flat (BHI-00184). The fluvial sands of the member of Taylor Flat dominate the lower cliffs of the White Bluffs.

Between 4.8 million years ago to the end of Ringold time at 3.4 million years ago, lacustrine deposits dominated Ringold Formation deposition. A series of three successive lakes is recognized along the White Bluffs and elsewhere along the margin of the Pasco Basin (BHI-00184). The lakes probably resulted from damming of the Columbia River farther downstream, possibly near the Columbia Gorge. The lacustrine and related deposits in the Pasco Basin are collectively called the Ringold Formation member of Savage Island.

At the end of Ringold time, western North America underwent regional uplift, resulting in a change in base level for the Columbia River system. Uplift caused a change from sediment deposition to regional incision and sediment removal. Regional incision is especially apparent in the Pasco Basin, where nearly 100 m (328 ft) of Ringold Formation sediment has been removed from the Hanford Area. The regional incision marks the beginning of Cold Creek time and the end of major deposition by the Columbia River.

Regional incision and erosion during Cold Creek time are most apparent in the surface elevation change of the Ringold Formation across the Hanford Site. As incision of the Columbia progressed eastward across Hanford, less erosion occurred on the surface of the Ringold Formation in the 200 West Area, leaving it at a higher elevation than in the 200 East Area. The surface of the Ringold Formation in the 200 West Area is consequently also older than that in the

200 East Area and thus was exposed to weathering processes for a much longer time. Less erosion of the 200 West Area surface accounts for the isolated remnants of the fluvial sands of the Ringold Formation member of Taylor Flat. At the north side of the 200 East Area, the ancestral Columbia River was able to cut completely through the Ringold Formation to the top of the basalt. The channel can be traced from Gable Gap across the eastern part of the 200 East Area and to the southeast. The greatest amount of incision is near the current river channel.

In the Pasco Basin, the Cold Creek unit (CCU) records most of the geologic events between the incision by the Columbia River and the next major event, the Missoula floods. The older Ringold surface at the 200 West Area was exposed to weathering, resulting in the formation of a soil horizon on its surface. Because the climate was becoming arid, the resulting soil became a pedogenically altered, carbonate-rich, cemented paleosol. The development of this carbonate-rich paleosol is much greater in the 200 West Area than in the 200 East Area due to longer exposure of the surface. This ancient paleosol is referred to as the lower Cold Creek unit (CCU_l) subunit.

Concurrently, eolian sediments and minor fine-grained flood deposits from streams originating from the nearby ridges were deposited on the paleosol, resulting in a wide variety of sediments that are called the upper subunit of the Cold Creek unit (CCU_u). Because of the long time interval (approximately 3.4 to 2 million years ago), several localized paleosols similar to the lower CCU were able to develop in the upper CCU. Throughout Cold Creek time, streams from the Rattlesnake, Yakima, and Umtanum Ridges were carving channels to the Cold Creek drainage area, depositing basaltic gravels in their stream beds. These form the sidestream alluvial facies of the CCU.

During Cold Creek time in the central Pasco Basin, the Columbia River flowed through Gable Gap, depositing gravels of mixed lithologies in a sand matrix. These gravels, informally called the “pre-Missoula gravels” (*Skagit/Hanford Nuclear Project, Preliminary Safety Analysis Report*, Vol. 1 [PSPL 1981]), overlie the Ringold Formation and are up to 25 m (82 ft) thick. The 200 East Area lies along the boundary between these two geologic environments, undergoing significantly more erosion than 200 West Area but with some soil development occurring in areas. There may have been other periods of fluvial deposition near the 200 East Area that reworked the existing Ringold gravels. The difficulty and uncertainty in distinguishing between these similar units is reflected in the differing choices for geologic contacts and their differing descriptions between reports.

During the Pleistocene Epoch, cataclysmic floods inundated the Pasco Basin several times when ice dams failed in northern Washington (“Quaternary Geology of the Columbia Plateau” [Baker et al. 1991]). Current interpretations suggest as many as 40 flooding events or more occurred as ice dams holding back glacial Lake Missoula repeatedly formed and broke. In addition to larger major flood episodes, there were probably numerous smaller individual flood events. Deciphering the history of cataclysmic flooding in the Pasco Basin is complicated, not only because of floods from multiple sources but also because the paths of Missoula floodwaters migrated and changed course with the advance and retreat of the Cordilleran Ice Sheet.

Along with sedimentological evidence for cataclysmic flooding in the Pasco Basin, high-water marks and faint strandlines occur along the basin margins. Temporary lakes were created when flood waters were hydraulically dammed, resulting in the formation of the short-lived Lake Lewis behind Wallula Gap. High-water mark elevations for Lake Lewis, inferred from ice-rafted erratics on ridges, range from 370 to 385 m (1,214 to 1,261 ft) above sea level.

The sediment deposited by the cataclysmic flood waters has been informally called the Hanford formation because the best exposures and most complete deposits are found on the Hanford Site. The coarse-grained flood facies (gravel-dominated facies of DOE/RL-2002-39, *Standardized Stratigraphic Nomenclature for Post-Ringold-Formation Sediments Within the Central Pasco Basin*) is generally confined to relatively narrow tracts within or near flood channelways. The plane-laminated sand facies (sand-dominated facies of DOE/RL-2002-39), on the other hand, occurs as a broad sheet over most of the central basin. Paleocurrent indicators within beds of plane-laminated sands are unidirectional, generally toward the south and east within the Pasco Basin.

Rhythmite facies (interbedded silt and sand-dominated facies of DOE/RL-2002-39) occur in slackwater areas around the margins of the basin and were deposited by multidirectional currents, including upvalley currents. Individual rhythmites become finer and thinner both laterally and vertically upward.

Recent studies using the magnetic polarity of the Hanford formation sediments have shown that the earliest floods may have occurred as long ago as 2 million years. Four magnetic polarity reversals have been found in sediments from core holes in the 200 East Area ("Magnetostratiphic Evidence from the Cold Creek Bar for Onset of Ice-Age Cataclysmic Floods in Eastern Washington During the Early Pleistocene" [Pluhar et al. 2006]). These polarity reversals have paleosols at the top of each reversed sequence of sediments. The oldest sediments occur in the ancestral Columbia River channels where the pre-Missoula sediments occur. The age of the Hanford formation in the 200 West Area is more difficult to determine because only normal-polarity sediments occur there.

Since the end of the Pleistocene, the main geologic process has been wind. After the last Missoula flood drained from the Pasco Basin, winds moved the loose, unconsolidated material until vegetation was able to stabilize it. Stabilized sand dunes cover much of the Pasco Basin, but there are areas, such as along the Hanford Reach National Monument, where sand dunes remain active.

3.3 GEOLOGIC FRAMEWORK OF THE HANFORD SITE

As discussed in Section 1, the events occurring throughout the Pacific Northwest and Columbia Basin are reflected in the sedimentary record in the Pasco Basin and consequently the Hanford Site. This section provides a description of the large geologic framework for the Hanford Site.

3.4 STRUCTURAL GEOLOGY

The Cold Creek syncline (Figure 3-4) lies between the Umtanum Ridge-Gable Mountain uplift and the Yakima Ridge uplift and is an asymmetric and relatively flat-bottomed structure. The Cold Creek syncline began developing during the eruption of the CRBG and has continued to subside since that time. The 200 Areas lie on the northern flank, and the bedrock dips gently (approximately 5°) to the south. The 300 Area lies at the eastern end of the Cold Creek syncline where it merges with the Pasco syncline. The deepest parts of the Cold Creek syncline, the Wye Barricade depression and the Cold Creek depression, are approximately 12 km (7.5 mi) southeast of the 200 Areas and southwest of the 200 West Area, respectively (Figure 3-4).

Figure 3-4. Geologic and Geomorphic Map of the 200 Areas and Vicinity.

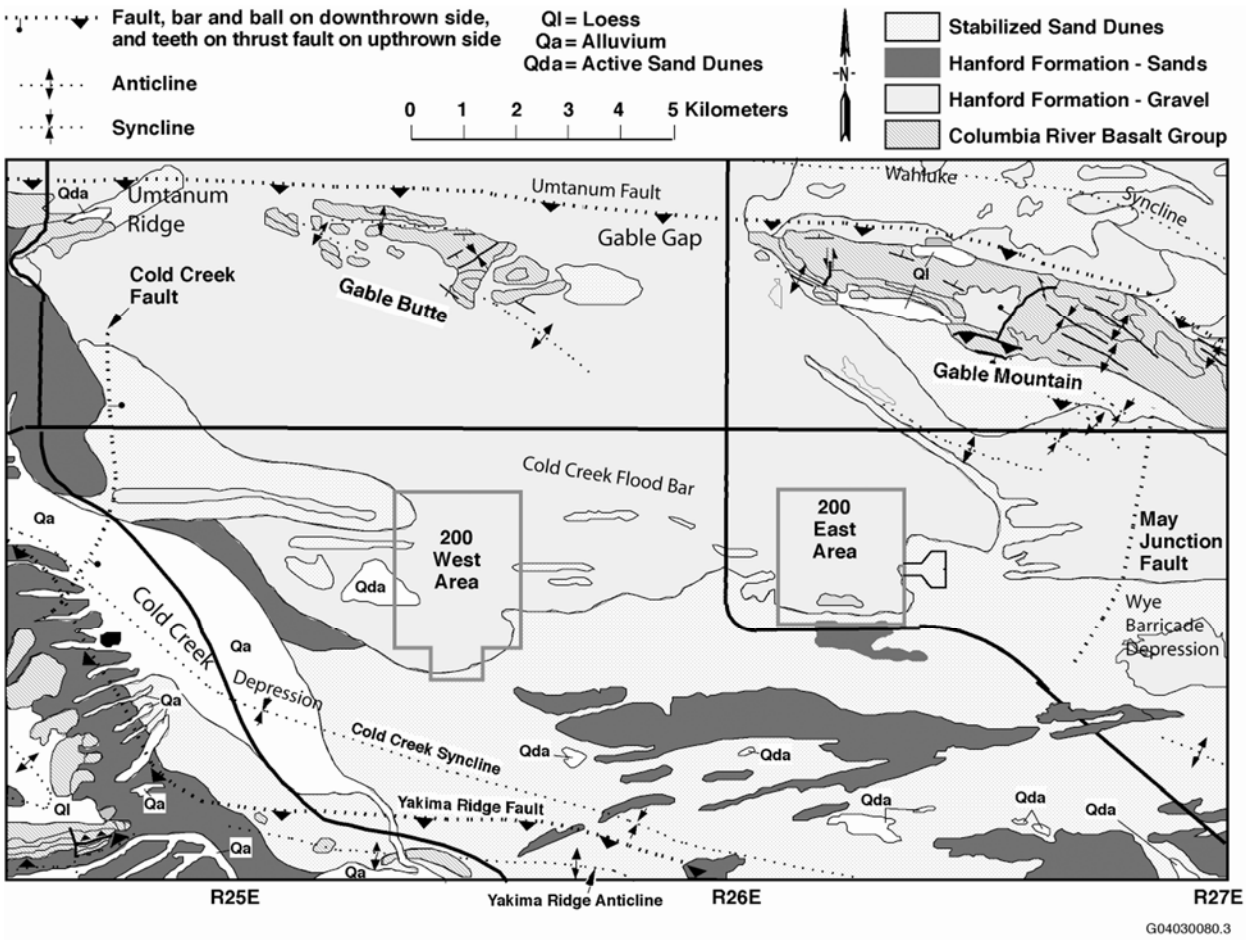

The Wahluke syncline north of Gable Mountain is the principal structural unit that contains the 100 Areas. The Wahluke syncline is an asymmetric and relatively flat-bottomed structure similar to the Cold Creek syncline. The northern limb dips gently (approximately 5°) to the south. The steepest limb is adjacent to the Umtanum Ridge-Gable Mountain structure.

The Umtanum Ridge-Gable Butte-Gable Mountain structural trend (Figure 3-4) is a segmented anticlinal ridge extending for a length of 110 km in an east-west direction and passes north of the

200 and 300 Areas and south of the 100 Areas. The Southeast anticline and Gable Mountain-Gable Butte is the easternmost portion of this ridge.

The Yakima Ridge uplift extends from west of Yakima, Washington, to the center of the Pasco Basin, where it forms the southern boundary of the Cold Creek syncline south of the 200 West Area (Figure 3-4). The easternmost surface expression of the Yakima Ridge uplift is represented by an anticline that plunges eastward into the Pasco Basin (RHO-BWI-ST-4, *Geologic Studies of the Columbia Plateau – A Status Report: October 1979*). The eastern extension of Yakima Ridge is mostly buried beneath late Cenozoic sediments and has much less structural relief than the rest of Yakima Ridge.

The 200 East Area sits on the eastern part of the Cold Creek bar, which is along the northern flank of the Cold Creek syncline (Figure 3-4). Another deep structural low, the Wye Barricade depression, developed along the Cold Creek syncline southeast of the 200 East Area. The May Junction fault is a normal fault that marks the western boundary of the depression.

The 200 East Area sits at the southern end of a series of secondary doubly plunging anticlines and synclines that are associated with the Umtanum Ridge-Gable Mountain anticlinal structure. Waste Management Areas A, AX, B-BX-BY, and C in the 200 East Area lie near the southern flank of the closest secondary anticline. A fault was recently detected during drilling of seismic test boreholes at the Waste Treatment Plant. The fault caused some displacement in the Pomona Basalt that lies beneath the Elephant Mountain Member but is not thought to have caused any displacement in younger basalts or overlying sediments (PNNL-16407, *Geology of the Waste Treatment Plant Seismic Boreholes*).

3.5 STRATIGRAPHY OF THE HANFORD SITE

The generalized stratigraphy of the Pasco Basin and Hanford Site is shown in Figure 3-3. The principal rocks exposed at the surface of the surrounding ridges are the CRBG and intercalated sedimentary rocks of the Ellensburg Formation. In the low-lying basins and valleys, these are overlain by younger sedimentary rocks of the Ringold Formation, CCU, and the Pleistocene cataclysmic flood deposits of the Hanford formation.

3.5.1 Columbia River Basalt Group and Ellensburg Formation

The Elephant Mountain Member is the uppermost basalt flow beneath the 200 Areas and much of the Hanford Site. Where folds and faults have formed basalt ridges, other flows from the Saddle Mountains, Wanapum, and Grande Ronde Formations are exposed.

The Ellensburg Formation is intercalated with and overlies the CRBG in the Pasco Basin and includes epiclastic and volcaniclastic sedimentary rocks ("Stratigraphic and Lithologic Variations in the Columbia River Basalt" [Waters 1961]; USGS Bulletin 1457-G). At the Hanford Site, the Ellensburg Formation consists of sediments deposited by the ancestral Clearwater (now the course followed by the Snake River) and Columbia Rivers. Relatively few boreholes in the 200 Areas penetrate the Ellensburg Formation. Those boreholes that do

penetrate the Ellensburg Formation generally find tuffaceous siltstones and sandstones, with conglomerates marking ancient main river channels. The Ellensburg stratigraphy of the Hanford Site has been discussed in more detail in Fecht et al. (1987).

3.5.2 Post-Columbia River Basalt Group Sediments

The Hanford Site and tank farms are situated on a sequence of Ringold Formation, CCU, and Hanford formation sediments overlying the CRBG. The upper Miocene to middle Pliocene record of the Columbia River system in the Columbia Basin is represented by the upper Ellensburg and Ringold Formations. Except for local deposits (e.g., the CCU), there is a hiatus (erosion or lack of sedimentation) in the stratigraphic record between the end of the Ringold Formation deposition (3.4 Ma) and the beginning of Pleistocene (1.6 Ma) time (DOE/RW-0164, *Consultation Draft Site Characterization Plan. Reference Repository Location, Hanford Site, Washington*; DOE/RL-2002-39).

Pleistocene to recent sediments overlying the CRBG at the Hanford Site include cataclysmic flood gravels and slackwater sediments of the Hanford formation; terrace gravels of the Columbia, Snake, and Yakima Rivers; and eolian deposits.

3.6 GEOLOGY OF THE CENTRAL PLATEAU

The Central Plateau encompasses the 200 East Area, 200 West Area, and the area between. Because of the need to understand the geologic controls on movement of contaminants in the vadose zone and groundwater, the Central Plateau has become one of the best characterized areas on the Hanford Site. The geology of the Hanford Site has largely been determined using samples from numerous boreholes.

Figure 3-5, a fence diagram of the Central Plateau area, depicts the geology above the CRBG. By necessity, Figure 3-5 is highly generalized, depicting the overall consistency of stratigraphy between the 200 East Area and 200 West Area. The major differences are in the thicknesses of the units in response to the geologic history. For example, the Hanford formation thickens to the east as the Ringold Formation thins. This variation is a response to the downcutting by the Columbia River after Ringold Formation time and then further erosion and filling of the erosional channels by Missoula Flood deposits.

3.6.1 Basalt

The uppermost basalt flow beneath the Central Plateau is the Elephant Mountain Member (RHO-BWI-ST-14, *Subsurface Geology of the Cold Creek Syncline*, Chapter 3 – Wanapum and Saddle Mountains Basalts of the Cold Creek Syncline Area). The top of basalt surface dips to the southwest beneath the 200 West Area and to the south-southwest beneath the 200 East Area. Low-amplitude secondary folds such as the one to the northeast of the 200 East Area may occur throughout the area and have probably not been fully identified. Between the 200 East Area and Gable Gap to the north, the Elephant Mountain has been eroded to expose underlying basalt

flows. There is also a suspected window eroded through the Elephant Mountain near the northeast corner of the 200 East Area.

Figure 3-5. Fence Diagram of Sediment Overlying the Columbia River Basalt Group in the Central Plateau, Hanford Site.

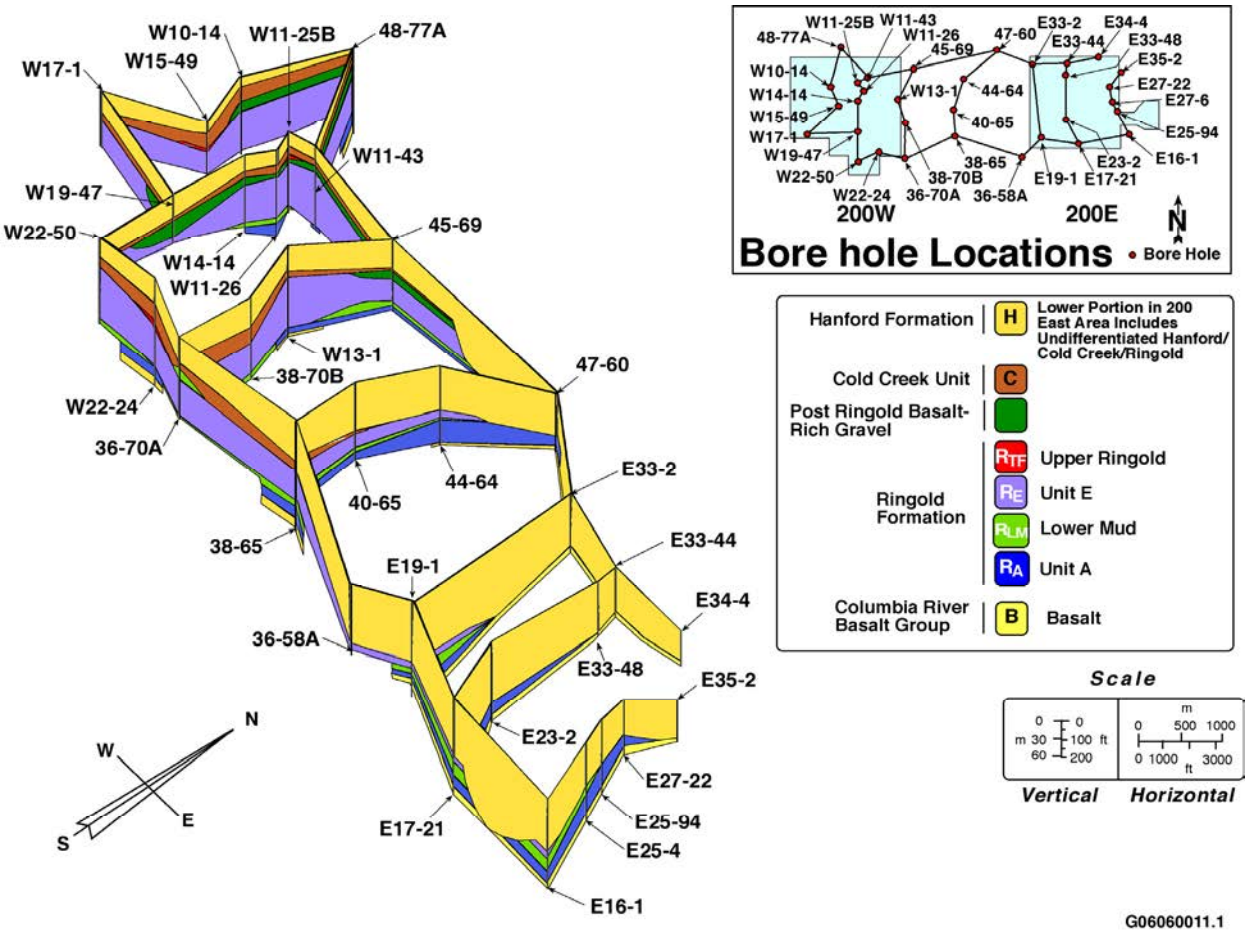

3.6.2 Ringold Formation

The Ringold Formation at the Hanford Site is up to 185 m (607 ft) thick in the deepest part of the Cold Creek syncline south of the 200 West Area and 170 m (55 ft) thick in the western Wahluke syncline near the 100 B Area. The Ringold Formation pinches out against the Gable Mountain, Yakima Ridge, Saddle Mountains, and Rattlesnake Mountain anticlines. It is largely absent in the northern and northeastern parts of the 200 East Area. It consists of semi-indurated clay, silt, pedogenically altered sediment, fine- to coarse-grained sand, and granule to cobble gravel. Ringold Formation strata typically are below the water table on the Hanford Site, and the textural variations influence groundwater flow.

Studies of the Ringold Formation in the Pasco Basin indicate it contains significant stratigraphic variations (WHC-SD-EN-EE-004, *Revised Stratigraphy for the Ringold Formation, Hanford Site, South-Central Washington*, BHI-00184) that are best described on the basis of sediment

facies. Sediment facies in the Ringold Formation are defined on the basis of lithology, stratification, and pedogenic alteration.

In the Pasco Basin, the lower half of the Ringold Formation, the member of Wooded Island, is the main unconfined aquifer under the Hanford Site and contains five separate stratigraphic intervals dominated by the fluvial gravel facies. These gravels, designated units A, B, C, D, and E (Figure 3-5), are separated by intervals containing deposits typical of the overbank and lacustrine facies (WHC-SD-EN-EE-004). In the 200 Areas, only fluvial gravel units A and E occur. Between these two gravel units in many places is the lowermost of the fine-grained sequences, designated the lower mud sequence. Fluvial gravel units A and E correspond to the lower basal and middle Ringold Formation units, respectively, as defined by DOE/RW-0164. Gravel units B, C, and D do not correlate to any previously defined units (WHC-SD-EN-EE-004, BHI-00184) and do not occur beneath the tank farms.

The following discussion of the geology of the Central Plateau is based on interpretations of new and old wells for this report as well as geologic contact depths from PNNL-12261, *Revised Hydrogeology for the Suprabasalt Aquifer System, 200-East Area and Vicinity, Hanford Site, Washington*; PNNL-13858, *Revised Hydrogeology for the Suprabasalt Aquifer System, 200-West Area and Vicinity, Hanford, Washington*; and PNL-8971, *Three-Dimensional Conceptual Model for the Hanford Site Unconfined Aquifer System, FY 1993 Status Report*. Specific lithologic descriptions and unit distributions are discussed in more detail for each tank farm in Section 4.

Ringold unit A occurs throughout much of the Central Plateau and ranges from 0 to over 30 m (0 to 100 ft) thick. This unit is thickest to the north and south of the 200 West Area. Beneath the 200 West Area, the top of this gravel unit dips to the southwest into the Cold Creek depression, while beneath the 200 East Area, the unit dips to the south into the Cold Creek syncline except in the northern part where it has been eroded. Generally, unit A is a conglomerate with clasts of basalt and other lithologies in a silty sand matrix intercalated with beds of sand and silt. The sediments may be strongly cemented with silica or calcite in places.

The Ringold Formation lower mud unit has had a more complex history in the 200 Areas. The lower mud has been eroded from beneath most of the 200 East Area. There is also a poorly defined channel cut through the lower mud unit in the northeastern corner of the 200 West Area. The lower mud unit ranges in thickness from 0 to 30 m (0 to 103 ft). Thickness of the lower mud increases in the Cold Creek depression, representing subsidence during deposition of the fine-grained sediments. The lower mud is thinnest beneath the 200 East Area and increases to the south. There is a broad zone of decreased thickness that runs southeast from the 200 West Area and may trace an old river channel from early in Ringold Formation unit E time. This unit consists primarily of lacustrine silt and clay, with at least one well-developed paleosol noted in the 200 West Area. It is an aquitard, separating the suprabasalt confined aquifer in unit A from the unconfined aquifer in unit E.

Unit E of the member of Wooded Island is by far the thickest of the Ringold Formation units present in the Central Plateau. It consists of well-rounded gravel in a sand and silt matrix deposited by major rivers. Gravel lithologies are varied with sources outside the Columbia Basin. Cementation varies from well- to poorly-indurated. Unit E ranges from 0 to over 90 m

(0 to 300 ft) in thickness. This variation in thickness is due in part to continued subsidence of the Cold Creek syncline and in part to erosion during the CCU and Hanford formation times. Increasing thicknesses to the west of the 200 West Area and to the south of the 200 East Area are a combination of both processes. Main channels during both Cold Creek and Hanford floods went through Gable Gap and across the northeastern part of the 200 East Area, removing unit E from most of that area and leaving a complicated surface in the 200 East Area.

In the Pasco Basin, the upper part of the Ringold Formation includes members of Taylor Flat and Savage Island (BHI-00184). The member of Taylor Flat consists of a sequence of fluvial sands and overbank deposits while the member of Savage Island consists of lacustrine sediments. The member of Savage Island is found only along the White Bluffs in the eastern Pasco Basin and corresponds to the upper Ringold Formation unit as originally defined by "Ringold Formation of Pleistocene Age in Type Locality, the White Bluffs, Washington" (Newcomb 1958). In the 200 West Area, erosional remnants of the member of Taylor Flat consists of fine-grained fluvial sand and overbank facies with localized stringers of calcium carbonate. Member of Taylor Flat sediments are found beneath parts of the T, TX, and TY tank farms and in the vicinity of the U tank farm and are discussed in more detail in Section 4.

3.6.3 Pliocene to Pleistocene Transition

Two main alluvial units of the Pliocene to Pleistocene transition are recognized at the Hanford Site—the CCU and the pre-Missoula gravels. Recently, the pre-Missoula gravels have been tentatively incorporated into the CCU (DOE/RL-2002-39); both are discussed together here.

The laterally discontinuous CCU overlies the tilted and truncated Ringold Formation in an unconformable relationship in the western Cold Creek syncline in the vicinity of the 200 West Area (DOE/RL-2002-39). To the east, the pre-Missoula gravels replace the calcrete and silt-dominated subunits of the CCU. The CCU appears to be correlative to other sidestream alluvial, eolian, and pedogenic deposits found near the base of the ridges bounding the Pasco Basin on the north, west, and south. These sedimentary deposits are inferred to have a late Pliocene to early Pleistocene age on the basis of stratigraphic position and magnetic polarity of interfingering loess units (DOE/RW-0164). At a coarse scale, the surfaces of the Ringold Formation and the CCU in the 200 West Area dip to the south. This surface also dips to the east between the 200 West and 200 East Areas. Local trends of the CCU are discussed in more detail for each of the tank farms in Section 4.

3.6.3.1 Pre-Missoula Gravels – Central Pasco Basin. The pre-Missoula gravels disconformably overlie the Ringold Formation in much of the central basin and may extend into areas in or near the 200 East Area. The nature of the contact between the pre-Missoula gravels and the overlying Hanford formation is not clear. In addition, it is unclear whether the pre-Missoula gravels overlie or interfinger with the CCU. In this appendix, we include the pre-Missoula gravels in the CCU because they overlie the Ringold Formation and underlie the Hanford formation. The gravel lying on basalt beneath much of the northern half of the 200 East Area has been variously interpreted as Ringold Formation unit A, as gravels deposited during Cold Creek time, or as part of the cataclysmic Hanford flood deposits that include some

reworked Ringold. The difficulty in distinguishing between these units is reflected in the cross sections for the 200 East waste management areas.

3.6.3.2 Cold Creek Unit – 200 East Area. The CCU as described above is largely absent from the 200 East Area. The exact origin of the sedimentary deposits overlying the CRBG and underlying the Hanford formation is uncertain and still open to interpretation. These deposits beneath the Hanford formation have been called the Hf/CCU (undifferentiated Hanford/Cold Creek) (HNF-5507, *Subsurface Conditions Description of the B-BX-BY Waste Management Area*) and undifferentiated Hanford formation/CCU/Ringold Formation unit (Hf/CCU/RF) (RPP-8531, *Vadose Zone Geology of Boreholes 299-W10-27 and 299-W11-39 T-TX-TY Waste Management Area Hanford Site, South-Central Washington*). In this report, they are placed in the CCU or lower Hanford gravel/CCU undifferentiated because they represent sediments deposited between the late Pliocene and early Pleistocene Epochs. This is the age range of the CCU in the 200 West Area. By assigning these deposits to this unit, only the age is implied, not the origin of the deposits.

HNF-5507 recognized two facies of the Hf/CCU beneath the 200 East Area tank farms: a fine-grained eolian/overbank silt (silt facies CCU), up to 10 m thick, and a sandy gravel to gravelly sand facies CCU. The thick, silt-rich interval is believed to be a pre-Pleistocene fluvial flood deposit because silty layers associated with Ice Age flood deposits of the Hanford formation in this area are generally much thinner (i.e., a few centimeters or less) (HNF-5507). Where the silt unit is absent, the gravel sequence below the silt unit is indistinguishable from similar-appearing facies of the overlying Hanford formation (HNF-5507). If the thick silt layer predates the Hanford formation, however, then the underlying gravels also must predate the Hanford formation. Thus, the gravel sequence beneath the silt layer must belong to either a mainstream alluvial facies of the ancestral Columbia River (pre-Missoula gravels) or the Ringold Formation.

3.6.4 Quaternary Stratigraphy of the Pasco Basin

Quaternary sediments, as much as 100 m thick within the Pasco Basin, overlie the Ringold Formation and/or CCU at the tank farms. The most extensive of these is the Pleistocene-aged Hanford formation (Figure 3-3), but the sediments also include eolian deposits and recent alluvium.

Eolian Deposits. Loess deposits at the Hanford Site contain a detailed Quaternary record; five units are represented within the Pasco Basin (WHC-MR-0391, *Field Trip Guide to the Hanford Site*). These units are informally referred to as L1 through L5 and differentiated on the basis of 1) position relative to other stratigraphic units, 2) color, 3) soil development, and 4) paleomagnetic polarity.

Hanford Formation. The Hanford formation is the main stratigraphic unit at the surface of the tank farms. The Hanford formation consists of pebble to boulder gravel, fine- to coarse-grained sand, and silt. These deposits are divided into three facies: 1) gravel-dominated, 2) sand-dominated, and 3) sand- and silt-dominated. These facies are referred to as coarse-grained deposits, plane-laminated sand facies, and rhythmite facies, respectively, in DOE/RW-0164. The rhythmites also are referred to as the Touchet Beds. The Hanford

formation is thickest beneath the Cold Creek bar, particularly in the vicinity of the 200 East Area, where it is over 100 m thick.

The gravel-dominated facies association generally consists of coarse-grained basaltic sand and granule to boulder gravel. These deposits display massive bedding, plane to low-angle bedding, and large-scale planar cross-bedding in outcrop. The gravel facies dominates the Hanford formation in the 100 Areas north of Gable Mountain, the northern part of the 200 East and West Areas, and the eastern part of the Hanford Site including the 300 Area. The gravel-dominated facies was deposited by high-energy flood waters in or immediately adjacent to the main cataclysmic flood channelways.

The sand-dominated facies association consists of fine- to coarse-grained sand and granule gravel displaying plane lamination and bedding and, less commonly, plane bedding and channel-fill sequences in outcrop. These sands may contain small pebbles and rip-up clasts in addition to pebble-gravel interbeds and silty interbeds less than 1 m thick. The silt content of these sands is variable. These sands typically are basaltic, commonly being referred to as black, gray, or salt-and-pepper sands. This facies is most common in the central Cold Creek syncline, in the central to southern parts of the 200 East and 200 West Areas. The laminated sand facies was deposited adjacent to main flood channelways during the waning stages of flooding. The facies is transitional between the gravel-dominated facies and the rhythmite facies.

The interbedded sand- and silt-dominated facies association consists of thinly bedded, plane-laminated and ripple cross-laminated silt and fine- to coarse-grained sand that commonly display normally graded rhythmites a few centimeters to several tens of centimeters thick (RHO-BWI-ST-4; DOE/RW-0164; DOE/RL-2002-39). This facies is found throughout the central, southern, and western Cold Creek syncline within and south of the 200 East and 200 West Areas. These sediments were deposited under slackwater conditions and in back-flooded areas (DOE/RW-0164).

Cataclysmic floods inundated the Pasco Basin several times during the Pleistocene when ice dams failed in northern Washington and Idaho. Net erosion by these floods was minimal and probably associated with only the earliest floods; later floods only partially incised into older flood deposits before backfilling. Recent work on subdividing the Missoula flood deposits at the Hanford Site has shown that paleomagnetic polarity is a useful technique ("Paleomagnetic and Geochemical Applications to Tectonics and Quaternary Geology: Studies at Coso Volcanic Field, CA and the Channeled Scabland, WA" [Pluhar 2003]; Pluhar et al. 2006). In a detailed study at the 200 East Area, four magnetic polarity reversals were recognized. These reversals were equated to the Brunhes normal subchron (present to 780,000 years BP) and the Matuyama reversal subchron (780,000 to 1.76 Ma). The Matuyama reversal has a normal excursion at 1 Ma, which Pluhar attributed to the normally magnetized sediments between the upper and lower reversal. The age of the lowest reversal is constrained by the lower limit of 1.76 Ma of the Matuyama subchron.

In the 200 West Area, mainly normally polarized sediments were found with two possible reversed horizons. Pluhar et al. (2006) interpreted the Hanford formation at the 200 West Area

as being deposited during the Brunhes normal subchron (present to 780,000 years BP) and the two possible reversals as short magnetic excursions during the Brunhes subchron.

The results of the Pluhar et al. (2006) study suggest that the Hanford formation sediments at the 200 East Area are older than those in the 200 West Area. This further implies that the Hanford subdivisions—upper coarse-dominated (H1), sand-dominated (H2), and lower coarse-dominated (H3) (BHI-00184)—are not the same flooding event in both areas and, thus, cannot be correlated across the Cold Creek bar.

3.6.5 Clastic Dikes

Clastic dikes are vertical to subvertical sedimentary structures that cross-cut normal sedimentary layering and could locally affect the vertical and horizontal movement of water and contaminants. Clastic dikes are a common geologic feature of Pleistocene flood deposits of the Hanford formation, although they also have been found in the underlying Ringold Formation and in CRBG and intercalated sedimentary interbeds. Clastic dikes on the Hanford Site have been described in detail in BHI-01103, *Clastic Injection Dikes of the Pasco Basin and Vicinity: Geologic Atlas Series*.

Clastic dikes typically occur in swarms and as regularly shaped polygonal patterns, irregularly shaped polygonal patterns, pre-existing fissure fillings, and random occurrences. Regular polygonal networks resemble four- to eight-sided polygons. Dikes in irregularly shaped polygon networks generally are cross-cutting in both plane and cross section, resulting in extensive segmentation of the dikes.

Clastic dikes typically show a wide range in width, depth, length, and orientation. They are especially common within the sand- and silt-dominated facies of the Hanford formation (Figure 3-6). The vertical extent of clastic dikes has been observed to range from 30 cm to more than 55 m (~1 to 180 ft), while width ranges from about 1 mm to greater than 2 m (0.04 in. to more than 6.6 ft). Deep exposures of clastic dikes typically show that they have many twists and turns as they are followed deeper. Most do not penetrate through the Hanford formation but typically will turn horizontally into a layer where they end. This horizontal bend has been interpreted as a key to the initial formation of the dikes. These dikes are interpreted as de-watering phenomena and the bend from vertical to horizontal is the point where the original clastic dike formed (the horizontal bed) and then broke upward to the surface as the wet sediment de-watered.

An example of the scale and spacing of clastic dikes is shown in Figure 3-7. In this figure, mapped clastic dikes south of the 200 West Area are projected on the S-SX WMA in 200 West Area. In this area these clastic dikes occur in the slackwater Touche Beds and planar-laminar silts and sands.

The hydrologic properties of a 2-m wide clastic dike near the 200 West Area have been investigated in “Influence of Clastic Dikes on Vertical Migration of Contaminants at the Hanford Site” (Murray et al. 2007). They concluded that “the highly heterogeneous nature of the system led to complex behavior, with the relative flux rates in the matrix and clastic dike being highly

dependent on the recharge rates that were imposed on the system." Their study suggested that "the potential role of clastic dikes in vertical transport at the Hanford Site would depend on the leakage rate, and that areas of contaminant deposition formed at high flow rates might become isolated at low flow rates, and vice-versa."

Figure 3-6. Typical Clastic Dike in Touchet Beds of the Hanford Formation. Picture taken in the Walla Walla valley near Touchet, Washington.

3.6.1 Volcanic Ash Deposits

Volcanism in the Cascade Range has been active throughout the Pleistocene Epoch (approximately 2 million years to 10,000 years BP), and throughout the Holocene Epoch (10,000 years BP to present). The eruption history of the Holocene best characterizes the most likely types of activity in the next 100 years. Many volcanoes have been active in the last 10,000 years, including Mount Mazama (Crater Lake) and Mount Hood in Oregon, and Mount St. Helens, Mount Adams, Mount Baker, and Mount Rainier in Washington. The Quaternary

sediments recorded these eruptions in the form of ash deposits that are interlayered with the sediments.

Figure 3-7. Projection of a Hypothetical Network of Clastic Dikes onto Waste Management Area S-SX.

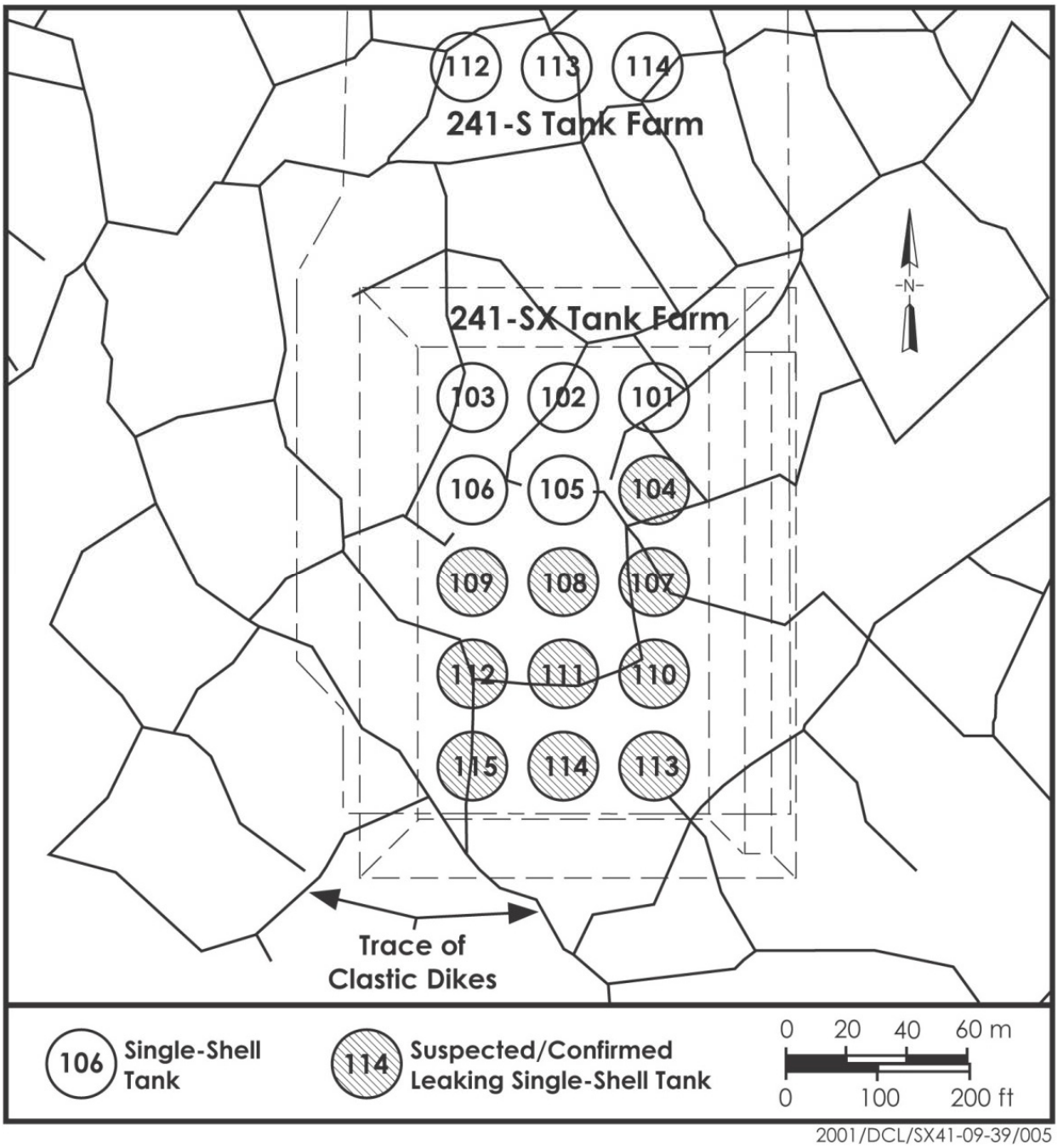

Reference: HNF-4936, *Subsurface Physical Conditions Description of the S-SX Waste Management Area*.

3.6.2 Surface Soil

BNWL-243, *Soil Survey Hanford Project in Benton County Washington* lists and describes 15 different soil types on the Hanford Site, varying from sand to silty and sandy loam. The 200 East Area consists of the Burbank Loamy Sand, the Ephrata Sandy Loam, and the Rupert Sand. The Rupert Sand has now been reclassified as the Quincy Sand [PNL-6415, *Hanford Site National Environmental Policy Act (NEPA) Characterization*]. The 200 West Area consists of the Quincy Sand and the Burbank Loamy Sand. The SST WMAs in the 200 East Area are developed in the Burbank Loamy Sand and the Ephrata Sandy Loam. The SST WMAs in the 200 West Area are developed mainly in the Quincy Sand.

The Burbank Loamy Sand is dark-colored, coarse-textured soil underlain by gravel. The surface soil is usually about 40 cm (16 in.) thick but can be 76 cm (30 in.) thick. The gravel content of the subsoil ranges from 20 to 80%. The surface of the Ephrata Sandy Loam is dark-colored, and the subsoil is dark grayish-brown, medium-textured soil underlain by gravelly material, which may continue for many feet. The Quincy Sand (formerly Rupert Sand) is brown to grayish-brown coarse sand grading to dark grayish-brown at about 90 cm (35 in.). Quincy Sand developed under grass, sagebrush, and hopsage in coarse sandy alluvial deposits that were mantled by windblown sand.

Soil horizons have been disturbed or removed over much of the surface within the 200 East and West Area boundaries. It can still be found in undisturbed areas within and between these areas.

3.6.3 Perched Water

Perched water has been encountered locally in the Central Plateau and the 200 Areas. The H1-H2 contact and the Cold Creek unit fine-grained (CCU_u) facies appear to have controlled perched water in localized areas across the 200 West Area, such as east of the T SST WMA, below the U trenches, and under the S-10 Pond. In the 200 East Area, perched water has been encountered at the top of the fine-grained facies of the CCU at the B/BY/BX SST WMA. East of the 200 East Area at B Pond, perched water was encountered on top of the Ringold Formation lower mud. At B Pond, the Ringold Formation has been removed above the lower mud so that the Hanford formation directly overlies it.

3.7 LOCAL GEOLOGY IN VICINITY OF WASTE MANAGEMENT AREA C

This section of the report describes the local geology of the Waste Management C area.

Data referred to in this section were obtained from published reports, unpublished data on surface geologic studies, and from borehole data. Some graphics are directly from various published reports, leading to a mixture of English and metric units. Where possible, both units are shown.

The information discussed in this document is derived from PNNL-15301, *RCRA Assessment Plan for Single-Shell Tank Waste Management Area T*; RPP-14430, *Subsurface Conditions*

Description of the C and A-AX Waste Management Areas; and more recent ground water monitoring reports. The data used here include historic and current water-table elevations; hydraulic properties including hydraulic conductivity, effective porosity, specific yield, and transmissivity; historic and current groundwater flow directions and flow rates as determined by measured hydraulic properties; and the concentrations and distributions of contaminants in the unconfined aquifer.

Unless otherwise specified, all groundwater chemistry data are from the Hanford Environmental Information System (HEIS) data base and are available from Flour Hanford, Inc. Most groundwater chemistry data collected since the mid-1980s were collected under strict regulatory requirements for the *Resource Conservation and Recovery Act of 1976* (RCRA) or *Comprehensive Environmental Response, Compensation, and Liability Act of 1980* (CERCLA). PNNL-13080, *Hanford Site Groundwater Monitoring: Setting, Sources, and Methods* describes the sampling methods, analytical methods, and quality control and data management practices used to collect and evaluate these data. Groundwater data collected before the mid-1980s are not as well documented and, in a general way, the older the data, the less is known about the data quality. Most of the information presented and discussed in this document is updated from previously published sources by including the latest analytical results from groundwater sampling. Table 3-1 lists the most used sources of groundwater hydrology and geochemistry information.

The detailed description of geologic and stratigraphic relationships are provided for the general area beneath WMA C and some adjoining areas of the 200 East Area, the A-AX tank farm area (Figure 3-8). The discussion of these relationships is based on a compilation of historical information (HW-61780, *Subsurface Geology of the Hanford Separation Areas*; ARH-LD-127, *Geology of the 241-A Tank Farm*; ARH-LD-128, *Geology of the 241-AX Tank Farm*; ARH-LD-132, *Geology of the 241-C Tank Farm*; RHO-ST-23, *Geology of the Separation Areas, Hanford Site, South-Central Washington*; WHC-SD-EN-TI-012, *Geologic Setting of the 200 East Area: An Update*; HNF-2603, *A Summary and Evaluation of Hanford Site Tank Farm Subsurface Contamination*; PNNL-12261) and some new interpretations allowed by new borehole emplacement and research conducted in calendar year 2003 (PNNL-14538, *Borehole Data Package for RCRA Wells 299-E25-93 and 299-E24-22 at Single-Shell Tank Waste Management Area A-AX, Hanford Site, Washington*; PNNL-14656, *Borehole Data Package for Four CY 2003 RCRA Wells 299-E27-4, 299-E27-21, 299-E27-22, and 299-E27-23 at Single-Shell Tank, Waste Management Area C, Hanford Site, Washington*). The most recent detailed description of the A, AX, and C tank farms is that in RPP-15808, *Subsurface Conditions Description of the U Waste Management Area*, and most of the discussion presented below is built on that report.

Table 3-1. Stratigraphic Terminology and Unit Thickness for the A-AX and C Tank Farms. (3 sheets)

Stratigraphic Symbol	Formation	Facies/ Subunit	Description	A-AX	C
				Thickness	Thickness
Backfill	NA	Backfill – Anthropogenic	Gravel-dominated consisting of poorly to moderately sorted cobbles, pebbles, and coarse to medium sand with some silt derived from coarse-grained Hanford formation (H1 unit) excavated around tanks (ARH-LD-127, ARH-LD-128, ARH-LD-132, RPP-14430); occasional layers of sand to silty sand occur near the base of the backfill sequence.	10 m	10 m
H1	Hanford formation	Unit H1 – (Gravel-dominated facies association). Cataclysmic flood deposits (high-energy)	Gravel-dominated flood sequence; composed of mostly poorly sorted, basaltic, sandy gravel to silty sandy gravel. Equivalent to the upper gravel sequence discussed in PNL-6820, the Q_{fg} documented in Open File Report 94-8, coarse-grained sequence (H1 unit) of RPP-14430 and gravel facies of unit H1 of RPP-8681, and gravel-dominated facies association of DOE/RL-2002-39.	20–30 m	10–30 m
H2	Hanford formation	Unit H2 – (Sand-dominated facies association). Cataclysmic flood deposits (moderate energy)	Sand-dominated flood sequence; composed of mostly horizontal to tabular cross-bedded sand to gravelly sand. Some sand beds capped with thin layers of silty sand to sandy silt. Equivalent to Fine-Grained Sequence (H2 unit) of RPP-14430 and unit H2 of RPP-8681, the sandy sequence of PNL-6820 and WHC-SD-EN-TI-012, to Q_{fs} documented in Open File Report 94-8, and sand-dominated facies association of DOE/RL-2002-39.	30–65 m	45–>70 m

Table 3-1. Stratigraphic Terminology and Unit Thickness for the A-AX and C Tank Farms. (3 sheets)

Stratigraphic Symbol	Formation	Facies/ Subunit	Description	A-AX	C
				Thickness	Thickness
H3	Hanford formation	Unit H3 – (Gravel-dominated facies association). Cataclysmic flood deposits (high-energy)	Gravel-dominated flood sequence; composed of open framework gravel and poorly sorted, basaltic, sandy gravel to silty sandy gravel. Equivalent to the lower coarse-grained unit of the Hanford formation of PNL-6820, to the lower gravel sequence of WHC-SD-EN-TI-012, and to the Hanford formation, H3 sequence of Lindsey et al. (1994).	0–20 m	Not specifically identified as a separate and distinguishable unit in the area of WMA C but may be present and indistinguishable with the lower gravel-dominated sequences belonging to the CCU and Ringold Formation Unit A sediments in the area of WMA C
CCU_u/R	Undifferentiated Cold Creek unit and Ringold Formation	Upper subunit	Silty sequence; locally thick layer of silt overlying the gravelly sediments of the lower subunit. Silt facies is light olive-brown to tan colored, massive, well-sorted, fine, calcareous silt to sand with pedogenetic traces (i.e., root casts).	0–6 m	Not specifically identified as a separate and distinguishable unit in the area of WMA C
CCU_l/R	Undifferentiated Cold Creek unit and Ringold Formation	Lower subunit	Lower gravel sequence equivalent to pre-Missoula gravels; sandy gravel to gravelly sand beneath the silt-dominated facies and above the top of basalt. Occurs as muddy, sandy gravel to sandy gravel. Moderate to uncemented with some caliche fragments. These sediments may be indistinguishable and may include sediments belonging to the lower H3 gravel-dominated facies associated with the Hanford formation in vicinity of WMA C.	0–>15 m	0 – 25 m
R_{wi}	Ringold	R_{wi} unit – Ancestral Columbia River System braided-stream deposits	Coarse-grained Ringold Formation sequence, consisting of mostly moderately sorted, quartzitic sandy gravel to silty sandy gravel. Equivalent to middle Ringold Formation unit (DOE/RW-0164) and the Ringold Formation unit E gravels (RPP-14430; RPP-8681).	Probably not present	Probably not present

Table 3-1. Stratigraphic Terminology and Unit Thickness for the A-AX and C Tank Farms. (3 sheets)

Stratigraphic Symbol	Formation	Facies/ Subunit	Description	A-AX	C
				Thickness	Thickness

CCU_u/R = upper Cold Creek unit/Ringold Formation.
CCU_l/R = lower Cold Creek unit/Ringold Formation.
H1 = Hanford formation, unit H1; equivalent to upper sand-dominated.
H2 = Hanford formation, unit H2; equivalent to middle sand-dominated.
H3 = Hanford formation, unit H3; equivalent to lower sand-dominated.
NA = not applicable.
Q_{fg} = Quaternary flood gravels.
Q_{fs} = Quaternary flood silt and sand.
R_{wi} = Ringold Formation, member of Wooded Island.

References:
ARH-LD-127, *Geology of the 241-A Tank Farm*
ARH-LD-128, *Geology of the 241-AX Tank Farm*
ARH-LD-132, *Geology of the 241-C Tank Farm*
DOE/RL-2002-39, *Standardized Stratigraphic Nomenclature for Post-Ringold-Formation Sediments Within the Central Pasco Basin*
DOE/RW-0164, *Consultation Draft Site Characterization Plan. Reference Repository Location, Hanford Site, Washington*
Lindsey et al. 1994, "Geohydrologic Setting of the Hanford Site, South-Central Washington"
Open File Report 94-8, *Geologic Map of the Richland 1:100,000 Quadrangle, Washington*
PNL-6820, *Hydrogeology of the 200 Areas Low-Level Burial Grounds – An Interim Report*, Volumes 1 and 2
RPP-8681, *Vadose Zone Geology of Boreholes 299-E33-45 and 299-E33-46 B-BX-BY Waste Management Area Hanford Site, South-Central Washington*
RPP-14430, *Subsurface Conditions Description of the C and A-AX Waste Management Area*
WHC-SD-EN-TI-012, *Geologic Setting of the 200 East Area: An Update*

Figure 3-8. Fence Diagram of the A, AX and C Tank Farms.

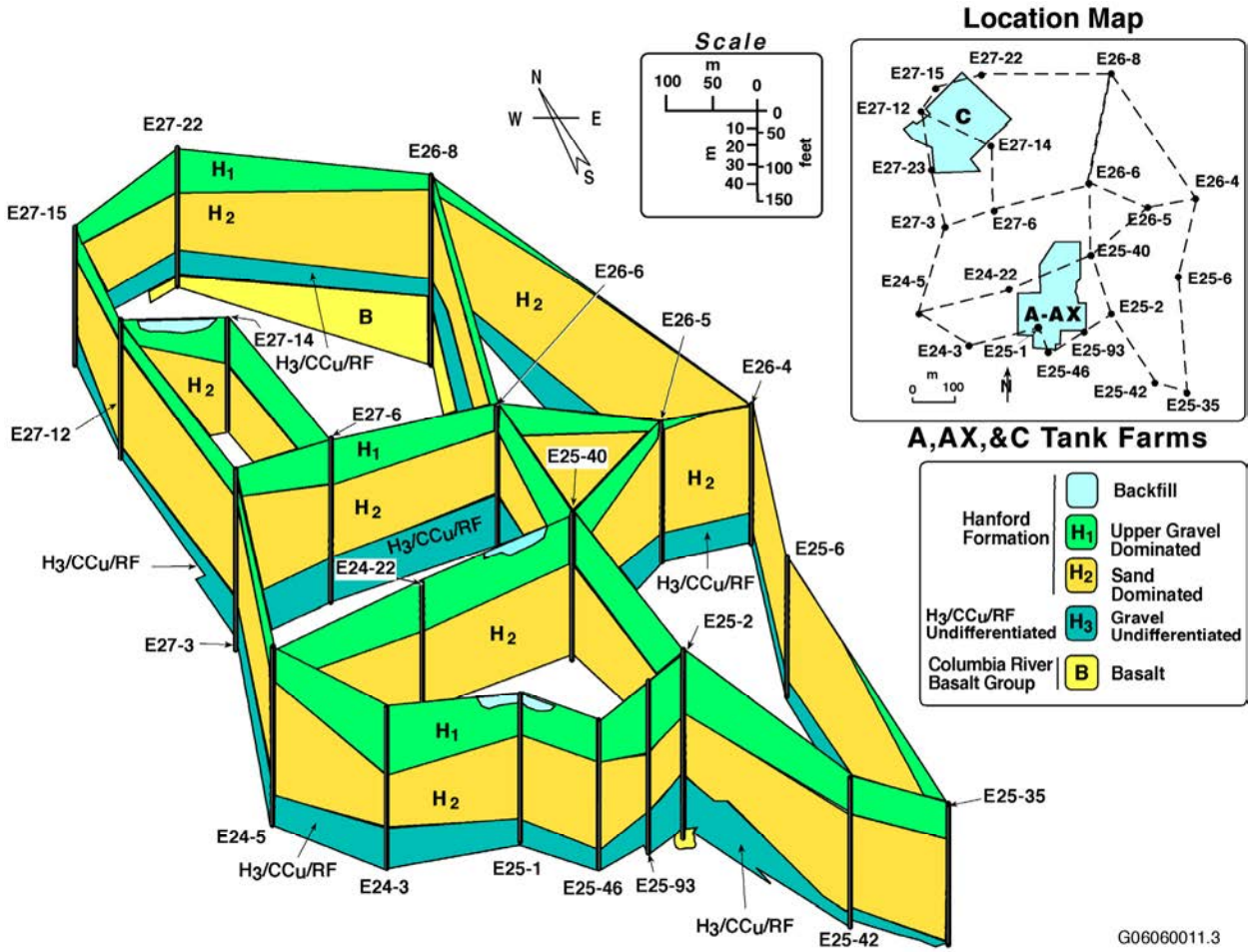

Numerous wells have been drilled over the years in the vicinity of these SSTs. Table 3-2 provides geologic contacts for those wells used in the following geologic discussion and cross sections. For some wells, several interpretations of stratigraphic contacts or "picks" have been rendered by various authors over the years. Most of the illustrations presented here reflect picks represented by RPP-15808 with some modification arising from new well logs. This current list of hydrostratigraphic picks are now modified to be consistent with those provided in RPP-RPT-56356, Rev. 1 *Development of Alternative Geologic Models of Waste Management Area C.*

The A, AX, and C tank farms were built in Hanford formation sediments. Based on RPP-15808, seven stratigraphic units lie beneath WMAs A-AX and C. From oldest to youngest, the primary geologic units are:

- CRBG

- A lower gravel-dominated sequence that has been locally interpreted as including either:
  - An undifferentiated combination of a CCU fine unit and/or Ringold Formation sediments (CCU/R)
  - An undifferentiated combination of Hanford formation gravel and/or CCU gravel and/or Ringold Formation, unit A sediments (H3/CCU/R), or
  - A lower gravel-dominated sequence belonging to the Hanford formation (H3 unit)

Table 3-2. Stratigraphic Contact Elevations for Boreholes in Waste Management Areas A-AX and C. (2 sheets)

Well No.	Ground Elevation in meters[a]	Contact Elevation in meters[a]						
		Top Backfill/ Eolian Sand	Top H1	Top H2	Top H3	Top CCU_u/R	Top CCU_l/R	Top of Basalt
E24-4[b]	213.03	213.03	204.2[c]	191.7	NP	NP	NP	—
E24-5	213.1	—	213.1	196.3	NP	NP	133.8	—
E24-13	210.6	—	210.6	174.0	NP	128.3	122.2	—
E24-20[b]	210.11	—	210.11	175	NP	126.3[d]	124.7	—
E25-1	211.5	—	202.1	185.6	NP	132.3	126.2	—
E25-2	206.3	—	202.1	169.8	143.9	128.6	125.6	98.1
E25-6	201.8	—	NP	201.8	143.9	121.0	119.5	—
E25-7	201.2	—	NP	201.2	143.3	NP	120.4	—
E25-35	205.7	—	205.7	184.4	141.7	126.5	123.4	—
E25-41	204.8	—	204.8	174.3	143.9	127.1	122.5	—
E25-42	209.1	—	209.1	182.9	140.2	NP	126.5	—
E25-46	212.8	—	212.8	184.4	129.5	126.5	—	—
E25-48	208.2	—	208.2	180.7	141.1	128.9	122.8	—
E25-93	207.3	—	203.9	170.7	132.6	NP	114.3	—
E26-4	197.8	—	197.8	193.5	157.0	129.5	126.5	—
E26-5	198.7	—	198.7	192.6	154.5	NP	128.6	—
E26-6[b]	199	199	194.2[c]	180.8	NP	125.0[d]	123.7	—
E26-8[b]	189.2	189.2	NP	186.2[c]	147.8	NP	NP	113
E27-3[b]	208.9	—	208.9	198.2	131.2	NP	—	102.5

Table 3-2. Stratigraphic Contact Elevations for Boreholes in Waste Management Areas A-AX and C. (2 sheets)

Well No.	Ground Elevation in meters[a]	Contact Elevation in meters[a]						
		Top Backfill/ Eolian Sand	Top H1	Top H2	Top H3	Top CCU_u/R	Top CCU_l/R	Top of Basalt
E27-4[b]	204.7	—	204.7	188.7	132.4	—	—	—
E27-6	205.7	—	205.4	175.3	128.0	126.2	102.4	—
E27-12[b]	201.5	—	201.5	190.9	131.4	—	—	—
E27-13[b]	204.1	—	204.1	191.9	131.6	—	—	—
E27-14[b]	200.8	—	200.8	173.6	128.6	—	—	—
E27-15[b]	199.2	199.2	196.1	180.9	129.1	—	—	—
E27-21[b]	205.0	—	205	186.4	121.8	—	—	—
E27-22[b]	192.6	—	192.6	169.1	122.2	—	—	110.9
E27-23[b]	205.7	—	205.7	197	131.4	—	—	—

[a] Multiply by 3.281 to convert meters to feet.

[b] Used in RPP-RPT-56356, Rev. 1, *Development of Alternative Geologic Models of Waste Management Area C* see Table 4-7.

[c] RPP-RPT-56356, Rev. 1, *Development of Alternative Geologic Models of Waste Management Area C* did not account for eolian sands and ground surface elevation was used for the top of the unit in that document.

[d] RPP-RPT-56356, Rev. 1, *Development of Alternative Geologic Models of Waste Management Area C* in the close vicinity of Waste Management Area Hanford H3 unit, Cold Creek Unit, and Ringold formation cannot be differentiated and used this value for the undifferentiated H3/CCu/RF.

References:
WMP-22817, *Geologic Contacts Database for the 200 Areas of the Hanford Site*.
RPP-14430, *Subsurface Conditions Description of the C and A-AX Waste Management Area*, Table 2-2.

NP = unit not present
CCU_u/R = undifferentiated Cold Creek unit/Ringold Formation fine-grained sediments.
CCU_l/R = undifferentiated Cold Creek unit/Ringold Formation coarse-grained sediments.
H1 = Hanford formation, unit H1; equivalent to upper gravel-dominated.
H2 = Hanford formation, unit H2; equivalent to sand-dominated.
H3 = Hanford formation, unit H3; equivalent to lower gravel-dominated.
R_{wia} = Ringold Formation, Member of Wooded Island, unit A.

- A sand-dominated sequence (H2 unit) belonging to the Hanford formation
- An upper gravel-dominated sequence (H1 unit) belonging to the Hanford formation
- Recent deposits.

The CCU is equivalent to the “Plio-Pleistocene Unit” that was previously used in RPP-15808.

3.7.1 Columbia River Basalt Group

The Elephant Mountain Member is the uppermost basalt flow beneath the A, AX, and C tank farms. It lies at an elevation of approximately 100 m (328 ft) above mean sea level and dips gently to the southwest toward the axis of the Cold Creek syncline (ARH-LD-127, ARH-LD-128, ARH-LD-132, DOE/RW-0164). Up to 15 m (50 ft) of topographic relief exists on the basalt surface as a result of tectonic deformation and/or erosion.

3.7.2 Undifferentiated Lower Gravel-Dominated Sediments

Waste Management Areas A-AX and C lie along the edge of a paleochannel that eroded much or all of the Ringold Formation during CCU and/or Hanford time. Because of the difficulty in distinguishing reworked Ringold Formation gravels and pre-Missoula mainstream Columbia River gravels from original Ringold Formation gravels, these units are undifferentiated here (H3/CCU/R). A similar problem arises with fine-grained sediments overlying the basal gravels. In places, these fine-grained layers appear to correlate to Ringold Formation sediments, based in part on color, but in other areas appear to be more closely related to CCU or even Hanford formation sediments. Therefore, the lower fine-grained sediments are also undifferentiated here.

Gravelly facies immediately overlying basalt within most of the study area have been interpreted as belonging to an undifferentiated combination of H3/CCU/R gravel units. An exception is in the northeast of WMA C near borehole 299-E26-8, where the top of basalt has been interpreted as rising above the undifferentiated combination of CCU_l/R sediments, leaving the gravel-dominated Hanford formation sediments lying directly on top of basalt. The CCU_l/R sediments consist of predominantly sandy pebble- to cobble-sized gravel with occasional boulders. Mineralogically, the sand fraction consists of 15 to 60% basalt grains with generally less than 1 wt% calcium carbonate. The total thickness of this unit is less than 27 m (90 ft), based on a limited number of boreholes where the upper and lower boundaries are represented. The top of the undifferentiated combination of H3/CCU/R gravels ranges from about 120 to 130 m (390 to 425 ft) elevation above mean sea level.

The fine-grained unit, H3/CCU/R, is found in most boreholes beneath WMA A-AX but not beneath WMA C. It occurs at a depth of about 79 m (260 ft) and ranges in thickness from 0 to 7 m (0 to 21 ft). Descriptions of this unit vary significantly, which may be due to 1) subjective descriptions and/or interpretations by different drillers and geologists; 2) heterogeneities within the unit, which may include multiple lithologic units (i.e., CCU silts overlying Ringold Formation mud); or 3) a combination of the above. Where present, this fine-grained unit is described in about half of the boreholes as a blue-, gray-, or olive-colored clay or mud; remaining borehole logs describe the unit as a tan to brown sandy silt to “heavy” silt, which may display a laminated to mottled structure. The former description fits that of Ringold Formation paleosol facies (DOE/RW-0164), whereas the latter fits descriptions for the Cold Creek silt facies (HNF-5507), interpreted as eolian-overbank in origin. Unlike most other fine-grained units in the 200 Areas, the undifferentiated Cold Creek silt and/or Ringold Formation mud unit is generally noncalcareous, containing only a few weight percent or less calcium carbonate.

Some gross gamma-ray logs show a moderate increase in activity occasionally accompanied by an increase in moisture. The water table was higher in the past; thus, the increased moisture content may be a remnant of a higher water table.

3.7.3 Hanford Formation Sediments

The Hanford formation makes up the majority of the suprabasalt sedimentary sequence beneath WMAs A-AX and C, ranging in thickness from 61 to 83 m (200 to 275 ft). The Hanford formation has been divided into three informal units (H1, H2, and H3 from top to bottom) in the 200 East Area. These units do not correspond to similarly named units in the 200 West Area.

The H3 unit is the Hanford formation's lower gravel-dominated sequence in the area and overlies undifferentiated Cold Creek/Ringold Formation deposits. This sequence is equivalent to the lower coarse-grained unit of the Hanford formation of PNL-6820, *Hydrogeology of the 200 Areas Low-Level Burial Grounds—An Interim Report*, to the lower gravel-dominated sequence of WHC-SD-EN-TI-012, and to the Hanford formation H3 sequence of "Geohydrologic Setting of the Hanford Site, South-Central Washington" (Lindsey et al. 1994).

The H3 unit consists of clast-supported, sandy, pebble to boulder gravel to matrix-supported pebbly sand. This unit appears in the east and southeast parts of the study area but appears to be missing from beneath most of WMA A-AX and all of WMA C. The unit is probably absent from these areas because of lateral facies changes that take place between gravel-dominated facies to the north and sand-dominated facies to the south away from the axis of primary flood channel that exists north and east of the study area. The surface of the H3 unit slopes to the south and west, with the highest elevations occurring in the northeast and east portions of the study area.

The H2 unit is continuous beneath WMAs A-AX and C. It overlies the undifferentiated CCU/R units or the H3 unit where present. The H2 unit is equivalent to the middle sand unit (PNL-6820), the fine sequence of WHC-SD-EN-TI-012, and the Hanford formation H2 sequence of Lindsey et al. (1994).

Dominantly a fine- to coarse-grained sand, the H2 unit also contains lenses of silty sand to slightly gravelly sand. Minor sandy gravel to gravelly sand beds occur sporadically. Consolidation ranges from loose to compact. Cementation is very minor or absent. Silt lenses and thinly interbedded zones of silt and sand are common but are not abundant in the H2 unit. These thin (<0.3 m [1 ft]) fine-grained zones generally cannot be correlated between boreholes and are not reflected in the gross gamma-ray logs or moisture data. Sampling intervals are probably too large to detect such thin zones. The fine structure observed in some older gross gamma-ray logs may reflect changes in the silt content that were not detected during drilling.

The upper portion of H2 may have been scoured by a southeast-trending Ice Age flood channel, associated in part with deposition of the overlying gravelly H1 unit. This is indicated by a south to southeast-trending trough present at the top of the H2 unit. Furthermore, over 40 m (130 ft) of relief exists on top of the H2 unit at right angles to the axis of this trough.

The H1 upper gravel sequence is equivalent to the upper coarse-grained unit of PNL-6820, the upper gravel sequence of WHC-SD-EN-TI-012, and the Hanford formation H1 sequence of Lindsey et al. (1994). This unit consists of predominantly loose, sandy gravel to gravelly sand, with minor beds of sand to silty sand. Coarser beds may contain boulder-sized materials. Occasional thin, discontinuous lenses of fine sand and silt may also be present.

The H1 unit thickens near the center of the study area and beneath WMA A-AX where it reaches approximately 30 m (100 ft) thick.

3.7.4 Clastic Dikes

No clastic dikes have been observed in WMA C. This is probably because sediment at WMA C is reworked Ringold sediment and course-grained sediment of the Hanford Formation. Clastic dikes have been observed, however, in the Waste Treatment Plant (WTP) excavations and in the Integrated Disposal Facility (IDF) excavation. In both localities, they occur within the sand- and silt-dominated facies of the Hanford formation (Figure 3-9) which are absent in the C WMA. The vertical extent of clastic dikes in those localities is limited. Excavations at the IDF show that clastic dikes extending from the surface make abrupt bends and become nearly horizontal (Figure 3-10).

3.7.5 Recent Deposits

Two types of recent deposits are present in WMAs A-AX and C: 1) eolian sand and silt and 2) backfill material. Backfill is found within the tank farms and other disturbed areas. Fine to medium sand to silty sand caps the sedimentary sequence outside the tank farms. These fine-grained eolian deposits are up to 6 m (20 ft) thick and contain up to 10 wt% calcium carbonate associated with recent soil development.

3.8 TECTONIC DEVELOPMENT OF THE HANFORD SITE

The geologic history of the Pacific Northwest from the Precambrian to the present and the resulting geologic structures that have developed at the Hanford Site significantly affect principally the seismic hazards of the Site (WHC-SD-W236A-TI-002, *Probabilistic Seismic Hazard Analysis, DOE Hanford Site, Washington*). This section summarizes the principal tectonic events in the development of the Hanford Site and their hazards.

The principal tectonic processes in the Hanford area have been north-south compression and subsidence. The present structure of the Columbia Basin and Hanford Site is the product of this compression that began in the early Tertiary prior to the eruption of the CRBG; that compression continues today. This pattern of deformation has produced the Yakima Fold Belt but this area overlies a large, mostly hidden Tertiary basin that began subsiding in the Eocene (approximately 55 Ma) and continues today.

Figure 3-9. Clastic Dikes in the Excavated Wall of the Integrated Disposal Facility. Arrows show the abrupt change from vertical to nearly horizontal.

Figure 3-10. Clastic Dikes to Right of Figure 3-9.

The rates of deformation (folding, faulting and subsidence) in the Columbia Basin and Hanford Site were greatest during the eruption of the basalt flows in the Miocene (17 Ma). The main form of tectonism has been subsidence of the basin with the Yakima Fold Belt superimposed on this subsidence. The rate of subsidence of the basin and rate of local folding and faulting of the anticlinal ridges have both declined since the Miocene. The present rate of ridge growth is estimated at 0.04 mm/yr and the rate of subsidence in the basin is estimated at 3×10^{-3} mm/yr. More recent work using deformation rates determined from the Global Positioning System ("Fault locking, block rotation and crustal deformation in the Pacific Northwest" [McCaffrey et al. 2007]) has determined similar rates of ridge deformation.

Microseismicity, high *in situ* stress conditions, and the geometry of Quaternary-Holocene faulting indicate that the basin is still experiencing N-S compression (Reidel et al. 1994). Although known late Cenozoic faults are found exclusively on the anticlinal ridges, earthquake focal mechanisms and strain measurements suggest that most stress release is occurring in the synclinal areas. The high *in situ* stress in the Cold Creek syncline can explain the microseismicity in the region but the absence of microseismicity associated with the anticlinal ridges may result from a component of aseismic or below detection limit seismic slip, or the fault zones may be locked up.

3.9 SEISMIC ACTIVITY AND EARTHQUAKES ON THE HANFORD SITE

Tectonic studies have concluded that earthquakes can occur in the following six different tectonic environments (earthquake sources) at the Hanford Site (WHC-SD-W236A-TI-002).

- **Major Geologic Structures**. Reverse/thrust faults in the CRBG associated with major anticlinal ridges such as Rattlesnake Mountain, Yakima Ridge, and Umtanum Ridge could produce some of the largest earthquakes (7.0 M_c).

- **Secondary faults**. These faults are typically smaller (1 to 20 km) than the main reverse/thrust faults that occur along the major anticlinal ridges (up to 100 km). Secondary faults can be segment boundaries (tear faults) and small faults of any orientation that formed along with the main structure.

- **Swarm areas (see Figure 3-11)**. Small geographic areas not known to contain any geologic structures produce clusters of events (swarms), usually in the CRBG in synclinal valleys. These clusters consist of a series of small shocks with no outstanding principal event. Swarms occur over a period of days or months and the events may number into the hundreds and then quit, only to start again at a later date. This differs from the sequence of foreshocks, mainshock, and trailing-off aftershocks that have the same epicenter or are associated with the same fault system. In the past, swarms were thought to occur only in the CRBG. Most swarm areas are in the basalt but swarm events also appear to occur in all. There are seven earthquake swarm areas that are recognized in the Hanford Seismic Network area but this list will be updated as new swarm areas develop. The Saddle Mountains swarm area, Wooded Island swarm area, Wahluke swarm area, Coyote Rapids swarm area, and Horse Heaven Hills swarm area are typically active at

one time or another during the year (Figure 3-11). The other earthquake swarm areas are active less frequently.

- **The entire Columbia Basin**. The entire basin, including the Hanford Site, could produce a "floating" earthquake. A floating earthquake is one that, for seismic design purposes, can happen anywhere in a tectonic province and is not associated with any known geologic structure. Seismic interpretation classifies it as a random event for purposes of seismic design and vibratory ground motion studies.

- **Basement source structures**. Studies (WHC-SD-W236A-TI-002) suggest that major earthquakes can originate in tectonic structures in the crystalline basement. Because little is known about geologic structures in the crystalline basement beneath the Hanford Site, earthquakes cannot be directly tied to a mapped fault. Earthquakes occurring in the crystalline basement without known sources are treated as random events.

- **The Cascadia Subduction Zone**. This source has been postulated to be capable of producing a magnitude 9 earthquake. Because this source is along the western boundary of Washington State and outside the Hanford Seismic Network, the Cascadia Subduction Zone is not an earthquake source that is monitored at the Hanford Site, so subduction zone earthquakes are not reported here. Because any earthquake along the Cascadia Subduction zone can have a significant impact on the Hanford Site or can be felt like the February 2001 Nisqually earthquake, UW monitors and reports on this earthquake source for the DOE. Ground motion from any moderate or larger Cascadia Subduction Zone earthquake is detected by Hanford seismic monitoring arrays and reported (see Section 5.0).

Since records have been kept, most of the earthquakes at the Hanford Site have originated in the CRBG layer. The crystalline basement has had the next greatest amount of earthquakes followed by the pre-basalt sediments.

Beginning in January 2009, the Pacific Northwest National Laboratory's seismic monitoring array began recording numerous small earthquakes in the Wooded Island earthquake swarm area (Figure 3-11) (PNNL-19071, *Annual Hanford Seismic Report for Fiscal Year 2009*). From January to June, over 1,600 earthquakes were recorded with over 250 events per month. July marked the decline in earthquake activity with only 10 to 15 events per month occurring until activity leveled out in September. The largest earthquake occurred on May 13, 2009 and had a coda Magnitude of 3.0. A few of the larger earthquakes were felt locally.

Most earthquakes were shallow and occurred in the CRBG. The estimated depths were between 1 km and 2.3 km. The U.S. Geological Survey reported that this swarm event resulted in uplift of the Earth's surface of 35 mm ["InSAR measurement of surface deformation at the Hanford Reservation associated with the 2009 Wooded Island earthquake swarm (Invited)" (Wicks et al. 2009)].

Figure 3-11. Earthquake Swarm Areas in the Vicinity of the Hanford Site.

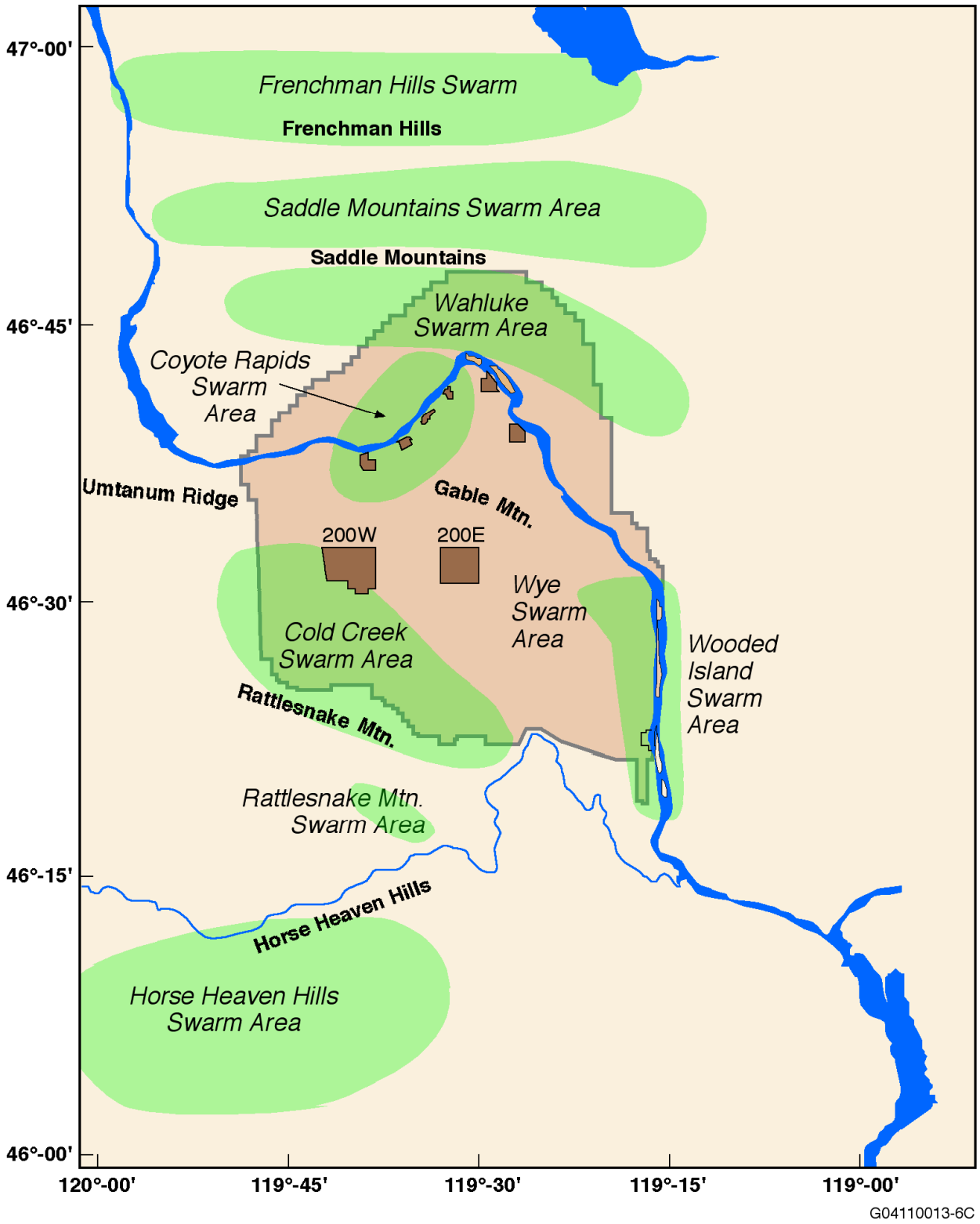

3.10 GEOLOGIC HAZARD ASSESSMENT

3.10.1 Volcanic Hazard Assessment

Two types of volcanic hazards have affected the Hanford Site in the past 20 million years:

- Continental flood basalt volcanism that produced the CRBG, which underlies the Hanford Site, outcropping in the surrounding ridges, which is no longer a hazard
- Volcanism associated with the Cascade Range, which still remains a hazard due to ash fall.

3.10.2 Seismic Hazard Assessment

A seismic hazard analysis was completed for the Hanford Site (WHC-SD-W236A-TI-002). Previous seismic hazard analyses were done for Washington Public Power Supply System WNP 1/4 and WNP/2, which also are located on the Hanford Site.

The following potential seismic sources were determined to be the major contributors to the seismic hazard in and around the Hanford Site.

- Crustal sources:
  - Fault sources related to the Yakima Folds
  - Shallow basalt sources that account for the observed seismicity within the CRBG and not associated with the Yakima Folds
  - Crystalline basement source region.
- Cascadia subduction zone earthquakes.

4.0 VADOSE ZONE SYSTEM AT WASTE MANAGEMENT AREA C

This section provides a detailed discussion of the vadose zone hydrology in vicinity of the WMA C Area. The foundation of the understanding the hydrogeologic system at WMA C is rooted in the geologic framework and history of the Hanford Site and the central Plateau presented in Chapter 3.

The vadose zone, the region between the ground surface and the water table, is host to the underground storage tanks and related facilities in WMA C and 1) contains the chemical and radionuclide contaminants which have leaked into subsurface from past leaks and unplanned releases from tanks and ancillary facilities and 2) will receive chemical and radiological contaminant that will be released out of wastes remaining in tanks and ancillary facilities in the future. Key features, processes, and events operating within the local-scale vadose zone system of the WMA C area play a key role in controlling contaminant migration from WMA facilities through the vadose zone to underlying groundwater.

The geology of the vadose zone underlying WMA C forms the media through which the contaminants move and provides the basis with which to interpret and extrapolate the physical and geochemical properties that control the migration and distribution of contaminants. Of particular interest are the interrelationships between the coarser- and finer-grained facies, and the degree of contrast in their physical and geochemical properties. While the exact distribution of these alternating units is not known, their contrast appears to have a strong influence on the distribution of leak and recharge waters and dissolved tank waste constituents.

Important factors (i.e., features and processes affecting moisture and contaminant transport) are presented in this section; in particular, the state of knowledge on vadose zone hydrology, field variables such as matric potential and moisture content for tank farm soils as well as vadose zone hydraulic properties. Also discussed is state-dependent anisotropy (also referred to as tension-dependent or moisture-dependent anisotropy) – an important field-scale process that enhances fluid flow and therefore contaminant migration in the lateral direction. The section concludes with a discussion of vadose zone flow and transport properties that would be appropriate to use in numerical modeling of local-scale flow and transport at the WMA C.

4.1 KEY FEATURES OF THE VADOSE ZONE

Key features have been identified as potentially important to consider in conceptual models of the vadose zone at WMA C and in the scope of the WMA C PA calculations and related sensitivity analyses. A list of potential key features were identified in the WMA C PA Working Session held on March 30 through April 1, 2010 that was focused on FEPs. The FEPs for the vadose zone were identified for two time periods: 1) the time extending from the operational period through the end of the retrieval, remediation, and correction action period and 2) future projected conditions.

The FEPs identified for past to present conditions and for projected future conditions are summarized in Tables A-1 through A-4 in Appendix A. The key general features that were

identified for the vadose zone for these time periods include the following general categories: 1) the geometry, physical, hydraulic, and transport properties of the major hydrogeologic units; 2) the occurrence of potential preferential pathways (i.e., river channels, sloping beds, clastic dikes, etc.); 3) the existence of potential made-made preferential pathways (i.e., unsealed dry wells, groundwater wells, and boreholes); 4) the general moisture conditions in the vadose zone; and 5) current soil and water chemistry and contamination in the vadose zone. They are discussed briefly in this section.

Properties of the Major Hydrogeologic Units: The SST and related facilities at WMA C were constructed in Hanford formation sediments. Based on recent work by RPP-14430 and PNNL-15955, *Geology Data Package for the Single-Shell Tank Waste Management Areas at the Hanford Site*, seven stratigraphic units, including the underlying CRBG, have been identified beneath WMAs A-AX and C. As indicated in Section 3.7, the primary hydrogeologic geologic units overlying the underlying basalt bedrock in the area of these two WMAs include the following units:

- A lower gravel-dominated sequence that has been locally interpreted as including either :
  - An undifferentiated combination of CCU fine unit and/or Ringold Formation (CCU/R)
  - An undifferentiated combination of Hanford formation gravel and/or CCU gravel and/or Ringold Formation, unit A (H3/CCU/R), or
  - A lower gravel-dominated sequence belonging to the Hanford formation (H3 unit)
- A sand-dominated sequence belonging to the Hanford Formation referred to as the H2 unit
- An upper gravel-dominated sequence belonging to the Hanford formation referred to as the H1 unit, and
- Recent deposits composed of eolian sands and silts and local backfill.

The CCU is equivalent to the “Plio-Pleistocene Unit” in RPP-14430. All interpretations of major units along lines of section in the general area of WMA C are shown in Figure B-1 of Appendix B and are provided in Figures B-2 through B-8. Three of the seven cross sections (Sections A-A’, D-D’, and G-G’ shown in Figures B-2, B-5, and B-8) illustrate the distribution and thicknesses of these units relevant to the vadose zone in the immediate vicinity of WMA C.

Descriptions of the general properties of these units relevant to the WMA C are provided in Section 3.7 and Appendix B. As mentioned in Section 3.7, interpretations in some of the boreholes and wells identify an undifferentiated gravel-dominated unit below the Hanford formation H2 sands that is considered to be made up of combinations of the lower Hanford formation H3 unit, the Cold Creek gravels and the sandy-gravels belonging to the Ringold Formation at some locations due to difficulties in distinguishing the characteristics of the

three underlying units. This indistinguishable unit is typically identified using the H3/CCU/RF or CCU/Rf designation. As indicated in Section 3.7, sediments specifically belonging to the Hanford formation H3 unit have not been identified as a separate and distinguishable unit in geologic logs from wells and/or boreholes at the WMA C.

Potential Natural Preferential Pathways: Previous work in SST WMAs and WMA C has identified a number of potential naturally-occurring preferential pathways for water flow and transport in the vadose zone. These have included the occurrence of broad stratigraphic features and heterogeneities such as river channel deposits, or changes in contrasting soil texture or cross-cutting vertical features such as clastic dikes, that could enhance moisture movement and/or contaminant transport. Some of these features are discussed in Section 3.7 and their potential effects are discussed briefly in Section 4.2.3.

Potential Man-Made Preferential Pathways: About 70 dry wells have been drilled at WMA C. The wells are not a direct contributor to vadose zone water contamination; rather they provide a potential preferential pathway for the rapid downward movement of any existing contamination through the vadose zone. The construction of almost all the wells at the SST farms is not in compliance with *Washington Administrative Code* (WAC) 173-160, "Minimum Standards for the Construction and Maintenance of Wells," which came into existence in 1973. Newly constructed wells (C4297) are constructed in accordance with WAC 173-160, which establishes minimum construction standards including sealing requirements to prevent water movement between aquifers.

These wells are much shallower than groundwater wells; the deepest vadose zone monitoring well is 143 ft below ground surface (bgs), while depth to groundwater varies from 233 ft to 280 ft bgs. A total of 10 groundwater monitoring wells also exist outside the fence of WMA C that could have offered the potential pathways in the past. As a part of the closure process, both the dry wells and groundwater monitoring will be properly sealed and decommissioned so that they do not present a preferential pathway in the future.

However, assuming that some waste is left in the ground after closure, an engineered surface barrier will likely be placed above the farm and all drywells within the tank farm are expected to be decommissioned. Assuming that some waste and contamination within the vadose zone is left in place, some post-closure monitoring will be required, but the form that such monitoring will take has yet to be determined. Whether groundwater monitoring wells will be decommissioned as part of closure is yet to be determined because decisions about any cover design including its aerial extent have not been reached. Some of the groundwater monitoring wells could be candidates for such monitoring. If groundwater monitoring wells are used for monitoring they will be properly sealed and decommissioned so that they do not present a preferential pathway in the future.

A discussion of these features as potential preferential pathways is discussed in 3.2.2.9 of RPP-RPT-44042, *Recharge and Waste Release within Engineered System in Waste Management Area C*.

Moisture Conditions: Direct characterization of moisture conditions has been limited to what can be inferred from neutron logging of dry wells as a part of tank farm monitoring and detailed collection of moisture content data in specific characterization boreholes. A summary of the limited characterization borehole data is presented in Section 4.3.

Current Contamination of the Vadose Zone: A summary of selected vadose characterization data that form the basis for the current understanding of the role of the vadose zone in the groundwater pathway at the WMA C is provided in Appendix C of this document. These characterization data and information include a review of selected historical information and data collected at three general locations within WMA C and data collected at the same general areas during Phase 1 characterization. This discussion also includes results of surface geophysical explorations and some recent spectral gamma logging of a groundwater monitoring well hydraulically upgradient of the WMA C.

These characterization data were presented during the WMA C PA Working Sessions related to the Assessment Context (September 1 through 3, 2009) and the Soil Inventory (October 27 through 29, 2009). More detailed discussions of this characterization data were included in Appendix B of RPP-RPT-41918, *Assessment Context for Performance Assessment for Waste in C Tank Farm Facilities after Closure*.

4.2 FACTORS AFFECTING MOISTURE MOVEMENT IN VADOSE ZONE

Figure 4-1 illustrates a vertical cross-section of an outcrop at the Hanford Site. As the figure suggests, the natural subsurface flow systems can be extremely variable. The heterogeneous nature is manifested in the spatial variability in physical and hydraulic properties of Hanford sediments (WHC-EP-0883, *Variability and Scaling of Hydraulic Properties of 200 Area Soils, Hanford Site*). Subsurface heterogeneity is therefore a rule rather than an exception. Of particular importance is the spatial variability in moisture retention and unsaturated hydraulic conductivity relationships within a geologic unit as well as among different units.

When soil is not saturated, soil moisture moves through interconnected pores that are filled with water and, to a lesser extent, as film flowing around particle surfaces in pores that also contain air. With increasing water content, more pores fill with water, and the rate of downward water movement increases. When considering water infiltration through the unsaturated zone, the total potential in the soil, ϕ, can be expressed mathematically as the sum of both pressure head, h, and an elevation head, Z, using the following expression:

$$\phi = h\,(\Theta_v) + Z$$

Where pressure head, h, is a function of the volumetric water content, Θ_v. Pressure head is expressed as a negative pressure due to the soil water attraction. Pressure head increases with increasing amounts of soil moisture.

Figure 4-1. A Cross-sectional View of Heterogeneous Sediments in 200 Areas.

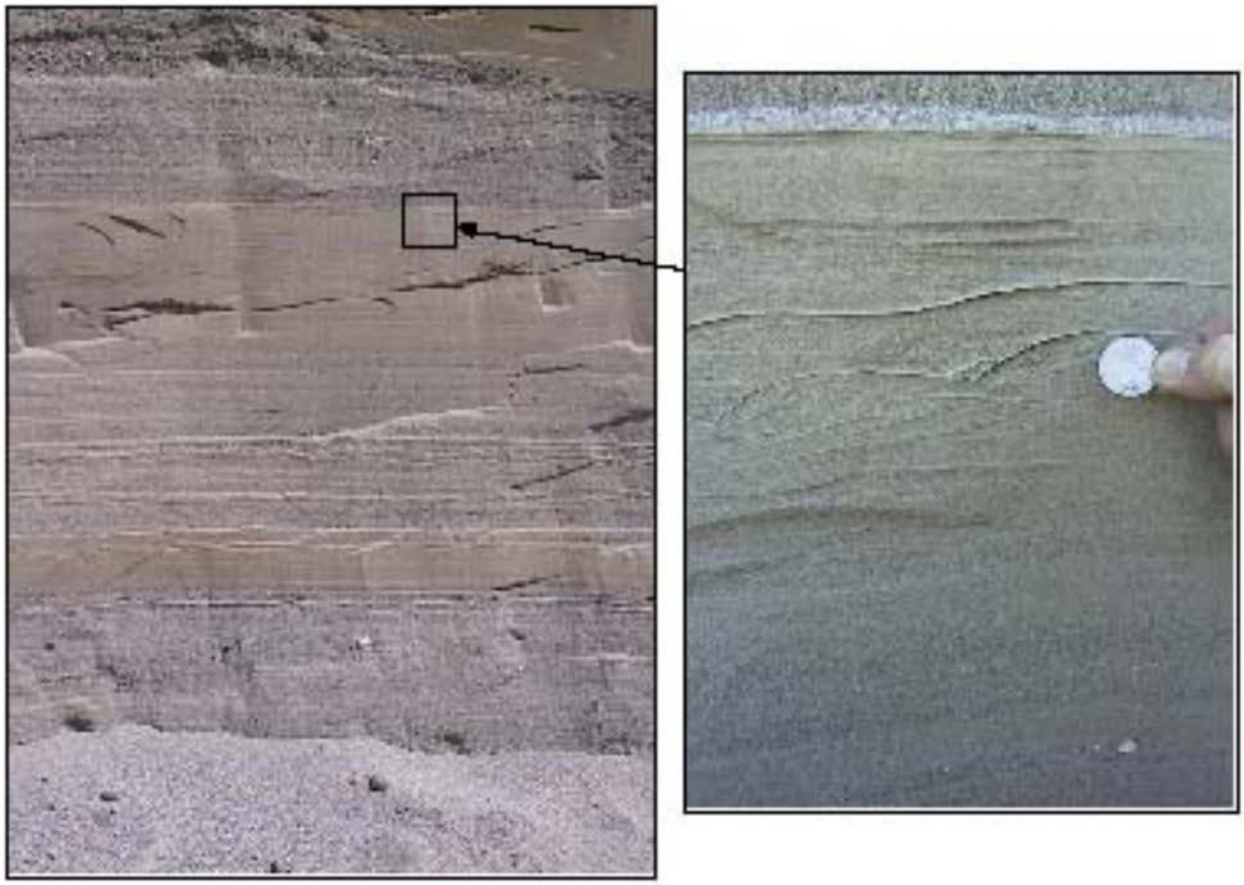

The graphical expression that is typically used to show the non-linear functional relationship between the pressure head, *h* (also referred to as matric potential, ψ), and the corresponding soil volumetric water content, Θ_v, is called the soil moisture retention curve.

Under unsaturated flow conditions, hydraulic conductivity for a particular soil is not a constant property as it would be under fully saturated conditions and is a function of volumetric water content. Unsaturated hydraulic conductivity, K, increases with increasing pressure head and water content. The relationship between unsaturated hydraulic conductivity, K and *h* or the corresponding Θ_v is also a nonlinear function.

4.2.1 Water Retention and Unsaturated Hydraulic Conductivity

Water retention (*h* versus Θ_v) and the relationships between unsaturated hydraulic conductivity and moisture content (K versus Θ_v) are determined experimentally. As expected, different types of media have different moisture retention characteristics. However, a fundamental porous medium characteristic that influences retention behavior is the sediment particle size distribution, and therefore the pore size distribution for a particular sample. As indicated in Figure 4-2, the moisture content of porous media decreases as the pressure head (or matric potential) becomes more negative. Generally speaking, the rate of reduction in Θ_v as the pressure head *h* becomes more negative depends on the soil pore size distribution. For instance, sandy sediments tend to

have a narrow pore-size distribution (i.e., a relatively large number of large pores and only a few small pores). Therefore, sandy materials tend to have a rapid reduction in Θ_v as h becomes more negative. In contrast, fine-textured materials such as silty sediments have a widespread pore-size distribution and the reduction in moisture content is therefore much gentler (see Figure 4-2).

Figure 4-2. Typical Moisture Retention (volumetric moisture content, Θ_v, versus decreasing pressure head, *h*) Curves for a Fine-textured (e.g., silt) and a Coarse-textured (e.g., coarse sand) Sediment; (the curves represent fit through the experimental data).

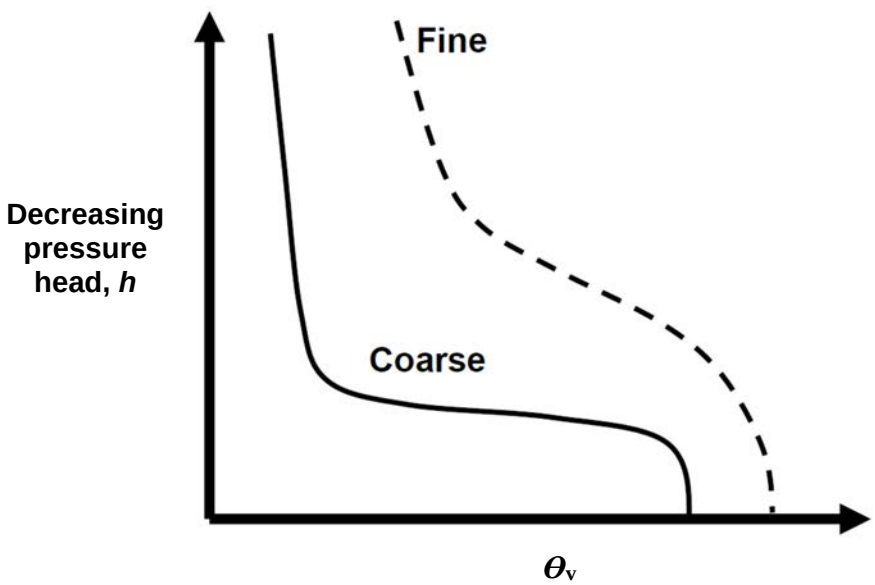

Figure 4-3. Typical Unsaturated Hydraulic Conductivity, K(*h*) versus Pressure Head, *h* Relation for a Fine-textured (e.g., silt) and a Coarse-textured (e.g., coarse sand) Sediment; (the circles represent the experimental data).

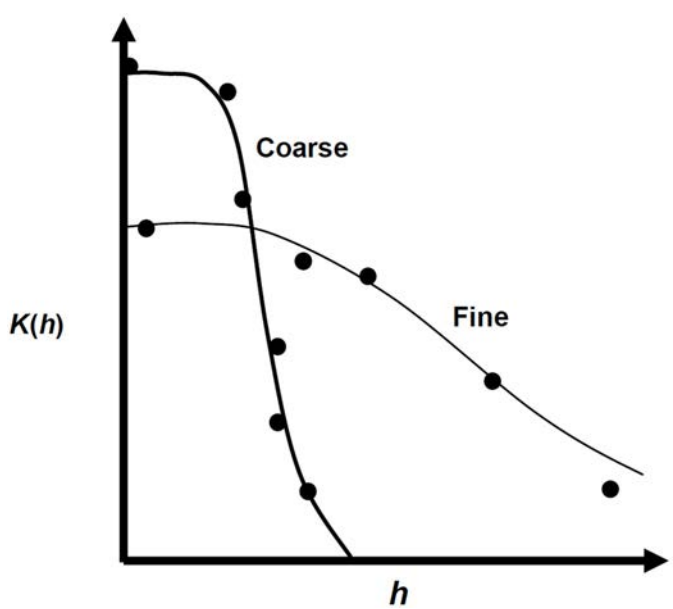

Figure 4-3 illustrates the relationship of unsaturated hydraulic conductivity and pressure head which go with the moisture retention curves for the fine-textured and coarse-textured sediments shown in Figure 4-2. For both fine- and coarse-textured media, the unsaturated hydraulic conductivity (K) decreases with a greater decrease in moisture content (Θ_v); the reduction in K with a reduction in Θ_v is highly nonlinear. The conductivity will asymptotically approach a limiting value after a threshold value of moisture content (i.e., residual water content) is reached. That is, media with moisture content less than the threshold value virtually cannot transmit any significant amount of remaining moisture, because of its being attached to solids or forming films that are isolated from each other.

A review of the functional relationships provided in Figures 4-2 and 4-3 indicates the potential impact and enhancement of hydraulic and contaminant transport characteristics of sediments in the vadose zone when a soil profile is wetted, as occurred from intentional and unintentional releases from tanks and pipelines at various tank farm areas during the historical period. The functional relationships also show the potential reduction of the hydraulic and contaminant transport characteristics of the vadose zone sediments with drying of the soil profile in response to emplacement of an engineered surface barrier in the future.

The functional relationships provided in Figures 4-2 and 4-3 are also generally obtained from measurements made as the soil samples are dried. If, at the end of the drying process, the laboratory measurements were continued by rewetting the soil sample, a new retention and unsaturated hydraulic conductivity would be obtained. This phenomenon is known as hysteresis and could be an important process to consider during the historical period when alternate wetting and drying of the soils occurred.

To illustrate the effects of media heterogeneity on unsaturated flow, consider the case where a fine-textured material overlies a coarse-textured material. Suppose the pressure heads (matric potentials) in the two materials are more negative than the cross-over pressure head h in their conductivity curves (Figure 4-3). In such a case, moisture in the fine-textured material will not be able to flow into the coarse material below because of its low conductivity (Figure 4-3). In other words, there exists a significant presence of air in the coarse-textured material below, and water from the fine-textured material cannot enter the coarse-textured material unless the pressure head is built up high enough (toward saturation) in the fine-textured material to expel the air in the underlying coarse-textured material. Such a behavior is counter-intuitive, given the fact that the saturated hydraulic conductivity for the coarse-textured material is larger than that of the fine-textured material. Nonetheless, during unsaturated flow conditions (i.e., beyond the cross-over point in Figure 4-3 toward more negative h), the unsaturated hydraulic conductivity for the underlying coarse-textured material is much smaller than that of the overlying fine-textured material. This phenomenon is called the capillary barrier effect, and it has been used as a fundamental principle in the design of earth liners for landfills, and “umbrellas” for waste storage facilities to prevent infiltrating moisture migrating below from the surface. As shown in Figure 4-3, up to the cross-over point, the fine-textured material is also a barrier to the flow from any overlying coarse-textured material. This situation also enhances lateral spreading of fluid and solute migration.

In field-scale problems (Sisson and Lu site, T-106 tank leak site) in 200 Areas, we see evidence of such natural capillary breaks during unsaturated flow wherever fine-textured layers are underlain by coarser sediments. The capillary breaks created due to textural discontinuities allow flow to occur laterally until the pressure head, h (or matric potential, ψ) in the fine layer is sufficient to overcome the entry pressure head of the underlying coarse layer.

4.2.2 Moisture Dependent Anisotropy

In addition to heterogeneity and textural discontinuities which are ubiquitous with Hanford sediments, an important characteristic is anisotropy (i.e., directional dependence of hydraulic conductivity). Anisotropy in unsaturated hydraulic conductivity and the consequent lateral migration have a strong impact on contaminant fate and transport within the vadose zone. In general, anisotropy in the hydraulic conductivity varies with the observation scale as well as the scale of heterogeneity within the observation scale. In the following paragraphs, we will examine the hydraulic conductivity anisotropy at two observation scales, namely, a pore-scale anisotropy and a field-scale anisotropy.

Pore-scale hydraulic conductivity anisotropy is of interest when we determine the macroscopic hydraulic conductivity over a certain volume of the soil (e.g., a soil core). Within the soil volume, one likely will find that depositional processes cause flat particles (minerals) to orient themselves with the longer dimension parallel to the plane on which they settle. This produces flow channels parallel to the bedding plane, which allow fluid flow with little resistance. Fluid flow in the direction perpendicular to the flat surface of particles, however, must detour and take more tortuous and longer paths than for flow parallel to the bedding plane. Therefore, under the same hydraulic gradient, more flow can occur through a soil core if the gradient is parallel to the bedding plane than if it is perpendicular to the bedding plane. The bulk hydraulic conductivity of the soil core in the direction parallel to the bedding (K_h) is thus greater than in the direction perpendicular to the bedding (K_v). The soil core thus possesses a pore-scale anisotropy in hydraulic conductivity.

In contrast to pore-scale anisotropy, field-scale anisotropy due to hydraulic conductivity arises from the fact that when we determine the hydraulic conductivity in a field situation, we often employ Darcy's law that assumes homogeneity of the medium over a relatively large flow domain. In essence, we seek to describe effective properties for the media in a large control volume (much larger than the core dimension) that likely includes numerous large-scale structural heterogeneities (such as stratification, cross-bedding, clay lenses, structural discontinuities, etc.). Such anisotropy effects are evident in the experimental work of "Quantifying the Effects of Small-Scale Heterogeneities on Flow and Transport in Undisturbed Cores from the Hanford Formation" (Pace et al. 2003), who found, at lower water contents, a greater conductivity for the Hanford sediment cores parallel to bedding than in sediment cores perpendicular to bedding.

To illustrate impacts of field-scale unsaturated hydraulic conductivity anisotropy on simulated moisture movement, let us assume that Figure 4-4a represents the observed plume due to infiltration into a relatively dry, stratified medium (e.g., Figure 4-1) having heterogeneous and anisotropic properties. In Figure 4-4b, the schematic "classical isotropy" indicates the expected,

simulated plume behavior for an equivalent homogeneous medium (EHM) (i.e., if we assume that the heterogeneous medium is replaced by a homogeneous medium) having isotropic properties ($K_h=K_v$). Note that a constant anisotropy implies that the unsaturated hydraulic conductivity (K) as a function of pressure head (or moisture content) maintains the identical ratio for K parallel to bedding to K perpendicular to bedding. This is illustrated in Figure 4-4d, where the K_h/K_v is constant regardless of variability in pressure head, h or saturation in a partially saturated medium. In case where the media is assumed to be isotropic ($K_h=K_v$), the moisture plume moves predominantly in the vertical than in the lateral direction (Figure 4-4b).

Figure 4-4. Schematics Illustrating Comparison of (a) an Observed Plume with Simulations using (b) an Isotropic, and (c) a Variable Moisture Dependent Anisotropy for Unsaturated Hydraulic Conductivity (K); (d) Constant and Variable Anisotropy; Kh is Horizontal Hydraulic Conductivity Parallel to Bedding and Kv is Vertical Hydraulic Conductivity Perpendicular to Bedding; ψ is Matric Potential or Pressure Head (*h*).

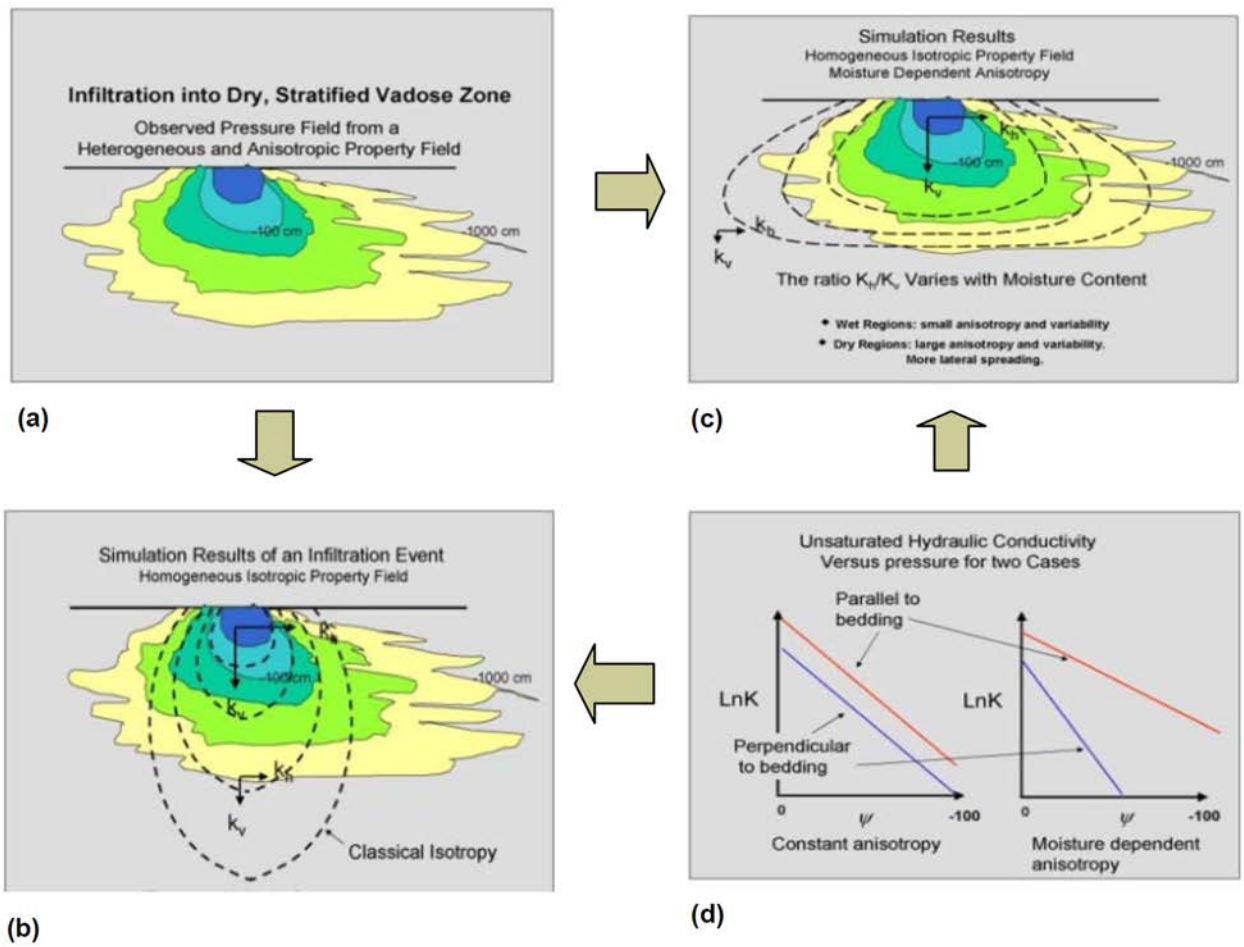

Image courtesy of Professor Jim Yeh, University of Arizona.

Compared to the observed plume, the vertical extent of the plume is clearly overestimated (Figure 4-4b). In case where a constant anisotropy (K_h/K_v=constant) in unsaturated hydraulic

conductivity is assumed (Figure 4-4d), the moisture plume travels more in the lateral than in the vertical direction. Illustrated in Figure 4-4c is the simulated moisture content distribution with a moisture-dependent anisotropy in unsaturated hydraulic conductivity. The moisture content distributions in both Figure 4-4a (observed plume) and Figure 4-4c (simulated plume) show significant lateral movement. The anisotropy in unsaturated hydraulic conductivity retards vertical movement of moisture but enhances lateral spreading (Figures 4-4a and 4-4c). With the moisture-dependent anisotropy, a greater lateral spreading is evident (Figure 4-4c) than in an isotropic profile (Figure 4-4b). As shown in Figure 4-4d, unlike constant anisotropy, for moisture-dependent anisotropy, K_h/K_v is a function of pressure head or moisture content. Also, as shown in Figure 4-4d, as the pressure head, h becomes more negative or as the medium gets drier, for moisture-dependent anisotropy, the K_h/K_v ratio becomes larger. The effects of moisture-dependent anisotropy on moisture plume dynamics are further illustrated for the plume resulting from field injection experiments at the Sisson and Lu site in 200 East Area.

4.2.3 Influence of Preferential Pathways

In addition to the conventional homogeneous approaches to modeling porous medium flow, preferential flow – a process whereby water and contaminants move along preferential pathways, which are not included in the homogeneous medium model – is of interest in analysis of moisture flow through vadose zone soils. Preferential pathways can be natural (e.g., clastic dikes) or manmade (e.g., unsealed monitoring wells). Although preferential flow has been recognized and widely studied under saturated or near saturated flow conditions ("Modeling Tritium and Chloride 36 Transport Through an Aggregated Oxisol" [Nkedi-Kizza et al. 1983], "Solute Transfer through Columns of Glass Beads" [De Smedt and Wierenga 1984]), there is little evidence of it in arid and semiarid climates or under low water fluxes, particularly where soils are coarse-grained such as those under the tank farms. Typically, under natural recharge conditions, meteoric precipitation at arid sites is usually too low to invoke preferential flow; much of the water in the dry soils is simply adsorbed onto the grain surfaces and cannot move along preferred pathways. The flux of natural infiltration from precipitation is generally low, but somewhat higher fluxes developed over the years from inadvertent application of water to wash down contaminants found in surface soils to deeper soils following releases, the use of water to excavate soils around surface facilities (often referred as hydroexcavation), and releases from raw water lines (either deliberate or inadvertent). Potential preferential pathways during release events from tank leaks in the near-field include wetting front instability or 'fingering' flow. Wetting front instability, reported in petroleum related literature, is a special case of interface instability during immiscible fluid displacement in porous media. The phenomenon is triggered by unfavorable differences between the viscosities and densities of two fluids across their interface, which is a condition that can potentially exist during release events, for example, at S-SX tank farm. However, unlike S-SX tank farm conditions where the ionic strength of the plume is extremely high, such conditions are not expected to dominate fluid and contaminant migration during release events at other tank farms.

Among potential preferential pathways, the probability of encountering clastic dikes beneath tank farms is substantial. For example, numerous clastic dikes occur at the US Ecology site southwest of the 200 East Area that may serve as conduits for preferential flow. While a clastic dike can potentially increase flow rate, it is less likely to intersect large segments of leaked

wastes, and when it does, the cross-sectional area of the intersection is small (DOE/RL-96-61, *Hanford Site Background: Part 3, Groundwater Background*).

Therefore, the presence of clastic dikes in unsaturated media appears unlikely to contribute much to the transport to groundwater of the bulk quantity of leaked wastes and, based on the results of WMA S-SX FIR simulations (RPP-7884, *Field Investigation Report for Waste Management Area S-SX*), are not expected to contribute significantly to long-term risk in terms of higher peak concentrations for long-lived mobile radionuclides. However, attempts at previous modeling efforts to simulate the effects of clastic dikes have not always adequately represented the geometry and extent of these features. Thus, additional simulations that can better approximate the tabular and three-dimensional (3D) characteristics of clastic dikes may be needed to portray the hydraulic and contaminant transport attributes of clastic dikes more realistically. The conceptual models to be used for Phase 2 WMA specific risk assessments will be developed and documented in a collaborative process involving Ecology. The appropriate modeling of clastic dikes will be evaluated.

Finally, a circumstantial evidence of predominantly porous medium flow is provided by site characterization data for various FIRs. For example, based on the field data (e.g., S-SX 41-09-39 and slant boreholes), and the observation of an apparent ion exchange front for the cations, it can be postulated that the contaminant plume is more likely traveling through the far-field vadose zone sediments via porous media flow as opposed to traveling through preferred pathways. If the latter flow conditions were controlling the plume movement at the SX tank farm, it would be unlikely to encounter the well-developed ion exchange front throughout the borehole profiles.

4.3 MOISTURE CONTENT AND MATRIC POTENTIAL MEASUREMENTS AT WASTE MANAGEMENT AREA C

Soil matric potential and moisture content characterize the existing state of drainage for vadose zone sediments at tank farms. In this section, we provide, for tank farm soils, a summary of matric potential (pressure head) as well as moisture content information collected as part of field investigation reports for WMAs C, B-BX and S-SX.

As part of site characterization for the WMA C FIR, attempts were made to determine the soil water status and use the data to evaluate the occurrence of drainage within the WMA (PNNL-15503, *Characterization of Vadose Zone Sediments Below the C Tank Farm: Borehole C4297 and RCRA Borehole 299-E27-22*). Matric potential data were obtained from the RCRA borehole 299-E27-22 outside of WMA C and the borehole C4297 within WMA C.

4.3.1 Matric Potential Data

Figure 4-5 shows the matric potentials (in MPa) as a function of depth for borehole 299-E27-22, with the potentials shown as absolute values. Matric potentials for three of the samples (27.0, 72.0, and 74.5 ft bgs) suggest very dry conditions; these appear to be erroneous because of inadvertent drying of the samples or weighing errors. The red line, labeled “theoretical value” in Figure 4-5, is the theoretical line that represents the steady-state unit gradient condition. Matric

potential values to the left of the unit gradient line suggest a draining profile. The general trend for the data from borehole 299-E27-22 is that the matric potentials are consistent with those of a draining profile.

4.3.2 Moisture Content Data

Figure 4-6 illustrates the gravimetric moisture content (θ_g) as a function of depth for sediments from the RCRA borehole 299-E27-22. Figure 4-6 is based on θ_g measurements of continuously-cored (19 to 111 ft bgs) as well as selectively-cored (111 to 230 ft bgs) samples from the borehole. The moisture content profile correlates well with the lithology shown in Figure 4-6. The only region with elevated moisture is in the Hanford formation H1 unit, and corresponded to a thin, fine-medium sand to silty fine-sand lens at ~48 ft bgs. The rest of the Hanford formation H1 unit was rather dry, with a mean θ_g of 2.6 wt%. The next zone of elevated moisture was found at the contact of the Hanford formation H1 and H2 units at ~82 ft bgs, with a θ_g of 12.5 wt%. The final zone of elevated moisture was in the Hanford formation H2 unit at ~98 ft bgs and corresponded to a thin, fine to coarse sand contact. The rest of the Hanford formation H2 unit was relatively dry, with a mean θ_g of 2.5 wt%. Below the Hanford formation, the Cold Creek upper sub-unit is believed to have been penetrated by the final split-spoon core sample collected. The sample was composed of gravel and was quite dry. No core samples were obtained from borehole 299-E27-22 in the lower Cold Creek sub-unit or the Ringold units.

The gravimetric moisture content profile as a function of depth for borehole C4297 within WMA C is shown in Figure 4-7. The profile is based on θ_g measurements for 37 core liners and 119 grab samples. The backfill split-spoon samples had average moisture content (θ_g) of 5.0% by weight with very little variation. The Hanford formation H1 split-spoon samples (40 to 65 ft bgs) had a mean θ_g of 2.9% with less variability than the backfill material. The Hanford formation H2 sub-unit split-spoon samples had an average θ_g of 3.1% with little variability among the samples. The average θ_g of the H1 unit samples measured in borehole C4297 was about one half of one percent by weight lower than the average for the same stratigraphic unit at the RCRA borehole 299-E27-22. The average θ_g of the H2 unit samples measured in C4297 sediments was about one half of one percent by weight higher than the average for the same stratigraphic unit at the RCRA borehole 299-E27-22. Based on moisture data at the two boreholes, it cannot be stated that tank farm operations have caused increased moisture accumulation. Rather, it appears that the moisture content data reflect natural heterogeneities at the two borehole sites.

As shown in Figure 4-8, for the C4297 core samples, the measured matric potentials were generally much less than the gravity potential from the shallowest core at 19.5 ft bgs down to the deepest core taken at 195.25 ft bgs, representing both the Hanford formation H1 and H2 units. Matric potential values to the left of the unit gradient line (the red line labeled “theoretical value” in Figure 4-5) suggest a draining profile. Only one sample, collected at 150 ft bgs, had a measured matric potential in excess of the theoretical matric potential line plotted in Figure 4-5; this could be an artifact of inadvertent drying during sample storage. The general trend for the data from C4297 is that the matric potentials were consistent with those of a draining profile.

Figure 4-5. Matric Potentials Measured by Filter Paper Technique on Core Samples from Borehole 299-E27-22.

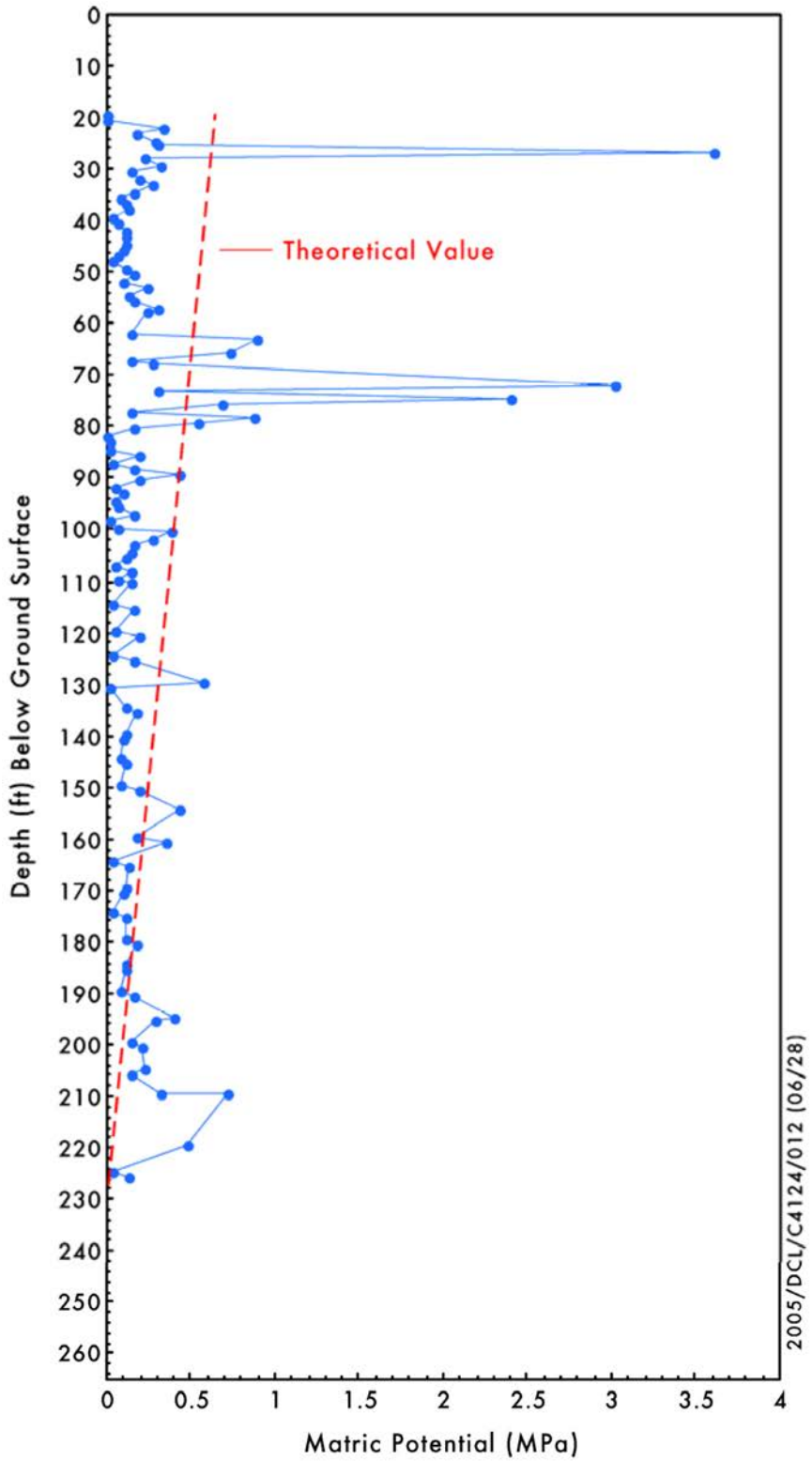

Reference: PNNL-15503, *Characterization of Vadose Zone Sediments Below the C Tank Farm: Borehole C4297 and RCRA Borehole 299-E27-22.*

Figure 4-6. Borehole 299-E27-22 Lithology and Gravimetric Moisture Content Measurements (the shaded areas in light blue and gray are regions of increased moisture).

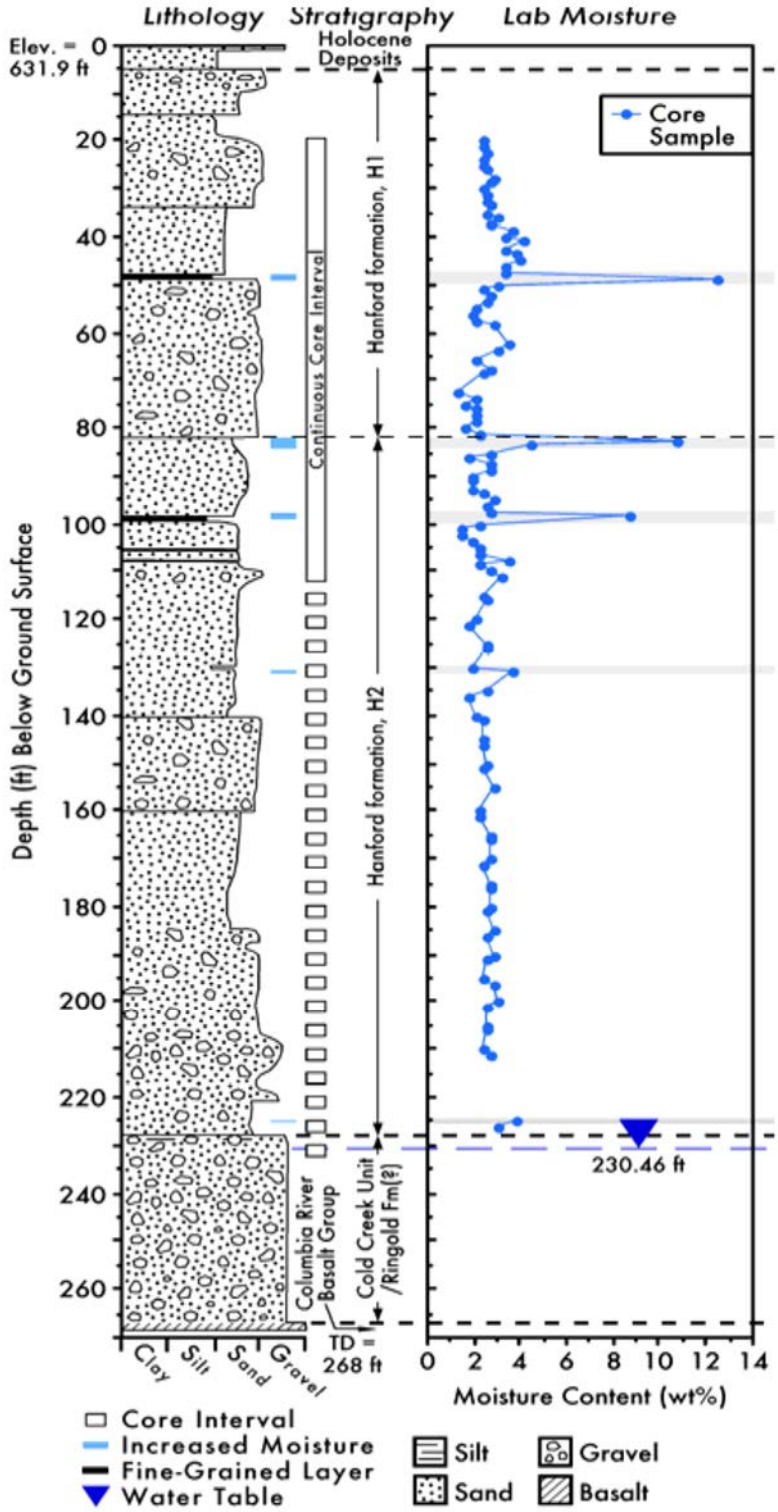

Reference: PNNL-15503, *Characterization of Vadose Zone Sediments Below the C Tank Farm: Borehole C4297 and RCRA Borehole 299-E27-22.*

Figure 4-7. Borehole C4297 Lithology and Gravimetric Moisture Content Measurements (the shaded areas in light blue and gray are regions of increased moisture).

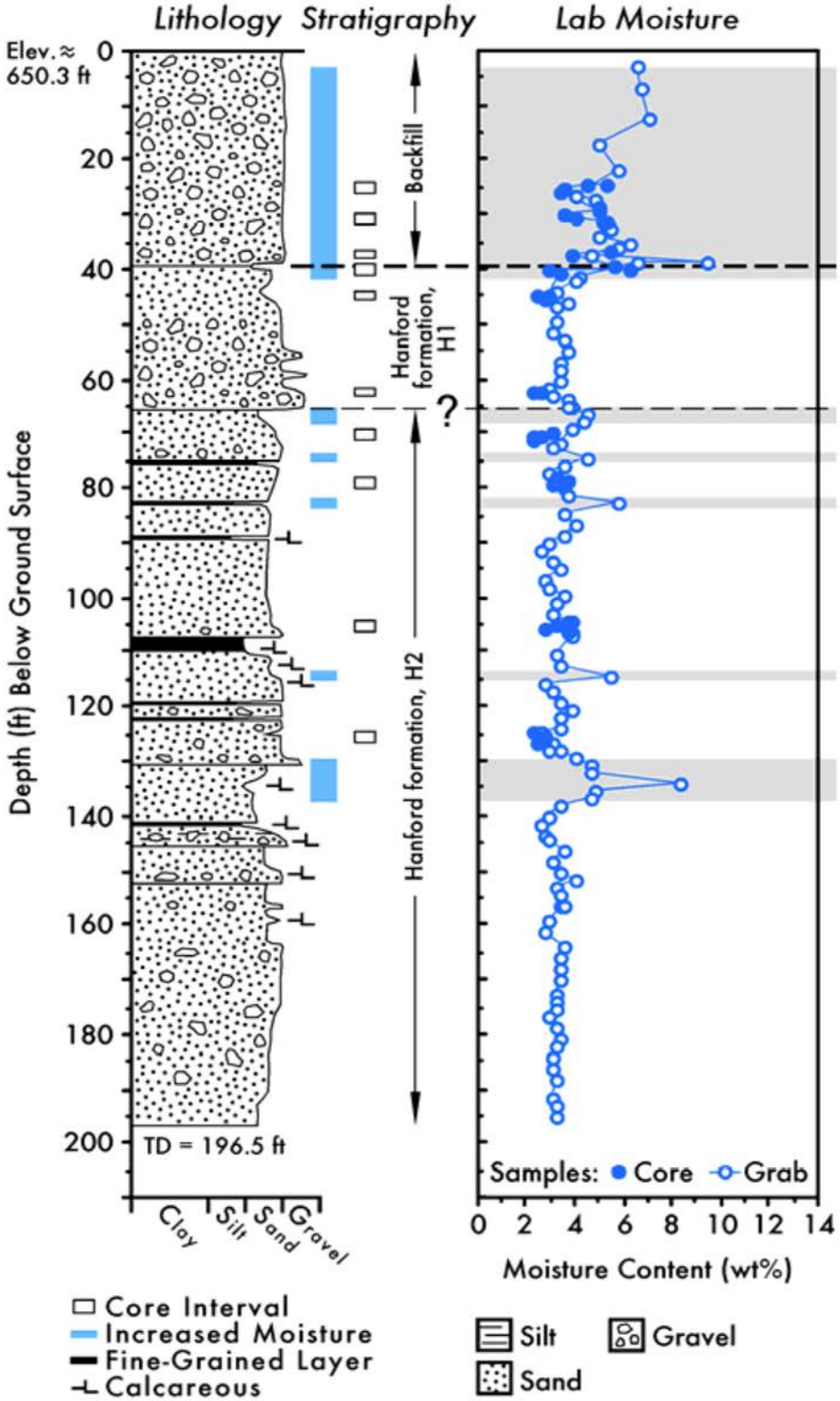

Reference: PNNL-15503, *Characterization of Vadose Zone Sediments Below the C Tank Farm: Borehole C4297 and RCRA Borehole 299-E27-22.*

Figure 4-8. Matric Potential for Borehole C4297 Samples (measured after cores were sub-sampled).

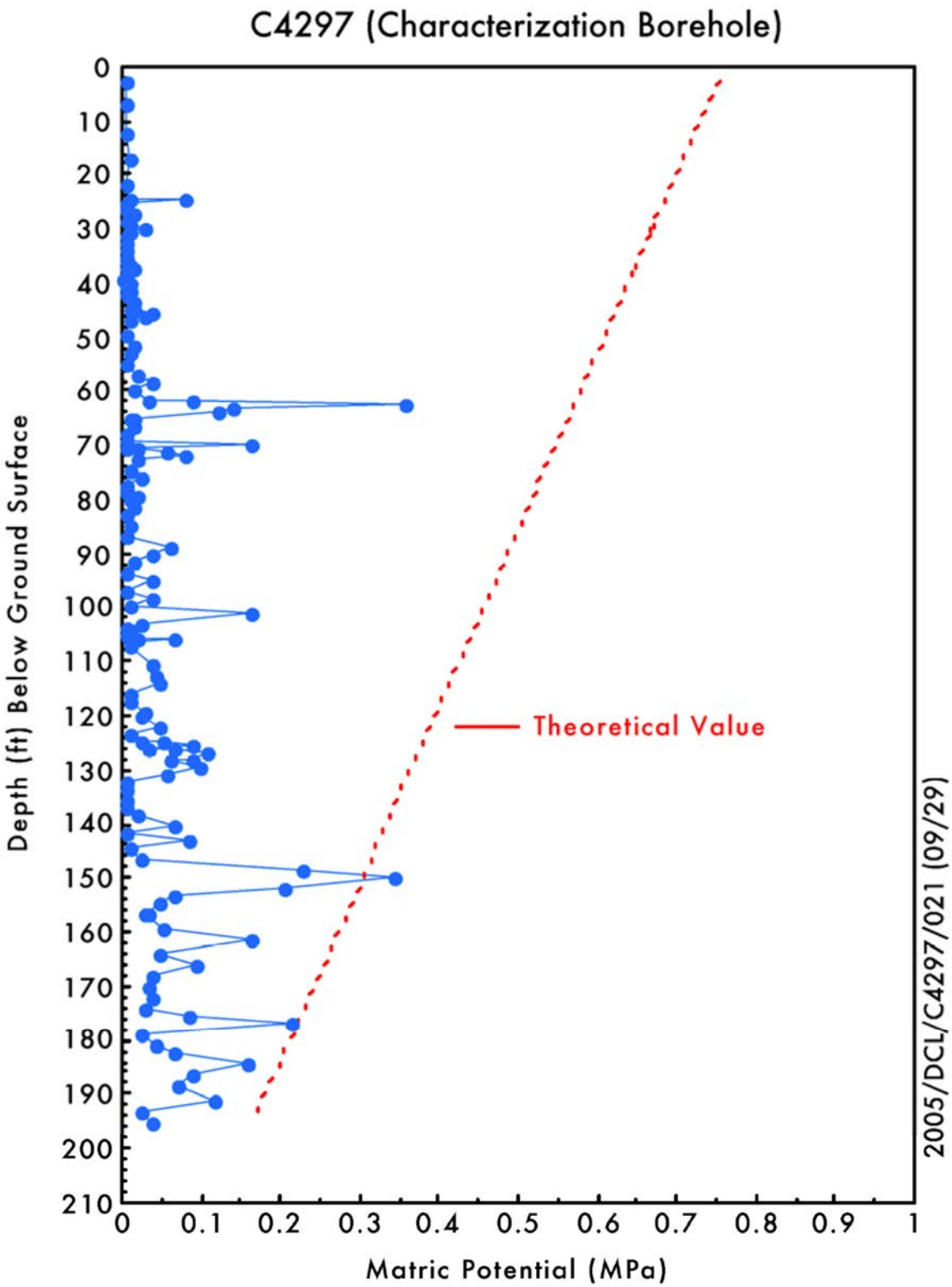

Reference: PNNL-15503, *Characterization of Vadose Zone Sediments Below the C Tank Farm: Borehole C4297 and RCRA Borehole 299-E27-22.*

4.4 ALTERNATIVE CONCEPTUAL MODELS OF VADOSE ZONE FLOW AND TRANSPORT AT WASTE MANAGEMENT AREA C

Alternative conceptual models of vadose zone flow and transport were developed and described as part of the Field Investigation Report for WMA C (RPP-35484, *Field Investigation Report for Waste Management Areas C and A-AX*) and the data quality objective (DQO) for Phase 2 Characterization Activities (RPP-RPT-38152, *Data Quality Objectives Report Phase 2 Characterization for Waste Management Area C RCRA Field Investigation/Corrective Measures Study*), and include input from the Nez Perce. Five initial alternative models were presented in the WMA C PA Working Session on Assessment Context on September 1 through 3, 2009 and were included in Section 9.3 of RPP-RPT-41918, Rev. 0 as a starting point to facilitate discussion of viable alternative models during this working session.

These alternative models include:

- A Phase 1 Alternative Model
- A Modified Phase 1 Alternative Model to Account for Additional Recharge
- An Alternative Based on Contaminant Movement Down Stratigraphic Dip (Nez Perce)
- An Alternative Based on Preferential Pathway
- An Alternative Based on Unknown Leak Event.

The order of their presentation in this list is not intended to imply a preference of one over the other. Final alternative model(s) selected for consideration in the integrated WMA C PA may likely reflect elements of one or more of these alternative models

A summary of these conceptual models of the vadose zone, that contain many of the FEPs that have been identified to date, were described for conditions prevalent in the past and projected future conditions. These conceptual models will undergo revisions if additional FEPs identified in the screening process are found to be important and should be considered in the WMA C PA. They are provided in this report for reference in Appendix D.

4.5 RECOMMENDED FLOW AND TRANSPORT PROPERTIES

This section provides recommendations for effective estimated values of flow and transport parameters that will be used to evaluate flow and transport through the vadose zone at WMA C. Specific flow-related parameters considered include fitting parameters associated with models that will be used to evaluate the relationship between capillary pressure and moisture content (i.e., moisture retention characteristics), and the relation of these factors with saturated and unsaturated hydraulic conductivity. An additional flow related parameter will also include estimates of macroscopic anisotropy that will be used to evaluate the effect of tension dependent anisotropy in flow calculations with the vadose zone.

4.5.1 Flow Properties

Discussion of the key features of the sediments within the vadose zone system up to this point has stressed the heterogeneous nature of the sands and gravelly-sands associated with the major hydrogeologic units. The challenge in the PA for WMA C is the development of a suitable approach for treatment of these features given the scale of the flow and transport analysis and limited amount of characterization data and information that is available to define the levels of heterogeneity at the scales of interest.

For purposes of the initial PA for WMA C, the technical approach that has been adopted is to approximate the hydraulic properties of the vadose system with composite properties developed from flow-related parameters acquired from limited sampling of the major hydrogeologic units across the Hanford Site. The composite properties would be used to represent the major units in a proposed denominator case that would provide a basis against which results from other alternative models with other treatments of system heterogeneities could be compared. The effect of system heterogeneities on system performance will eventually be evaluated using a variety of approaches that include:

- Development of alternative conceptual models that consider major features of heterogeneity that can be identified from available characterization data and information

- Evaluation of range of hydraulic properties in proposed sensitivity cases that could represent the range of hydraulic properties observed during characterization

- One or more sensitivity cases that would attempt to evaluate the effect of system heterogeneities by developing realistic distributions of hydraulic properties based on geostatistical analysis or treatment of available data and information.

Specific flow-related parameters considered include fitting parameters associated with models that will be used to evaluate the relationship between capillary pressure and moisture content (i.e., moisture retention characteristics), and the relation of these factors with saturated and unsaturated hydraulic conductivity. An additional flow related parameter will also include estimates of macroscopic anisotropy that will be used to evaluate the effect of tension dependent anisotropy in flow calculations with the vadose zone.

Specific development of numerical implementation of alternative conceptual models, particularly those that will consider major features of heterogeneity, will be presented in a data package and presentations used in the Numeric Codes working session to be held January 25 through 27, 2011.

4.5.1.1 Moisture Retention Data. Information on particle-size distributions, moisture retention, and saturated hydraulic conductivity is available for 183 samples in the 200 Areas [RPP-RPT-35222, *Far-Field Hydrology Data Package for the RCRA Facility Investigation (RFI) Report*]. These data are corrected for gravel content. Once corrected, hydraulic parameters are determined by fitting the data using a moisture retention model developed in “A Closed-form

Equation for Predicting the Hydraulic Conductivity of Unsaturated Soils" (van Genuchten 1980) using the following empirical relationship.

$$\theta(h) = \theta_r + (\theta_s - \theta_r)\left\{1 + [\alpha h]^n\right\}^{-m} \tag{4-1}$$

where:

- θ = volumetric moisture content [dimensionless]
- h = matric potential or pressure head, which, for notational convenience, is considered as being positive (i.e., tension [cm])
- θ_r = residual moisture content [dimensionless]
- θ_s = saturated moisture content [dimensionless]
- α = a fitting parameter (cm^{-1})
- n = a fitting parameter [dimensionless]
- m = 1 - 1/n.

Combining the van Genuchten model with "A New Model for Predicting the Hydraulic Conductivity of Unsaturated Porous Media" (Mualem 1976) model for unsaturated conductivity:

$$K(h) = \frac{K_s\left\{1 - (\alpha h)^{mn}\left[1 + (\alpha h)^n\right]^{-m}\right\}^2}{\left[1 + (\alpha h)^n\right]^{m\ell}} \tag{4-2}$$

where:

- $K(h)$ = unsaturated hydraulic conductivity [cm/s]
- K_s = saturated hydraulic conductivity [cm/s]
- ℓ = pore-connectivity parameter [dimensionless], estimated by Mualem to be about 0.5 for many soils.

It is well recognized that the estimated unsaturated conductivities, based on saturated conductivity and the van Genuchten retention model, can differ by up to several orders of magnitude with measured conductivities at the dry end (e.g., "Evaluation of van Genuchten-Mualem Relationships to Estimate Hydraulic Conductivity at Low Water Contents" [Khaleel et al. 1995]).

A simultaneous fit of both laboratory-measured moisture retention and unsaturated conductivity data was used in this work, and all five unknown parameters θ_r, θ_s, α, n, and K_s, with m=1-1/n (van Genuchten 1980) were fitted to the data via a code named RETention Curve (RETC) (EPA/600/2-91/065, *The RETC Code for Quantifying the Hydraulic Functions of Unsaturated Soils*). Thus, in order to obtain a better agreement with experimental data for the region of interest (i.e., relatively dry moisture regime), K_s is treated as a fitted parameter during the curve fitting process. The pore size distribution factor, ℓ (Mualem 1976) was kept fixed at 0.5 during the simultaneous fitting.

Specific values for composite van Genuchten-Mualem parameters for the major hydrogeologic units identified at WMA C for use in the SST PA (DOE/ORP-2005-01, *Initial Single-Shell Tank System Performance Assessment for the Hanford Site*) were made in RPP-RPT-35222. These recommended values, which are summarized in Table 4-1, are also recommended as initial estimates of these parameters for use in the WMA C PA. A detailed discussion of the basis for these recommended values are provided in Section 6 of RPP-RPT-35222.

Table 4-1. Composite van Genuchten-Mualem Parameters for Various Strata at Waste Management Area C.

Strata	Number of Samples	θ_s	θ_r	α 1/cm	n	ℓ	Fitted K_s cm/s
Backfill	10	0.1380	0.0100	0.0210	1.374	0.5	5.60E-4
Sandy H2	12	0.3819	0.0443	0.0117	1.6162	0.5	9.88E-5
Gravelly Sand H3/CCU/R	8	0.2688	0.0151	0.0197	1.4194	0.5	5.15E-4
Gravelly Sand H1	11	0.2126	0.0032	0.0141	1.3730	0.5	2.62E-4
Plio-Pleistocene*/ Ringold Sandy Gravel	10	0.1380	0.0100	0.0210	1.374	0.5	5.60E-4

Reference: RPP-RPT-35222, *Far-Field Hydrology Data Package for the RCRA Facility Investigation (RFI) Report*.

*This lower sandy gravel unit that was formerly called the Plio-Pleistocene unit is the equivalent of the Cold Creek (Pre-Missoula Gravels) unit referred to in other tables of parameters provided in Section 4.5.

A similar set of recommended input data sets for use in vadose zone modeling for large-scale Hanford assessments are presented in PNNL-14702, *Vadose Zone Hydrogeology Data Package for Hanford Assessments*. Hydraulic property data for the vadose zone simulations were derived from the laboratory measurements of 284 soil samples (both repacked and split-spoon samples) taken from the 100 and 200 Areas. These data were selected from a catalog of vadose zone hydraulic properties (PNNL-13672, *A Catalog of Vadose Zone Hydraulic Properties for the Hanford Site*, Rev. 1) and a subsequent prototype database (WMP-17524, *Vadose Zone Hydraulic Property Letter Reports*). Because the hydraulic property data are limited in the spatial location of samples and the soil types represented, individual stochastic data sets were developed to represent ten different soil classes. These ten classes build on the six soil classes originally identified by WHC-EP-0883 and are based on texture (i.e., particle size), International Society of Soil Science classification, and moisture retention curve characteristics.
Four additional soil classes were incorporated to separate out the CCU (formerly referred to as the Plio-Pleistocene unit) sediment, add additional detail for the Hanford formation sand-dominated sediment, and add a new class for very coarse gravel. The resulting 10 soil hydraulic property classes and their associated hydraulic property distributions were later correlated to the hydrostratigraphic units used in the 17 geographic area templates. Table 4.5 in PNNL-14702 describes the hydraulic-property soil classes assembled for a large-scale Hanford assessment.

PNNL-14702 prepared statistical distributions of van Genuchten model (van Genuchten 1980) parameters (α, n, Θ_R, Θ_S, Sr), saturated hydraulic conductivity (Ks) data developed from laboratory data described in a catalog of vadose zone hydraulic properties by PNNL-13672,

PNNL-13672 Rev. 1, and a subsequent prototype database (WMP-17524). Ideally, all parameters in this database should be based on gravel-corrected data derived using the same gravel-correction procedure. Some of the parameters are known to have been based on gravel-corrected data derived using the Gardner method (e.g., "Correcting Laboratory-Measured Moisture Retention Data for Gravels" [Khaleel and Relyea 1997]), but it is not clear that all samples were treated in a consistent manner.

Gravel percentages are included in Tables 4.5 to 4.9 of PNNL-14702 to indicate which soil classes might be affected. Values for residual saturation (S_r) are statistically derived from the sample population where the raw residual water content (Θ_R) for an individual sample was divided by the raw saturated content (Θ_S) for that sample. Effective porosity is assumed to be equal to the saturated water content (Θ_S).

Estimated mean values of van Genuchten-Mualem parameters from PNNL-14702 from site-wide samples presented in Table 4.5 of that document that would considered to be appropriate for consideration in the WMA C PA are summarized in Table 4-2.

Table 4-2. Statistical Mean Values of van Genuchten-Mualem Parameters for Site-Wide Samples.

Soil Class	Count	α (1/cm)	n	θ_R (cm^3/cm^3)	θ_s (cm^3/cm^3)	K_s (cm/sec)	Sr	% Gravel
Backfill (Bf)	6	0.019	1.4	0.03	0.262	5.98E-04	0.103	33.5
Hanford formation								
Silty sand (Hss)	38	0.008	1.91	0.07	0.445	8.58E-05	0.162	0.2
Fine sand (Hfs)	36	0.027	2.16	0.03	0.379	3.74E-04	0.086	0.6
Coarse Sand (Hcs)	81	0.061	2.03	0.03	0.349	2.27E-03	0.08	2.6
Gravelly Sand (Hgs)	16	0.014	2.12	0.03	0.238	6.65E-04	0.14	25.8
Sandy Gravel (Hg)	28	0.017	1.72	0.02	0.167	3.30E-04	0.134	51.4
Gravel (Hrg)	40	0.007	1.83	0.02	0.102	1.46E-03	0.2	67.6
Cold Creek Unit								
Silt dominated (CCUl)	9	0.005	2.25	0.04	0.419	5.57E-05	0.097	0.4
Caliche (CCUl)	14	0.011	1.74	0.05	0.281	8.45E-04	0.185	16.7
Ringold Formation								
Gravel Dominated (Rg)	18	0.008	1.66	0.03	0.177	4.13E-04	0.135	46.1

Reference: PNNL-14702, *Vadose Zone Hydrogeology Data Package for Hanford Assessments*.

Data on physical and hydraulic parameters are also needed for clastic dikes to model their effect on flow and contaminant. Such physical and hydraulic data (i.e., bulk density, particle size distribution, moisture retention, saturated and unsaturated hydraulic conductivities) for clastic dike infilling materials were developed in RPP-20621, *Far-Field Hydrology Data Package for*

the Integrated Disposal Facility Performance Assessment, Appendix F – Physical and Hydraulic Measurements of FY1998 Clastic Dike Samples. A summary of these physical and hydraulic conductivities are provided in Table 4-3.

Table 4-3. van Genuchten-Mualem Parameters, Saturated Hydraulic Conductivity and Bulk Density for Several Clastic Dikes.

Sample	θ_s (cm^3/cm^3)	θ_r (cm^3/cm^3)	α (1/cm)	n (-)	Saturated Hydraulic Conductivity (cm/s)	Bulk Density (g/cm^3)
1	0.424	0.063	0.0839	1.33	5.97E-04	1.57
2A	0.446	0.019	0.0762	1.98	4.70E-03	1.50
2B	0.443	0.023	0.0741	1.84	3.14E-03	1.51
3A	0.424	0.025	0.0143	2.49	3.41E-03	1.46
3B	0.448	0.050	0.0593	1.54	1.14E-03	1.52
4A	0.454	0.030	0.0092	1.97	1.84E-03	1.49
4B	0.425	0.021	0.0823	2.09	5.43E-03	1.57

Reference: RPP-20621, *Far-Field Hydrology Data Package for the Integrated Disposal Facility Performance Assessment*, Appendix F. Physical and Hydraulic Measurements of FY1998 Clastic Dike Samples.

4.5.1.2 Macroscopic Anisotropy. RPP-RPT-35222 proposed a stochastic model approach to evaluate tension-dependent anisotropy for major sediment units found in WMA C. Variable, tension-dependent anisotropy provides a framework for up-scaling small-scale measurements to the effective (up-scaled) properties for the equivalent, large scale vadose zone. The specific details and equations associated with the proposed methods are described in section 6.7.2 in RPP-RPT-35222.

Results of application of the approach in RPP-RPT-35222 for major sediment units found within WMA C are summarized in Table 4-4.

Table 4-4. Macroscopic Anisotropy Parameters for Various Strata at Waste Management Areas C and S-SX Based on Polmann (1990) Model.

Strata/Material Type	Number of Samples	$<LnK_s>$	$\sigma^2_{LnK_s}$	p	ζ	λ cm	A
Backfill (1)	10	-15.76	3.56	-1.1E-04	1.84E-04	30	0.00371
Sandy H2 (2)	12	-14.59	1.50	-7.2E-04	6.55E-04	50	0.00620
Gravelly Sand H3/CCU/R (3)	8	-15.30	1.83	-5.6E-04	5.16E-04	50	0.00415
Gravelly Sand H1 (4)	11	-14.85	1.94	-2.6E-04	2.50E-04	30	0.00368
Cold Creek unit (pre-Missoula Gravels)/Ringold Sandy Gravel (5)	10	-15.76	3.56	-1.1E-04	1.84E-04	30	0.00371

See Appendix D of RPP-13310, *Modeling Data Package for an Initial Assessment of Closure of the C Tank Farm*, Rev. 1 for description of the variables.
Reference: Application of Stochastic Methods to Transient Flow and Transport in Heterogeneous Unsaturated Soils, Ph.D. Thesis (Polmann 1990).

4.5.2 Transport-Related Properties

Specific transport parameters considered include estimate of bulk density, diffusivity and macro-dispersivity which are used to estimate the effect of concentration gradients and hydraulic gradients on the process of diffusion and dispersion in contaminant transport calculations. Other transport parameters considered include recommended estimates of constituent-specific distribution coefficients (kds) which will be used to approximate the effect of chemical factors affecting contaminant-specific mobility or retardation in the transport process.

4.5.2.1 Bulk Density. In the WMA C PA, bulk density estimates, when combined with contaminant-specific distribution coefficients, are required to retardation factors for different specific species. Recommendations, taken from RPP-RPT-35222 for composite bulk density estimates for sediments found within WMA C, are provided in Table 4-5.

Table 4-5. Effective Bulk Density (g/cm^3) Estimates at Waste Management Area C.

Strata/Material Type	E[ρ_b]
Backfill	2.13
Sandy H2	1.76
Gravelly sand H3/CCU/R	1.94
Gravelly sand H1	2.07
Plio-Pleistocene*/Ringold gravels	2.13

* This lower sandy gravel unit that was formerly called the Plio-Pleistocene unit is the equivalent of the Cold Creek (Pre-Missoula Gravels) unit referred to in other tables of parameters provided in Section 4.5.

References: RPP-13310, *Modeling Data Package for an Initial Assessment of Closure of the C Tank Farm*
RPP-17209, *Modeling Data Package for an Initial Assessment of Closure of the S and SX Tank Farms.*

4.5.2.2 Diffusivity. For purposes of the WMA C PA, we will assume that the effective, large-scale diffusion coefficients for all strata at a WMA are a function of volumetric moisture content, θ, and can be expressed using the "Permeability of Porous Solids" (Millington and Quirk 1961) empirical relation:

$$D_e(\theta) = D_0 \frac{\theta^{10/3}}{\theta_s^2} \tag{4-3}$$

where:

$D_e(\theta)$ = effective diffusion coefficient of an ionic species as a function of moisture content
D_0 = molecular diffusion coefficient for the same species in free water.

The molecular diffusion coefficient for all species in free water was assumed to be 2.5×10^{-5} cm^2/sec (WHC-SD-WM-EE-004, *Performance Assessment of Grouted Double-Shell Tank Waste Disposal at Hanford*).

4.5.2.3 Dispersivity

4.5.2.3.1 Macro-dispersivity Estimates for Nonreactive Species. The Gelhar and Axness equation (Stochastic Subsurface Hydrology [Gelhar 1993]) is used to estimate asymptotic values of macro-dispersivity. To account for the effects of unsaturated flow, a modified version is used:

$$A_L(<h>) = \sigma_{LnK}^2 \lambda \tag{4-4}$$

where the longitudinal macro-dispersivity depends on the mean tension $< h >$.

To apply Equation 4-4, an estimate of the vertical correlation scale for unsaturated conductivity is needed. A correlation length of the order of about 50 cm was obtained for saturated hydraulic conductivity for sediments near the C tank farm (RPP-13310, *Modeling Data Package for an Initial Assessment of Closure of the C Tank Farm*). For unsaturated conditions, an increase in the variance of log unsaturated conductivity is expected to be compensated in part by a decrease in the correlation scale of log unsaturated conductivity. A correlation length of 30 cm is assumed for log unsaturated conductivity for all strata. Table 4-6 provides the log unsaturated conductivity variances and the estimated longitudinal (A_L) and transverse (A_T) macro-dispersivities for various strata. The transverse dispersivities are estimated as one tenth of the longitudinal values ("A Critical Review of Data on Field Scale Dispersion in Aquifers" [Gelhar et al. 1992]).

Table 4-6. Nonreactive Macro-dispersivity Estimates for Various Strata at Waste Management Areas C.

Strata	σ_{LnK}^2	Correlation length, λ cm	A_L cm	A_T cm
Backfill	4.54	30	~150	15
Sandy H2	4.60	30	~150	15
Gravelly Sand H3/CCUl/R	4.95	30	~150	15
Gravelly Sand H1	3.19	30	~100	10
Plio-Pleistocene*/Ringold Sandy Gravel H3/CCUl/R	4.54	30	~150	15

Note: See Section 6.8.7 of RPP-RPT-35222, *Far-Field Hydrology Data Package for the RCRA Facility Investigation (RFI) Report* for description of variables.

*This lower sandy gravel unit that was formerly called the Plio-Pleistocene unit is the equivalent of the Cold Creek (Pre-Missoula Gravels) unit referred to in other tables of parameters provided in Section 4.5.

4.5.2.3.2 Heterogeneous Sorption Enhanced Macrodispersivities for the Reactive Species. The net effect of sorption is to retard the velocity at which the contaminant migrates through the

porous media. Because sorption for specific contaminants may be a function of soil properties, as the soil properties experience spatial variability, the sorption also varies (Gelhar 1993; NUREG/CR-6114, *Auxiliary Analyses in Support of Performance Assessment of a Hypothetical Low-Level Waste Facility: Groundwater Flow and Transport Simulation*, Vol. 3). Stochastic analysis developed by Gelhar (1993) was recommended for evaluating macro-dispersivity enhancement that considers the effect of sorption for various strata in WMA C in the modeling data package reports (RPP-13310; RPP-17209, *Modeling Data Package for an Initial Assessment of Closure of the S and SX Tank Farms*; and RPP-RPT-35222).

In RPP-RPT-35222, this macro-dispersivity enhancement was only developed for consideration for uranium. This theoretical basis for this treatment is described more fully in Section 6.8.8 of this specific data package. The resulting estimates of macro-dispersivity for uranium for the key sediment units at WMA C are provided in Table 4-7.

4.5.3 Contaminant-Specific Distribution Coefficients

Contaminant migration rates are element-specific because of the varying degrees of their chemical reactivity with soils (PNNL-13037, *Geochemical Data Package for the 2005 Hanford Integrated Disposal Facility Performance Assessment*). Some contaminants are largely non-sorbing (i.e., technetium) and migrate with recharge water. Others are highly reactive and migrate very slowly (i.e., cesium).

Table 4-7. Results for Macro-dispersivity Enhancement that Considered Sorption Based on a K_d of 0.6 mL/g for Various Strata in Waste Management Area C.

Strata	$\overline{K}_d$	$\sigma_{Kd}/\overline{K}_d$	$\overline{R}$	$\sigma_R/\overline{R}$	$\overline{P}_b$	$\overline{\theta}$	σ^2_{LnK}	γ	ζ	$\lambda_n\lambda_1$	A_{11}/A_o
Backfill/Cold Creek (pre-Missoula gravels)/ Ringold Sandy Gravel	0.6	0	11.94	0.43	2.13	0.066	4.54	0.26	0.38	1	1.067
Sandy H2	0.6	0	14.31	0.67	1.76	0.115	4.60	0.13	0.58	1	1.063
Gravelly Sand H3/CCU/R	0.6	0	14.31	0.50	1.94	0.086	4.95	0.20	0.42	1	1.062
Gravelly Sand H1	0.6	0	11.36	0.38	2.07	0.081	3.19	0.32	0.72	1	1.120

Adapted from RPP-RPT-35222, *Far-Field Hydrology Data Package for the RCRA Facility Investigation (RFI) Report*; see Section 6.8.8 of RPP-RPT-35222 for description of variables.

Chemical reactions that occur when contaminants interact with soil solid phases and retard contaminant migration relative to water flow through the vadose zone are often represented in risk and performance assessments by an adsorption isotherm that makes use of a distribution coefficient (K_d). The K_d value is a lumped parameter and, as a result, neglects many of the chemical complexities of the adsorption processes such as saturation of adsorption sites and aqueous complexation.

The simplest type of adsorption isotherm is a linear adsorption isotherm that is defined using the distribution coefficient, K_d (in mL/g or m^3/kg) as seen in Equation 4-5:

$$S = K_d * C \tag{4-5}$$

where:

S (g/g) = concentration of solute adsorbed onto the solid phase
C (g/ml) = concentration of the solute in solution.

A linear isotherm (or K_d) approach is generally applied as a constant property of the vadose zone and groundwater system, and forms the basis of the general retardation factor (Rf) through the relationship in Equation 4-6 (Groundwater [Freeze and Cherry 1979]):

$$Rf = 1 + (\rho/\theta)K_d = Vw/Vc \tag{4-6}$$

where:

ρ = bulk density of the media
θ = effective porosity of the media
Vw = water velocity in the media
Vc = contaminant velocity in the media.

The lower the value of K_d, the lower the retardation factor, and the faster a species migrates through the subsurface. For a non-adsorbing species, $K_d = 0$, Rf reduces to 1, and the species migrates at the water flow velocity.

The K_d value is the ratio of contaminant mass attached to soil solids versus mass dissolved in solution. The advantage of this approach is that K_d values can be easily incorporated in modeling transport. The disadvantage is that K_d values are entirely empirical and are used to represent many different kinds of chemical reactions that are dependent on the contaminant of interest, the soil solid phases present in the vadose zone, and the soil water chemistry. The effects of physical variables (moisture content and gravel fraction) and reactions (colloid formation and migration) can be also incorporated in the K_d approach.

It is recognized that, at WMA C, the sorption characteristics of any one constituent are potentially variable as a function of the heterogeneous nature of physical, textural and chemical properties of the sediments encountered during the transport process. It is likewise acknowledged that the use of a constant K_d model may not provide an adequate approximation for predicting the effects of the adsorption process in situations where spatial mineralogical and hydrochemical characteristics within the vadose zone are variable. This could be particularly true in close proximity to source release areas where unique chemistry associated with tank waste release could have a significant effect on sorption and reactive process for selected constituents. However, the use of spatial and temporal variation in K_ds to account for specific mineralogical and chemical heterogeneity is limited because of general lack of characterization data and information that could support such an approach.

The potential presence of ligands and chelating agents in tank wastes can have some influence and enhance the mobility of some metal constituents. PNNL-13895, *Hanford Contaminant Distribution Coefficient Database and Users Guide* notes specific examples of such agents enhancing the potential mobility of two normally immobile constituents such as americium and cobalt. Discussion of the effect on mobility of these two constituents in the presence of ligands and chelating agents such as ethylenediaminetetraacetic acid are discussed in detail in PNNL-13895.

The attachment (by adsorption or precipitation) of strongly sorbing radionuclides to colloidal-size materials (1 nm to 1 μm) that may be transported by mobile pore fluids is also potentially an important transport mechanism (Cation and Anion Adsorption at the Oxide/Solution Interface in Systems Containing Binary Mixtures of Adsorbents: An Investigation of the Concept of Adsorptive Additivity [Honeyman 1984]; "Migration of Plutonium in Ground Water at the Nevada Test Site" [Kersting et al. 1999]; "Subsurface Transport of Contaminants" [McCarthy and Zachara 1989]; "Review on Subsurface Colloids and Colloid-Associated Contaminant Transport in Saturated Porous Media" [Sen and Khilar 2006]). While little evidence exists at Hanford to support this type of transport mechanism at the field scale, the potential impacts from colloid development to enhance mobility of certain constituents may need to be considered. Susceptible contaminants include those of very low solubility (e.g., americium, plutonium, and thorium) or those that strongly adsorb to mineral phases of clay-size (e.g., <2.0 μm) particles (e.g., $^{137}Cs+$). Mobile colloids are generated when subsurface water systems experience chemical perturbations that cause (1) relatively rapid, in-situ precipitation events; or (2) ionic strength induced particle disaggregation (McCarthy and Zachara 1989, "Chemical Factors Influencing Colloid-Facilitated Transport of Contaminants in Porous Media" [Roy and Dzombak 1997]). These conditions have occurred at Hanford as caustic, saline tank wastes have been neutralized by dissolution and precipitation reactions with surface sediments, and as low ionic strength recharge waters resulting from meteoric water infiltration and infrastructure water losses have migrated behind relatively small volumetric releases of tank wastes causing salinity fronts.

Laboratory studies also show that colloid formation can be significant at tank waste plume fronts as high waste Na^+ displaces Ca^{2+}, Mg^{2+}, and Sr^{2+} from the exchanger phase and induces the supersaturation of calcite and other phases ("Colloid Formation at Waste Plume Fronts" [Wan et al. 2004a], "Geochemical Evolution of Highly Alkaline and Saline Tank Waste Plumes during Seepage through Vadose Zone Sediments" [Wan et al. 2004b]). The colloid load so produced accumulates in the aqueous phase and significantly exceeds the concentrations produced by salinity gradients ("In Situ Mobilization of Colloids and Transport of Cesium in Hanford Sediments" [Flury et al. 2002]; Wan et al. 2004b). The precipitation reactions neutralize and lower pH at the plume front allowing for supersaturation and precipitation of other phases including uranyl solids ("Geochemical Processes Controlling Migration of Tank Wastes in Hanford's Vadose Zone" [Zachara et al. 2007]) that may also migrate for unknown distances as colloidal material.

Away from the near-field source zones along the total thickness of the vadose zone and the length of the groundwater flow path, field characterization has shown that the unique chemistry and pH conditions from the source zone are buffered as it equilibrates with the background

chemical and mineralogical characteristics of natural sediments and concentrations of constituents of concern generally become low relative to the adsorption capacity of the sediments. For these far-field conditions, a constant K_d model can provide a reasonable approximation of the sorption process.

Use of variable or compartmentalized K_d values is one way to deal with spatially variable mineralogy and hydrochemistry that result in significant variability in K_d values along different components with the combined vadose zone-groundwater flow path. In this approach, different K_d values are used for different spatial compartments. Each compartment is assumed to have an average representative mineralogy, hydrochemistry, and associated K_d value. In principal, this approach could be used to deal with adsorption due to unique chemical characteristics in close proximity to the source release zones.

The specific details of K_d implementation in models used in the initial WMA C PA will be developed and will be presented in a data package and presentations made during the Numeric Codes working session scheduled for January 25 to 27, 2011.

Tables 4-8 and 4-9 list the contaminant distribution coefficient (K_d) bins that are recommended for used in the WMA C PA for various contaminants. Contaminant K_d values are adapted from:

- Guidance provided in Washington State Department of Ecology Toxics Clean-up Program Publication No. 94-145, *Model Toxics Control Act Cleanup Levels & Risk Calculations (CLARC) Version 3.1*
- EPA/540/R-95/128, *Soil Screening Guidance: Technical Background Document*
- Letter EM-ER-01-115, "K_d Values for INTEC Groundwater Modeling"
- EDF-ER-275, *Engineering Design File – Fate and Transport Modeling Results and Summary Report*
- A Practical Guide to Groundwater and Solute Transport Modeling (Spitz and Moreno 1996)
- Risk Assessment Information System, http://rais.ornl.gov/
- Section 4.3 of PNNL-14702
- PNNL-13895.

Distribution coefficients are only provided for those constituents with known toxicological effects. Should new information on toxicology require that new constituent be considered, K_d estimates for these contaminants can be added at some later time.

Table 4-8. Distribution Coefficients (mL/g) for Non-Radiological Constituents that are Part of the Waste Management Area C Inventory. (5 sheets)

CAS	Constituent	Group	Part Of	K_d (mL/g)	K_d Source	To Be Used in WMA C PA K_d		
						Denominator	Minimum	Maximum
7429-90-5	Aluminum	Inorganic	Both	1,500	ORNL	5	—	—
7440-36-0	Antimony	Inorganic	Both	45	CLARC 3.1	5	—	—
7440-38-2	Arsenic	Inorganic	Both	29	CLARC 3.1	5	—	—
7440-39-3	Barium	Inorganic	Both	41	CLARC 3.1	5	—	—
7440-41-7	Beryllium	Inorganic	Both	790	CLARC 3.1	5	—	—
7440-42-8	Boron	Inorganic	Both	3	ORNL	2	—	—
7440-43-9	Cadmium	Inorganic	Both	6.7	CLARC 3.1	5	—	—
18540-29-9	Chromium	Inorganic	Both	0	PNNL-13895	0	—	—
7440-48-4	Cobalt	Inorganic	Both	45	ORNL	5	—	—
7440-50-8	Copper	Inorganic	Both	22	CLARC 3.1	5	—	—
57-12-5	Cyanide	Inorganic	Both	0	conservative assumption	0	—	—
16984-48-8	Fluoride	Inorganic	Both	150	ORNL 12/8/08	5	—	—
7439-89-6	Iron	Inorganic	Both	25	ORNL	5	—	—
7439-93-2	Lead	Inorganic	Both	10,000	WAC 173-340	5	—	—
7439-93-2	Lithium	Inorganic	Both	300	ORNL	5	—	—
7439-96-5	Manganese	Inorganic	Both	65	ORNL	5	—	—
7439-97-6	Mercury	Inorganic	Both	52	CLARC 3.1	5	—	—
7439-98-7	Molybdenum	Inorganic	Both	20	ORNL	5	—	—
7440-02-0	Nickel	Inorganic	Both	65	CLARC 3.1	5	—	—
14797-55-8	Nitrate	Inorganic	Both	0	conservative assumption	0	—	—
14797-65-0	Nitrite	Inorganic	Both	0	conservative assumption	0	—	—
7723-14-0	Phosphorus	Inorganic	Both	3.5	ORNL	2	—	—
7782-49-2	Selenium	Inorganic	Both	5	CLARC 3.1	5	—	—
7440-22-4	Silver	Inorganic	Both	8.3	CLARC 3.1	5	—	—
7440-24-6	Strontium	Inorganic	Both	25	100 Area RDR/RAWP, DOE/RL-96-17	5	—	—
7440-28-0	Thallium	Inorganic	Both	71	CLARC 3.1	5	—	—
7440-31-5	Tin	Inorganic	Both	250	ORNL 12/8/08	5	—	—
7440-32-6	Titanium	Inorganic	Both	1,000	ORNL	5	—	—
7440-61-1	Uranium	Inorganic	Both	2	TC&WM EIS, PNNL-15503 and PNNL-15617	0.6	0.2	2
7440-62-2	Vanadium	Inorganic	Both	1,000	CLARC 3.1	5	—	—

Table 4-8. Distribution Coefficients (mL/g) for Non-Radiological Constituents that are Part of the Waste Management Area C Inventory. (5 sheets)

CAS	Constituent	Group	Part Of	K_d (mL/g)	K_d Source	To Be Used in WMA C PA K_d		
						Denominator	Minimum	Maximum
7440-66-6	Zinc	Inorganic	Both	62	CLARC 3.1	5	—	—
75-34-3	1,1 Dichloroethane	Organic	Both	0.053	CLARC 3.1 Kd=Koc/1,000	0.02	—	—
71-55-6	1,1,1-Trichloroethane	Organic	Both	0.135	CLARC 3.1 Kd=Koc/1,000	0.1	—	—
79-34-5	1,1,2,2-Tetrachloroethane	Organic	Both	0.079	CLARC 3.1 Kd=Koc/1,000	0.02	—	—
127-18-4	1,1,2,2-Tetrachloroethene	Organic	Both	0.265	CLARC Kd=Koc/1,000	0.2	—	—
76-13-1	1,1,2-Trichloro-1,2,2-trifluoroethane	Organic	Both	0.2247	ORNL	0.2	—	—
79-00-5	1,1,2-Trichloroethane	Organic	Both	0.075	CLARC 3.1 Kd=Koc/1,000	0.02	—	—
79-01-6	1,1,2-Trichloroethylene	Organic	Both	0.094	CLARC 3.1 Kd=Koc/1,000	0.02	—	—
92-52-4	1,1'-Biphenyl	Organic	CMS_SAP	6.25	ORNL	5	—	—
75-35-4	1,1-Dichloroethene	Organic	Both	0.065	CLARC 3.1 Kd=Koc/1,000	0.02	—	—
57-14-7	1,1-Dimethylhydrazine	Organic	CMS_SAP	0.012	ORNL Kd=Koc/1,000	0	—	—
120-82-1	1,2,4-Trichlorobenzene	Organic	Both	1.659	CLARC 3.1 Kd=Koc/1,000	1	—	—
107-06-2	1,2-Dichloroethane	Organic	Both	0.038	CLARC 3.1 Kd=Koc/1,000	0.02	—	—
78-87-5	1,2-Dichloropropane	Organic	CMS_SAP	0.047	CLARC 3.1 Kd=Koc/1,000	0.02	—	—
106-99-0	1,3-Butadiene	Organic	CMS_SAP	0.0438	ORNL	0.02	—	—
541-73-1	1,3-Dichlorobenzene	Organic	CMS_SAP	0.434	ORNL	0.2	—	—
106-46-7	1,4-Dichlorobenzene	Organic	Both	0.616	CLARC 3.1 Kd=Koc/1,000	0.6	—	—
100-25-4	1,4-Dinitrobenzene	Organic	CMS_SAP	0.2201	ORNL	0.2	—	—
123-91-1	1,4-Dioxane	Organic	CMS_SAP	0.001	ORNL	0	—	—
95-95-4	2,4,5-Trichlorophenol	Organic	Both	1.597	CLARC 3.1 Kd=Koc/1,000	1	—	—
88-06-2	2,4,6-Trichlorophenol	Organic	Both	0.381	CLARC 3.1 Kd=Koc/1,000	0.2	—	—
121-14-2	2,4-Dinitrotoluene	Organic	Both	0.0955	CLARC 3.1 Kd=Koc/1,000	0.02	—	—
78-93-3	2-Butanone(MEK)	Organic	Both	0.027	ORNL	0.02	—	—
95-57-8	2-Chlorophenol	Organic	Both	0.388	CLARC 3.1 Kd=Koc/1,000	0.2	—	—
110-80-5	2-Ethoxyethanol	Organic	Both	0.001	ORNL	0	—	—
591-78-6	2-Hexanone	Organic	CMS_SAP	0.01302	ORNL	0	—	—
126-98-7	2-Methyl-2-propenenitrile	Organic	CMS_SAP	0.01283	ORNL	0	—	—
95-48-7	2-Methylphenol (o-cresol)	Organic	Both	0.443	ORNL	0.2	—	—
79-46-9	2-Nitropropane	Organic	Both	0.02495	ORNL	0.02	—	—
67-64-1	2-Propanone (Acetone)	Organic	Both	0.000575	CLARC 3.1 Kd=Koc/1,000	0	—	—
88-85-7	2-sec-Butyl-4,6-dinitrophenol (Dinoseb)	Organic	CMS_SAP	3.54	ORNL	2	—	—
107-05-1	3-Chloropropene (Allyl chloride)	Organic	CMS_SAP	0.0396	ORNL Kd=Koc/1,000	0.02	—	—
108-10-1	4-Methyl-2-pentanone (MIBK)	Organic	Both	0.8	ORNL	0.6	—	—

Table 4-8. Distribution Coefficients (mL/g) for Non-Radiological Constituents that are Part of the Waste Management Area C Inventory. (5 sheets)

CAS	Constituent	Group	Part Of	K_d (mL/g)	K_d Source	To Be Used in WMA C PA K_d		
						Denominator	Minimum	Maximum
106-44-5	4-Methylphenol (p-cresol)	Organic	Both	0.434	ORNL	0.2	—	—
83-32-9	Acenaphthene	Organic	Both	4.898	CLARC 3.1 Kd=Koc/1,000	2	—	—
75-05-8	Acetonitrile	Organic	CMS_SAP	0.045	ORNL	0.02	—	—
98-86-2	Acetophenone	Organic	CMS_SAP	0.0462	ORNL	0.02	—	—
107-02-8	Acrolein (propenal)	Organic	CMS_SAP	0.00276	ORNL	0	—	—
107-13-1	Acrylonitrile	Organic	CMS_SAP	0.0083	ORNL	0	—	—
309-00-2	Aldrin*	Organic	Both	48.69	CLARC 3.1 Kd=Koc/1,000	5	—	—
319-84-6	alpha-BHC*	Organic	CMS_SAP	1.762	CLARC 3.1 Kd=Koc/1,000	1	—	—
71-43-2	Benzene	Organic	Both	0.062	CLARC 3.1 Kd=Koc/1,000	0.02	—	—
56-55-3	Benzo(a) anthracene	Organic	CMS_SAP	357	CLARC 3.1 Kd=Koc/1,000	5	—	—
50-32-8	Benzo(a)pyrene	Organic	Both	969	CLARC 3.1 Kd=Koc/1,000	5	—	—
205-99-2	Benzo(b)fluoranthene	Organic	CMS_SAP	1230	CLARC 3.1 Kd=Koc/1,000	5	—	—
207-08-9	Benzo(k)fluoranthene	Organic	CMS_SAP	1230	CLARC 3.1 Kd=Koc/1,000	5	—	—
319-85-7	beta-BHC*	Organic	CMS_SAP	2.139	CLARC 3.1 Kd=Koc/1,000	2	—	—
117-81-7	Bis(2-ethylhexyl)phthalate	Organic	CMS_SAP	111.1	CLARC 3.1 Kd=Koc/1,000	5	—	—
74-83-9	Bromomethane	Organic	CMS_SAP	0.009	CLARC 3.1 Kd=Koc/1,000	0	—	—
85-68-7	Butylbenzylphthalate	Organic	Both	13.75	CLARC 3.1 Kd=Koc/1,000	5	—	—
75-15-0	Carbon disulfide	Organic	Both	0.0457	CLARC 3.1 Kd=Koc/1,000	0.02	—	—
56-23-5	Carbon tetrachloride	Organic	Both	0.152	CLARC 3.1 Kd=Koc/1,000	0.1	—	—
108-90-7	Chlorobenzene	Organic	Both	0.224	CLARC 3.1 Kd=Koc/1,000	0.2	—	—
75-45-6	Chlorodifluoromethane	Organic	CMS_SAP	0.0318	ORNL Kd=Koc/1,000	0.02	—	—
75-00-3	Chloroethane	Organic	CMS_SAP	0.02374	ORNL	0.02	—	—
75-01-4	Chloroethene(vinyl chloride)	Organic	Both	0.0186	CLARC 3.1 Kd=Koc/1,000	0	—	—
67-66-3	Chloroform	Organic	Both	0.053	CLARC 3.1 Kd=Koc/1,000	0.02	—	—
74-87-3	Chloromethane	Organic	CMS_SAP	0.0143	ORNL	0	—	—
218-01-9	Chrysene	Organic	CMS_SAP	398	CLARC 3.1 Kd=Koc/1,000	5	—	—
156-59-2	Cis-1,2-dichlorobenzene	Organic	CMS_SAP	0.0355	CLARC 3.1 Kd=Koc/1,000	0.02	—	—
108-94-1	Cyclohexanone	Organic	Both	0.01515	ORNL	0	—	—
53-70-3	Dibenz(a,h)anthracene	Organic	Both	1789	CLARC 3.1 Kd=Koc/1,000	5	—	—
75-71-8	Dichlorodifluoromethane	Organic	CMS_SAP	0.04864	ORNL	0.02	—	—
75-09-2	Dichloromethane (methylene chloride)	Organic	Both	0.01	CLARC 3.1 Kd=Koc/1,000	0	—	—
60-57-1	Dieldrin*	Organic	Both	25.55	CLARC 3.1 Kd=Koc/1,000	5	—	—
60-29-7	Diethyl ether	Organic	Both	0.004395	ORNL	0	—	—

Table 4-8. Distribution Coefficients (mL/g) for Non-Radiological Constituents that are Part of the Waste Management Area C Inventory. (5 sheets)

CAS	Constituent	Group	Part Of	K_d (mL/g)	K_d Source	To Be Used in WMA C PA K_d		
						Denominator	Minimum	Maximum
84-74-2	Di-n-butylphthalate	Organic	Both	1.567	CLARC 3.1 Kd=Koc/1,000	1	—	—
117-84-0	Di-n-octylphthalate	Organic	Both	83,200	CLARC 3.1 Kd=Koc/1,000	5	—	—
72-20-8	Endrin*	Organic	Both	10.81	CLARC 3.1 Kd=Koc/1,000	5	—	—
141-78-6	Ethyl Acetate	Organic	Both	0.006131	ORNL	0	—	—
100-41-4	Ethylbenzene	Organic	Both	0.204	CLARC 3.1 Kd=Koc/1,000	0.2	—	—
106-93-4	Ethylene dibromide (1,2, Dibromoethane)	Organic	CMS_SAP	0.0438	ORNL	0.02	—	—
107-21-1	Ethylene glycol	Organic	CMS_SAP	0.001	ORNL	0	—	—
206-44-0	Fluoranthene	Organic	Both	49.1	CLARC 3.1 Kd=Koc/1,000	5	—	—
58-89-9	gamma-BHC (Lindane)*	Organic	Both	1.352	CLARC 3.1 Kd=Koc/1,000	1	—	—
76-44-8	Heptachlor	Organic	Both	9.528	CLARC 3.1 Kd=Koc/1,000	5	—	—
118-74-1	Hexachlorobenzene	Organic	Both	80	CLARC 3.1 Kd=Koc/1,000	5	—	—
87-68-3	Hexachlorobutadiene	Organic	Both	53.7	CLARC 3.1 Kd=Koc/1,000	5	—	—
67-72-1	Hexachloroethane	Organic	Both	1.78	CLARC 3.1 Kd=Koc/1,000	1	—	—
193-39-5	Indeno (1,2,3-cd) pyrene	Organic	CMS_SAP	3470	CLARC 3.1 Kd=Koc/1,000	5	—	—
78-83-1	Isobutanol	Organic	Both	0.37	ORNL	0.2	—	—
108-39-4	m-Cresol (3-Methylphenol)	Organic	Both	0.434	ORNL	0.2	—	—
67-56-1	Methanol	Organic	CMS_SAP	0.001	ORNL	0	—	—
60-34-4	Methylhydrazine	Organic	CMS_SAP	0.0133	ORNL Kd=Koc/1,000	0	—	—
122-39-4	N,N-Diphenylamine	Organic	CMS_SAP	1.887	ORNL	1	—	—
91-20-3	Naphthalene	Organic	Both	1.191	CLARC 3.1 Kd=Koc/1,000	1	—	—
71-36-3	n-Butyl alcohol (1-butanol)	Organic	Both	0.00692	CLARC 3.1 Kd=Koc/1,000	0	—	—
110-54-3	n-Hexane	Organic	CMS_SAP	3.41	CLARC 3.1 Kd=Koc/1,000	2	—	—
98-95-3	Nitrobenzene	Organic	Both	0.119	CLARC 3.1 Kd=Koc/1,000	0.1	—	—
924-16-3	n-Nitrosodi-n-butylamine	Organic	CMS_SAP	1.651	ORNL	1	—	—
621-64-7	N-nitroso-di-n-propylamine	Organic	Both	0.024	CLARC 3.1 Kd=Koc/1,000	0.02	—	—
10595-95-6	n-Nitrosomethylethylamine	Organic	CMS_SAP	0.0435	ORNL Kd=Koc/1,000	0.02	—	—
62-75-9	N-Nitroso-N,N-dimethylamine	Organic	CMS_SAP	0.03821	ORNL	0.02	—	—
95-50-1	o-Dichlorobenzene	Organic	Both	0.379	CLARC 3.1 Kd=Koc/1,000	0.2	—	—
75-21-8	Oxirane	Organic	CMS_SAP	0.001435	ORNL	0	—	—
82-68-8	Pentachloronitrobenzene (PCNB)	Organic	CMS_SAP	2.406	ORNL	2	—	—
87-86-5	Pentachlorophenol	Organic	Both	0.592	CLARC 3.1 Kd=Koc/1,000	0.2	—	—
108-95-2	Phenol	Organic	Both	0.0288	CLARC 3.1 Kd=Koc/1,000	0.02	—	—
129-00-0	Pyrene	Organic	Both	67.99	CLARC 3.1 Kd=Koc/1,000	5	—	—

Table 4-8. Distribution Coefficients (mL/g) for Non-Radiological Constituents that are Part of the Waste Management Area C Inventory. (5 sheets)

CAS	Constituent	Group	Part Of	K_d (mL/g)	K_d Source	To Be Used in WMA C PA K_d		
						Denominator	Minimum	Maximum
110-86-1	Pyridine	Organic	Both	0.03301	ORNL	0.02	—	—
100-42-5	Styrene	Organic	CMS_SAP	0.912	CLARC 3.1 Kd=Koc/1,000	0.6	—	—
108-88-3	Toluene	Organic	Both	0.14	CLARC 3.1 Kd=Koc/1,000	0.1	—	—
8001-35-2	Toxaphene*	Organic	CMS_SAP	95.82	CLARC 3.1 Kd=Koc/1,000	5	—	—
126-73-8	Tributyl phosphate	Organic	Both	1.89	ORNL	1	—	—
75-69-4	Trichlorofluoromethane	Organic	Both	0.04864	ORNL	0.02	—	—
121-44-8	Triethylamine	Organic	CMS_SAP	0.1072	ORNL	0.1	—	—
1330-20-7	Xylenes	Organic	Both	0.233	CLARC 3.1 Kd=Koc/1,000	0.2	—	—
12674-11-2	Aroclor 1016	Organic	Both	107.3	CLARC 3.1 Kd=Koc/1,000	5	—	—
11104-28-2	Aroclor 1221	Organic	Both	10.3	ORNL	5	—	—
11141-16-5	Aroclor 1232	Organic	Both	10.3	ORNL	5	—	—
53469-21-9	Aroclor 1242	Organic	Both	44.8	ORNL	5	—	—
12672-29-6	Aroclor 1248	Organic	Both	43.9	ORNL	5	—	—
11096-82-5	Aroclor 1260	Organic	Both	822.4	CLARC 3.1 Kd=Koc/1,000	5	—	—
11097-69-1	Aroclor 1254	Organic	Both	75.6	ORNL	5	—	—
100-02-7	4-Nitrophenol	Organic	TankDQO	0.309	ORNL	0.2	—	—
57-74-9	Chlordane	Pesticides	CMS_SAP	51.31	CLARC 3.1 Kd=Koc/1,000	5	—	—
—	DDT/DDD/DDE (total)	Pesticides	CMS_SAP	677.9	CLARC 3.1 Kd=Koc/1,000	5	—	—

CAS = Chemical Abstracts Service
DQO = data quality objective
ORNL = Oak Ridge National Laboratory
WMA C PA = Waste Management Area C Performance Assessment

References:

DOE/EIS-0391, *Draft Tank Closure and Waste Management Environmental Impact Statement for the Hanford Site, Richland, Washington* (TC & WM EIS).
DOE/RL-96-17, *Remedial Design Report Remedial Action Work Plan for the 100 Area (100 Area RDR/RAWP)*.
PNNL-13895, *Hanford Contaminant Distribution Coefficient Database and Users Guide*.
PNNL-15503, *Characterization of Vadose Zone Sediments Below the C Tank Farm: Borehole C4297 and RCRA Borehole 299-E27-22*.
PNNL-15617, *Characterization of Vadose Zone Sediments from C Waste Management Area: Investigation of the C-152 Transfer Line Leak.*
WAC 173-340, "Model Toxics Control Act – Cleanup," *Washington Administrative Code*, as amended.
Washington State Department of Ecology Toxics Clean-up Program Publication No. 94-145, *Model Toxics Control Act Cleanup Levels & Risk Calculations (CLARC) Version 3.1* (CLARC 3.1).

Table 4-9. Distribution Coefficients (mL/g) for Radiological Constituents that are Part of the Waste Management Area C Inventory. (2 sheets)

Constituent	Part Of	Radionculide[1] K_d (mL/g)	Hanford Measured K_d[2]			WMA C Measured K_d[3]			To Be Used in WMA C PA K_d		
			Best	Minimum	Maximum	Recommended	Minimum	Maximum	Denominator	Minimum	Maximum
Tritium	Both	—	0	0	0	—	—	—	0	—	—
Carbon-14	Both	—	7	0	100	—	—	—	5	0	—
Cobalt-60	Both	0.1	—	—	—	—	—	—	0.1	—	—
Nickel-63	Both	34	—	—	—	—	—	—	5	—	—
Selenium-79	Both	—	0	0	1	—	—	—	0	—	—
Strontium-90	Both	—	22	10	50	—	—	—	5	—	—
Technetium-99	Both	—	0	0	0.1	0	0	0.51	0	—	—
Antimony-125	Both	45	—	—	—	—	—	—	5	—	—
Tin-126	CMS_ SAP	250	—	—	—	—	—	—	5	—	—
Iodine-129	Both	—	0.1	0	0.2	—	—	—	0.1	0	0.2
Cesium-137	Both	—	100	10	1,000	—	—	—	5	—	—
Europium-152	Both	—	200	10	1,000	—	—	—	5	—	—
Europium-154	Both	—	200	10	1,000	—	—	—	5	—	—
Europium-155	Both	—	200	10	1,000	—	—	—	5	—	—
Thorium-228	CMS_ SAP	20	—	—	—	—	—	—	5	—	—
Thorium-230	Both	20	—	—	—	—	—	—	5	—	—
Thorium-232	Both	20	—	—	—	—	—	—	5	—	—
Thorium-234	CMS_ SAP	20	—	—	—	—	—	—	5	—	—
Uranium-233	Both	—	0.8	0.2	4	1	1.09	8.32	0.6	0.2	2
Uranium-234	Both	—	0.8	0.2	4	1	1.09	8.32	0.6	0.2	2
Uranium-235	Both	—	0.8	0.2	4	1	1.09	8.32	0.6	0.2	2
Uranium-236	Both	—	0.8	0.2	4	1	1.09	8.32	0.6	0.2	2
Uranium-238	Both	—	0.8	0.2	4	1	1.09	8.32	0.6	0.2	2
Uranium-238	Both	—	0.8	0.2	4	1	1.09	8.32	0.6	0.2	2
Neptunium-237	Both	—	200	100	500	—	—	—	5	—	—
Plutonium-239/240	Both	—	190	62	620	—	—	—	5	—	—

Table 4-9. Distribution Coefficients (mL/g) for Radiological Constituents that are Part of the Waste Management Area C Inventory. (2 sheets)

Constituent	Part Of	Radionculide[1] K_d (mL/g)	Hanford Measured K_d[2]			WMA C Measured K_d[3]			To Be Used in WMA C PA K_d		
			Best	Minimum	Maximum	Recommended	Minimum	Maximum	Denominator	Minimum	Maximum
Plutonium-241	CMS_ SAP	—	190	62	620	—	—	—	5	—	—
Americium-241	Both	82	—	—	—	—	—	—	5	—	—
Curium-242	Both	86	—	—	—	—	—	—	5	—	—
Curium-243	CMS_ SAP	86	—	—	—	—	—	—	5	—	—
Curium-244	CMS_ SAP	86	—	—	—	—	—	—	5	—	—
Niobium-94	Tank DQO	—	—	—	—	—	—	—	—	—	—
Ruthenium/ Rhodium-106	Tank DQO	0	—	—	—	—	—	—	0	—	—
Cesium-134	Tank DQO	62	—	—	—	—	—	—	5	—	—
Cerium/ Praseodymium-144	Tank DQO	35	—	—	—	—	—	—	5	—	—
Radium-226	Tank DQO	3	—	—	—	—	—	—	2	—	—
Actinium-228	Tank DQO	1 to 10	—	—	—	—	—	—	5	—	—
Curium-243/244	Tank DQO	82	—	—	—	—	—	—	5	—	—

[1] K_d not measured on the Hanford Site taken from Oak Ridge National Laboratory Risk Assessment System

[2] K_d measured on the Hanford Site; please see PNNL-13895, *Hanford Contaminant Distribution Coefficient Database and Users Guide* and PNNL-14702, *Vadose Zone Hydrogeology Data Package for Hanford Assessments*.

[3] K_d estimated at WMA C based on the ratio of contaminant in the pore water to that on the sediment; please see PNNL-15503, *Characterization of Vadose Zone Sediments Below the C Tank Farm: Borehole C4297 and RCRA Borehole 299-E27-22* and PNNL-15617, *Characterization of Vadose Zone Sediments from C Waste Management Area: Investigation of the C-152 Transfer Line Leak*.

DQO = data quality objective
PA = performance assessment
WMA = waste management area

Many of the bulk distribution coefficient (K_d) for non-radiological constituents that are listed in Tables 4-7 are taken directly from tables in the "Chemical-Specific Parameter Values - Physical and Chemical Properties" Section of Ecology Publication No. 94-145. The publication has been superseded by the establishment of CLARC Database located at https://fortress.wa.gov/ecy/clarc/Reporting/CLARCReporting.aspx

Contaminant K_d values for many of the organic chemicals were estimated using the organic carbon partition coefficients (K_{oc}) method described in EPA 402-R-99-004A, *Understanding Variation in Partition Coefficient, K_d, Values*, and an estimated fractional organic carbon content for Hanford Site sediments of 0.03% (PNNL-14702).

Contaminants for which inventory estimates exist and that do not have an assigned K_d value are assumed to have a $K_d = 0$. A soil material description of low organic, low salt, with a near-neutral pH is assumed.

With the exception of uranium, no WMA C-specific measurements for K_d exist so a single value is shown. For uranium, however, PNNL-15503 and PNNL-15617, *Characterization of Vadose Zone Sediments from C Waste Management Area: Investigation of the C-152 Transfer Line Leak* present estimated uranium K_ds from 83 samples taken within WMA C from uranium concentrations on the sediments and in the pore water. For uranium, it was found that the natural background concentrations must be separated from Hanford-added material in discussing risk potential. Natural uranium is almost entirely resistant to water leaching and becoming mobile, whereas the material added by Hanford activities appears to have some mobility. The range for uranium K_ds related to Hanford activities based on samples taken at WMA C ranged from 1.09 to 8.32 and these reports recommended a value of 1.0 for WMA C. However, to be consistent with "Technical Guidance Document for Tank Closure Environmental Impact Statement Vadose Zone and Groundwater Revised Analyses" (http://www.hanford.gov/orp/uploadfiles/TCEIS-Vadose.pdf), this report is recommending a value 0.6 mL/g with sensitivities of 0.2 mL/g and 2.0 mL/g because of the greater range of uranium K_d observed in the 200 Areas of Hanford (PNNL-13895, *Hanford Contaminant Distribution Coefficient Database and Users Guide*, Rev. 1).

Because of relatively large number of constituents, the approach used in the WMA C PA will not explicitly evaluate each specific K_d designated for each constituent. To minimize the number of required simulations, the analysis will focus on examination of modeling results using a specified number of K_d classes within which each constituent would be assigned. Because of the time-frame of interest, the assessment will primarily focus on a limited range of K_ds (0 to 5 mL/g). At this point, we anticipated using a total of eight K_d classes (0, 0.02, 0.1, 0.2, 0.6, 1.0, 2.0, and 5.0 mL/g). For each particular constituent of interest, it would be assigned to the next lowest K_d class based on its designated K_d value. For example, if a constituent's designated K_d is a value of 0.55 mL/g, it would be assigned to the 0.2 mL/g K_d class. The assigned K_d to be used is shown in the denominator case.

Based on input received during the review of this data package during the Natural System working session held May 25 to 27, 2010, and in subsequent review of the modeling cases focused on the Natural System during the Engineered System working session held in January 25

to 27, 2010, alternative models are proposed that would examine the effect of using non-linear adsorption isotherms. Commonly used non-linear adsorption isotherms include those based on the Freundlich and Langmuir approaches. These cases would be used to evaluate uranium mobility based on data and analysis performed in the B-Complex area that does not appear to follow a linear isotherm. Specific parameterization of these specific sensitivities will be developed and evaluated at a later date using scoping calculations.

Freundlich sorption isotherm is a more general equilibrium isotherm. It is shown graphically in Figure 4-9 and mathematically given by

$$S = K_f C^N$$

where K_f is the Freundlich adsorption constant, N is the Freundlich exponent, C is the solution concentration (mg/L), and S is the adsorbed concentration in mg/kg (Ground Water Contamination – Transport and Remediation [Bedient et al. 1994]).

Figure 4-9. Example Plots of Freundlich Isotherm in Terms of S versus C using Freundlich Adsorption Constant (K_f) Ranging from 1 to 10 and and Freundlich Exponent (N) of 0.6.

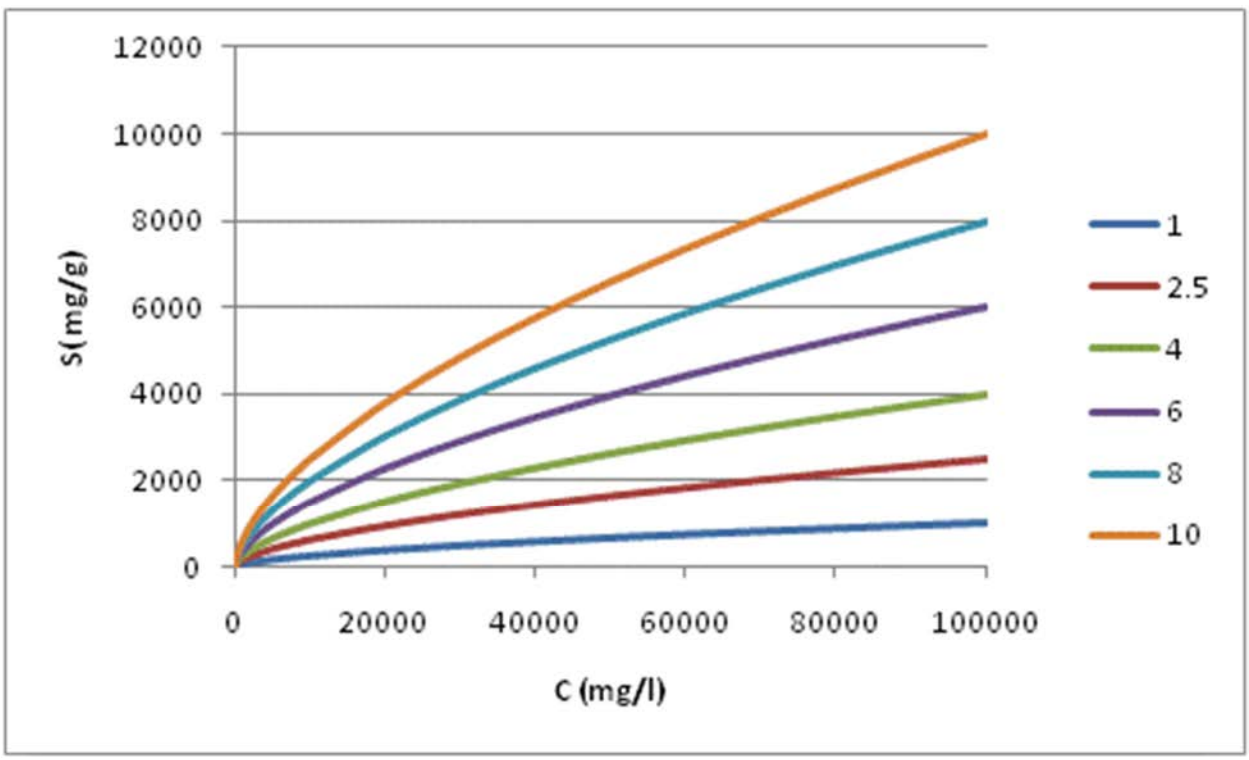

The Langmuir Isotherm is based on the concept that a solid surface possesses a finite number of sorption sites. When all the sorption sites are filled, the surface will no longer sorb solute from solution. The Langmuir isotherm is given by

$$S = \frac{\alpha\beta C}{1 + \alpha C}$$

where α is an absorption constant related to the binding energy (L/mg), and β is a maximum amount of solute that can be sorbed by the solid (mg/kg) (see Figure 4-10). C is the solution concentration (mg/L) and S is the adsorbed concentration in mg/kg (Bedient et al. 1994).

Figure 4-10. Example Plots of Langmuir Adsorption Isotherm in Terms of S versus C Using a Binding Energy Constant (α) Ranging from 0.001 to 1 L/mg and Maximum Amount of Solute Sorbed onto Solid (β) of 100 mg/kg.

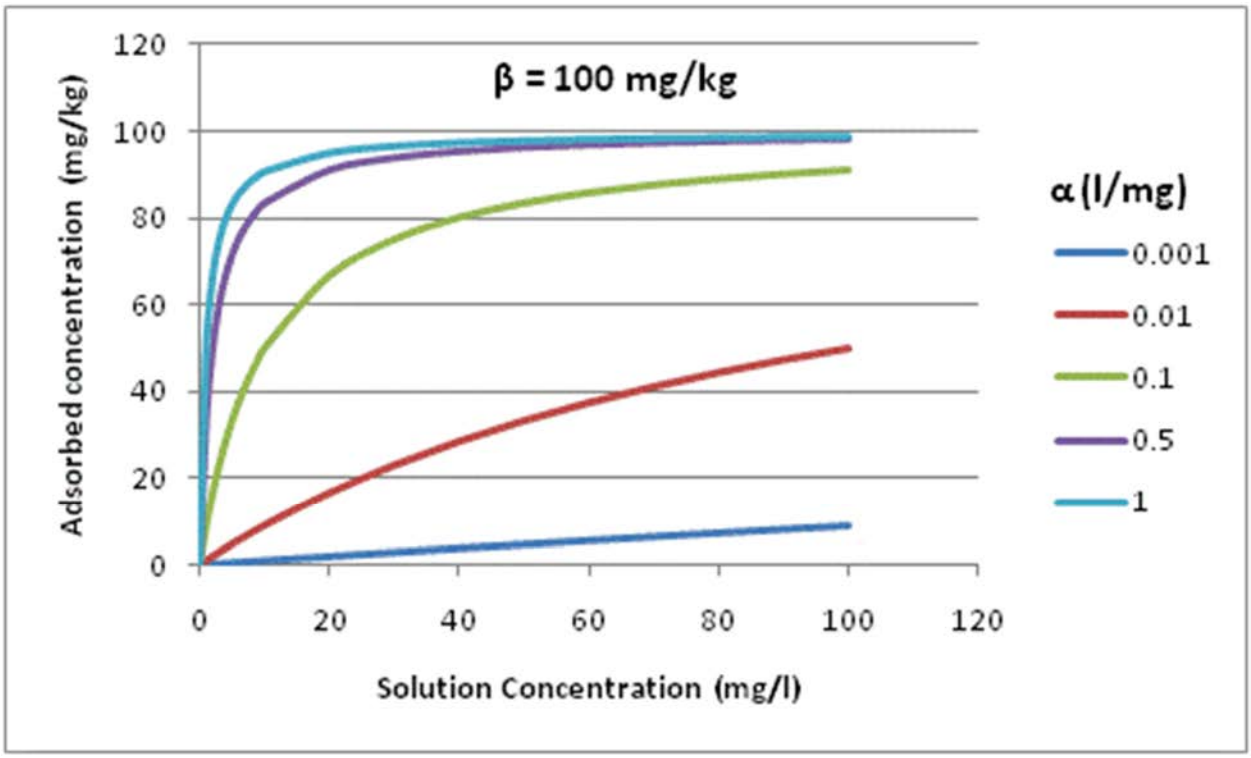

5.0 GROUNDWATER SYSTEM AT WASTE MANAGEMENT AREA C

This section provides a summary of the groundwater system at WMA C which includes a brief description of the uppermost unconfined aquifer system including a discussion of the historic and recent groundwater data collected beneath the 200 East Area with emphasis on the C Tank Farm. Most of the information in this section is derived from RPP-23748, *Geology, Hydrogeology, Geochemistry, and Mineralogy Data Package for the Single-Shell Tank Waste Management Areas at the Hanford Site* and PNNL-15301. This section also provides a summary of potential key FEPs operating within the unconfined aquifer and the associated conceptual models of groundwater flow and transport that may need to be considered in the WMA C PA. Finally, this section provides recommendations for groundwater flow and transport properties that would be appropriate to use in numerical modeling of local-scale flow and transport at WMA C.

Key features have been identified as potentially important to consider in conceptual models of the vadose zone at WMA C and in the scope of the WMA C PA calculations and related sensitivity analyses. A list of potential key FEPs have not been specifically discussed in a WMA C PA Working Session to date. A summary of FEPs related to the groundwater system are presented for consideration in Appendix E. The FEPs are identified for two time periods: 1) the time extending from the operational period through the end of the retrieval, remediation, and correction action period and 2) future projected conditions. The FEPs identified for past to present conditions and for projected future conditions are summarized in Tables E-1 through E-3 in Appendix E. The key general features that were identified for the groundwater for these time periods include the following general categories.

Properties of the Major Hydrogeologic Units: The SST and related facilities at WMA C are constructed in Hanford formation sediments, and below the water table at depth of about 80 m these facilities are underlain by an undifferentiated unit composed of Hanford formation gravel and/or CCU (l) gravel and/or Ringold Formation, unit A referred to as the H3/CCU/R unit.

Descriptions of the general properties of the units within the unconfined aquifer beneath WMA C are provided in Section 3.7 and Appendix B. All interpretations of major units along lines of section in the general area of WMA C are shown in Figure B-1 of Appendix B and are provided in Figures B-1 through B-7. Three of the seven cross sections (Sections A-A', D-D', and G-G' shown in Figures B-1, B-4, and B-7) illustrate the distribution and thicknesses of these units relevant to the unconfined aquifer in the immediate vicinity of WMA C. Discussions of hydraulic properties of these sediments are presented in Sections 5.2 and 5.5.1. A discussion of transport properties of these sediments is given in Section 5.6.

General Flow Conditions in the Groundwater: Since the start of Hanford Site operations in the mid-1940s, artificial recharge from wastewater disposal facilities has been several times greater than the estimated recharge from natural sources. This caused an increase in the water-table elevation over most of the Hanford Site and the formation of groundwater mounds beneath major wastewater disposal facilities. In vicinity of WMA C, long-term hydrographs of water-level measurements suggests that unconfined aquifer has risen as much as 5 m in response to the artificial recharge from nearby wastewater disposal facilities. More detailed discussions of

regional flow in the unconfined aquifer and hydraulic impacts from past operations are provided in Sections 5.1 and 5.3.

Current Water Chemistry and Contamination in Groundwater: Waste releases from past operations at WMA C and nearby facilities has also had a significant impact to water quality in the immediate vicinity of WMA C. A detailed discussion of these impacts is provided in Section 5.4.

5.1 UPPERMOST AQUIFER SYSTEM

Aquifers at the Hanford Site are divided into 1) confined, and 2) suprabasalt or unconfined, aquifer systems. The regional, confined aquifer system occurs within the CRBG and extends from western Idaho through eastern Washington and northeastern Oregon (RHO-BWI-ST-4). Basalt-confined aquifers beneath the Hanford Site are grouped into three separate hydrogeologic units corresponding to the three basalt formations discussed above: from deepest to shallowest, the Grande Ronde, Wanapum, and Saddle Mountains (DOE/RW-0164). The basalt-confined aquifers are composed of intraflow zones (mainly flow tops) between the relatively impermeable interiors of basalt flows. The unconfined aquifer system occurs within fluvial, lacustrine, and glacio-fluvial sediments deposited on top of the Columbia River Basalts.

The sediment above the basalt in which groundwater occurs is subdivided into the glacio-fluvial sands and gravels of the Hanford formation, the fluvial-lacustrine sediments of the Ringold Formation, and the CCU which is primarily reworked sediment of the Ringold Formation. The suprabasalt aquifer system is approximately 180 m thick near the center of the Cold Creek syncline but thins laterally, anticlinal basalt ridges that extend above the water table. It is thickest in the Wye Barricade depression and the Cold Creek Depression (see Figure 3-4). A generalized east to west geologic cross section showing the position of the water table and major stratigraphic units beneath the Hanford Site is shown in Figure 5-1.

The base of the suprabasalt aquifer in the vicinity of WMA C is the basalt surface. Sediment below SST WMA C consists primarily of the undifferentiated lower sands and gravels associated with the Hanford formation, CCU, and the Ringold Formation (Unit A) which lie in an eroded channel caused by the cataclysmic floods of the Pleistocene. Away from SST WMA C where the Ringold Formation is present in the suprabasalt aquifer, the silt and clay horizon of the formation's hydrogeologic unit 8 (lower mud unit) forms a confining layer that separates the suprabasalt aquifer into the uppermost and unconfined aquifer and an underlying confined or semi-confined aquifer in the Ringold Formation. The hydrogeologic unit 8 occurs at or above the water table east of the 200 East Area and in an area between the 200 East and 200 West Areas. The lower mud unit thus creates a thinning of the unconfined aquifer and a barrier to eastward groundwater flow in very localized areas.

The general direction of groundwater flow is primarily from natural recharge areas on the basalt ridges west of the Hanford Site to discharge along the Columbia River (see Figure 5-2). The general west to east flow was interrupted locally by artificial groundwater mounds that developed in the unconfined aquifer in the 200 Areas due to artificial recharge from liquid waste

disposal operations that began in the 1940s. Artificial recharge, estimated to be 10 times natural recharge, created large water-table mounds primarily below the 200 East and 200 West Areas. Since cessation of these discharges, the water table has declined about 6 m in the 200 East Area from the highest, historic water levels and flow directions of the unconfined aquifer are returning to pre-Hanford Site directions toward the east. A component of groundwater flow and contaminant transport also exists to the north, between Gable Mountain and Gable Butte.

Figure 5-1. Generalized Geologic Cross-Section through the Hanford Site.

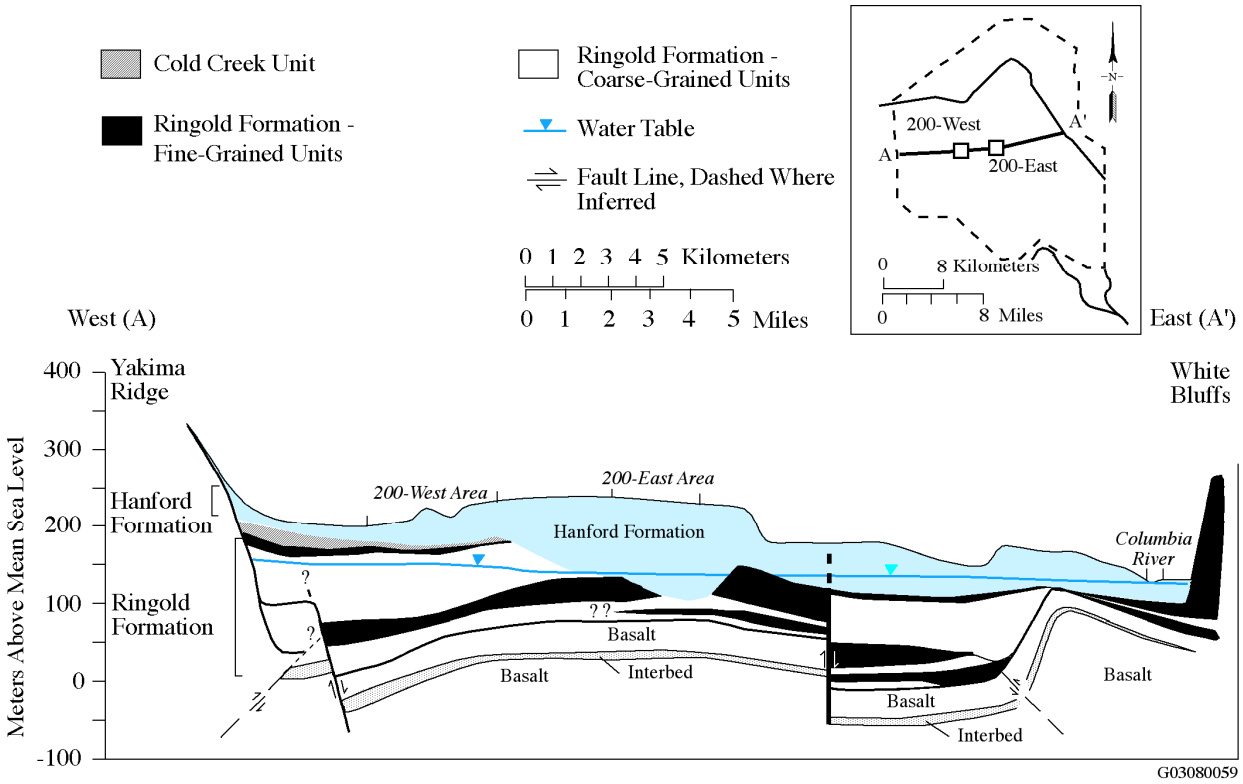

Note: Location of cross-section A-A' is shown as west-east line on outline of Hanford Site in upper right.

Recharge from agricultural activities offsite and west of the Hanford Site also has affected the groundwater. The continued use of irrigation upgradient of the Hanford Site is expected to sustain recharge to the unconfined aquifer.

The regional-scale interpretation of the water-table elevation in Figure 5-2 from DOE/RL-2008-66, *Hanford Site Groundwater Monitoring for Fiscal Year 2008* infers a groundwater flow divide likely occurs in the 200 East Area with southeast flow in the southern part of this area (Figure 5-3). However, small differences in water elevations make it difficult to define the exact location of this groundwater divide.

In the Northwest quadrant of 200 East Area near the WMA B-BX-BY and LLWMA 1, the average flow direction has been interpreted in DOE/RL-2008-66 to be to the north-northwest through Gable Gap.

Figure 5-2. Hanford Site and Outlying Areas Water Table Map, March 2008.

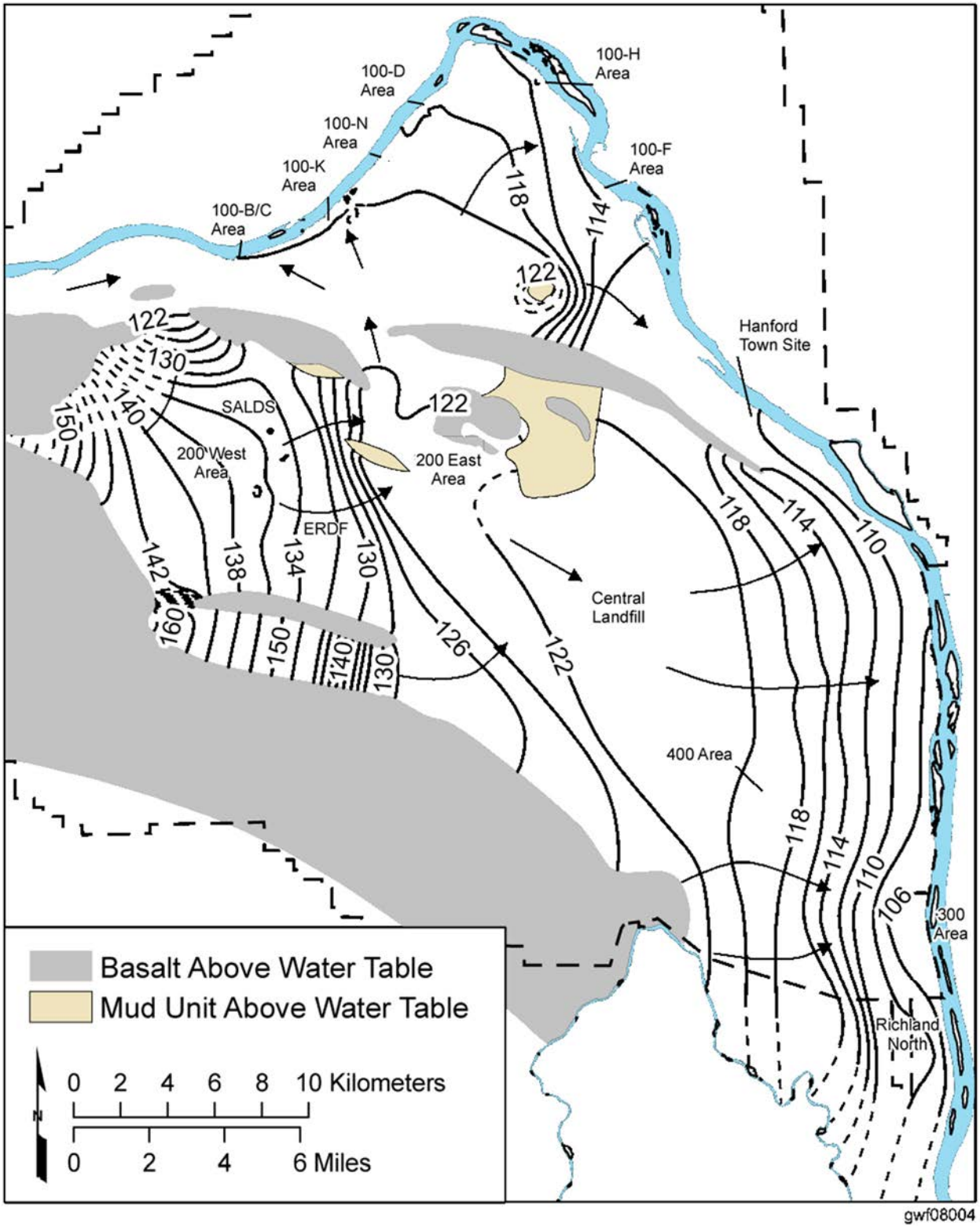

Modified from DOE/RL-2008-66, *Hanford Site Groundwater Monitoring for Fiscal Year 2008.*

Figure 5-3. Distribution of Water-Table Elevations, March 2008.

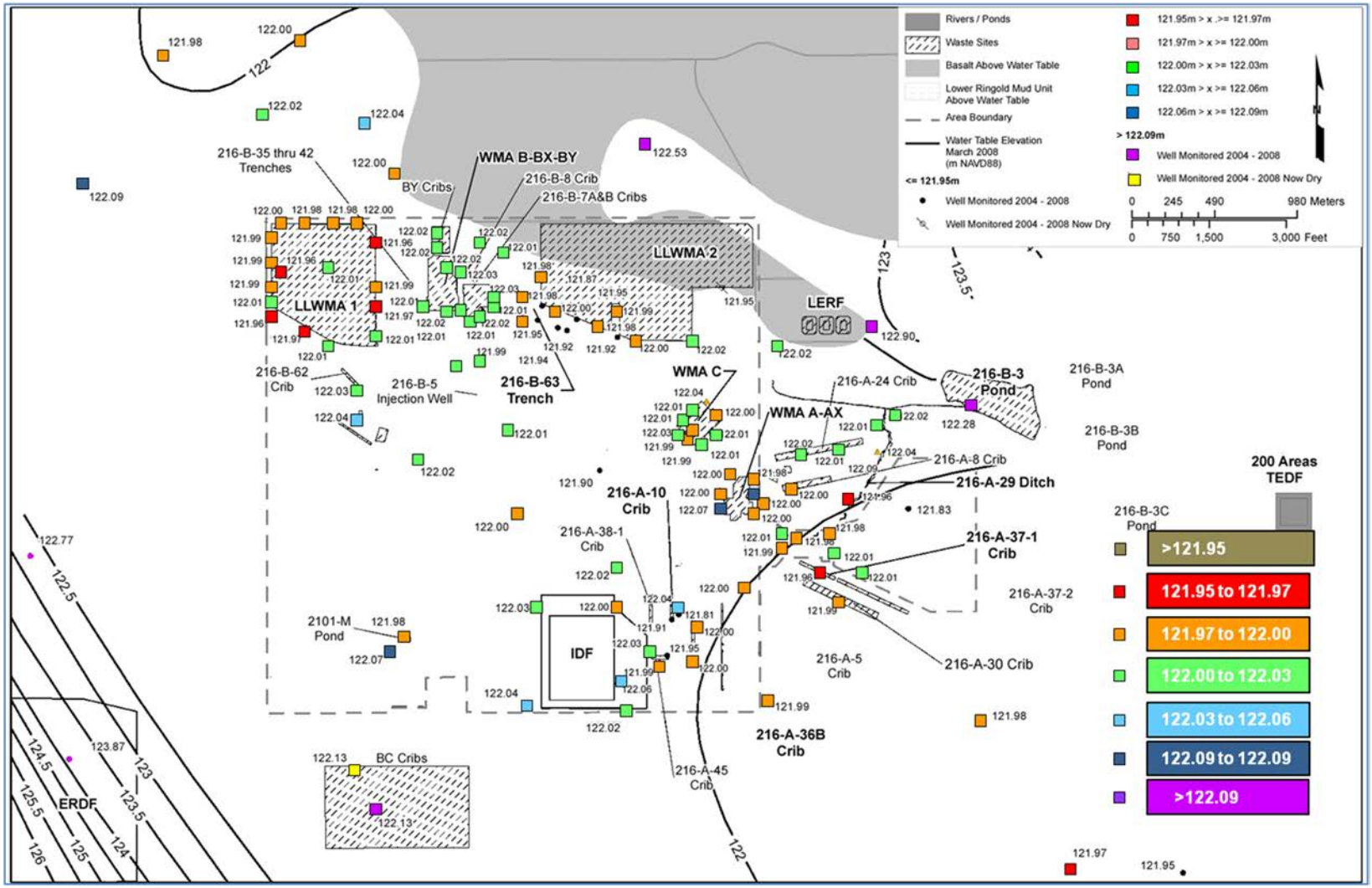

Modified from DOE/RL-2008-66, *Hanford Site Groundwater Monitoring for Fiscal Year 2008.*

ERDF = Environmental Restoration Disposal Facility
IDF = Integrated Disposal Facility
LLWMA = Low-Level Waste Management Area
TEDF = Treated Effluent Disposal Facility
WMA = Waste Management Area

The local-scale flow directions along the southern boundary of the 200-BP-5 Operable Unit and central part of 200 East Area are uncertain. The range in water table elevations is only a few centimeters across the 200 East Area and the water level measurements in wells exhibit spatial variability (see Figure 5-3). In the vicinity of the WMA C, the average flow direction is currently inferred – based in part on water-level measurements and in evaluation and interpretation of local-scale plume migration – to be to the south and southwest. Methods being used to reduce uncertainty in these measurements include higher resolution well elevation surveys and gyroscopic surveys to determine borehole deviation from vertical.

5.2 AQUIFER PROPERTIES

This section describes the aquifer properties beneath the 200 East Area and specifically SST WMA C. This discussion includes a summary of data and information collected on hydraulic properties, aquifer thickness, and groundwater flow directions and flow rates in these areas. This section also describes historic changes in the aquifer conditions due to past fuel processing operations and associated waste disposal to cribs and ponds. Changes in the aquifer properties during the past 60 years have large implications for direction and rate of contaminant movement in the aquifer and for residual vadose zone contamination where the water table has decreased in elevation.

The base of the unconfined aquifer in most of the 200 East Area is generally regarded as the basalt surface, and the supra-basalt aquifer system consists entirely of the unconfined aquifer. The unconfined aquifer consists primarily of hydrogeologic unit 1 (undifferentiated Hanford formation and coarse-grained CCU deposits) and hydrogeologic unit 9 (Ringold Formation unit A) beneath the SST WMAs in the 200 East Area (see Figure 5-4). Hydrogeologic unit 8, the lower mud unit, has been removed from beneath almost all of the 200 East Area and is not present beneath any of the SST farms in the area.

Table 5-1 contains a list of wells near SST WMA C in 200 East Area that penetrate through the entire unconfined aquifer and have March 2008 water level measurements. The location of these wells is provided in Figure 5-5. Also in Table 5-1 are calculated thicknesses for the unconfined aquifer. There are very little data for WMA C and nearby A-AX WMA. The thickness of the uppermost aquifer generally increases from north to south as the top of basalt dips into the Cold Creek syncline. The unconfined aquifer beneath the SST WMAs in the 200 East Area ranges from between 0 and 7 m beneath WMA B-BX-BY which lies to the west of SST WMA C, to about 9 to 10 m beneath WMA C, to about 27 m beneath WMA A-AX.

General groundwater flow directions and general flow rates are given in Table 5-2 for the SST WMA C (DOE/RL-2008-66). The principal vector of groundwater flow, as the table indicates, is to the southwest. Information on the direction of flow is generally based from the examination of changes in contaminant plume movement over several years. Information on the variability/uncertainty is very limited based on the flat gradient and the small number of samples taken in any given year on contaminants of interest.

Figure 5-4. Comparison of Major Hydrologic Units and Geologic Stratigraphy at Hanford.

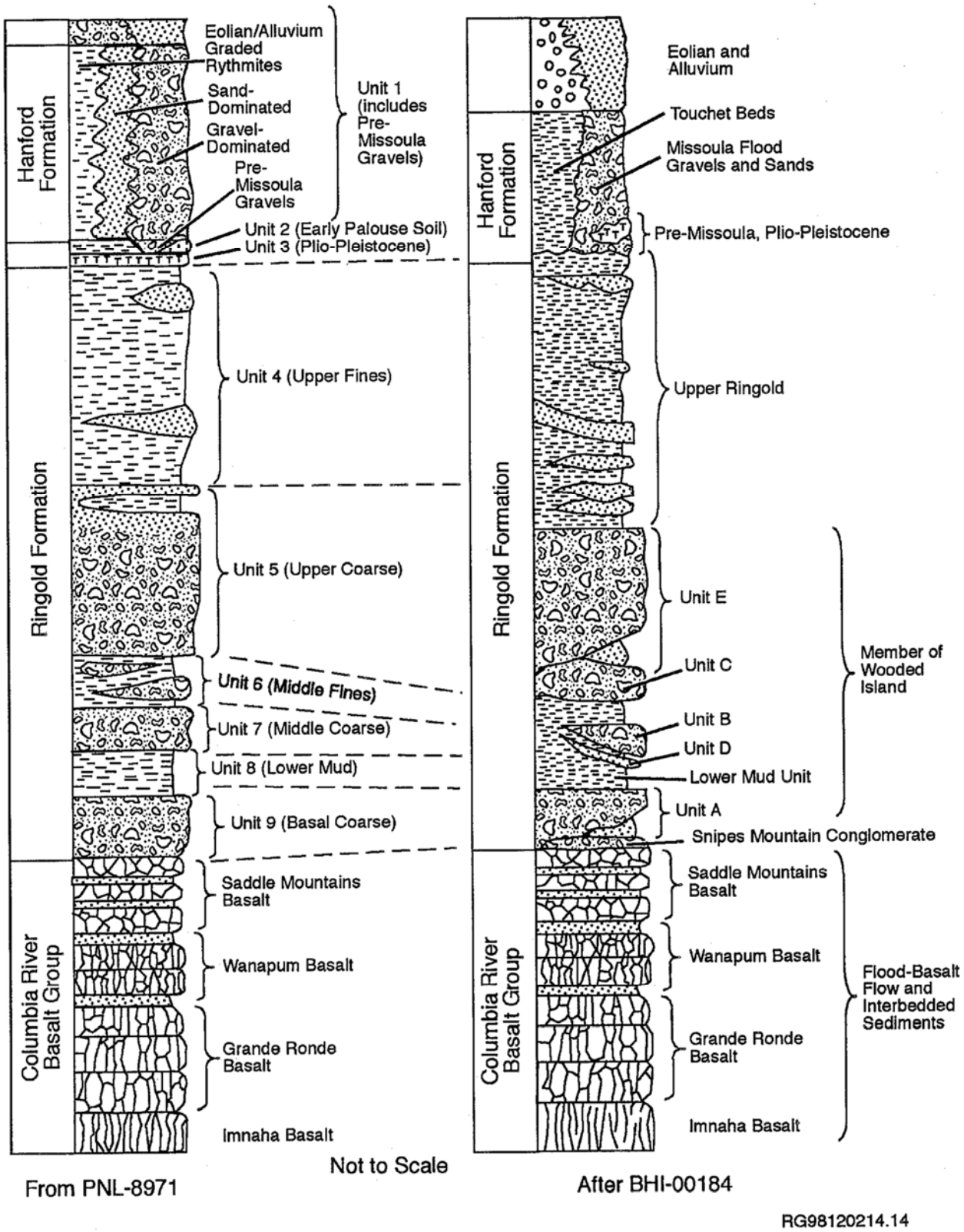

Adapted from PNNL-13080, *Hanford Site Groundwater Monitoring: Setting, Sources, and Methods.*

Table 5-1. Thickness of the Unconfined Aquifer Beneath the A-AX and C Single-Shell Tanks in 200 East Area.

Well Name	Well Location	Elevation of Top of Basalt[(a)] (m amsl)	Elevation of Water Table[(b)] (m amsl)	Aquifer Thickness (m)
Waste Management Area A-AX				
299-E25-2	East side of WMA A-AX	94.49	121-95-121.97	27.46-27.48
299-E24-8	~ 550 m southwest of WMA C	95.71	121.90	26.19
Waste Management Area C				
299-E26-8	~ 300 m east of WMA C	113.02	121.85	8.83
299-E27-22	North corner of WMA C	112.38	122.03 -122.05	9.65-9.67

(a) Top of basalt elevation from PNNL-13024, *RCRA Groundwater Monitoring Plan for Single-Shell Tank Waste Management Area C at the Hanford Site*; PNNL-13023, *RCRA Groundwater Monitoring Plan for Single-Shell Tank Waste Management Area A-AX at the Hanford Site*; PNNL-12261, *Revised Hydrogeology for the Suprabasalt Aquifer System, 200-East Area and Vicinity, Hanford Site, Washington*; RPP-14430, *Subsurface Conditions Description of the C and A-AX Waste Management Area*; Hanford Well Information System.

(b) March 2008 data except where noted.

amsl = above mean sea level WMA = waste management area

Multi-stress slug tests have been done at specific depth intervals one well at WMA C. The results of those tests (Table 5-3) indicate the ranges in hydraulic conductivity that can be expected within a single well. The data show that the hydraulic conductivity and the calculated flow velocity can be expected to vary by several orders of magnitude within a single well.

Several slug tests were done prior to 1997 in wells near 200 East Area SST farms. Table 5-4 gives the resulting hydraulic conductivity and transmissivity data from those tests. In most cases, the analyses of the data from these tests are less well documented than are more recent analyses. The original source for the data should be consulted for details of testing and analysis. The hydraulic conductivities obtained from the earlier slug test (Table 5-4) are generally lower than those measured in the more recent tests (Table 5-3).

The differences in hydraulic properties among wells and within single wells illustrate the difficulty in assigning accurate values to specific hydrogeologic units. The differences are due to different testing and analysis methods used through time, different assumed values for certain parameters such as effective porosity, and natural variation in lithologic properties that affect the hydraulic properties. As more hydrologic data become available, perhaps the relatively large ranges of some hydraulic properties will decrease. Until then, the existing data set must be considered plausible within the uncertainties in the analyses.

Figure 5-5. Well Location Map for Waste Management Area C.

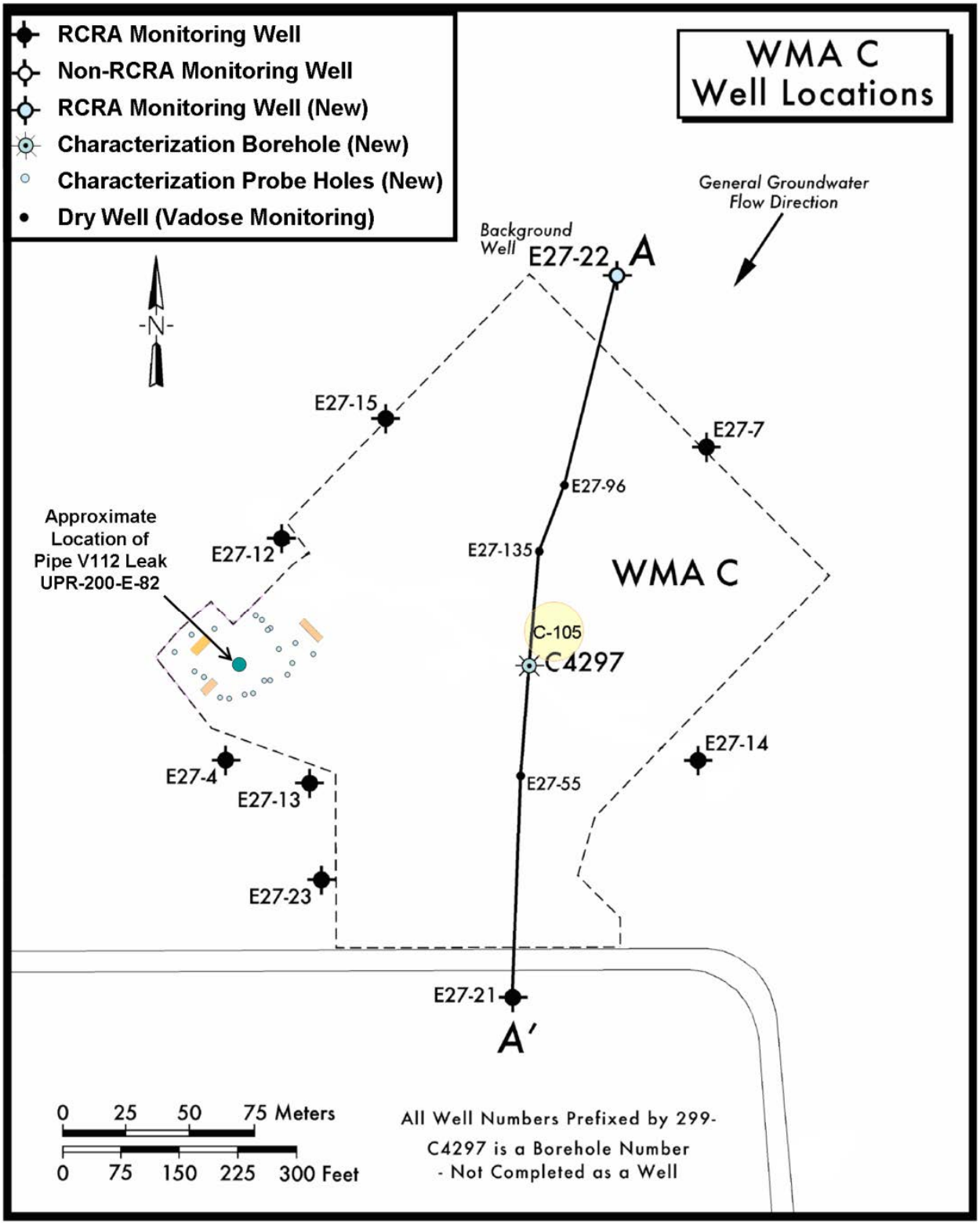

Modified from DOE/RL-2008-66, *Hanford Site Groundwater Monitoring for Fiscal Year 2008*.

RCRA = *Resource Conservation and Recovery Act of 1976* WMA = Waste Management Area

Table 5-2. General Estimated Groundwater Flow Directions and Flow Rates for Single-Shell Tank Waste Management Areas A-AX and C in the 200 East Area.

Waste Management Area	Groundwater Flow Direction	Gradient	Hydraulic Conductivity (m/d)	Groundwater Flow Rate* (m/day)
A-AX	SE	0.00002	1,981	0.13 to 0.4
C	SW	0.00002	1,000 to 2,000	0.2 to 0.4

Source: DOE/RL-2008-66, *Hanford Site Groundwater Monitoring for Fiscal Year 2007*.

*Groundwater flow rates are calculated using the Darcy equation (flow rate = (hydraulic conductivity × hydraulic gradient)/effective porosity).

Table 5-3. Results from Slug Testing of Wells at 200 East Area Single-Shell Tank Farms.[a]

Well[b]	Hydraulic Conductivity (m/day)	Specific Storage (m)	Calculated Groundwater Flow Rate (m/day)
Waste Management Area C			
299-E27-22[d,e] (75.1 – 75.9)	1900 – 2100[c]	Not available	0.14[f]
299-E27-22[d,e] (76.8 – 77.4)	0.04[c]	Not available	2.67E-05[f]
299-E27-22 [d,e] (81.4 – 81.7)	6000 – 6900[c]	Not available	0.46[f]
299-E27-23[a]	100 – 108[c]	Not available	0.0072[f]

(a) PNNL-13378, *Results of Detailed Hydrologic Characterization Tests – Fiscal Year 1999*; PNNL-13514, *Results of Detailed Hydrologic Characterization Tests – Fiscal Year 2000*; PNNL-14186, *Results of Detailed Hydrologic Characterization Tests – Fiscal Year 2002*; PNNL-14804, *Results of Detailed Hydrologic Characterization Tests – Fiscal Year 2003*; except where noted.

(b) All hydrologic tests conducted in hydrologic unit 1 (Hanford formation).

(c) High K (oscillatory) analysis method.

(d) Numbers in parentheses are depth intervals tested (meters below ground surface).

(e) PNNL-14656, *Borehole Data Package for Four CY 2003 RCRA Wells 299-E27-4, 299-E27-21, 299-E27-22, and 299-E27-23 at Single-Shell Tank, Waste Management Area C, Hanford Site, Washington*.

(f) Estimated using maximum hydraulic conductivity from this table and effective porosity of 0.3 and hydraulic gradient of 0.00002 from DOE/RL-2008-66, *Hanford Site Groundwater Monitoring for Fiscal Year 2008*.

5.3 CHANGES IN GROUNDWATER FLOW DIRECTION

Water levels beneath 200 East Area rose as much as 9 m (well 699-45-42, located near 216-B pond [B Pond]) because of artificial recharge from liquid waste disposal operations at the B Pond area. The largest volumes of discharge were to the B Pond system east of the 200 East

Area, the 216-A-25 (Gable Mountain) pond system north of the 200 East Area, and several of the Plutonium Uranium Extraction (PUREX) Plant cribs east and south of WMA A-AX and WMA C. Figure 5-6 shows the liquid discharge history for the two pond systems. The Gable Mountain pond system is estimated to have received approximately 307 billion L of effluent and B Pond to have received about 240 billion L of effluent (DOE/RL-92-05, *B Plant Source Aggregate Area Management Study Report*). These large volumes disposed to the ponds (and, lesser volumes to cribs and ditches) artificially recharged the unconfined aquifer creating large water-table mounds. The increase in water-table elevation was most rapid from 1954 to 1963, increasing as much as 0.6 m/year at times. The water table declined somewhat in the late 1960s and early 1970s, then increased again in the early 1980s before a final decline beginning in 1988 and continuing throughout the 1990s when wastewater discharges in the 200 East Area were reduced.

Table 5-4. Results of Pre-1997 Slug Testing at C Single-Shell Tank Waste Management Area in the 200 East Area.

Well Name	Hydraulic Conductivity (m/day)	Transmissivity* (m^2/day)
Waste Management Area C		
299-E27-13	54.9	232
299-E27-14	48.8	242
299-E27-15	118.9	520

*Transmissivity calculated by multiplying hydraulic conductivity by thickness of test interval.

Source: WHC-SD-EN-TI-147, *Hydrologic Testing at the Single-Shell Tanks, 1989.*

Past discharges to B Pond and 216-A-25 (Gable Mountain Pond) systems exerted significant effects on groundwater, not only in changes in head and flow direction, but also gradients and groundwater fluxes and the direction of contaminant transport from past water quality impacts near wastewater discharge facilities. Contaminant concentration in discharges to these large volume discharge facilities were generally dilute in comparison to contaminant concentration levels in wastewater discharges to cribs and trenches. The volume of relatively dilute water arising from pond discharges and associated water table mounds affected water quality as well, with some dilution of lower volume but higher contaminant content from local sources. Historical interpretation of water quality impacts from past operations needs to give careful consideration to the completion of local-scale groundwater wells in the uppermost part of the unconfined aquifer.

Figure 5-7 shows hydrographs for the area around SST WMA C. The hydrograph illustrates the changes in water-table elevation that have occurred since at least the mid 1950s. All data used to make the hydrographs were obtained from the HydroDat database (see data files on CD included in PNNL-15670, *Hanford Site Groundwater Monitoring for Fiscal Year 2005*).

Figure 5-6. Discharge History for and Location of the B Pond and the Gable Mountain Pond Systems.

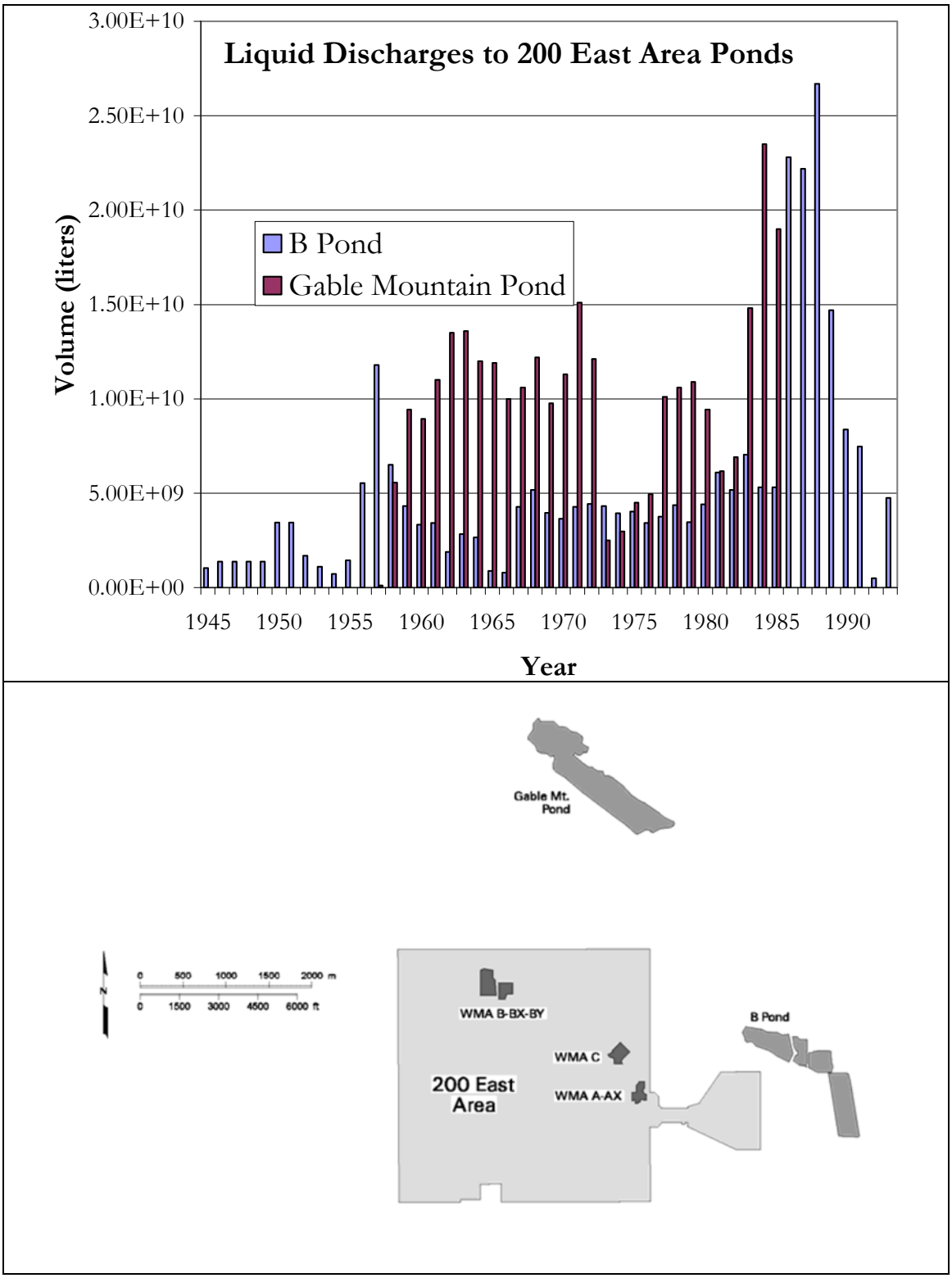

Reference: PNNL-15837, *Data Package for Past and Current Groundwater Flow and Contamination Beneath Single-Shell Tank Waste Management Areas*. Location map of the pond is adapted from PNNL-15837.

Figure 5-7. Hydrographs from Selected Wells in the Area of Waste Management Area C, 200 East Area.

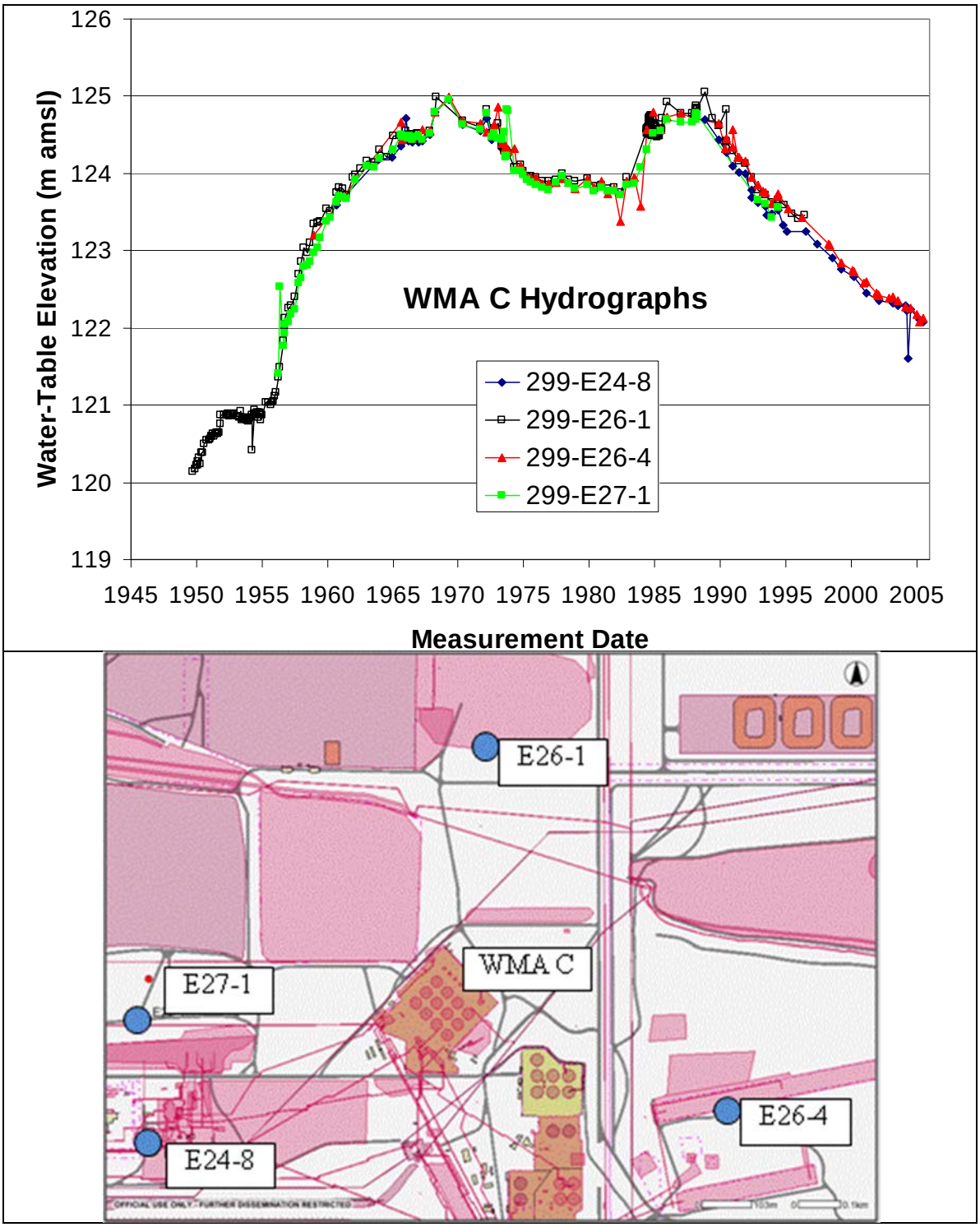

Note: Well 299-E24-8 is located about 650 m south-southwest of C Tank Farm; well 299-E26-1 is located about 450 m north of the C Tank Farm; well 299-E26-4 is located about 500 m southeast of the C Tank Farm; well 299-W27-1 is located about 500 m west of the C Tank Farm.

The hydrographs in this figure show a maximum in water-table elevation in about 1968 that corresponds to a time of high discharge to Gable Mountain pond (Figure 5-6). This maximum is followed by a minimum, centered around 1978, that corresponds to a minimum in the discharges to both pond systems. Finally, a second maximum is seen in 1986 to 1987 corresponding to peak discharge to the B Pond system. Hydrographs from A-AX and B-BY-BX SST WMAs show similar patterns (PNNL-15301).

Table 5-5 summarizes the changes in water-level elevations that have occurred beneath the SST WMA C since the beginning of the Hanford Site operations. The pre-Manhattan Project water table was at approximately 118 m above sea level in 200 East Area (BNWL-B-360, *Selected Water Table Contour Maps and Well Hydrographs for the Hanford Reservation, 1944-1973*). PNNL-13400, *Groundwater Flow and Transport Calculations Supporting the Immobilized Low-Activity Waste Disposal Facility Performance Assessment*, more recently modeled the elevation of the water table beneath the Hanford Site for the Immobilized Low-Activity Waste Performance Assessment. Their model resulted in a water-table elevation of about 116 to 118 m above sea level in the 200 East Area after all influences from the Hanford Site have dissipated.

Table 5-5. Historical Water Level Changes Beneath the 200 East Area Single-Shell Tank Farms.

Waste Management Area	Approximate Pre-Hanford Water-Table Elevation (m amsl)[(a)]	Estimated Post-Hanford Water-Table Elevation (m amsl)[(b)]	Approximate Maximum Water-Table Elevation (m amsl) and Date of Measurement	Approximate Current Water-Table Elevation (m amsl)[(c)]	Approximate Yearly Rate of Decline During the Past 5 Years (m/yr)
C	120 116 – 118	116 – 118	124.4 February 1990 (299-E27-13)	121.90 – 122.06	0.06

[(a)] BNWL-B-360, *Selected Water Table Contour Maps and Well Hydrographs for the Hanford Reservation, 1944-1973*.

[(b)] PNNL-13400, *Groundwater Flow and Transport Calculations Supporting the Immobilized Low-Activity Waste Disposal Facility Performance Assessment*.

[(c)] DOE/RL-2008-66, *Hanford Site Groundwater Monitoring for Fiscal Year 2008*.

amsl = above mean sea level.

All non-permitted discharges of liquid effluent to the ground were stopped in 1995. Since that time, continued changes have occurred in the water-table elevation. Table 5-5 also gives the average rate of water table decline in wells during the past 5 years. The average rate of decline was obtained by averaging the rate of decline in each monitoring well in the RCRA monitoring network between March 2003 and March 2008 (DOE/RL-2008-66).

The data show that the water table beneath SST WMA C is declining at a rate of about 0.11 m/year. At the current rate of decline, the water table will take between 30 and 50 years to reach the estimated post-Hanford water-table elevation (PNNL-13400).

Accompanying the changes in water level were changes in groundwater flow direction. Pre-Hanford Site groundwater flow direction was generally toward the east or southeast

(BNWL-B-360). Since 1944, liquid disposal to the B Pond, Gable Mountain Pond, and other disposal facilities has changed the flow direction several times during Hanford Site operations.

Table 5-6 gives historical groundwater flow directions and water-table gradients from the late 1950s to the year 2003 estimated from selected wells in close proximity to WMA C. The flow directions and gradients were calculated in PNNL-15301 using the three-point analysis method and water level measurements in the HydroDat database (see data files on CD included in PNNL-15670). The earlier historical flow directions are determined from water levels collected on relatively far-field wells between 1958 and 1994 whereas the latter flow directions were determined from measurements in wells in the RCRA monitoring network at WMA C from 1990 to 2003. The apparent variations in estimated flow directions in the northern part of the 200 East Area, including the area of the WMA C, may, in part, be influenced by the top of the basalt on the local-scale flow within the very thin unconfined aquifer. The top of the basalt, which forms the base of the unconfined aquifer in the area, is above the water table in the northeast corner of the 200 East Area and dips south to southwest. This surface is expected to influence local-scale flow directions especially near areas where the aquifer pinches out against the basalt. Also, the top of the basalt is an erosional surface with up to about 3.5 m of relief (PNNL-13404, *Hanford Site Groundwater Monitoring for Fiscal Year 2000*). Thus, local flow directions may differ greatly as water moves between high areas on the top of basalt.

The frequencies of historical groundwater flow directions in the area of WMA C between 1958 and 1994 and, separately, more recent flow direction between 1990 and 2003, are shown graphically in Figure 5-8. Examination of the frequency of calculated directions of groundwater from the far-field (Figure 5-8a) and local-scale wells (Figure 5-8b), shows that, while varying considerably between 1958 through 2003, groundwater flow directions in the area of WMA C have been generally toward the southwest over most of this period of time. Review of water-level measurements collected since 2003 and interpretations of plume migration during the past several years, discussed in Section 5.4.3, would continue to support the general observation of predominant groundwater flow direction to the south and southwest beneath the WMA C.

Interpretation of changes in the direction of groundwater flow prior to the period shown in the rose diagrams is very limited because of the small number of groundwater wells that were available to define water table conditions. Because of these limitations, the specific direction of groundwater flow in the immediate area of WMA C is difficult to determine and can only be inferred from the general regional interpretations of the water table provided prior to 1958.

Table 5-6. Water Levels, Groundwater Flow Directions, and Water-Table Gradients in the Area of Waste Management Area C from 1958 to 2003. (2 sheets)

Duration[a] (day)	Start Date	End Date	Water Levels (m amsl)			Groundwater Flow Direction[b]	Water-Table Gradient
			299-E26-1	299-E26-4	299-E27-1		
4	12/09/58	12/12/58	123.343	123.194	122.973	212.673	0.000433
1	08/18/65	08/18/65	124.48	124.660	124.500	328.459	0.000203
1	10/20/65	10/20/65	124.492	124.495	124.485	258.557	0.000009
4	01/03/66	01/06/66	124.559	124.486	124.485	188.628	0.000113
11	04/04/66	04/14/66	124.498	124.474	124.488	164.863	0.000029
1	05/20/66	05/20/66	124.498	124.474	124.463	199.422	0.000046
2	11/02/66	11/03/66	124.514	124.510	124.463	230.877	0.000056
11	03/28/67	04/07/67	124.462	124.568	124.436	308.904	0.000125
5	10/19/67	10/23/67	124.553	124.556	124.512	239.716	0.000046
1	05/18/70	05/18/70	124.675	124.678	124.631	239.428	0.000049
1	09/14/71	09/14/71	124.608	124.641	124.573	277.811	0.000055
6	03/15/72	03/20/72	124.824	124.538	124.771	152.595	0.000325
1	07/11/72	07/11/72	124.526	124.541	124.463	248.930	0.000073
5	10/03/72	10/07/72	124.59	124.635	124.518	267.052	0.000097
1	01/08/73	01/08/73	124.642	124.855	124.448	281.927	0.000331
1	08/13/73	08/13/73	124.279	124.352	124.210	280.928	0.000115
1	09/10/73	09/10/73	124.291	124.309	124.226	250.994	0.000076
1	04/11/74	04/11/74	124.078	124.328	124.037	313.189	0.000288
1	10/18/74	10/18/74	124.111	124.096	124.030	224.666	0.000090
1	01/08/75	01/08/75	124.038	124.026	123.988	221.536	0.000056
1	04/14/75	04/14/75	123.962	123.943	123.909	215.007	0.000061
1	07/07/75	07/07/75	123.965	123.950	123.884	224.666	0.000090
1	12/03/75	12/03/75	123.944	123.947	123.857	237.477	0.000096
1	06/15/76	06/15/76	123.904	123.870	123.814	213.979	0.000105
1	12/08/76	12/08/76	123.907	123.873	123.793	218.279	0.000130
1	07/01/77	07/01/77	123.916	123.876	123.878	186.664	0.000060
1	12/07/77	12/07/77	123.995	123.931	123.966	166.661	0.000077
1	06/01/78	06/01/78	123.91	123.886	123.869	203.768	0.000051
1	12/01/78	12/01/78	123.904	123.806	123.802	189.428	0.000153
1	12/01/79	12/01/79	123.928	123.931	123.857	237.928	0.000079
1	06/01/80	06/01/80	123.828	123.825	123.774	232.217	0.000060
1	12/01/80	12/01/80	123.852	123.907	123.826	297.966	0.000070
1	06/01/81	06/01/81	123.809	123.745	123.762	179.040	0.000087
1	12/01/81	12/01/81	123.819	123.800	123.762	216.359	0.000065
1	06/01/82	06/01/82	123.749	123.386	123.720	146.706	0.000409
1	12/01/82	12/01/82	123.944	123.904	123.845	212.603	0.000116
1	06/01/84	06/01/84	124.562	124.562	124.314	235.468	0.000274
1	12/01/84	12/01/84	124.709	124.788	124.515	257.542	0.000237

Table 5-6. Water Levels, Groundwater Flow Directions, and Water-Table Gradients in the Area of Waste Management Area C from 1958 to 2003. (2 sheets)

Duration[(a)] (day)	Start Date	End Date	Water Levels (m amsl)			Groundwater Flow Direction[(b)]	Water-Table Gradient
			299-E26-1	299-E26-4	299-E27-1		
9	06/12/85	06/20/85	124.588	124.565	124.549	203.569	0.000049
2	12/17/85	12/18/85	124.924	124.723	124.695	192.163	0.000330
4	12/08/87	12/11/87	124.771	124.711	124.671	203.112	0.000126
2	12/03/92	12/04/92	123.793	123.845	123.650	255.420	0.000172
2	06/09/93	06/10/93	123.729	123.760	123.607	249.787	0.000141
2	12/01/93	12/02/93	123.619	123.613	123.427	233.640	0.000212
1	06/03/94	06/03/94	123.653	123.735	123.558	275.430	0.000144
			299-E27-12	**299-E27-14**	**299-E27-7**		
1	06/28/90	06/28/90	124.297	124.312	124.331	228.635	0.000229
1	12/17/90	12/17/90	124.187	124.224	124.240	247.203	0.000316
1	06/17/91	06/17/91	124.056	124.117	124.097	301.756	0.000332
2	08/19/91	08/19/91	124.132	124.148	124.167	229.649	0.000233
2	03/04/92	03/05/92	123.76	123.953	123.990	258.790	0.001348
2	06/17/92	06/18/92	123.839	123.846	123.886	213.439	0.000388
1	12/16/92	12/16/92	123.733	123.749	123.777	223.989	0.000312
1	03/25/93	03/25/93	123.675	123.718	123.743	242.040	0.000415
1	12/15/93	12/15/93	123.516	123.532	123.551	229.649	0.000233
1	05/11/94	05/11/94	123.516	123.544	123.566	236.657	0.000315
1	12/09/94	12/09/94	123.498	123.523	123.545	234.665	0.000300
1	06/23/95	06/23/95	123.385	123.392	123.429	213.868	0.000360
2	10/30/95	10/30/95	123.398	123.395	123.432	205.009	0.000332
1	01/16/97	01/16/97	123.23	123.212	123.255	192.115	0.000361
1	06/10/97	06/10/97	123.199	123.249	123.225	315.891	0.000285
1	12/04/97	12/04/97	123.12	123.163	123.167	265.054	0.000277
1	06/08/98	06/08/98	123.065	123.020	123.033	117.982	0.000244
2	12/07/98	12/08/98	122.953	122.898	122.914	118.178	0.000298
1	06/03/99	06/03/99	122.843	122.831	123.728	207.362	0.008207
1	12/18/00	12/18/00	122.629	122.621	122.627	155.890	0.000055
1	06/20/01	06/20/01	122.571	122.574	122.574	271.893	0.000018
1	03/14/02	03/14/02	122.388	122.391	122.389	330.530	0.000019
1	12/16/02	12/16/02	122.442	122.410	122.520	197.195	0.000942
3	06/02/03	06/04/03	122.309	122.328	126.511	207.970	0.038467

Reference: RPP-23748, *Geology, Hydrogeology, Geochemistry, and Mineralogy Data Package for the Single-Shell Tank Waste Management Areas at the Hanford Site*.

[(a)] Duration is the length of time between the start and end dates.

[(b)] Groundwater flow direction is degrees azimuth clockwise from north (0º).

amsl = above mean sea level

Figure 5-8. Range of Groundwater Flow Directions in the Vicinity of 241-C Tank Farm Based on Analyses of Water-Level Measurements Made in Selected Wells between 1958 and 2003.

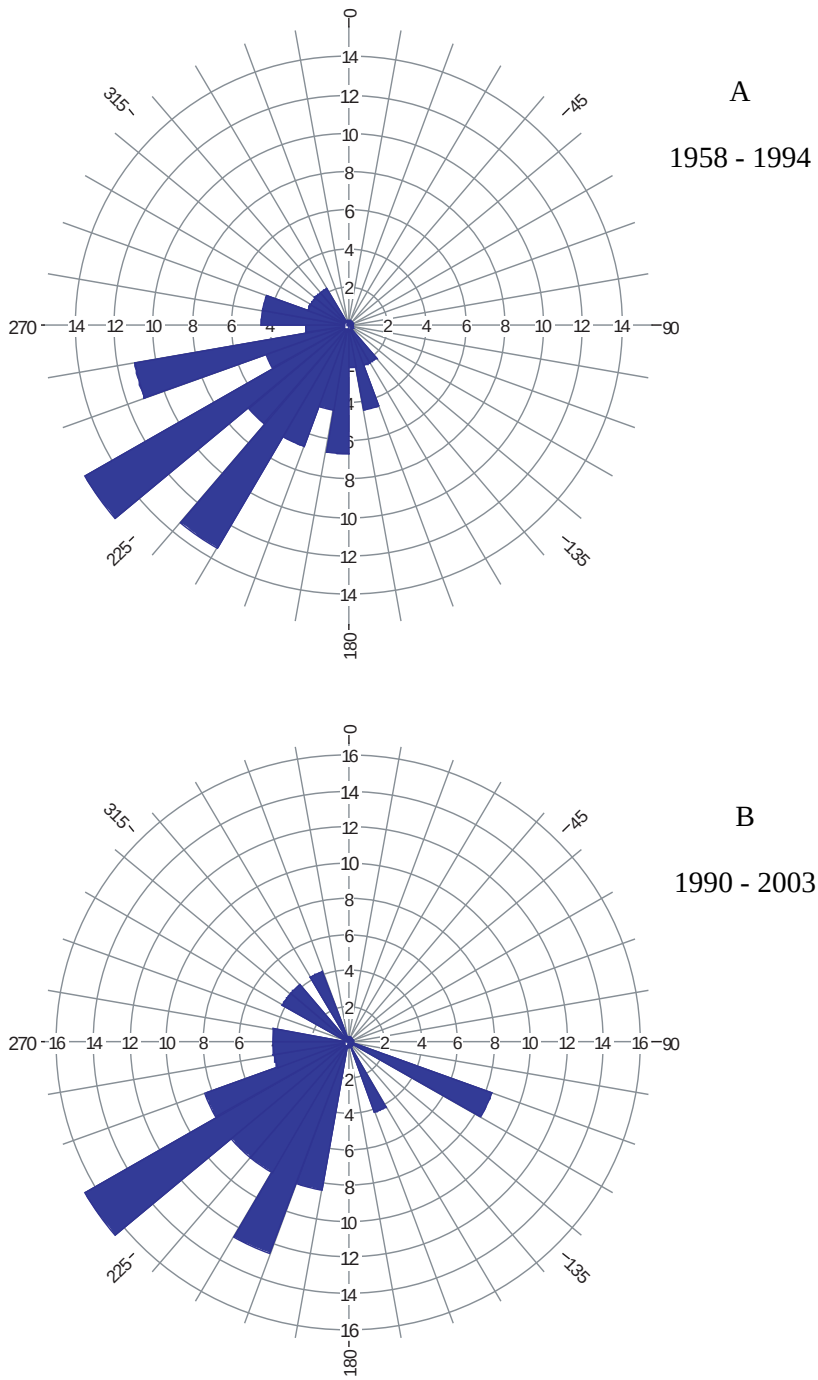

A. 1958 to 1994, wells 299-E26-1, 299-E26-4, and 299-E27-1, 45 measurements.
B. 1990 to 2003, wells 299-E27-12, 299-E27-14, and 299-E27-7, 24 measurements. Well 299-E26-1 is located about 450 m north of Waste Management Area C; well 299-E26-6 is about 500 m southeast of Waste Management Area C; well 299-E27-1 is about 550 m west of Waste Management Area C; the locations of all other wells are on Figure 5-4.
Reference: RPP-23748, *Geology, Hydrogeology, Geochemistry, and Mineralogy Data Package for the Single-Shell Tank Waste Management Areas at the Hanford Site*.

Interpretations of water-table conditions prior to 1958 can be found in three documents:

- Maps of water-table conditions in 1951 and 1955 depicted in BNWL-B-360
- Maps of water table conditions from 1951 through 1955 in HW-40469, *Changes in the Hanford Ground Water Table 1944-1955*
- A map of water-table conditions from 1948 in USGS-W-P-7, *Geologic and Hydrologic Features of the Richland Area, Washington, Relevant to the Disposal of Waste at the Hanford Operations of the Atomic Energy Commission; Interim Report No. 1*.

Because of the limited number of well measurements, the interpretations provided in these documents are appropriate for establishing a regional picture of water table conditions and would not be appropriate for resolving local-scale conditions. Interpretations of water-table conditions from these maps would suggest that discharges at B Pond also had a dominant influence on the unconfined aquifer in the late 1940s through the mid-1950s in 200 East Area. The discharges to B Pond created a saddle in the water table in 200 East Area. Under today's conditions, the actual position of the associated groundwater divide in directions of flow is difficult to discern based on the limited number of water table measurements. Based on the inferred regional water table interpretation, groundwater flow in the area south of WMA C was generally to the south and southeast; in an area north of WMA C, the flow direction appears to be to the north and northwest. However, because of the small number of wells and flatness of the hydraulic gradient in 200 East Area, the specific direction of groundwater flow in the immediate area of WMA C is difficult to determine.

5.4 GROUNDWATER GEOCHEMISTRY

This section is to describe the groundwater geochemistry beneath SST WMA C. A complete description of groundwater geochemistry beneath the 200 East Area WMAs is in RPP-23748 and PNNL-15301. General background chemistry for the Hanford Site is provided first. This is followed by discussions of background chemistry, a description of contaminant plumes associated with each WMA, and an accounting of the historical contamination specific to WMA C.

5.4.1 Background Groundwater Chemistry on Hanford Site

Natural chemical background for the Hanford Site is given from the work in DOE/RL-96-61. Hanford Site background is also described in terms of the water chemistry from samples of two upgradient wells used to monitor Hanford Site background. Local background for SST WMA C is given in subsequent sections using existing upgradient monitoring wells. Most of the information in this section is from RPP-23748 and PNNL-15301.

U.S. Department of Energy published a study of Hanford Site groundwater background in 1997 (DOE/RL-96-61). The study included historical groundwater monitoring data collected between

1989 and 1993 and new data collected specifically for the purpose of evaluating groundwater background.

An initial screening of the historical data eliminated all data from wells that (1) did not sample the unconfined aquifer, (2) were located within or proximal to known contaminated sites or contaminant plumes, and (3) contained halogenated hydrocarbons. Data from each well were then screened against a list of target constituents most likely to reflect concentration variations in response to contamination events. Wells were eliminated if they yielded samples with concentrations greater than a threshold concentration for the target constituents. The threshold values were obtained from a preliminary background determination in 1992 (DOE/RL-92-23, *Hanford Site Groundwater Background*). The remaining data were then put through a final screening by eliminating outliers (i.e., data that did not conform to the pattern established by other observations) (DOE/RL-96-61).

New groundwater data were collected from 45 wells located mostly in gaps in the geographic coverage of the historical data. There are several important differences between the historical data and the new data.

- The historical data were collected to monitor groundwater whereas the new data were collected specifically to determine background. Therefore, the historical data lack constituents important in considerations of background composition.

- The historical data have a temporal coverage that is lacking from the new data.

- The detection limits are substantially different for the two data sets. The detection limits for metals and radionuclides are significantly lower for the new data.

- The new data represent an internally consistent data set resulting from using the same laboratories and methods for all samples. This is not necessarily true for the older data.

The resulting Hanford Site groundwater background concentrations are given in Table 5-7. Data reported as equal to or less than the detection limit were assigned a value of one-half the detection limit for purposes of calculating the mean. In general, filtered samples were used for analyses of metals and radionuclides and unfiltered samples were used for anions.

Several variables affect the chemical composition of groundwater used for the Hanford Site groundwater background study. These variables are discussed in detail in DOE/RL-92-23 and include well construction, lithology of the sediment in the screened (or perforated) interval, the length of the screened or perforated interval, and recharge.

Table 5-7. Hanford Site Groundwater Background Concentrations. (4 sheets)

Analyte*	Data Set	Reason for Selection	Units	Geometric Mean	Geometric Standard Deviation	Number of Samples	Minimum	Maximum
Alkalinity as $CaCO_3$	New	More data	µg/L	118,650	1,183	30	80,000	170,000
Aluminum	*New*	*Lower DL*	*µg/L*	*1.23*	*3.92*	*32*	*0.5*	*187*
Americium-241	*New*	*Lower DL*	*fCi/L*	*0.732*	*2.11*	*16*	*0.05*	*1*
Ammonia	*New*	*Lower DL*	*µg/L*	*26.2*	*3,120*	*32*	*5*	*882*
Antimony	*Historical*	*No new*	*µg/L*	*23.8*	*1.92*	*15*	*9.47*	*53.9*
Antimony-125	*New*	*Lower DL*	*fCi/L*	*3.77*	*1.61*	*17*	*1.73*	*8.97*
Arsenic	New	Lower DL	µg/L	1.83	3.11	29	0.5	8.81
Barium	New	Lower DL	µg/L	31.2	2.58	32	0.5	94.1
Beryllium	*Historical*	*Lower DL*	*µg/L*	*0.583*	*2.91*	*17*	*0.2*	*2.5*
Beryllium-7	*Historical*	*No new*	*pCi/L*	*6.42*	*1.26*	*4*	*5.25*	*8.3*
Boron	Historical	No new	µg/L	20.3	1.56	7	12.6	45
Bromide	New	Lower DL	µg/L	61.9	1,721	32	15	235
Cadmium	*New*	*Lower DL*	*µg/L*	*0.274*	*2.57*	*32*	*0.05*	*0.5*
Calcium	Historical	More data	µg/L	36,518	1.33	25	19,200	79,683
Cesium-134	*Historical*	*No new*	*pCi/L*	*0.747*	*1.39*	*4*	*0.496*	*1.06*
Cesium-137	*New*	*Lower DL*	*fCi/L*	*2.26*	*2.79*	*17*	*0.643*	*29.5*
Chloride	Historical	More data	mg/L	7.05	0.0019	27	1.14	21.95
Chromium	*New*	*Lower DL*	*µg/L*	*0.893*	*2.16*	*27*	*0.5*	*4.41*
Cobalt	*New*	*Lower DL*	*µg/L*	*0.274*	*2.57*	*32*	*0.05*	*0.5*
Cobalt-60	*New*	*Lower DL*	*fCi/L*	*1.09*	*2.43*	*17*	*0.404*	*23*
Conductivity	Historical	More data	µS/cm	348,000	1,410	35	150,000	1,361,000
Copper	*New*	*Lower DL*	*µg/L*	*0.332*	*2.01*	*32*	*0.05*	*0.5*

Table 5-7. Hanford Site Groundwater Background Concentrations. (4 sheets)

Analyte*	Data Set	Reason for Selection	Units	Geometric Mean	Geometric Standard Deviation	Number of Samples	Minimum	Maximum
Cyanide	*New*	*No Historical*	*µg/L*	*5.43*	*1,407*	*25*	*5*	*26.7*
Dissolved oxygen	New	No Historical	µg/L	5,306	2,117	31	380	9,440
Eh	New	No Historical	mv	315	1.38	31	91	510
Europium-152	*New*	*Lower DL*	*fCi/L*	*12.9*	*1.51*	*17*	*5.39*	*24.1*
Europium-154	*New*	*Lower DL*	*fCi/L*	*8*	*1.52*	*17*	*3.43*	*18.3*
Europium-155	*New*	*Lower DL*	*fCi/L*	*2.33*	*1.87*	*17*	*0.969*	*11.7*
Fluoride	Historical	More data	mg/L	0.491	0.0018	28	0.267	5.85
Gross alpha	New	More data	pCi/L	1.09	2.03	19	0.25	3.02
Gross beta	New	More data	pCi/L	5.5	1.33	19	3.39	9.45
Iodine	*New*	*No Historical*	*µg/L*	*250*	*1,000*	*25*	*250*	*250*
Iodine-129	New	Lower DL	aCi/L	28.8	2.51	9	6.3	96.1
Iron	Historical	More data	µg/L	55.3	6.17	22	6	7,225
Lead	*New*	*Lower DL*	*µg/L*	*0.271*	*2.59*	*31*	*0.05*	*0.5*
Lithium	New	More data	µg/L	5,729	1,701	30	2,380	19,000
Magnesium	New	More data	µg/L	11,245	1.85	25	825	39,600
Manganese	New	More data	µg/L	2.22	9.25	32	0.05	94.4
Mercury	New	Lower DL	µg/L	0	5.34	27	0	0.012
Molybdenum	*New*	*Lower DL*	*µg/L*	*0.862*	*2.79*	*25*	*0.5*	*11.6*
Nickel	New	Lower DL	µg/L	0.686	1.9	31	0.27	2.56
Nitrate	New	More data	mg/L	5.68	3.36	26	0.085	28.063
Nitrite	*New*	*More data*	*mg/L*	*0.03*	*2.48*	*32*	*0.01*	*0.63*
Oxalate	*New*	*No Historical*	*µg/L*	*161*	*1,566*	*32*	*95*	*280*

Table 5-7. Hanford Site Groundwater Background Concentrations. (4 sheets)

Analyte*	Data Set	Reason for Selection	Units	Geometric Mean	Geometric Standard Deviation	Number of Samples	Minimum	Maximum
pH	Historical	More data	pH units	7.78	1.04	35	6.94	8.79
Phosphate	*New*	*Lower DL*	*µg/L*	*102*	*1,432*	*32*	*65*	*293*
Plutonium	*New*	*No Historical*	*µg/L*	*0.0038*	*2.15*	*25*	*0.001*	*0.005*
Plutonium-238	*New*	*Lower DL*	*fCi/L*	*0.064*	*2.64*	*16*	*0.015*	*0.485*
Plutonium-239/240	New	Lower DL	fCi/L	0.398	1.97	16	0.04	0.762
Potassium	Historical	No new	µg/L	4,578	1.71	25	768	10,000
Potassium-40	Historical	No new	pCi/L	77.3	2.12	10	12	188
Radium-226	New	Lower DL	fCi/L	18.2	1.6	17	7	41.5
Radium-228	New	Lower DL	fCi/L	32.3	1.72	17	12.8	75.6
Ruthenium-106	*New*	*Lower DL*	*fCi/L*	*1.63*	*1.89*	*17*	*0.607*	*5.92*
Selenium	New	Lower DL	µg/L	0.96	6.47	32	0.5	11.6
Silicon	Historical	No new	µg/L	13,691	2.03	7	2,966	23,900
Silver	*Historical*	*No new*	*µg/L*	*3.42*	*1.41*	*15*	*1.93*	*5*
Sodium	Historical	More data	µg/L	13,402	1.73	25	2,360	32,000
Strontium (elemental)	New	More data	µg/L	158	1.75	32	13.1	402
Strontium-90	New	Lower DL	fCi/L	4.78	2.39	14	0.641	15.6
Sulfate	New	More data	mg/L	27.1	1.54	28	11.19	71.21
Sulfide	*New*	*More data*	*µg/L*	*1.71*	*1.21*	*32*	*1.6*	*3.21*
Technetium-99	*Historical*	*No new*	*pCi/L*	*0.447*	*1.62*	*5*	*0.271*	*0.752*
Thallium	*Historical*	*No new*	*µg/L*	*1.14*	*1.35*	*4*	*0.883*	*1.73*
Thorium	*New*	*No Historical*	*µg/L*	*0.5*	*1*	*25*	*0.5*	*0.5*
Tin	*Historical*	*No new*	*µg/L*	*15.9*	*1.27*	*12*	*11.8*	*31.3*

Table 5-7. Hanford Site Groundwater Background Concentrations. (4 sheets)

Analyte*	Data Set	Reason for Selection	Units	Geometric Mean	Geometric Standard Deviation	Number of Samples	Minimum	Maximum
Titanium	*Historical*	*No new*	*µg/L*	*30*	*1*	*7*	*30*	*30*
Total carbon	New	No Historical	µg/L	30,325	1,174	32	20,990	43,175
Total dissolved solids	New	No Historical	µg/L	200,919	1.22	30	140,000	295,000
Total inorganic carbon	New	More data	µg/L	28,722	1,166	32	19,550	39,020
Total organic carbon	New	No Historical	µg/L	1,293	1,779	32	560	6,720
Tritium	*Historical*	*More data*	*pCi/L*	*63.9*	*1.63*	*15*	*27.8*	*131*
Uranium	New	More data	µg/L	2.57	2.85	25	0.5	12.8
Uranium-234	Historical	No new	pCi/L	0.75	1.1	2	0.7	0.803
Uranium-235	New	Lower DL	fCi/L	23.1	3.34	17	1.55	114
Uranium-238	New	Lower DL	fCi/L	721	1.89	17	150	2,440
Vanadium	*New*	*Lower DL*	*µg/L*	*1.83*	*4.19*	*32*	*0.5*	*16.7*
Zinc	*New*	*Lower DL*	*µg/L*	*1.27*	*9.22*	*32*	*0.05*	*1,270*
Zirconium	*Historical*	*No new*	*µg/L*	*25*	*1*	*7*	*25*	*25*

Reference: DOE/RL-96-61, *Hanford Site Background: Part 3, Groundwater Background*.

Note: Data rows entered in italics signify that >50% of the data were below the detection limit.

*Radionuclides with half-lives less than 1,000 years are decayed to June 1, 1997.

DL = detection limit.

The concentrations of major cations and anions in groundwater samples give a good indication of the quality of the groundwater and offer a useful tool for comparing groundwater samples. One useful way to depict major ion concentrations in groundwater is with Stiff diagrams. Stiff diagrams are a graphical means of representing the chemical analysis of major cations and anions in water samples ("The Interpretation of Chemical Water Analysis by Means of Patterns" [Stiff 1983]). Figure 5-9 shows the mean composition of the major cations and anions, as determined in the Hanford Site groundwater background study (DOE/RL-96-61), as a modified Stiff diagram. Nitrate has been added to the conventional Stiff diagram because nitrate is a major anion in much of the Hanford Site's contaminated groundwater. Although average groundwater compositions do not represent actual groundwater compositions, the charge balance for the average composition depicted in Figure 5-9 is +3.3%, which suggests that the representation in the figure describes Hanford Site background groundwater composition. Figure 5-9 shows that the Hanford Site's background groundwater is a calcium-bicarbonate dominated groundwater.

Figure 5-9. Modified Stiff Diagram Depicting Major Cation and Anion Compositions for Background Groundwater, Top of the Aquifer in the Hanford Site's Unconfined Aquifer.

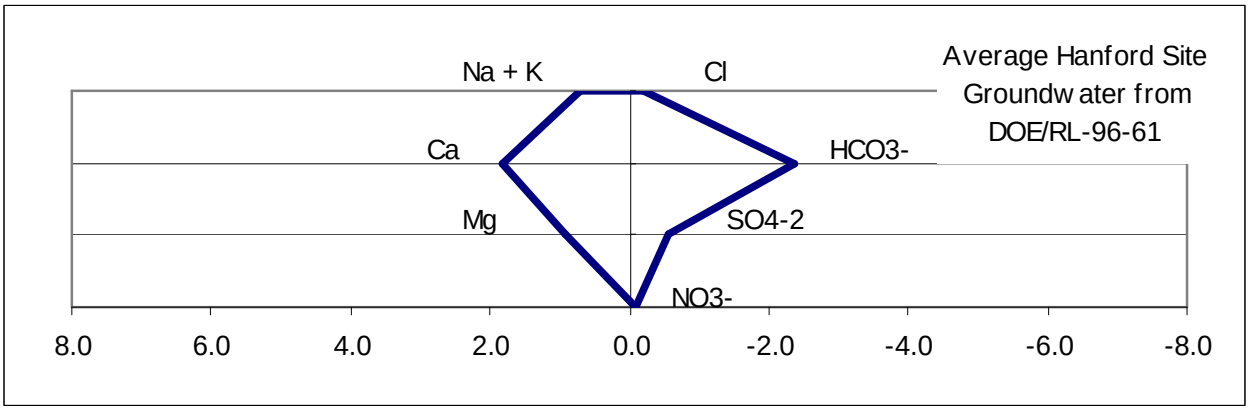

Note: Units for the x-axis are milliequivalents/liter with cations on the left and anions on the right.

Wells 699-19-88 and 699-49-100C were chosen because they are upgradient of all operating facilities at the Hanford Site and they are believed to be free of any Hanford Site contamination. As such, they are monitored as part of the Hanford Site Groundwater Monitoring Project and represent background conditions for Hanford Site groundwater.

Well 699-49-100C is located at the Yakima barricade. The well was drilled 2.4 m into basalt (total depth was 124.3 m bgs), completed with carbon steel casing in 1976, and perforated from 91.4 to 124.3 m bgs. The only records available for this well are an as-built diagram with driller's log that suggest that the water sampled from this well is from silty sandy gravels and sandy gravels of the Ringold Formation, member of Wooded Island of BHI-00184 or hydrogeologic units 5, 8, and 9 of PNL-8971.

Well 699-19-88 is located in the Dry Creek Valley, southwest of Highway 240. The well was drilled 8.5 m into basalt (total depth was 118.3 m bgs), completed with carbon steel casing in 1957, and perforated from 21.3 to 51.8 m bgs. The aquifer sampled is the Hanford formation

and consists of unconsolidated gravel from 21.3 to 30.5 m bgs, very hard cemented gravel from 30.5 to 39.6 m bgs, and sand, silt and gravel from 39.6 to 51.8 m bgs.

Neither of these wells samples the same formation as upgradient wells at any SST WMAs. However, monitoring wells in 200 East Area, and thus the WMA C, are screened in similar Hanford formation gravels. Also, both wells are located west of the 200 Areas and closer to the natural recharge area for the unconfined aquifer. The groundwater in that part of the aquifer is younger than the natural groundwater beneath the SST WMAs and is less altered by reaction with aquifer sediments. Up-gradient groundwater at most SST farms has been impacted by liquid disposal to cribs, ditches, and trenches. However, a few up-gradient wells at some tank farms are only slightly impacted and the general water composition from those wells resembles the groundwater composition of the background wells 699-49-100C and 699-19-88. Regardless of impacts from past-practice disposal facilities, groundwater from up-gradient wells at each SST farm is used as background for the tank farms when making up-gradient and down-gradient comparisons.

The average FY 2005 groundwater composition from the two up-gradient wells is given in Table 5-8 and a depiction of the major cations and anions is shown in Figure 5-10. The charge balances for the two analyses in Figure 5-10 are +3.5% for the 699-19-88 analysis and +1.9% for the well 699-49-100C analysis. Just as for the site-wide background groundwater, the up-gradient well groundwater is a calcium-bicarbonate dominated water type. Also, the groundwater from well 699-49-100C contains 12 mg/L nitrate suggesting that the groundwater at this location contains some nitrate contamination from up-gradient, probably agricultural, sources.

5.4.2 Background Groundwater Chemistry beneath Waste Management Area C

Up-gradient groundwater composition for WMA C is shown in Table 5-8 and Figure 5-10. The data in the table are the average FY 2005 concentrations in each up-gradient well at the WMA, available on the CD included in PNNL-15670. Data for the metals are from filtered samples; all other data are from unfiltered samples. Data flagged as suspect in the HEIS database have been excluded from the calculated averages. Charge balances for the analyses shown in Figure 5-10 are: +3.3% for well 299-E27-22 and +2.2% for well 299-E27-7.

The groundwater at WMA C is characterized as a calcium-sulfate water that is different than groundwater at any other SST WMA. Sulfate is also elevated in a few wells in the area of low-level burial ground WMA 2, north of WMA C, suggesting that the high sulfate found at WMA C is fairly regional in extent. The reason for the high sulfate is not known, but it does not reflect natural background conditions and may be related to leaching of the vadose zone caused by increased water levels associated with disposal at B Pond. Calcium, chloride, magnesium, and nitrate are also elevated relative to Hanford Site background groundwater.

Table 5-8. Average Fiscal Year 2005 Groundwater Composition in Upgradient Wells at Waste Management Area C.

Constituent (units)	Concentration	
	Well 299-E27-22	Well 299-E27-7
Alkalinity as $CaCO_3$ (µg/L)	94,000	87,250
Calcium (µg/L)	64,600	77,675
Cesium-137 (pCi/L)	Not detected	Not detected
Chloride (mg/L)	23.92	31.3
Chromium (µg/L)	Not detected	12.5
Cobalt-60 (pCi/L)	Not detected	Not detected
Cyanide (µg/L)	Not detected	31.03
Fluoride (mg/L)	0.16	0.15
Gross alpha (pCi/L)	Not analyzed	Not analyzed
Gross beta (pCi/L)	19.18	38.05
Iodine-129 (pCi/L)	Not analyzed	3.81
Iron (µg/L)	20.6	46.3
Magnesium (µg/L)	18,000	22,025
Nitrate (mg/L)	20.15	26.22
pH Measurement (pH units)	8.3	8.0
Potassium (µg/L)	8,285	7,915
Sodium (µg/L)	14,025	15,450
Specific Conductance (µS/cm)	535	649
Sulfate (mg/L)	113.85	156.5
Technetium-99 (pCi/L)	38.2	81.4
Total organic carbon (µg/L)	766	840
Tritium (pCi/L)	Not analyzed	987
Uranium (µg/L)	2.86	2.88

5.4.3 Groundwater Contamination beneath Waste Management Area C

This section discusses the current and historical groundwater contamination at WMA C. The evaluation of contamination includes descriptions of the types and concentrations of contaminants in the groundwater and the areal extent of contamination in the area. Much of the information in this section is taken from Chapter 2.10, “200 BP-5 Operable Unit” of PNNL-15670. Groundwater at WMA C is monitored to meet requirements of RCRA and the *Atomic Energy Act of 1954*. The objective of RCRA monitoring is to detect whether dangerous

waste constituents associated with the facility have compromised groundwater quality. Monitoring continued under an interim status indicator evaluation program at the WMA in FY 2005. Groundwater monitoring under the *Atomic Energy Act of 1954* tracks radionuclides beneath the WMA and surrounding vicinity.

Figure 5-10. Major Cation and Anion Composition of Groundwater from Upgradient Wells at Waste Management Area C.

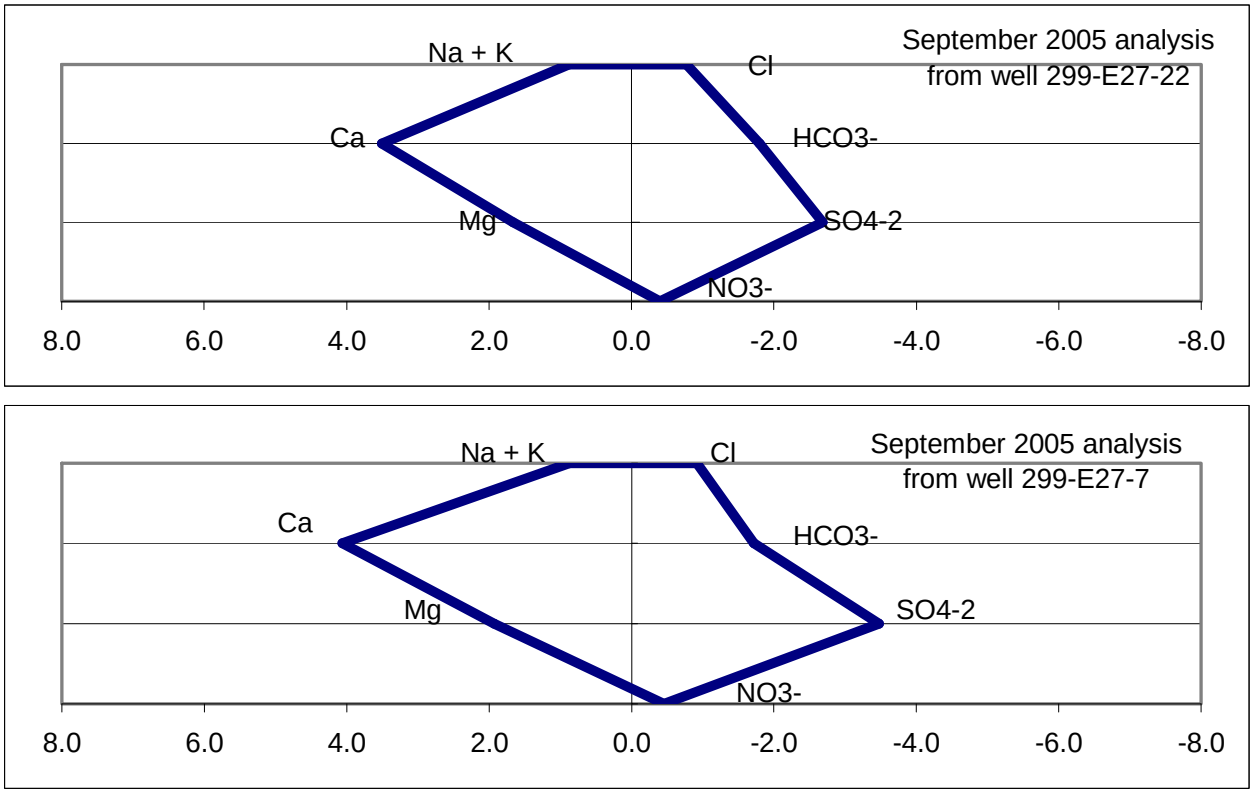

Note: Units for the x-axis are milliequivalents/liter with cations on the left and anions on the right.

5.4.3.1 Distribution of Selected Contaminants with Depth. Very little information is available concerning the vertical extent of contaminants in the uppermost aquifer beneath WMA C. Well 299-E27-22 is the only well in the area that has been sampled at more than one depth in the aquifer. Air-lifted groundwater samples were collected during drilling of well 299-E27-22 from five intervals in the aquifer. Samples were analyzed in the field for specific conductivity, nitrate, ^{99}Tc, and pH (PNNL-14656). Table 5-9 and Figure 5-11 show the analytical results. The data show that specific conductance, nitrate, and ^{99}Tc all increase with increasing depth, although the magnitude of the increase is not great. All concentrations are greater than Hanford Site background. However, well 299-W27-22 is an upgradient well and the magnitudes of the concentrations are less than the concentrations found in some downgradient wells at the time well 299-E27-22 was drilled. The latest (September 2005) sampling of well 299-E27-22 yielded a nitrate concentration of 24.8 mg/L and ^{99}Tc concentration of 30.2 pCi/L. These concentrations were obtained from the screened, upper 10 m of the aquifer and appear reasonable when compared with the depth discrete data in Figure 5-11.

Table 5-9. Depth-Discrete Water Sampling Results from Well 299-E27-22.

Sample Depth (m below water table)	Specific Conductivity (µS/cm)	pH	Nitrate (mg/L)	Tc-99 (pCi/L)
2.8 – 3.7	447	Not analyzed	14.2	10.9
5.0 – 5.9	412	8.11	16.2	Not detected
6.6 – 7.2	429	7.95	18.4	14
9.0	439	7.98	20.1	38.5
11.4	563	8.01	31.1	80.1
Hanford Site Background*	348	7.78	5.68	0.447

Reference: PNNL-14656, *Borehole Data Package for Four CY 2003 RCRA Wells 299-E27-4, 299 E27-21, 299-E27-22, and 299-E27-23 at Single-Shell Tank, Waste Management Area C, Hanford Site, Washington.*

*Data from DOE/RL-96-61, *Hanford Site Background: Part 3, Groundwater Background.*

Figure 5-11. Specific Conductance and Concentrations of Nitrate and Technetium-99 versus Depth below the Water Table in Well 299-E27-22.

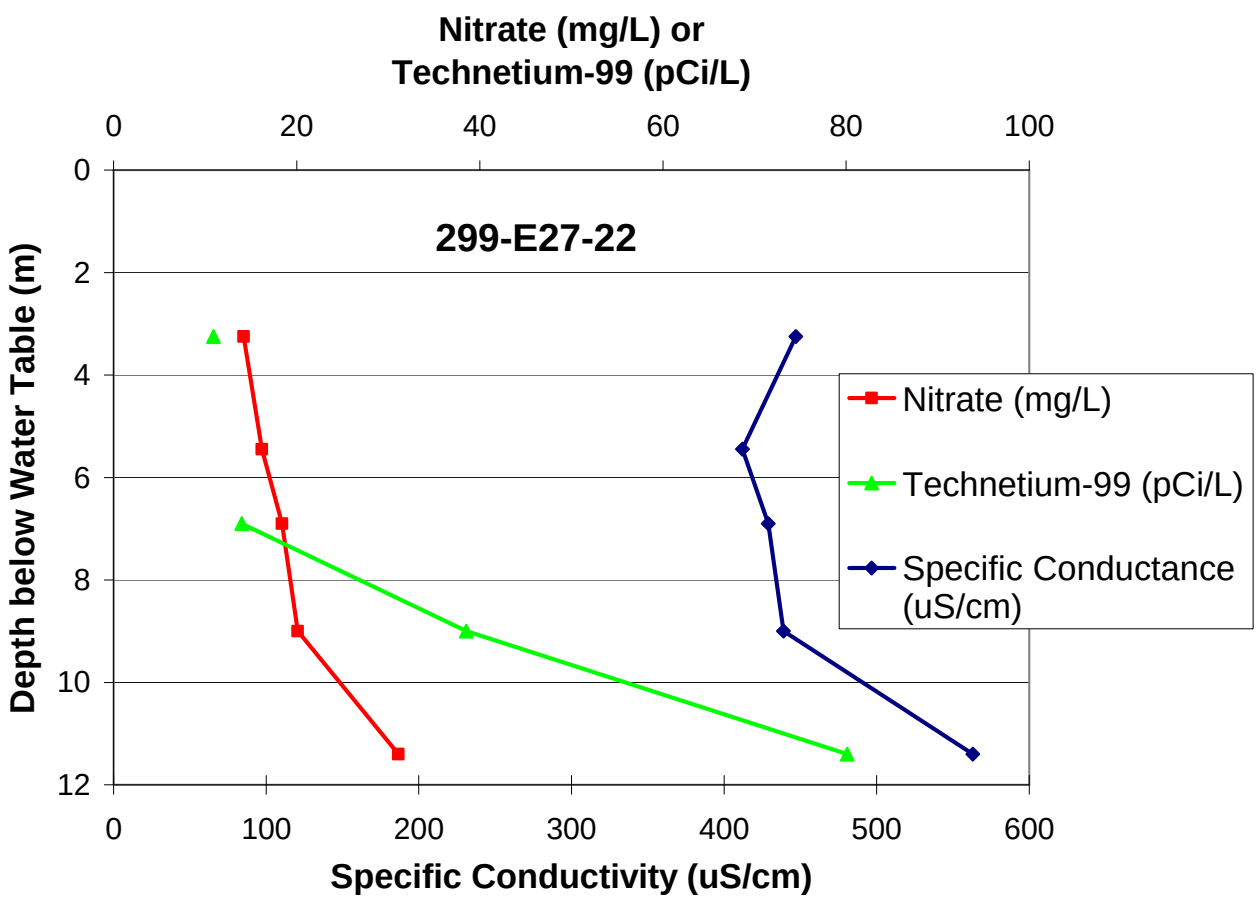

Data source: PNNL-14656, *Borehole Data Package for Four CY 2003 RCRA Wells 299-E27-4, 299 E27-21, 299-E27-22, and 299-E27-23 at Single-Shell Tank, Waste Management Area C, Hanford Site, Washington.*

5.4.3.2 Areal Distribution of Selected Contaminants. This section summarizes the aerial distribution of contaminants in groundwater at WMA C. Most of the information in this section is from Chapter 2.10 of PNNL-15670. Groundwater at WMA C contains elevated concentrations of calcium, chloride, cyanide, nitrate, sulfate, ^{99}Tc, ^{129}I, tritium and to lesser extents sodium and magnesium. Much of the tritium, nitrate, and ^{129}I at the WMA is attributed to regional plumes that extend across 200 East Area. However, a local area of high nitrate concentration exists beneath the WMA C and high ^{129}I is observed in one well at the WMA.

Few data are available before the early 1990s when most of the monitoring wells were drilled at the tank farm. The oldest well, well 299-E27-7, was drilled in 1982 and the oldest groundwater monitoring data associated with the well are gross beta values beginning in 1984, and nitrate concentrations beginning in 1985. Between 1984 and about 1998, gross beta values in well 299-E27-7 were only slightly greater than the Hanford Site background of 5.6 pCi/L (DOE/RL-96-61). Nitrate concentrations were close to or less than Hanford Site background concentrations (5.68 mg/L) until about 1992 when an increase in nitrate concentrations occurred, accompanied by increases in concentrations of most major cations and anions. Nitrate decreased to near background concentrations in 1993 and remained low until 1998.

Cobalt-60 was also detected at low levels in five wells at WMA C between 1991 and 1994. The highest concentration was 10.4 pCi/L in mid-1992. Although analyses for ^{60}Co have continued to the present, no ^{60}Co has been detected in the groundwater at WMA C since November 1994. There are no available data to assess groundwater contamination beneath WMA C prior to the early 1990s.

Because concentrations change over time, a time period must be chosen to examine spatial distribution patterns. For this purpose, the most recent data (average of FY 2005 sampling events) were chosen and these data are tabulated in Table 5-10. Data were then plotted and inspected for distribution patterns or groupings. Contour maps of contaminant concentrations were drawn to identify spatial patterns that might be indicative of source areas. The maps are shown in the series of Figures 5-12 through 5-15.

The data for ^{129}I in Table 5-10 are somewhat misleading because, in FY 2005, analyses for ^{129}I were made only on one sample from each of the two wells on the east side of the WMA. Prior to early 2001, ^{129}I was detected routinely in wells 299-E27-12, 299-E27-13, and 299-E27-15, located along the western edge of the WMA, at concentrations comparable to those in wells along the eastern edge. No analyses were done in the western wells since that time. The situation is similar for tritium in that tritium analyses from all wells done in 2004 and earlier showed concentrations similar to the concentrations for the two wells in Table 5-10 and to the regional trends.

Table 5-10. Average Concentration of Mobile Contaminants in Groundwater in the Vicinity of Waste Management Areas C for Fiscal Year 2005.[a]

Wells	NO_3 (mg/L)	CN (µg/L)	Ca (µg/L)	Na (µg/L)	Cl (mg/L)	SO_4 (mg/L)	^{129}I (pCi/L)	^{99}Tc (pCi/L)	Tritium (pCi/L)	Specific Conductance (µS/cm)[b]
299-E27-4	18.18	Not detected	47,900[c]	12,240[c]	10.55	70.42	Not analyzed	5,095	Not analyzed	388
299-E27-7	**26.22**	**31.03**	**77,675**	**15,450**	**31.30**	**156.5**	**3.81**	**81.4**	**987[d]**	**649[e]**
299-E27-12	9.19	Not detected	41,100	11,900	9.82	50.08	Not analyzed	60.3	Not analyzed	352
299-E27-13	12.4	Not detected	40,825	11,650	8.75	58.1	Not analyzed	2,170	Not analyzed	355
299-E27-14	46.70	Not detected	97,150	17,875	29.72	205.5	4.95	2,038	1,060[d]	771
299-E27-15	17.92	5.6[d]	50,825	15,825	14.85	88.85	Not analyzed	208	Not analyzed	453
299-E27-21	19.15	Not detected	42,500	13,700	8.52	63.2	Not analyzed	512	Not analyzed	369
299-E27-22	**20.15**	**Not detected**	**64,600**	**14,025**	**23.92**	**113.85**	**Not analyzed**	**38.2**	**Not analyzed**	**535**
299-E27-23[c]	25.56	Not detected	50,260	13,360	12.52	82.18	Not analyzed	1,904	Not analyzed	427
Hanford Site Background[f]	5.68	5.43	36,518	13,402	7.05	27.1	2.88E-6	0.447	63.9	348

[a] Average concentration of four, quarterly samples unless specified otherwise.
[b] Average of 16 analyses.
[c] Average of 5 analyses.
[d] One analysis.
[e] Average of 13 analyses.
[f] Background values are from DOE/RL-96-61, *Hanford Site Background: Part 3, Groundwater Background*.

Bold indicates upgradient wells.

Figure 5-12. Average Fiscal Year 2005 Tritium Concentration in the Area of Waste Management Area C, Top of the Aquifer.

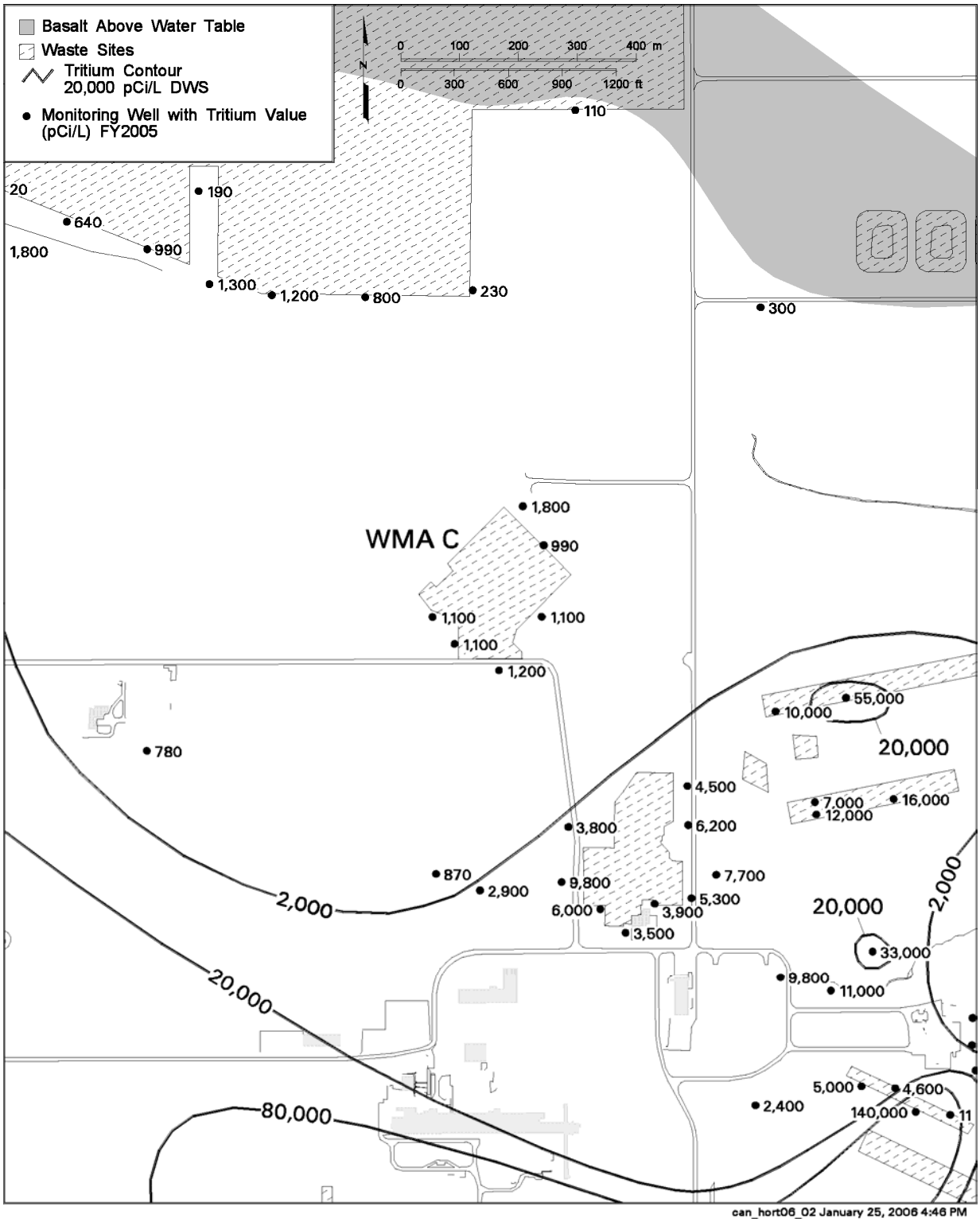

DWS = drinking water standard FY = fiscal year WMA = Waste Management Area

Reference: PNNL-15670, *Hanford Site Groundwater Monitoring for Fiscal Year 2005*.

Figure 5-13. Average Fiscal Year 2005 Iodine-129 Concentration in the Area of Waste Management Area C, Top of the Aquifer.

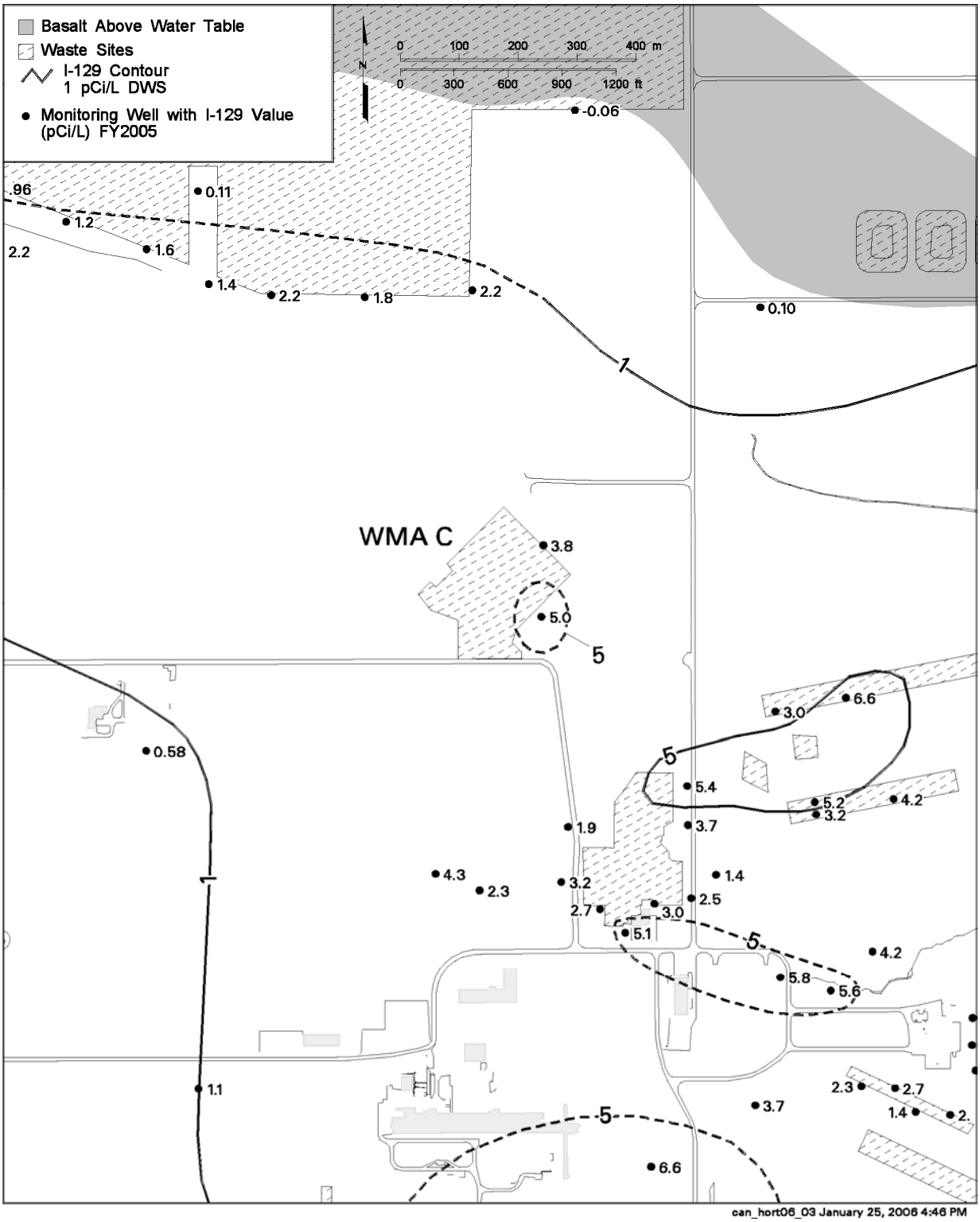

DWS = drinking water standard FY = fiscal year WMA = Waste Management Area

Reference: PNNL-15670, *Hanford Site Groundwater Monitoring for Fiscal Year 2005*.

Figure 5-14. Average June 2005 Nitrate Concentrations in the Area of Waste Management Area C, Top of the Aquifer.

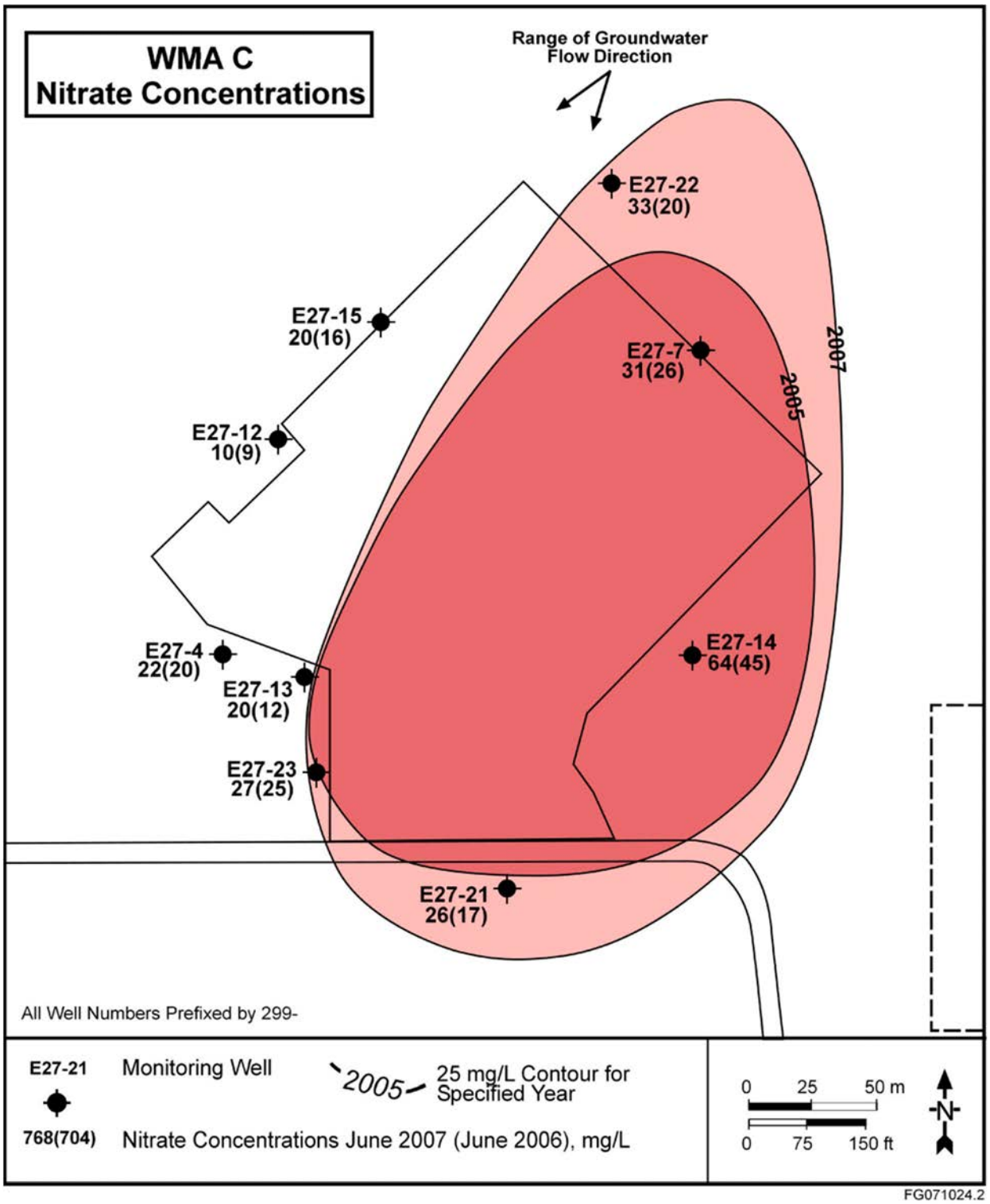

WMA = Waste Management Area

Reference: PNNL-15670, *Hanford Site Groundwater Monitoring for Fiscal Year 2005*.

Figure 5-15. Average Fiscal Year 2006 Technetium-99 Concentrations in the Area of Waste Management Area C, Top of the Aquifer.

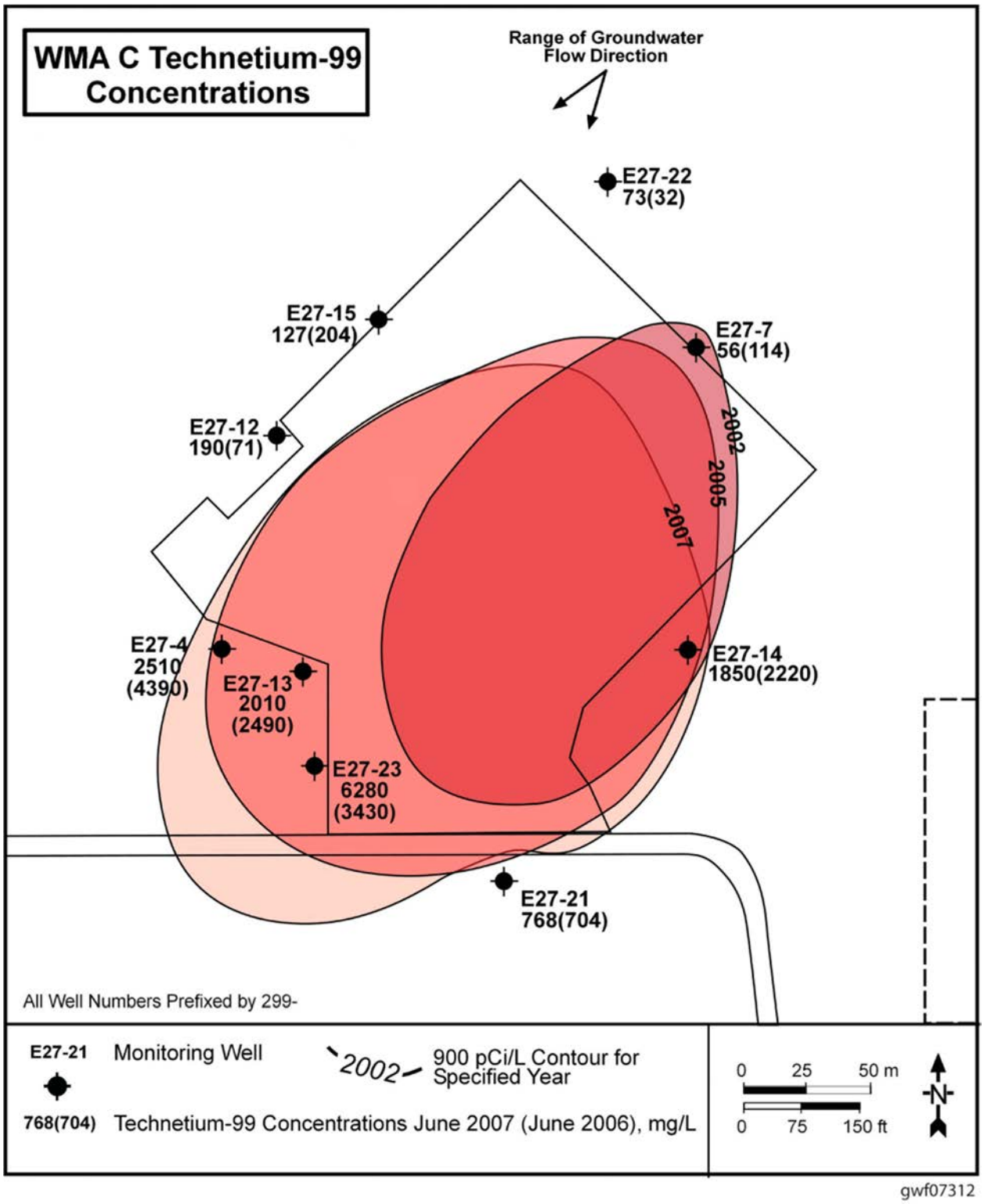

WMA = Waste Management Area

Tritium and ^{129}I are present in the unconfined aquifer beneath most of the 200 East Area (Figures 5-12 and 5-13, respectively) and both ^{129}I and tritium plumes have been mapped beneath the 200 East Area since at least the late 1970s (e.g., PNL-2899, *Radiological Status of the Ground-Water Beneath the Hanford Project January – December 1978*). The ^{129}I and tritium in the groundwater beneath WMA C is believed to be part of the regional 200 East Area plume, and are attributed to liquid discharges associated with the cribs and trenches near the PUREX facility.

A nitrate plume underlies much of the 200 East Area (Figure 5-14) and much of this plume also is attributed to discharges to various cribs and ditches throughout the 200 East Area. However, a local plume of nitrate occurs in the area of WMA C (Figure 5-14) and some of this nitrate may be from the WMA. Prior to about 1998, the nitrate concentration at WMA C was less than or near background levels. Beginning in about 1998, the nitrate concentration started to increase in all wells at WMA C. The highest concentrations historically were in the upgradient well 299-E27-7 on the northeast of the tank farms and well 299-E27-14 on the eastern side of the tank farm. These wells still had the largest nitrate concentrations in early 2005, but since about 2004, nitrate concentrations in some downgradient wells are similar to that in well 299-E27-7.

Figure 5-15 shows a plume map for ^{99}Tc in the top of the aquifer beneath WMA C in FY 2006. Elevated ^{99}Tc was first noted in the area during the late part of 2000 when concentrations began to increase from less than 100 pCi/L to 2,730 pCi/L in early 2002 in upgradient well 299-E27-7 (Figure 5-16). Subsequently the ^{99}Tc concentration rapidly decreased to pre-2002 values of less than about 500 pCi/L. The increase in ^{99}Tc was accompanied with an increase in sulfate and smaller increase in nitrate concentration (Figure 5-15). Both sulfate and nitrate concentrations continued to increase as the ^{99}Tc plume passed the well and both continue to increase today.

Water-quality changes in wells in the immediate vicinity of the WMA C for selected constituents (specific conductance, sulfate, nitrate, and ^{99}Tc), presented in Figure 5-17, provide an overall picture of groundwater impacts near WMA C going back to the early 1980s. The relationships among nitrate, sulfate, and ^{99}Tc are not constant from well to well at WMA C. Figure 5-18 shows concentrations for these constituents for four down-gradient wells. The concentrations of nitrate, sulfate, and ^{99}Tc began increasing simultaneously in well 299-E27-14 in 1998 to 1999 (Figure 5-18A). The sulfate and nitrate concentrations also began to increase in well 299-E27-13 in 1998. However, the ^{99}Tc concentration did not begin increasing in the latter well until about two years later in 2000 (Figure 5-18B). The other two down-gradient wells with significant ^{99}Tc, wells 299-E27-4 and 299-E27-23, were drilled after contamination arrived in the area such that the time of arrival of the contaminants is not recorded in the wells (Figure 5-18C and D). Figure 5-19 shows the ^{99}Tc/nitrate and ^{99}Tc/sulfate ratios (pCi/mg) in those wells at WMA C that have elevated ^{99}Tc. The ratios in the figure show that only in well 299-E27-14 do the concentrations of ^{99}Tc, nitrate, and sulfate track with each other. In all other wells the concentration of ^{99}Tc increases more rapidly than nitrate and sulfate, especially in wells 299-E27-13 and 299-E27-4. However, the presence of regional nitrate and sulfate plumes in the 200 East Area complicates the interpretation. These relationships show the difficulty in pinpointing a particular source for the contamination and it is likely that more than one source is involved.

Figure 5-16. Nitrate, Sulfate, and Technetium-99 Concentrations in Upgradient Well 299-W27-7 at Waste Management Area C.

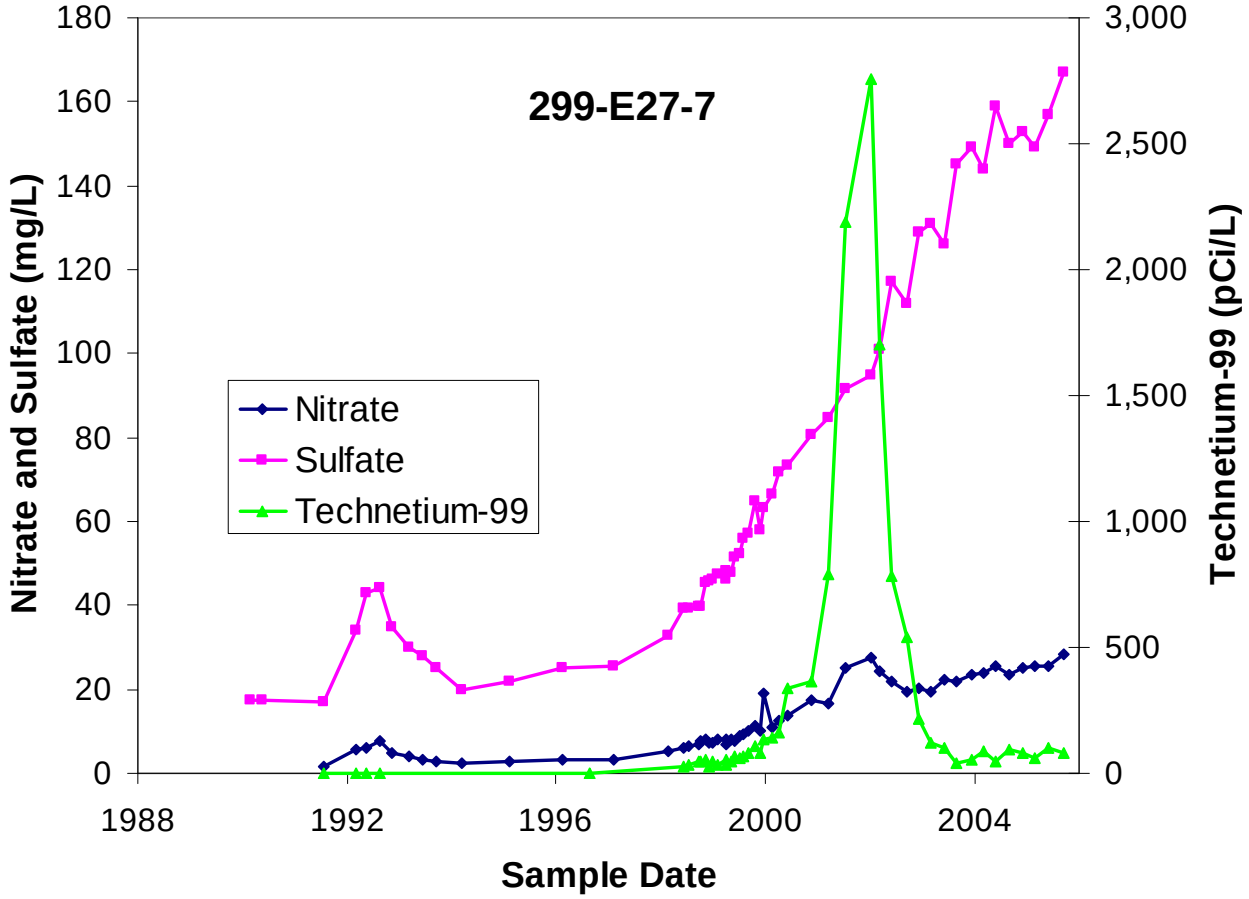

Several wells at WMA C have had detectable cyanide concentrations in the past five to six years although the concentrations have been erratic in most wells. The earliest detected cyanide in the area was in wells 299-E27-14 and 299-E27-15, located on the west and east sides of the WMA respectively, in the early 1990s. Both wells had one detectable occurrence of cyanide at less than 6 µg/L, but no subsequent analyses for cyanide were made until late in 2000 (Figure 5-20).

Since 2000, most wells in the WMA C monitoring network have shown sporadic cyanide concentrations in the groundwater. The highest concentrations have been in upgradient well 299-E27-7. Although this is the well that showed the earliest ^{99}Tc plume in the area, the high cyanide post-dates the passing of the ^{99}Tc plume by about 2 years. The fact that concentration increases and decreases of ^{99}Tc, cyanide, sulfate, and nitrate do not all coincide suggests that there is more than one source for the contaminants at WMA C. The identity of the specific sources has not been determined.

Figure 5-17. Selected Water Quality Showing Groundwater Impacts in Vicinity of Waste Management Area C. (1 of 5 sheets)

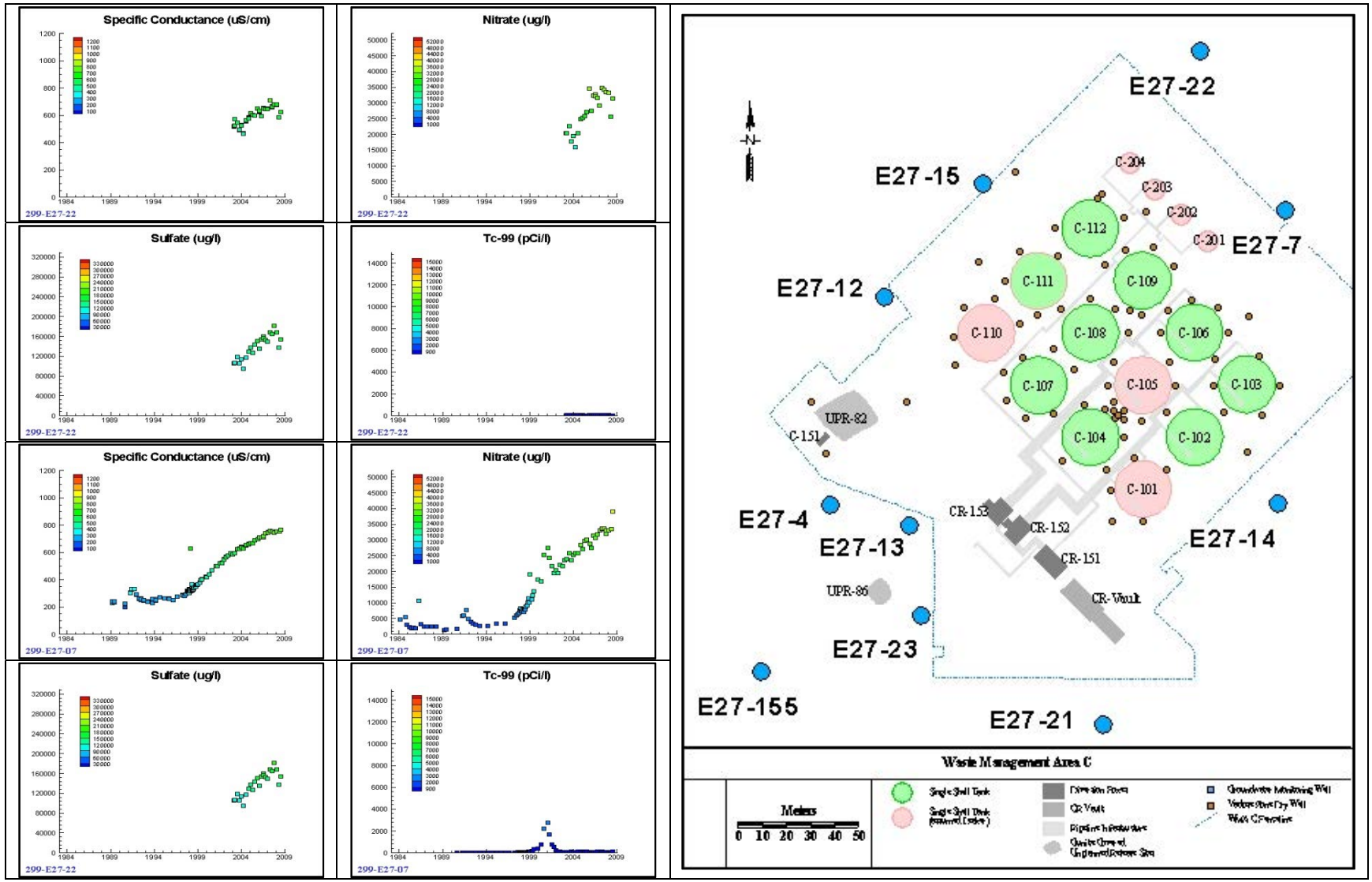

Figure 5-17. Selected Water Quality Showing Groundwater Impacts in Vicinity of Waste Management Area C. (2 of 5 sheets)

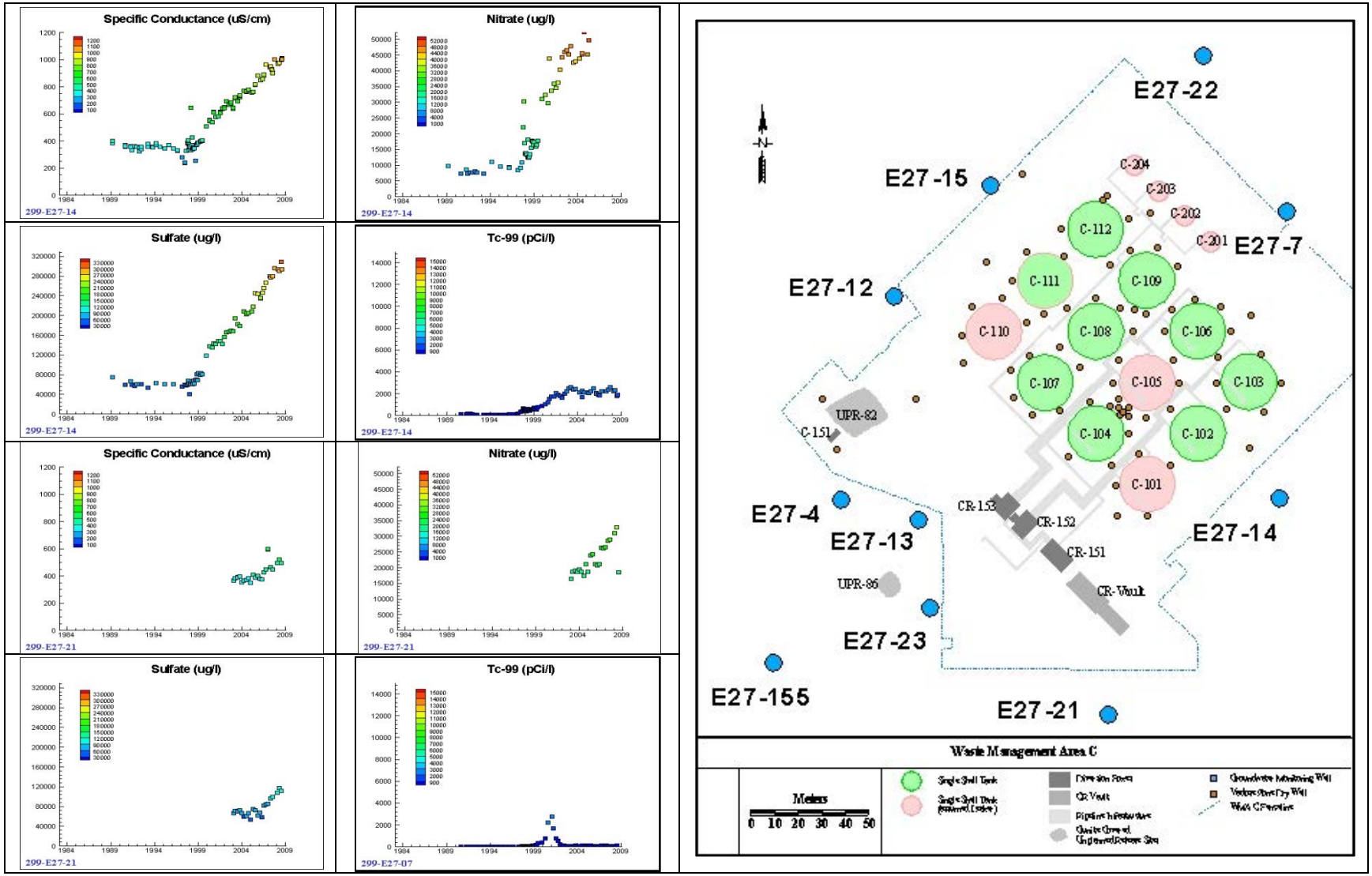

Figure 5-17. Selected Water Quality Showing Groundwater Impacts in Vicinity of Waste Management Area C. (3 of 5 sheets)

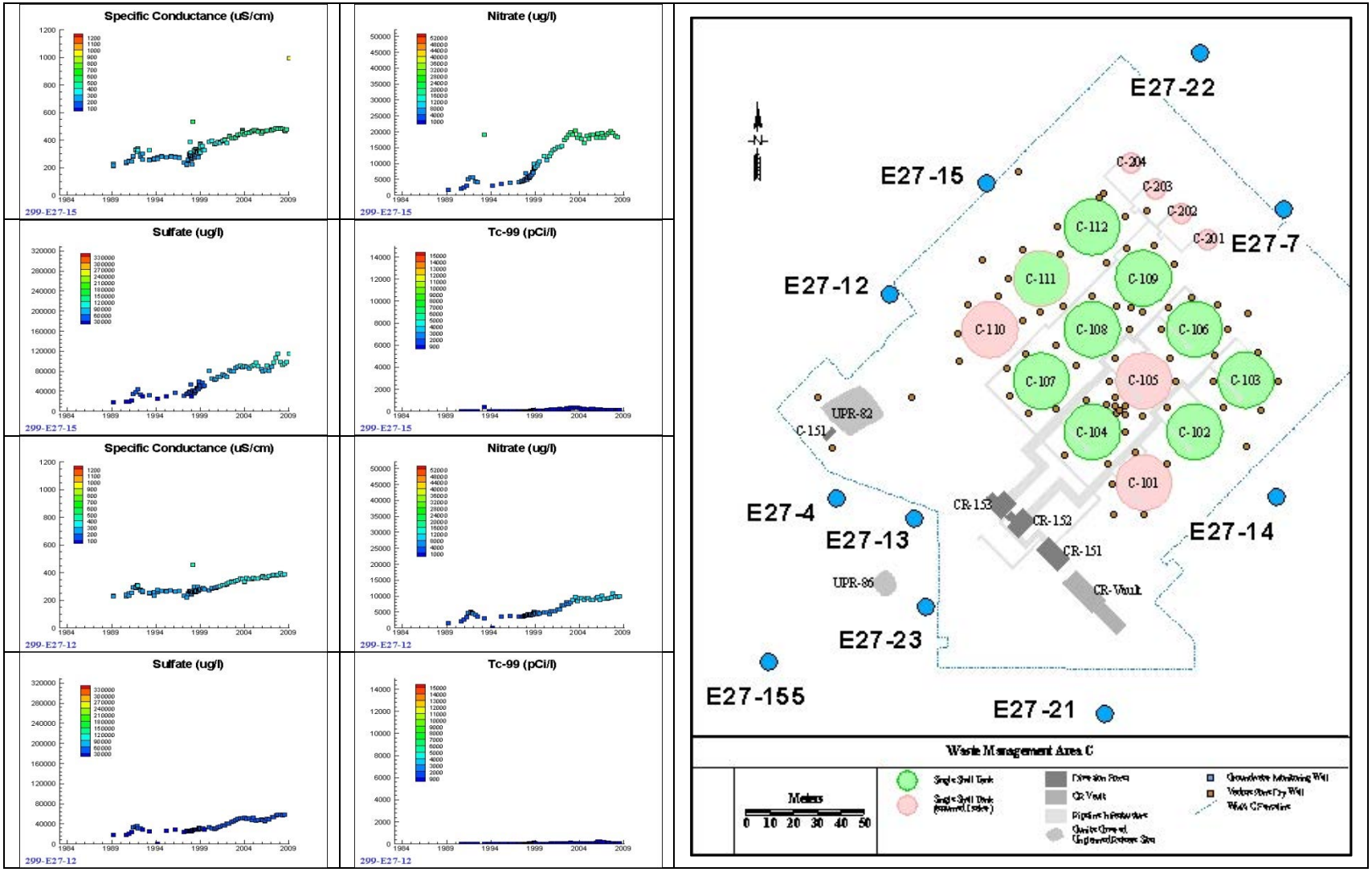

Figure 5-17. Selected Water Quality Showing Groundwater Impacts in Vicinity of Waste Management Area C. (4 of 5 sheets)

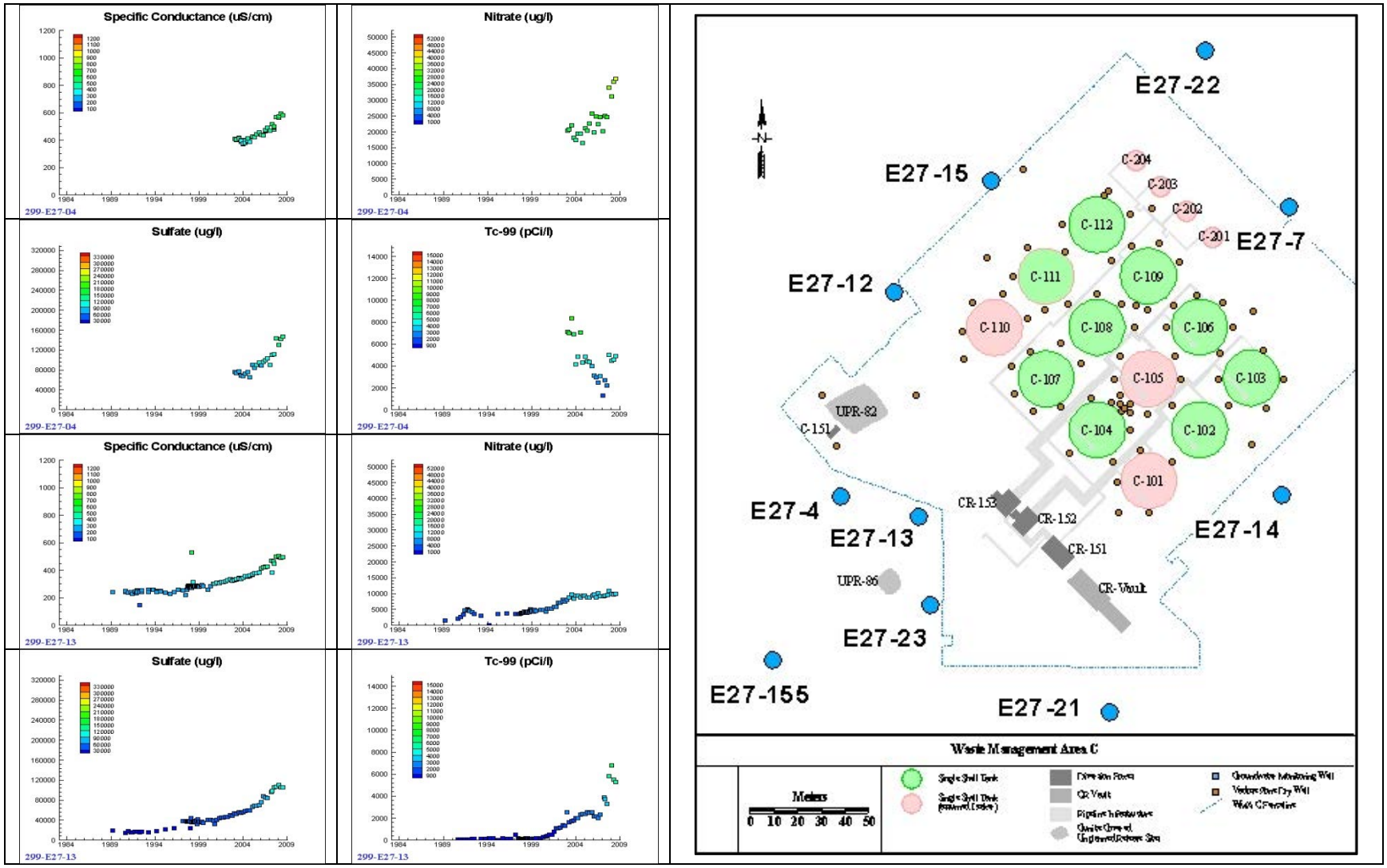

Figure 5-17. Selected Water Quality Showing Groundwater Impacts in Vicinity of Waste Management Area C. (5 of 5 sheets)

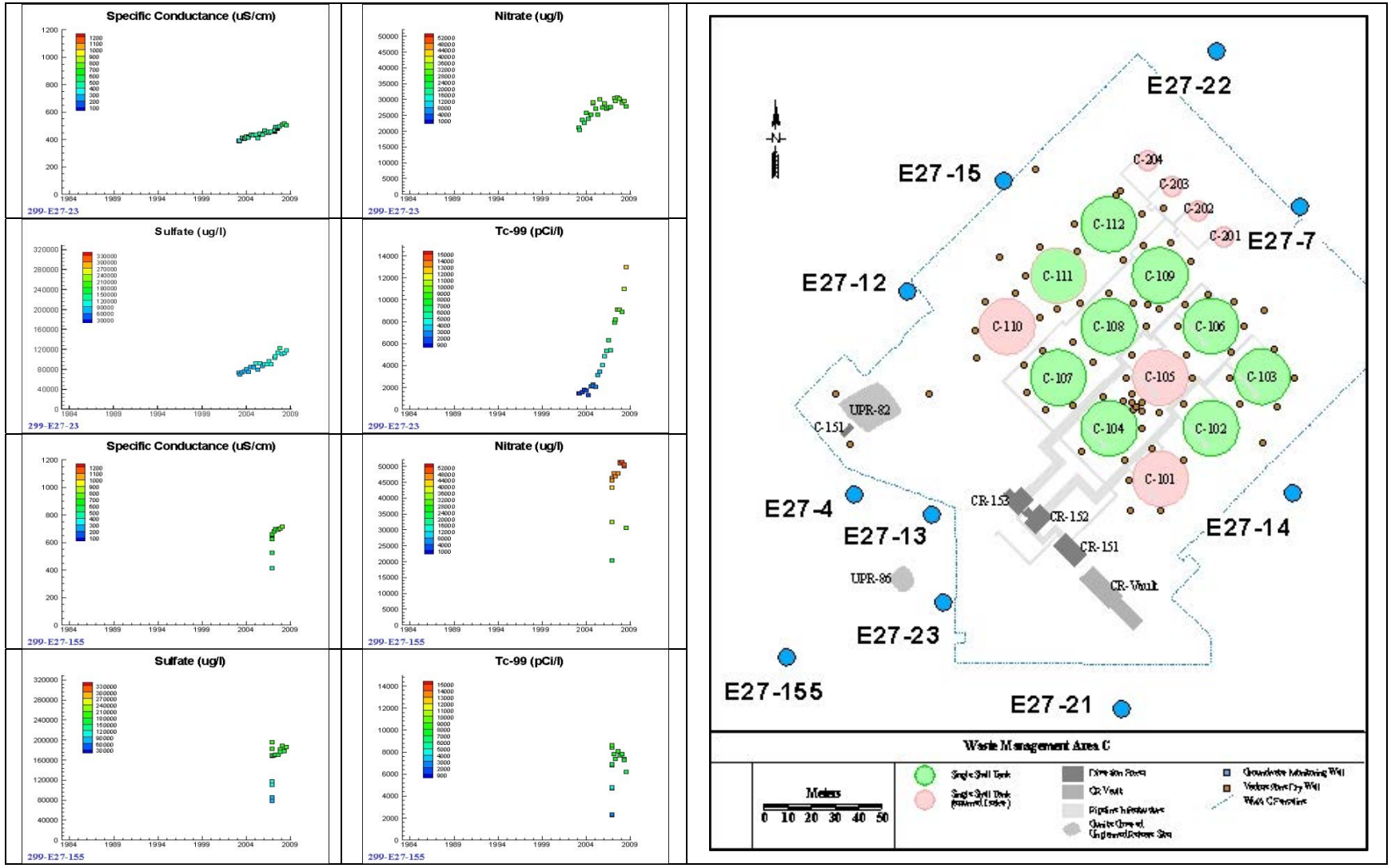

Figure 5-18. Sulfate, Nitrate, and Technetium-99 Concentrations in Selected Downgradient Wells at Waste Management Area C.

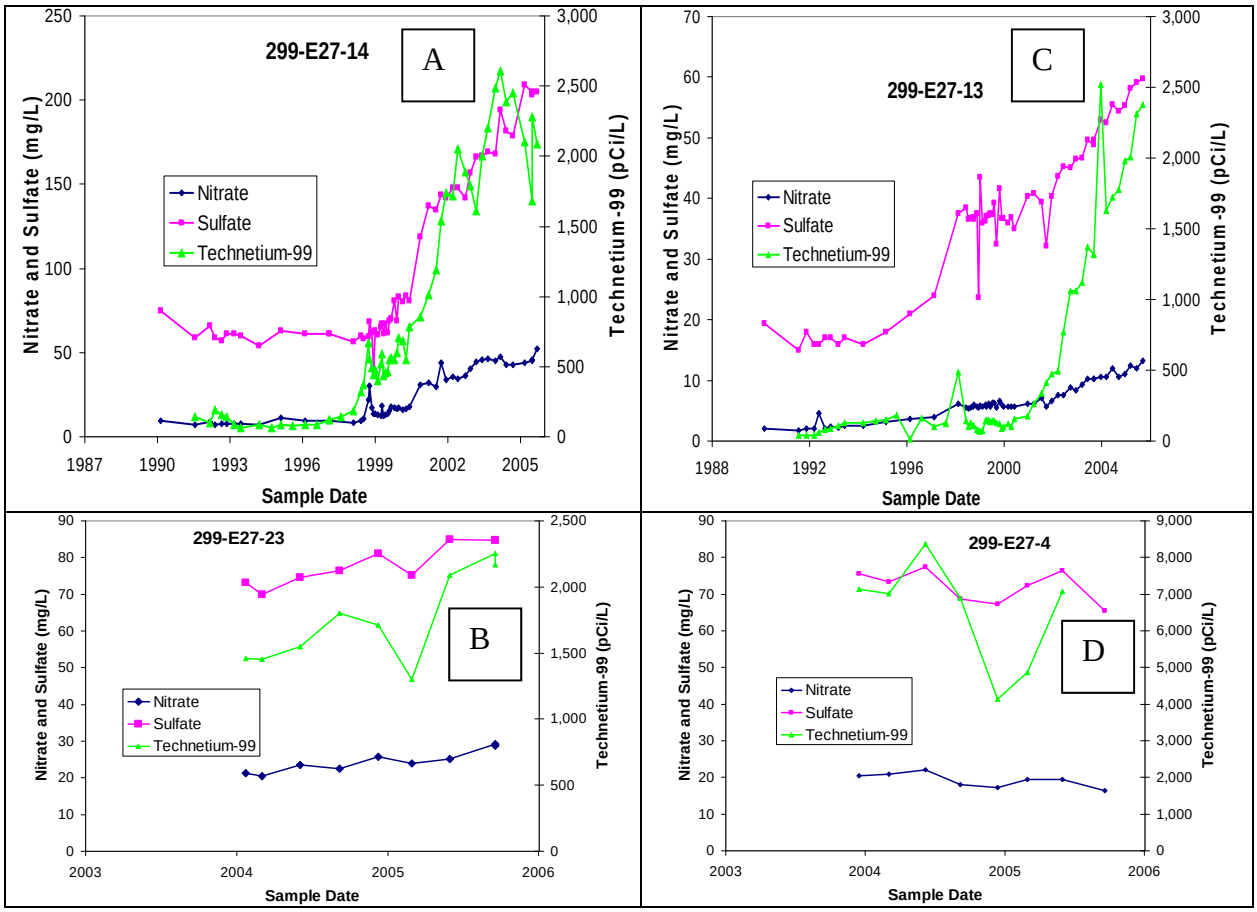

5.4.3.3 Comparison of Groundwater, Vadose Zone Pore Water, and Tank Leak Chemical Compositions. Nitrate, ^{99}Tc and other constituents like sulfate have been used to compare groundwater chemical composition with vadose zone pore water composition and estimated tank and crib waste chemical compositions [PNNL-13801, *Groundwater Quality Assessment Report for Waste Management Area S-SX (April 2000 through December 2001)*; PNNL-14594, *Characterization of Vadose Zone Sediments Below the TX Tank Farm: Boreholes C3830, C3831, C3832 and RCRA Borehole 299-W10-27*; PNNL-14849, *Characterization of Vadose Zone Sediments Below the T Tank Farm: Boreholes C4104, C4105, 299-W10-196, and RCRA Borehole 299-W11-39*] because these data are readily available for groundwater samples. Nitrate and ^{99}Tc also have very low distribution coefficients (PNNL-13895) and little, if any, fractionation of the two is expected in the vadose zone and aquifer (PNNL-15837, *Data Package for Past and Current Groundwater Flow and Contamination Beneath Single-Shell Tank Waste Management Areas*).

Specific efforts have been made in the past to correlate general groundwater chemistry characteristics with vadose zone pore water, tank waste chemistry to identify potential sources within WMA C of underlying groundwater contamination (see Section 4.3.6 in PNNL-15837). A summary of these efforts are provided in Appendix F of this report.

Figure 5-19. Technetium-99/Nitrate and Technetium-99/Sulfate Relationships for Selected Wells at Waste Management Area C (data for C4297 from PNNL-15503; all other data from Hanford Environmental Information System 1994).

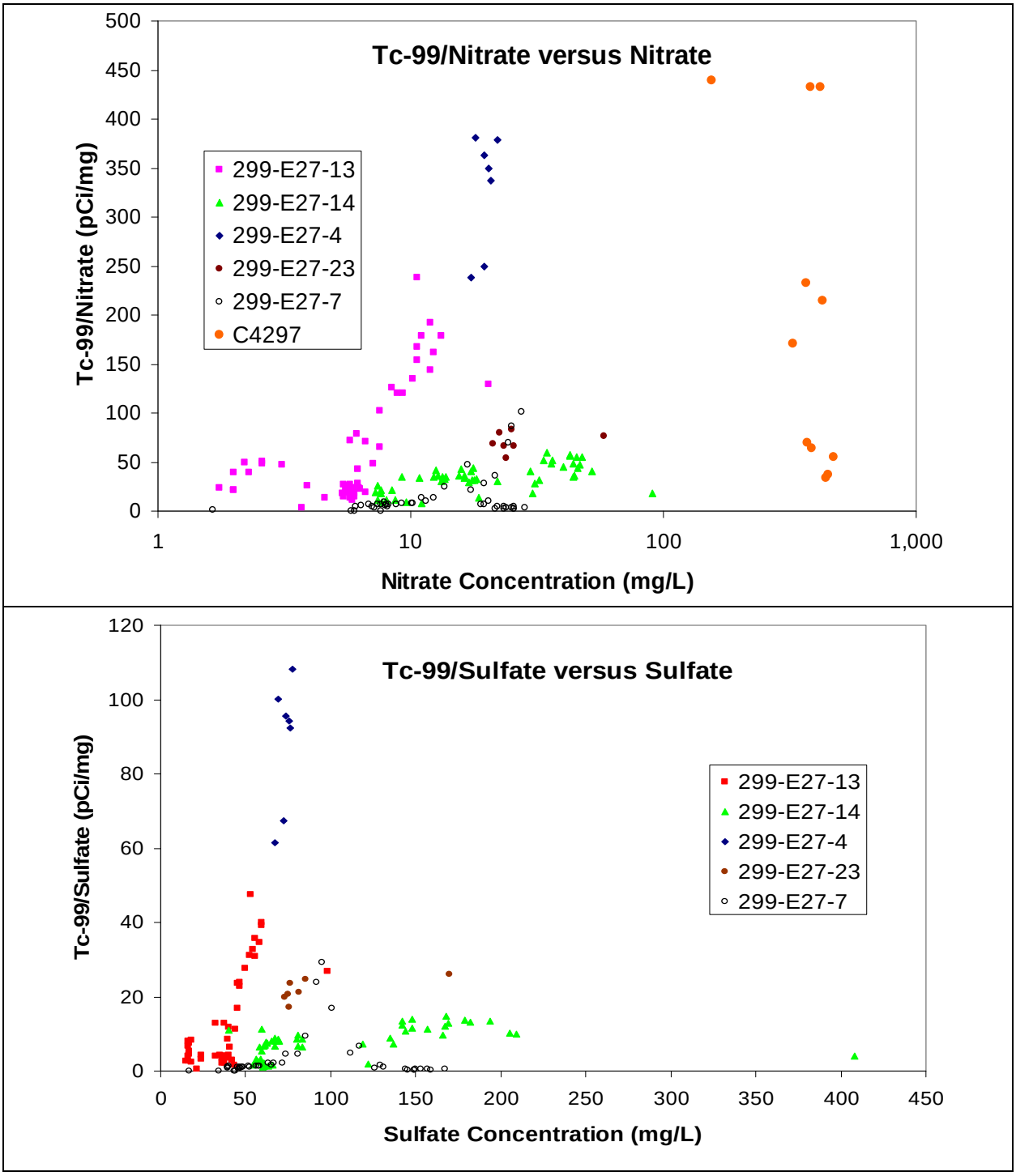

Reference: PNNL-15503, *Characterization of Vadose Zone Sediments Below the C Tank Farm: Borehole C4297 and RCRA Borehole 299-E27-22*, Rev. 1.

Figure 5-20. Cyanide Concentration in Wells at Waste Management Area C.

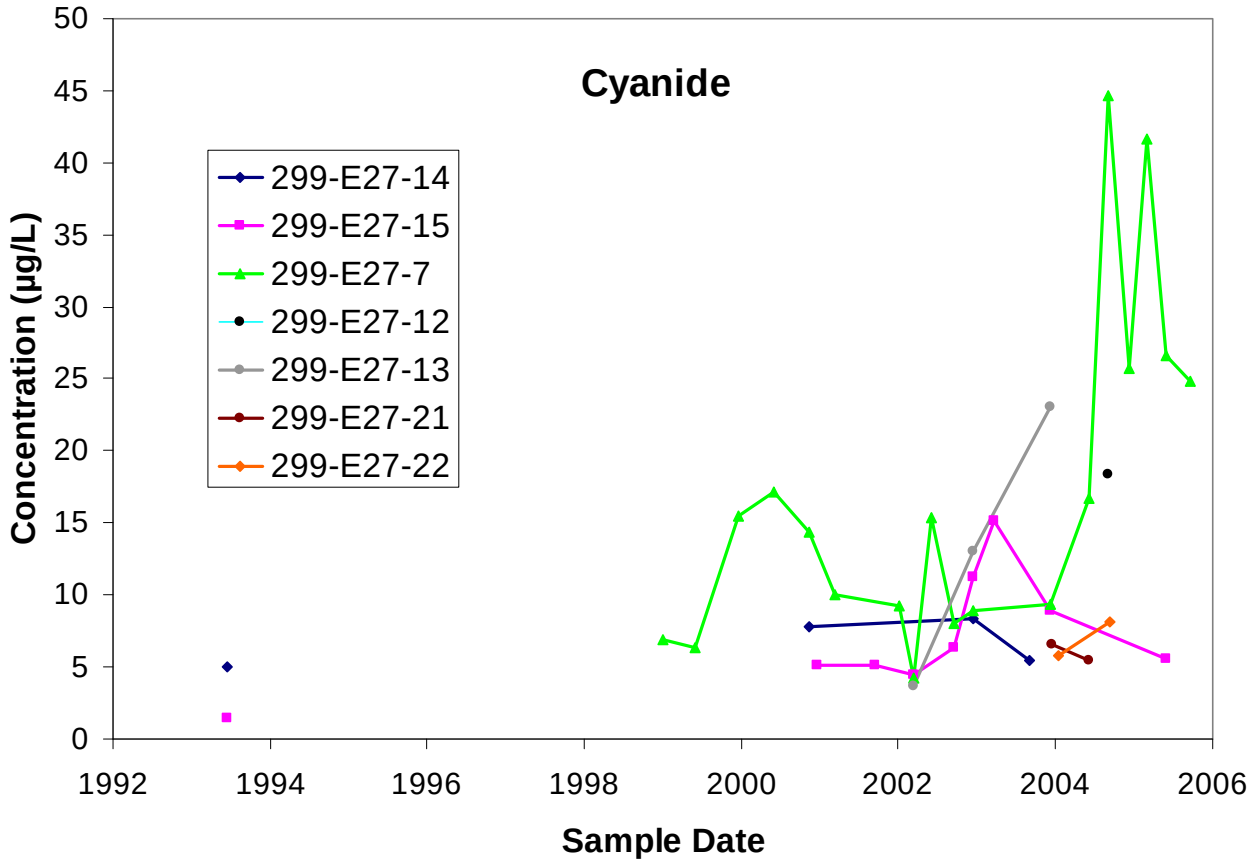

Results of these efforts have made the following conclusions:

- Comparison of the chemical ratios of $^{99}Tc/NO_3$ and $^{99}Tc/SO_4$ from the estimated tank fluids with those from groundwater analyses show that for some wells the tank fluids and groundwater ratios agree within an order of magnitude. For other wells, the ratios are not very similar.

- These comparisons allow for the possibility of tank waste from leaks associated with tanks C-110 and C-111 to have impacted groundwater. However, given the uncertainties in the tank fluid estimates and given the potential interferences in the groundwater ratios due to regional nitrate and sulfate plumes, a direct correlation is tenuous.

- No clear chemical fingerprint was found that indicates similarities among estimated tank fluid compositions at the time of suspected leaks, groundwater contaminant compositions, or C4297 pore water composition at WMA C.

5.5 CONCEPTUAL MODEL FOR THE GROUNDWATER PATHWAY AT WASTE MANAGEMENT AREA C

Following is a brief summary of the conceptual model of groundwater system relevant to the WMA C that addresses 1) key characteristics of unconfined aquifer system, 2) hydraulic and water quality impacts from historic past operations, and 3) projected future hydraulic and water quality impacts.

5.5.1 Key Characteristics of Unconfined Aquifer System

Groundwater is present in both unconfined and confined aquifers at the Hanford Site. The unconfined aquifer is contained in the unconsolidated to semi-consolidated Ringold and Hanford formations that overlie the basalt bedrock. In some areas, low permeability mud layers form aquitards that create confined hydraulic conditions in the underlying sediment.

Within 200 East and specifically in vicinity of the WMA C, groundwater is found at a depth of 80 m and about the uppermost unconfined aquifer is made of undifferentiated sands and gravels of the lower part of Hanford formation, the CCU, and the Ringold Formation that collectively range from 8 to 27 m thick.

Natural sources of recharge to the unconfined aquifer system occur due to the following.

- Infiltration of runoff from elevated regions along the western boundary of the Hanford Site.

- Infiltration of spring water along the flanks the unconfined aquifer bordering upland areas.

- Upwelling of groundwater that originates from the basalt-confined aquifer system (Note: There have been situations in the past where the head in the unconfined system has been greater than that in the confined system leading to discharge of groundwater along with contaminants from the unconfined aquifer to the confined system).

- Infiltration of precipitation falling across the Hanford Site (Note: Infiltration from precipitation is temporally dependent; i.e., infiltration from precipitation is greater during the winter months because of greater precipitation and reduced evapotranspiration when plants are dormant, and much less during other times of the year primarily because of increased evapotranspiration due to plant activity).

- Some recharge also takes place along the Yakima River.

Recharge from precipitation is highly variable, both spatially and temporally. It ranges from near zero to greater than 100 millimeters per year, depending on climate, vegetation, and soil texture ("Variations in Recharge at the Hanford Site" [Gee et al. 1992], PNL-10285, *Estimated Recharge Rates at the Hanford Site*). The highest rates of recharge from precipitation are associated with areas for which surface conditions are dominated by coarse-textured soil with

little or no vegetation; such conditions are found in all SST WMAs, including the area in and around WMA C.

Regionally, groundwater in the unconfined aquifer flows toward and discharges to the Columbia River across most of the Hanford Site. Some variation to this generalization occurs in some operation areas along the river where artificial recharge mounds are present or during times of high river stage.

Waste Management Area C is located in an area where the underlying water-table is very flat. The gradient in the vicinity of WMA C is consistent with the regional gradient of 0.00002 and existence of extremely permeable sands and gravels associated with the Hanford formation.

The regional-scale interpretation of the water-table elevation in Figure 5-2 from DOE/RL-2008-66 infers a groundwater flow divide likely occurs in the 200 East Area with southeast flow in the southern part of this area. However, small differences in water elevations make it difficult to define the exact location of this groundwater divide.

5.5.2 Hydraulic and Water Quality Impacts from Past Operations

Since the start of Hanford Site operations in the mid-1940s, artificial recharge from wastewater disposal facilities has been several times greater than the estimated recharge from natural sources. This caused an increase in the water-table elevation over most of the Hanford Site and the formation of groundwater mounds beneath major wastewater disposal facilities. In the vicinity of WMA C, long-term hydrographs of water-level measurements suggest that unconfined aquifer has risen as much as 5 m and the direction of local-scale groundwater flow has changed in response to the artificial recharge for nearby wastewater disposal facilities.

The water table declined somewhat in the late 1960s and early 1970s, then increased again in the early 1980s before a final decline beginning in 1988 and continuing throughout the 1990s when wastewater discharges in the 200 East Area were significantly reduced. At WMA C, water-table elevations have declined about 3m since the early 1990s.

In the vicinity of the WMA C, the average flow direction is currently inferred based in part on water-level measurements and in evaluation and interpretation of local-scale plume migration to be to the south and southwest. Groundwater flow rates in the area are on the order of 0.2 to 0.4 m/day with flow direction historically to the southwest but difficult to confirm.

Groundwater at WMA C contains elevated concentrations of calcium, chloride, cyanide, nitrate, sulfate, ^{99}Tc, ^{129}I, and tritium and to lesser extents sodium and magnesium. Much of the tritium, nitrate, and ^{129}I contamination at the WMA C are attributed to regional plumes that extend across 200 East Area from upgradient areas to the north and northeast. However, a local area of high nitrate concentration exists beneath the WMA C and high ^{129}I is observed in one well at the WMA. Potential causes for elevated concentrations of other components such as calcium include: 1) natural sources, since a major cation in the natural background groundwater chemistry is calcium, and 2) ion exchange in the vadose zone because of the presence of

high-sodium in tank farm waste streams that has the potential to displace calcium and make it more mobile.

A review of groundwater contamination data directly below the WMA C shows that concentration levels for several constituents (i.e., ^{99}Tc, ^{129}I, nitrate, antimony, and nickel) are above the maximum contaminant level (MCL). Of particular interest are rising trends in concentrations in down-gradient wells 299-E27-13 and 299-E27-23 where ^{99}Tc levels are rising to concentrations of about 7,000 and 13,000 pCi/l, respectively.

Two constituents (i.e., sulfate and aluminum) are found to be above the secondary MCL. In addition, other tank waste related contaminants are also present (i.e., cyanide) but are found at levels well below MCLs. However, a review of historical concentration levels of two key tank waste related constituents, ^{99}Tc and nitrate, among the wells local to the WMA C show no clear trends. Except for ^{129}I, only known sources in the general vicinity of the areas of groundwater contamination above MCLs and secondary MCLs appear to be potential waste areas within the WMA C.

A comparison of water quality impacts in groundwater and results of limited characterization of the vadose zone at the WMA C suggest the potential existence of other unknown source(s) of waste fluids and contaminants that may have contributed to groundwater contamination found within and near the WMA C and could further impact the groundwater at WMA C in the future (see Appendix C, Section C.1.3).

These conclusions have led to the need to consider a number of alternative conceptual models that include either 1) the potential effect of additional known or unknown sources of water or waste fluids or 2) preferential pathways of flow and transport and in the vadose zone, to explain current groundwater observations in vicinity of the WMA and vadose zone observations in borehole thought to be upgradient of WMA C source areas.

One way to test the validity of an alternative model and to develop confidence in the model's ability to forecast into the future is to perform history matching; i.e., run the model using historic release information/data to determine when releases from the SSTs reach groundwater. One of the major shortcomings of a thorough evaluation of conceptual models using history matching is that many of required data, information and parameters are incompletely known or known only within broad ranges.

As an alternative to broader site-wide history matching, some limited evaluations of alternative conceptual models have been performed using scoping calculations that would be applicable to past features, processes, and events at the WMA C. The results of some recently completed scoping analyses, which were presented in the Natural Systems Working Session held on May 25 through 27, 2010, provided a preliminary assessment of alternative conceptual models of recharge and of the vadose zone as they related to the depth of plumes at UPR-81, and the occurrence of groundwater plumes beneath WMA C in general. A complete description and results from these calculations along with the simplifying assumptions made in the analyses are provided in Appendix G.

This initial set of scoping calculations has been encouraging and would suggest that use of alternative conceptual models that consider the effects of reasonable amounts of additional water from operational use of water to estimates of natural recharge can be sufficient to approximate the general historical observations of contaminant arrival in the unconfined aquifer. Observations of these simple analyses lead to the following key findings.

- The existing depth of contamination at UPR-82 can likely be explained by current infiltration rates and past additions of water to the soil system.

- The existence of observed plumes in the unconfined aquifer does not require the postulation of an unknown fast path and can also be attributable to current infiltration rates and past additions of water to the soil system. However, this observation does not rule out the possibility that fast paths exist, but consideration of potential fast paths are not needed to fit the data.

5.5.3 Project Future Impacts

In the future, hydraulic and water quality conditions found beneath the WMA C are expected to change in the following manner.

- The effect of the historical wastewater discharges on the water table would dissipate and the water-level elevation in the unconfined aquifer would return to lower pre-Hanford conditions. Without any significant changes in land or water use either on site or up-gradient of the site, the current water-table at WMA C could likely decline another 3 to 5 m over the next 50 to 100 yrs before reaching this new lower equilibrium water table condition (see Table 5-5).

- Current interpreted directions of flow would be anticipated to change from the current south to southwesterly direction to a more south and southeasterly direction.

- Water-table and groundwater flow conditions could be influences with significant changes in land or water use nearby or up-gradient of the site.

- Water quality impacts from past contaminant releases to groundwater from the vadose zone or up-gradient sources could increase or decline locally as sources in the vadose zone continue to release to groundwater or up-gradient source pass beneath the site. Results of the SST PA suggest that existing sources of mobile contaminants within the vadose zone could continue to migrate downward and impact groundwater over the next 200 to 300 years.

- Eventually, mobile contaminants released from grouted residuals left in tanks and ancillary equipment would be first expected to impact groundwater about years 4000 to 6000 and peak in years 8000 to 10000.

5.6 RECOMMENDED FLOW AND TRANSPORT PROPERTIES

The following discussion presents recommended flow and transport properties that will be used to support an integrated, saturated and unsaturated, local-scale model that will be used to flow and transport simulations in the immediate vicinity of the WMA C. Results of these model simulation results will be used as input to regional-scale of groundwater flow and transport to evaluate water quality and risk impacts between the WMA C and points of regional discharge along the Columbia River.

The flow and transport properties that will be used in the regional-scale modeling efforts are based on the estimated parameters utilized in the site-wide groundwater model that has been developed and implemented within the framework of the TC&WM EIS (DOE/EIS-0391, *Draft Tank Closure and Waste Management Environmental Impact Statement for the Hanford Site, Richland, Washington*). The flow and transport properties used in the regional-scale modeling will not be specifically discussed as a part of this report. The reader is referred to the Appendices L (*Groundwater Flow Field Development*) and O (*Groundwater Transport Analysis*) in the TC&WM EIS for specific details of the development, calibration, and implementation of this site-wide groundwater flow and transport model.

Flow parameters such as saturated hydraulic conductivity, effective porosity, hydraulic gradient, and depth to water table are needed for the unconfined aquifer part of the integrated, saturated-unsaturated, local-scale model analysis up to the WMA C fence line. Recommendations for these specific parameters in RPP-13310 for the SST PA, which provide an initial set of estimates for these parameters for WMA C PA, are given in Table 5-11. Specific detailed discussions of the basis for these parameters are provided in Section 5 of RPP-13310.

Constituent-specific distribution coefficients that are recommended for use in the vadose zone pathway and summarized in Tables 4-8 and 4-9 within Section 4.5.3, provide the basis for the contaminant-specific distribution coefficients that will be used for contaminant transport calculations through the groundwater pathway.

Table 5-11. Recommended Parameter Values for Unconfined Aquifer Properties for Waste Management Area C.

Parameter	Estimated Value
Longitudinal Macro-dispersivity (m)[a]	62.5
Lateral Macro-dispersivity (m)[a]	12.5 m
Vertical Macro-dispersivity (m)[a]	0.0002 m
Molecular Diffusion Coefficient (cm^2/sec)[b]	2.5E-5
Distribution Coefficient (K_d)(mL/g)	Varies by contaminant (see Tables 4-15 and 4-16)
Depth to Water Table (m)	79 (259 ft)
Hydraulic gradient	0.00001
Saturated Hydraulic conductivity (m/day)	3,000
Effective porosity	0.25

Reference: RPP-13310, *Modeling Data Package for an Initial Assessment of Closure of the C Tank Farm*.

[a] These longitudinal, lateral, and vertical macro-dispersivity values are those recommended for use in regional-scale calculations of flow and contaminant in the unconfined aquifer. Recommendations for comparable dispersivities used in local-scale models that combine the unsaturated and saturated zone flow and contaminant transport can be found in Tables 4-6 and 4-7 of Section 4.5.2.

[b] The molecular diffusion coefficient for water is recommended in PNNL-14286, *STOMP Subsurface Transport Over Multiple Phases Version 3.0 User's Guide* and is used to calculate an effective diffusion coefficient for contaminant transport for all contaminants. The approach here is to use a conservative value of molecular diffusion coefficient for water to represent the effective diffusion coefficients for all constituents in the combined vadose zone and groundwater systems.

This page intentionally left blank.

6.0 SUMMARY OF PROPOSED CASES FOR VADOSE ZONE AND GROUNDWATER FLOW AND TRANSPORT

Assessment of water quality, dose, and risk impacts in the WMA C PA is expected to be accomplished using a combination of two separate but integrated models. A model of local-scale conditions of vadose zone and groundwater flow and transport will be used to assess impacts in the immediate area surrounding the WMA C. Releases from the WMA C generated for assessing impacts in the local-scale model will also be evaluated in a regional-scale groundwater flow and transport model to assess the same impacts at down-gradient points of assessment from the WMA fence line to the Columbia River.

This Section provides a summary of recommendations of proposed cases for both the local-scale and regional flow and transport models used in the WMA C PA.

6.1 LOCAL-SCALE VADOSE ZONE AND GROUNDWATER FLOW AND TRANSPORT

Based on the data and technical information presented in Sections 4 and 5, a range of cases are proposed to evaluate in the WMA C PA using the local-scale model of vadose zone and groundwater flow and transport. These cases will be examined with versions of the local-scale models that represent conditions observed during past operations as well as projected conditions for the post-closure period.

6.1.1 Conditions for Operational Period

As indicated in Appendix C, Section C.1.3, a review of general information found in groundwater and vadose zone characterization data within WMA C during the operational period suggests a discrepancy exists between observed data in the vadose zone and groundwater that needs to be examined. Because of the uncertainty in data and information related to the timing and location of past releases in the vadose zone, we have developed and will examine potential viable alternative conceptual models of vadose zone flow and transport for the WMA C. These models will need to consider a combination of factors that include:

- the potential effects of the hydraulic properties of stratigraphic units with depth in delaying vertical migration and enhancing lateral spreading
- the potential influences of other known or unknown sources in enhancing the migration of existing tank leak sources as they move through the vadose zone
- the possibility of features in the vadose zone that could enhance migration of contaminants along preferential pathways.

The resulting alternative conceptual models are described in Appendix D.

The local-scale flow and transport model of the WMA C that is developed for use in the WMA C PA will attempt to evaluate these alternative conceptual models to determine their applicability to our understanding of the impacts from past operations. These cases are provided in Table 6-1.

6.1.2 Conditions for Post-Closure Period

In addition to the general proposed cases examined with the local-scale model representing the past operation period, a set of other proposed cases are recommended for evaluation with local-scale flow and transport simulations that would be considered representative of conditions during the post-closure period. These cases are suggested to assess the effects of changing model parameters in four separate categories that include:

- Effects of alternative conceptual models of the vadose zone
- Effects of changing selected hydraulic properties of sediments in the vadose zone
- Effects of changing contaminant distribution coefficients
- Effects of changing hydraulic properties of the unconfined aquifer.

A summary of the proposed cases within these four categories are outlined in the following discussion.

6.1.2.1 Alternative Conceptual Models of Vadose Zone Flow and Transport. As discussed in Appendix D, several cases are proposed to examine the effects of alternative conceptual models on flow and transport (see Table 6-1). These cases evaluate the effect of discrete natural features potentially representing preferential pathways such as clastic dikes or sloping beds or man-made features such as unsealed dry wells, groundwater wells or boreholes. Results of running these cases using the local-scale flow and transport model will determine whether these proposed alternative conceptual model cases will be evaluated using the local-scale flow and transport model of the post-closure period.

6.1.2.2 Hydraulic Properties of Unsaturated Zone. A selected set of proposed simulations are recommended to evaluate the effects of hydraulic properties of unsaturated sediments at the WMA C. Sensitivity analysis associated with unsaturated flow parameters has been conducted in the past (DOE/RL-98-72, *Retrieval Performance Evaluation Methodology for the AX Tank Farm*; DOE/ORP-2000-24, *Hanford Immobilized Low-Activity Tank Waste Performance Assessment: 2001 Version*; SST PA [DOE/ORP-2005-01]). Historical work (e.g., DOE/ORP-2000-24 and the SST PA) indicates this feature of the system is generally of secondary importance to other key factors, such as recharge rates and inventory estimates of past releases. However, to account for sensitivity of unsaturated flow parameters in the WMA C PA, we propose a range of cases (Table 6-2) where the saturated hydraulic conductivity associated with unsaturated sediments at WMA C is changed by a scaling factor. In the proposed cases, the parameter variability is assumed to have a range that would be typical of saturated sands taken from the literature. A range from 0.1 to 500 m/day is recommended. This recommended range is reflective of hydraulic conductivity values for sands provided in Spitz and Moreno (1996). We would propose that recommended parameters for moisture-dependent anisotropy (see Section 4.5.1.2) be used in these cases.

Table 6-1. Proposed Simulation Cases Representing the Effects of Alternative Models on Vadose Zone Flow and Transport.

Alternative Model	Description Of Case	Basis For Parameterization
Based Phase 1 characterization model	Unsaturated hydraulic conductivity of the vadose zone units from RPP-RPT-35222 (see Table 4-1 of this report) with denominator case for recharge (Table 4-13 in RPP-RPT-44042 Rev. A), known sources of waste losses/leaks (Table 6-1 in RPP-RPT-42294, Rev. 0)	RPP-RPT-35222 RPP-RPT-42294, Rev. 0 RPP-RPT-44042, Rev. A
Based on consideration of hydraulic effects of: - clastic dike(s) - unsealed dry well - unsealed groundwater well	Unsaturated hydraulic conductivity of the vadose zone units from RPP-RPT-35222 (see Table 4-1 of this report) with denominator case for recharge (Table 4-13 in RPP-RPT-44042 Rev. A), known sources of waste losses/leaks (Table 6-1 in RPP-RPT-42294, Rev. 0) and effects of: • Natural preferred pathways (prescribed clastic dike) (see Sample 4B results in Table 4-5 of Appendix F of RPP-20621) • Man-made preferred pathways (prescribed unsealed dry well, groundwater well or borehole)	RPP-RPT-35222 RPP-RPT-42294, Rev. 0 RPP-RPT-44042, Rev. A Appendix F of RPP-20621
Based on consideration of hydraulic effects of dipping or sloping beds with breaks	Unsaturated hydraulic conductivity of the vadose zone units from RPP-RPT-35222 (see Table 4-1 of this report) with denominator case for recharge (Table 4-13 in RPP-RPT-44042 Rev. A), known sources of waste losses/leaks (Table 6-1 in RPP-RPT-42294, Rev. 0) and effects of prescribed sloping beds with breaks	RPP-RPT-35222 RPP-RPT-42294, Rev. 0 RPP-RPT-44042, Rev. A

References:
RPP-20621, *Far-Field Hydrology Data Package for the Integrated Disposal Facility Performance Assessment*, Appendix F. Physical and Hydraulic Measurements of FY1998 Clastic Dike Samples.
RPP-RPT-35222, *Far-Field Hydrology Data Package for the RCRA Facility Investigation (RFI) Report*.
RPP-RPT-42294, *Hanford Waste Management Area C Soil Contamination Inventory Estimates*.
RPP-RPT-44042, *Recharge and Waste Release within Engineered System in Waste Management Area C*.

Table 6-2. Proposed Simulation Cases Representing the Effects of Varying Hydraulic Conductivities on Vadose Zone Flow and Transport.

Proposed Cases	Description of Case Parameterization
Recommended unsaturated hydraulic properties (Proposed Denominator Case)	Unsaturated hydraulic conductivity of the vadose zone units from RPP-RPT-35222, *Far-Field Hydrology Data Package for the RCRA Facility Investigation (RFI) Report* (see Table 4-1 of this report) with recommended parameters for moisture-dependent anisotropy (see Table 4-4 of this report)
Higher values case of unsaturated hydraulic conductivity of the vadose zone units	Saturated hydraulic conductivity of the vadose zone units from RPP-RPT-35222 (see Table 4-1 of this report) of 500 m/day with recommended parameters for moisture-dependent anisotropy (see Table 4-4 of this report)
Lower values case of unsaturated hydraulic conductivity of the vadose zone units	Saturated hydraulic conductivity of individual units from RPP-RPT-35222 (see Table 4-1 of this report) of 0.1 m/day with recommended parameters for moisture-dependent anisotropy (see Table 4-4 of this report)
Homogeneous conditions (1)	Unsaturated hydraulic properties of the vadose zone units containing primarily sand (H2 sands unit) from RPP-RPT-35222 (see Table 4-1 of this report) with recommended parameters for moisture-dependent anisotropy (see Table 4-4 of this report)
Homogeneous conditions (2)	Unsaturated hydraulic properties of the vadose zone units containing primarily gravel (H1 gravelly sand unit) from RPP-RPT-35222 (see Table 4-1 of this report) with recommended parameters for moisture-dependent anisotropy (see Table 4-4 of this report)
Homogeneous conditions (3)	Unsaturated hydraulic properties of the vadose zone units containing primarily sand (H2 sands unit) from RPP-RPT-35222 (see Table 4-1 of this report) with assumed parameters to represent isotropic conditions
Homogeneous conditions (4)	Unsaturated hydraulic properties of the vadose zone units containing primarily gravel (H1 gravelly sand unit) from RPP-RPT-35222 (see Table 4-1 of this report) with assumed parameters to represent isotropic conditions
Heterogeous Conditions	A random field of hydraulic conductivity generated for available data on moisture content

Two other cases representing homogeneous conditions (i.e., one [1] representing the vadose zone as predominately sand and another [2] presenting the vadose zone as predominantly gravelly sand) are proposed. Two other homogeneous cases are also proposed (3 and 4) using the same unsaturated properties in cases 1 and 2 but with assumed parameters to represent isotropic conditions. A final sensitivity case is proposed that would examine the effect of a heterogeneous distribution of hydraulic conductivity in the vadose zone. In this case, a random field of hydraulic conductivity would be developed based in part on available data on moisture content and particle size distributions collected at wells and boreholes drilled in the vicinity of WMA C.

6.1.2.3 Contaminant Distribution Coefficients. A selected set of proposed simulation cases are recommended to evaluate the effects of distribution coefficients for certain key constituents of interest (technetium, iodine, chromium, and uranium) beneath WMA C. Table 6-3 presents a summary of the proposed denominator case, and maximum and minimum range cases of

contaminant K_d values for selected key contaminants affecting risk through the groundwater pathway. These K_d values are derived best estimates and ranges of recommended values for these constituents in Tables 4-8 and 4-9.

Table 6-3. Proposed Cases for Contaminant Distribution Coefficients (mL/g) for Non-Impacted Soils.

Contaminant	Proposed Denominator Case	Sensitivity Cases		
		Minimum Linear Adsorption Isotherm (K_d)	Maximum Linear Adsorption Isotherm (K_d)	Evaluation of Non-linear Adsorption Isotherms based on use of Freundlich and/or Langmuir Isotherms
Uranium	0.6	0.2	2	To be determined
Iodine-129	0.1	0.0	0.2	None proposed
Technetium-99	0	0	0.1	None proposed
Chromium	0	0	0.3	None proposed

Based on input received during the review of this data package during the Natural System working session held May 25 to 27, 2010, and in subsequent review of the proposed modeling cases during the Engineered System working session held July 25 to 27, 2010, another set of sensitivity cases are proposed that would examine the effect of using alternative non-linear adsorption isotherms using the Freundlich and Langmuir approaches. These cases would be used to evaluate uranium mobility. Specific parameterization of these specific sensitivity cases will be developed and evaluated at a later date using scoping calculations.

6.1.2.4 Unconfined Aquifer Parameters. A selected set of proposed simulations are recommended to evaluate the effects of hydraulic properties of the unconfined aquifer beneath WMA C. Saturated media variables that impact modeling results include horizontal hydraulic conductivity, effective porosity, and hydraulic gradient. In vicinity of WMA C, the saturated sediments making up the groundwater system includes undifferentiated and reworked Hanford formation Hr gravelly sand, CCU sands, and Ringold formation gravels. Based on the observation that the water table and associated hydraulic gradients in the vicinity of WMA C are flat, the effective hydraulic conductivities and transmissivities of the saturated sediments are postulated to be very high.

Hydraulic properties have been measured over the past 50 years and are documented in a number of reports (DOE/RW-0164; PNL-8337, *Summary and Evaluation of Available Hydraulic Property Data for the Hanford Site Unconfined Aquifer System*; and more recently, PNL-10886, *Development of a Three-Dimensional Ground-Water Model of the Hanford Site Unconfined Aquifer System: FY 1995 Status Report*). Hydraulic conductivities in the 200 East Area are generally much higher than in 200 West area and are highly dependent on the presence of fine or coarse-grained aquifer materials. Ranges of hydraulic properties shown in Tables 3-12 and 3-13 of the SST PA are based on PNL-10886 and were used to develop in the site-wide groundwater model (PNNL-13447, *Transient Inverse Calibration of Hanford Site-Wide Groundwater Model to Hanford Operational Impacts – 1943 to 1996*) prior to the recent groundwater model

developed as part of the TC&WM EIS. Much less information is available on the variability in porosity for either formation. Effective porosities shown in Tables 3-12 and 3-13 are the values generally used for the respective formations [RPP-6296, *Modeling Data Package for S-SX Field Investigation Report (FIR)*; RPP-9223, *Modeling Data Package for B-BX-BY Field Investigation Report (FIR)*]. Hydraulic gradients are based on the Hanford Site-wide groundwater model (PNL-10886; PNNL-13447) estimation of post-Hanford conditions. A set of initial estimates of the recommended ranges for aquifer properties for use in the sensitivity analysis are presented in Table 6-4.

Table 6-4. Unconfined Aquifer Properties for Waste Management Area C.

Property	Proposed Denominator Case	Minimum	Maximum
Hydraulic conductivity (m/day)	3,000	100	7.000
Effective porosity (unitless)	0.25 (Hanford gravel)	NC	NC
Hydraulic gradient (unitless)	0.00001	0.00002	0.0001
Depth to water table (m)	79	71	97

NC = not considered

Reference: DOE/ORP-2005-01, *Initial Single-Shell Tank System Performance Assessment for the Hanford Site.*

6.2 REGIONAL-SCALE GROUNDWATER FLOW AND TRANSPORT

Regional-scale flow and transport modeling that will be performed in support of the WMA C PA will rely on the regional-scale flow and transport modeling capability that has been developed under the TC&WM EIS. Since the TC&WM EIS is still undergoing technical review as a part of the public comment, we are deferring any specific recommendations for proposed cases as a part of this analysis. A number of cases for regional-scale flow and transport simulations will be suggested to assess the effects of changing model parameters in four categories that include:

- Effects of alternative future flow conditions with lower and higher water-table elevations and distributions
- Effects of varying contaminant distribution coefficients
- Effects of change hydraulic properties of the unconfined aquifer
- Effects of potential preferential pathways.

A final set of proposed cases for the regional scale model will be developed based on data and information contained in the final published version of the TC&WM EIS.

7.0 ADDITIONAL INFORMATION USED IN THE DEVELOPMENT AND IMPLEMENTATION PHASES OF THE WASTE MANAGEMENT AREA C PERFORMANCE ASSESSMENT

At the time this document was produced in August 2010, it reflected the understanding at that time of the geologic and hydrologic conditions present in the vadose and unconfined aquifer at WMA C. However, since the publication of Revision 1 of this document, new data/information became available to use in the WMA C PA. These updates include the following.

- Updates to the vadose zone stratigraphy based on the K-U-T geophysical logs from direct push sampling effort for RPP-RPT-58339, *Phase 2 RCRA Facility Investigation Report for Waste Management Area C* and previous K-U-T logging in groundwater wells and drywells within and around WMA C.

- Neutron probe moisture logging from the direct push sampling effort resulted in:

    - Updates to vadose zone hydraulic properties used in the modeling

    - Development of heterogeneous model of the vadose zone based on moisture contents.

- Updated transport properties of the vadose zone sediments.

- Updates to unconfined aquifer hydraulic properties based on CP-47631, *Model Package Report: Central Plateau Groundwater Model Version 3.4*.

7.1 UPDATES TO THE VADOSE ZONE STRATIGRAPHY BASED ON THE POTASSIUM-URANIUM-THORIUM GEOPHYSICAL LOGGING

In July of 2014, RPP-RPT-56356, *Development of Alternative Digital Geologic Models of Waste Management Area C* was published. This purpose of that report was to document the development of two alternative geologic models for WMA C. These geologic models are based on newly collected data from the direct push effort as documented in RPP-PLAN-39114 as well as older geophysical logging data collected from dry vadose zone monitoring wells and groundwater monitoring wells in the vicinity of WMA C. The first geologic model (Alternative Geologic Model I) was based on interpretations of K-U-T logging data along with geologic logs by WRPS and its subcontractors, while the second geologic model (Alternative Model II) is based interpretations of the same K-U-T data by Dr. Stan Sobcyzk of the Nez Perce.

Interpretations provided in the WRPS and Nez Perce alternative geologic models have identified the tops of the seven separate geologic units within WMA C. Descriptions of these units, provided below, are taken from Letter Report FS-NW-LT-5367, “Submittal of C Farm Geology/ Geophyics Review, Task 26” (see Appendix A of RPP-RPT-56356) and are provided in a shallow (upper) to deep (lower) sequence.

Backfill – Gravel-dominated, consisting of poorly- to moderately-sorted cobbles, pebbles, and coarse to medium sand with some silt derived from coarse-grained Hanford formation (H1 unit) excavated around tanks; occasional layers of sand to silty sand occur near the base of the backfill sequence.

Hanford H1 Unit – Hanford H1 unit is gravel-dominated, generally identified as gravel or very coarse sand comprising greater than 70% of the lithology. It is assumed to have been deposited in a high-energy environment (i.e., high-energy depositional system—pebble cobble gravels, sandy gravels, gravelly sands, very low percentage silt or very fine to fine sands and are represented by low total potassium concentrations usually 10 to 15 pCi/gr). Hanford H1 has low total gross gamma count rates (e.g., less than 150 to 200 counts per second for large diameter wells high-purity germanium tools, 70 to 80 counts per second total count rates and less than 2 pCi eq. Ra for processed logs in direct push boreholes logged with sodium iodide and/or bismuth germanate oxide tools).

Hanford H2 Sand Unit – Hanford H2 Sand unit is a sand-dominated facies generally identified as fining upward sequences of gravel, sandy/gravel to sand to very fine sand. It is assumed to have been deposited distant from the main channel/high energy flow, and is dominated by trough cross-bedded depositional features. These are represented on logs compared to H1 by an increase in gross gamma count rate of 25 to 30% with an associated potassium (K) increase. Some logs have only gradual gross gamma increases but still have easily recognizable percentage potassium increases. The increase in total gamma and potassium count rates is indicative of a higher felsic fine-grained component of the sediments.

Hanford H2 Coarse Gravelly Sand Unit – Hanford H2 Coarse Gravelly Sand unit is coarse sediments that underlie the H2 Sand Unit. This unit is the equivalent of the "H2 coarse" unit described in Letter Report FS-NW-LT-5367. Again, this is a gravel/coarse-grained facies, which is indicated by a 15 to 20% total gross gamma and potassium count rate reduction when compared to the H2 sands above it.

Hanford H2 Silt Unit – Hanford H2 Silt unit is only observed in deep groundwater wells and the presence of a mappable unit may not be readily identified. When present, a very strong potassium peak and occasionally strong natural uranium peak with or without a total gamma change is possible. Strongest evidence for the presence is observed on driller and geologist logs.

Undifferentiated Hanford H3 Gravels, Cold Creek and Ringold Unit – Waste Management Areas A-AX and C lie along the edge of a paleochannel that eroded much or all of the Ringold Formation during CCU and/or Hanford time. Because of the difficulty in distinguishing reworked Ringold Formation gravels and pre-Missoula mainstream Columbia River gravels from original Ringold Formation gravels, these units are undifferentiated here (H3/CCU/RF).

This unit is found in the vicinity of WMA C and consists of a significant thickness of basalt-dominated gravels as described by Pacific Northwest National Laboratory from

well 299-E27-155 drilling logs. Similar descriptions and log responses are present in other deep wells. The response is a significantly reduced total gamma count rate directly below the H2 silt that is not entirely attributable to the presence of groundwater. The top of groundwater is usually well below the overlying H2 unit. This facies is generally described as a coarse-grained open framework gravel to sandy gravel, high-energy system which in outcrop and drilled sample contains significant percentages of Ringold, Columbia River Basalt and far-derived granites, Belt Rocks, and other terrains from north of the Pasco Basin (multi-lithic).

Columbia River Basalt – Columbia River Basalt is only noted in one or two wells. The best evidence of basalt contact depths is from geologic logs.

The WRPS interpretation for the tops of these units is given in Table 3-1 of RPP-RPT-56356. The data in that table was further augmented by slant hole direct pushes installed after the receipt of FS-NW-LT-5367 (Table 3-2 of RPP-RPT-56356), and data from Hanford Site GeoContacts Database for groundwater wells in the vicinity of WMA C (Table 3-2 of RPP-RPT-56356).

The Nez Perce interpretation for the top of these units is given in Table 3-5 of RPP-RPT-56356. No modifications were made to this data and it was used exactly as given to create the model in the vicinity of WMA C. However, because of the need to expand the geologic model and to include the water table into the model, the data provided by the Nez Perce was supplemented with data from the last 10 lines of Table 3-3 of RPP-RPT-56356.

It should be noted that previous interpretations of the geologic strata within WMA C did not break out the H2 sands into three separate facies. However, both the Energy*Solutions* and the Nez Perce interpretations identified evidence that supported the delineation of the three facies within the H2 sands that is carried forward into the geologic models. Also, the unconfined aquifer is wholly contained within the undifferentiated H3/Cold Creek/Ringold unit in the vicinity of WMA C. The June 2013 water measurements (Table 3-4 of RPP-RPT-56356) at the groundwater wells were used to create the water table surface and provided a basis for dividing the undifferentiated H3/Cold Creek/Ringold unit into two separate layers; one associated with the vadose zone and one associated with the unconfined aquifer. Furthermore, the Nez Perce description of the H2 unit (see e-mail from S. Sobczyk to M. P. Bergeron, “WMA C geology” [Sobczyk, S., 2014-03-10]) includes the following:

> *In addition to the three layers in the Hanford H2, … there are numerous, discontinuous, low permeability laminations/lenses in the particularly in the upper portion of the H2 unit. These “lenses” parallel the overall dip of the H2, which is ~3% dip to the northeast.*

However, these discontinuous low-permeability laminations/lenses are not accounted for in the digital geologic models developed.

Two 3D digital geologic models of WMA C and surrounding areas were developed by creating surfaces representing the tops of these units (Figure 7-1a and 7-1b) using the elevations listed in those tables, along with the data for the top of the unconfined aquifer Table 3-4 of RPP-RPT-56356.

Figure 7-1(a). Cross-Sections through Waste Management Area C Alternative Geologic Model I Using Washington River Protection Solutions Interpretations.

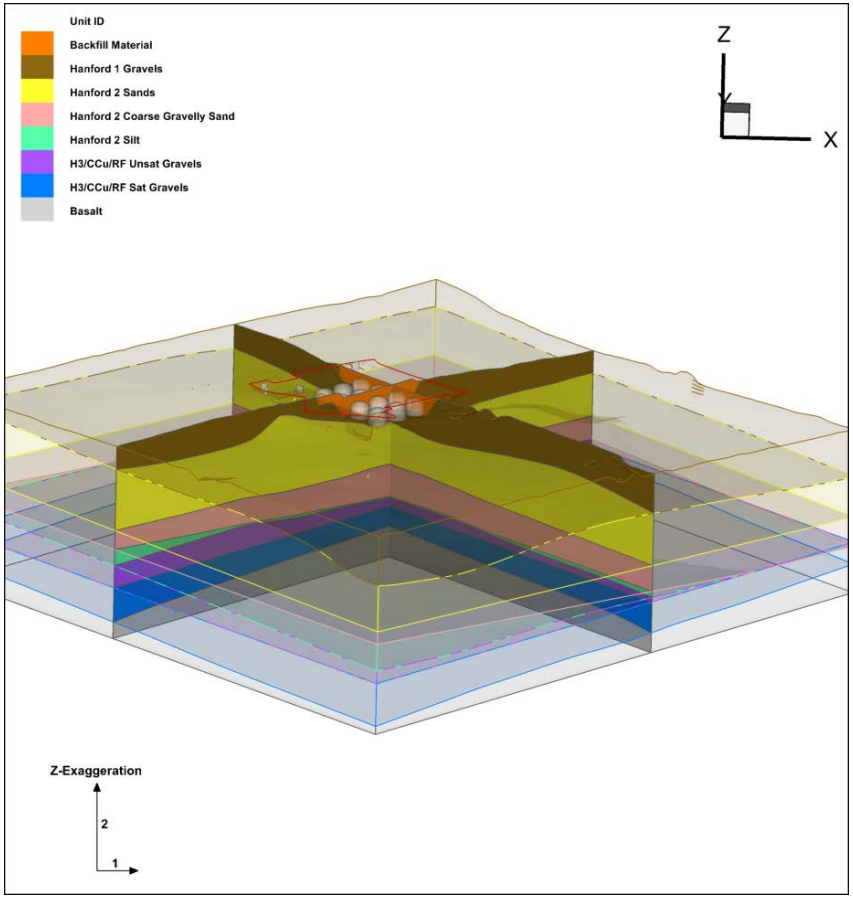

Figure 7-1(b). Cross-Sections through Waste Management Area C Alternative Geologic Model II Using Nez Perce Interpretations.

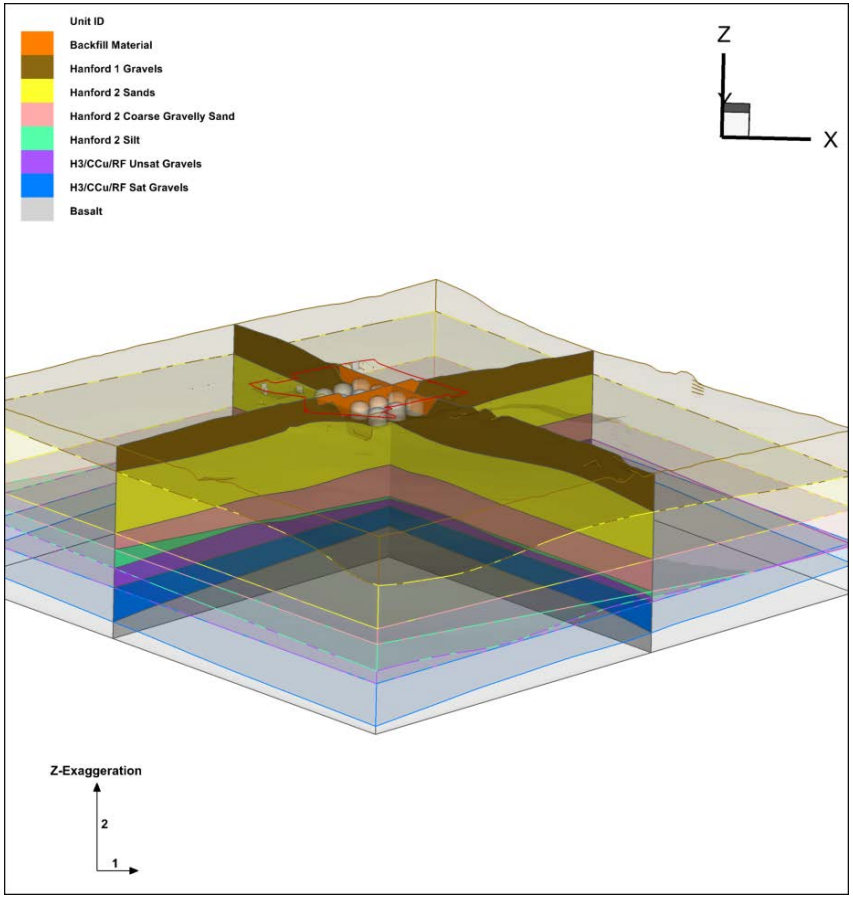

In discussing these models with the individuals who examined the geophysical logs, along with the geologists who have created geologic logs for wells drilled in the eastern half of the 200 East Area, a concern was raised about the H2 coarse layer and the H2 silt layer located right above the undifferentiated H3/CCU/RF layer at WMA C identified using the K-U-T logging data. Based on the considerations raised in those discussions which are documented in the following paragraph, it is recommended that for the Alternative Geologic Model I (WRPS), the three facies H2 (sand, coarse gravelly sand, and silt) be combined into one layer by the assignment of the same material properties for this model and the vadose zone model to be used in the WMA C PA.

The geophysical logs based on the K-U-T indicated that a silt layer similar to what is seen at WMA B-BX-BY is likely to be present at WMA C. However, a thorough examination was made of the drill cuttings stored at Hanford Geotechnical Sediment Library for two wells at WMA C and two wells at WMA B-BX-BY, along with an examination of the geologic logs of four groundwater wells installed at WMA C in 2004 (Section 7 of RPP-RPT-56356). For the wells near WMA B-BX-BY, the examination shows that there is a strong competent silt layer at depth that can and does cause a localized perched water condition in this general area. At WMA C, while there is a definite fining of the sands along with silt found at the same vertical location as indicated by the K-U-T geophysical logs, a competent silt layer on which water could perch was not observed in the geologic logs. While K-U-T logs definitely indicate a change in mineralogy, it does not appear that a competent silt layer at the bottom of the H2 unit is present in the wells for which there are good corresponding geologic logs/samples.

Additionally, only the groundwater wells were drilled deep enough to encounter this unit and for these groundwater wells, Letter Report FS-NW-LT-5367 placed the confidence of the picks for the tops of the units as low for the following reason: the majority of the groundwater wells with geophysical logs that were drilled in the WMA C used a Becker Hammer method. This makes the interpretation of the geophysical logs difficult due to the double-walled casing used by this method. The double casing walls (quadruple walls at joints) shields the gamma signature that would normally be used for correlations. Additionally, for the description of the H2 Silt unit (Letter Report FS-NW-LT-5367), the strongest evidence for the presence of this unit should be observed on driller's and geologist's logs and the coarse gravelly sand and silt were not observed in the geologist's logs.

In order to understand the differences between the models, four cross-sections of each model have been prepared. The plan view of WMA C showing locations of these cross-sections is given in Figure 7-2, along with the wells used to define the top of the units for each cross-section. Figure 7-3 provides the legend for the cross-sections. Cross-sections for each location given in Figure 7-2 are shown in Figures 7-4 through 7-7. In each of these four figures, three cross-sections are shown with each cross-section representing a different geologic model, thereby allowing the reader to compare the geologic models to each other along the selected section line. The upper cross-section (a) in the figures represents the Alternative Model I derived from the interpretations for the top of the units given in Letter Report FS-NW-LT-5367 and supplemented by Hanford Site GeoContacts Database. The middle cross-section (b) shows the modified Alternative Model I by combining all of the H2 Sand, H2 Coarse Gravelly Sand, and H2 Silt into one unit based on the geologic logs. The bottom cross-section is Alternative Model II with the top of units picked by Dr. Stan Sobcyzk.

Figure 7-2. Locations of Cross-Sections at Waste Management Area C Shown in Figures 7-4 through 7-7.

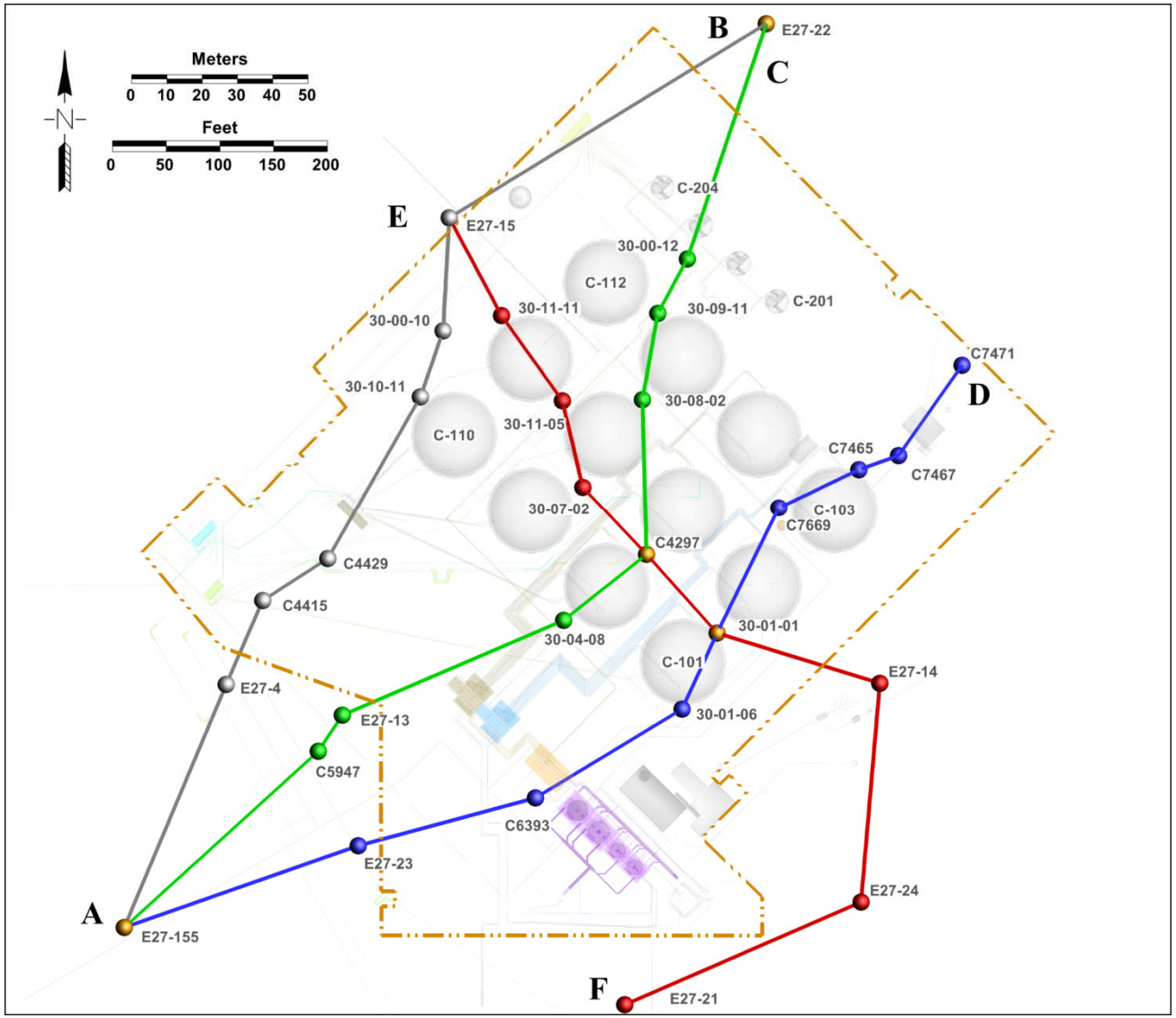

Figure 7-3. Legend for Cross-Sections

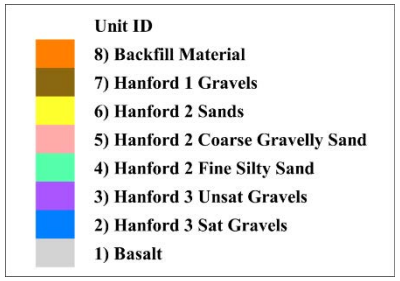

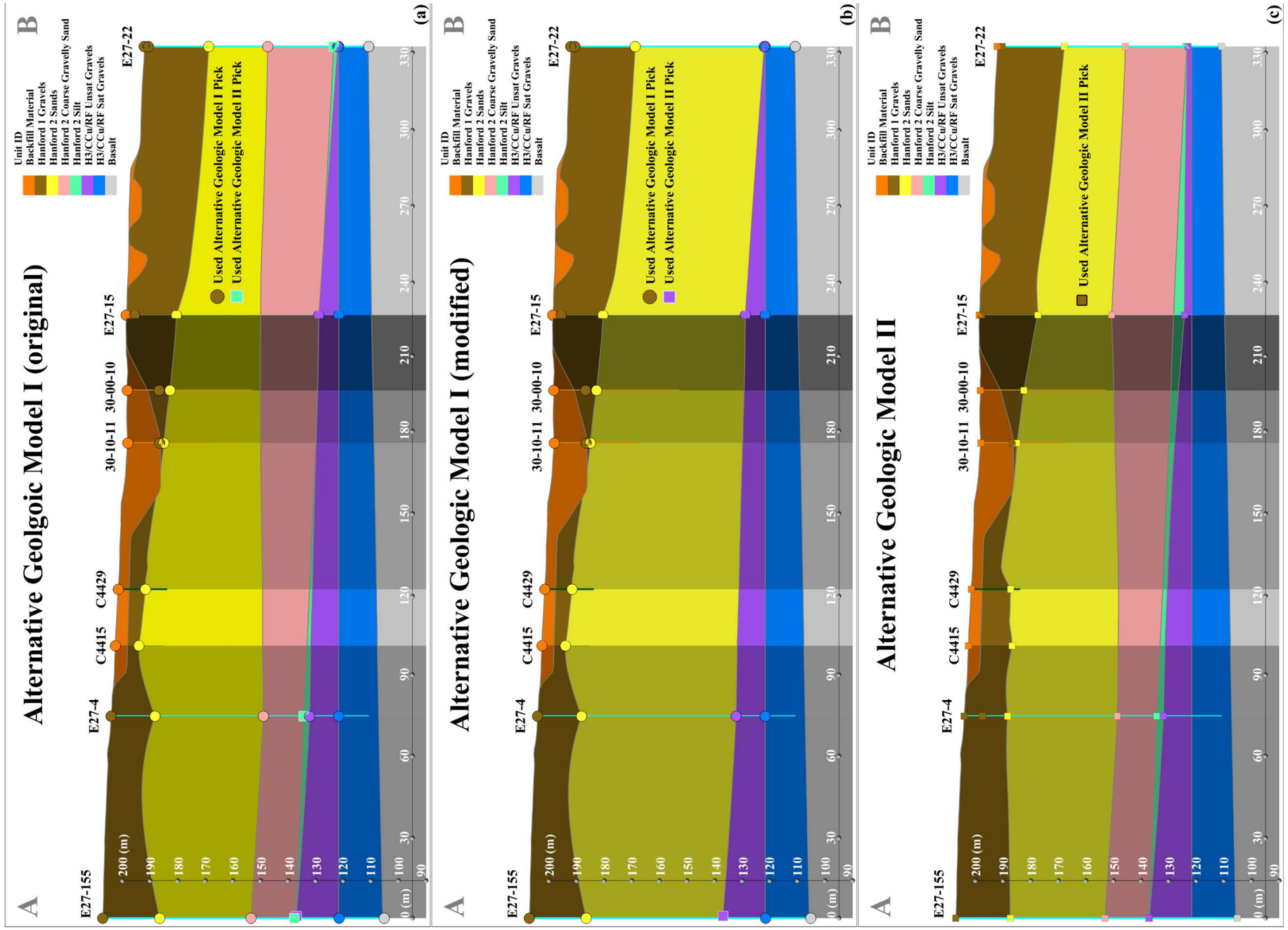

Figure 7-4. West Cross-Section A to B (gray) for Different Alternative Models.

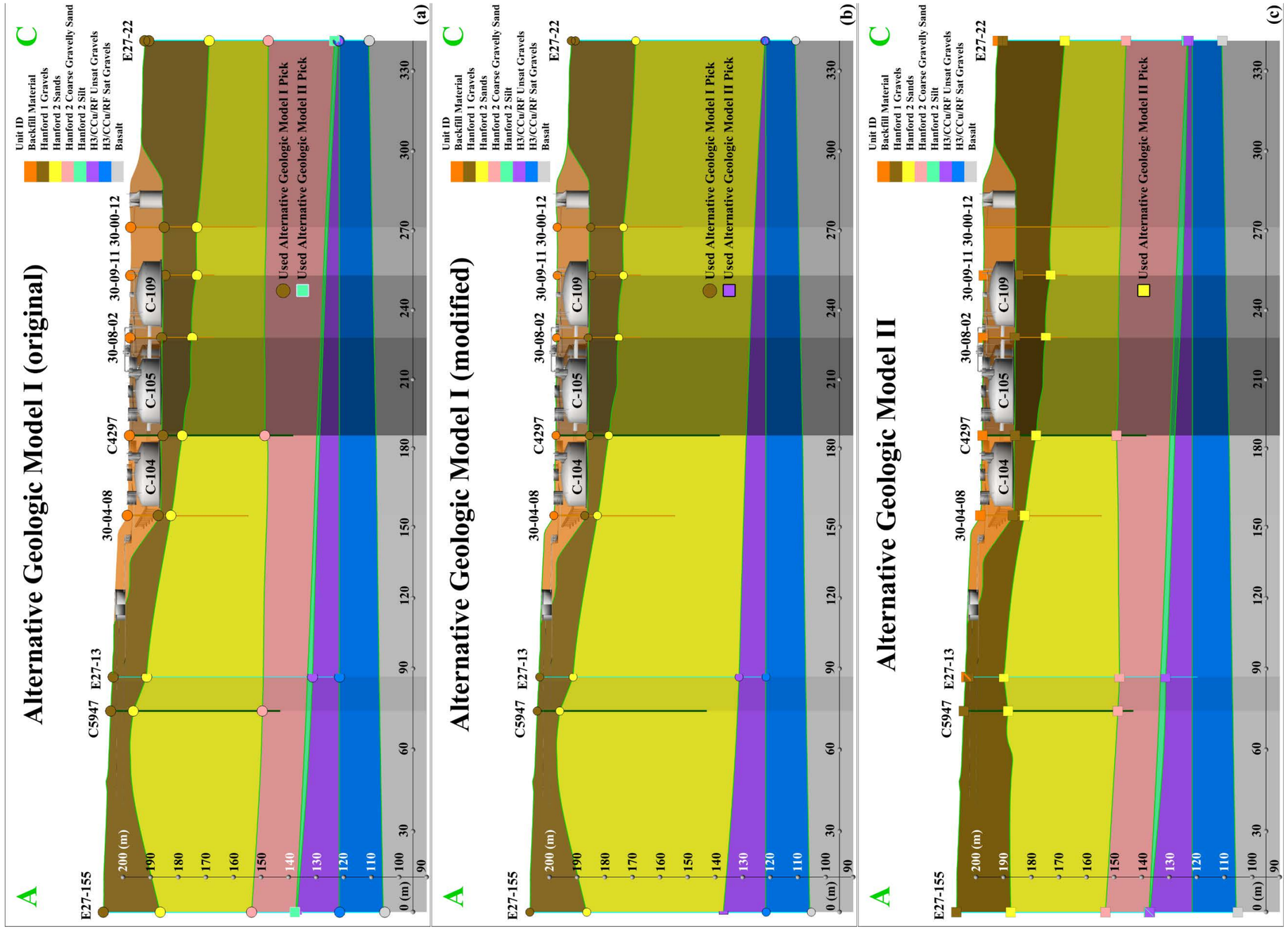

Figure 7-5. Middle Cross-Section A to C (green) for Different Alternative Models.

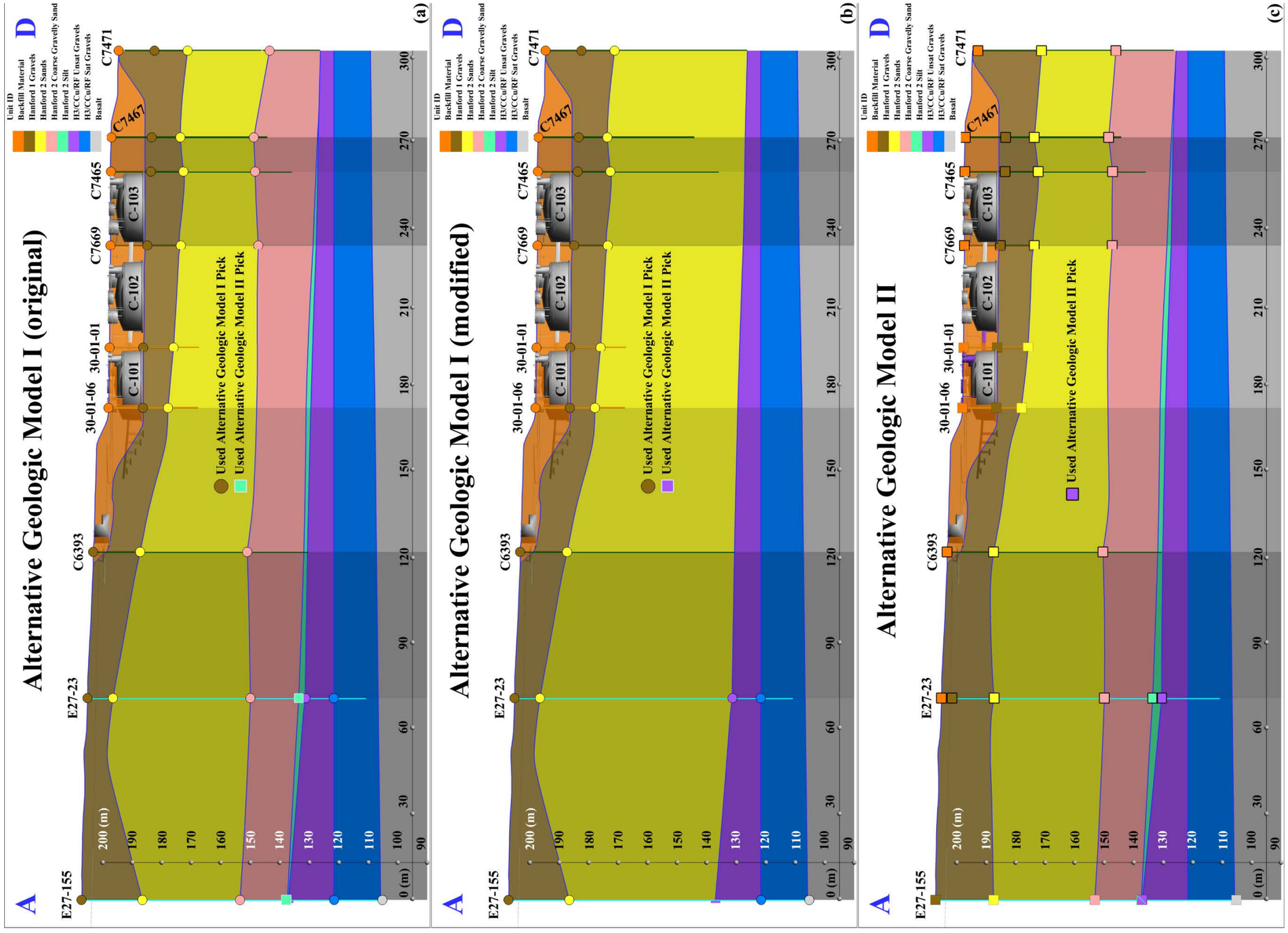

Figure 7-6. East Cross-Section A to D (blue) for Different Alternative Models.

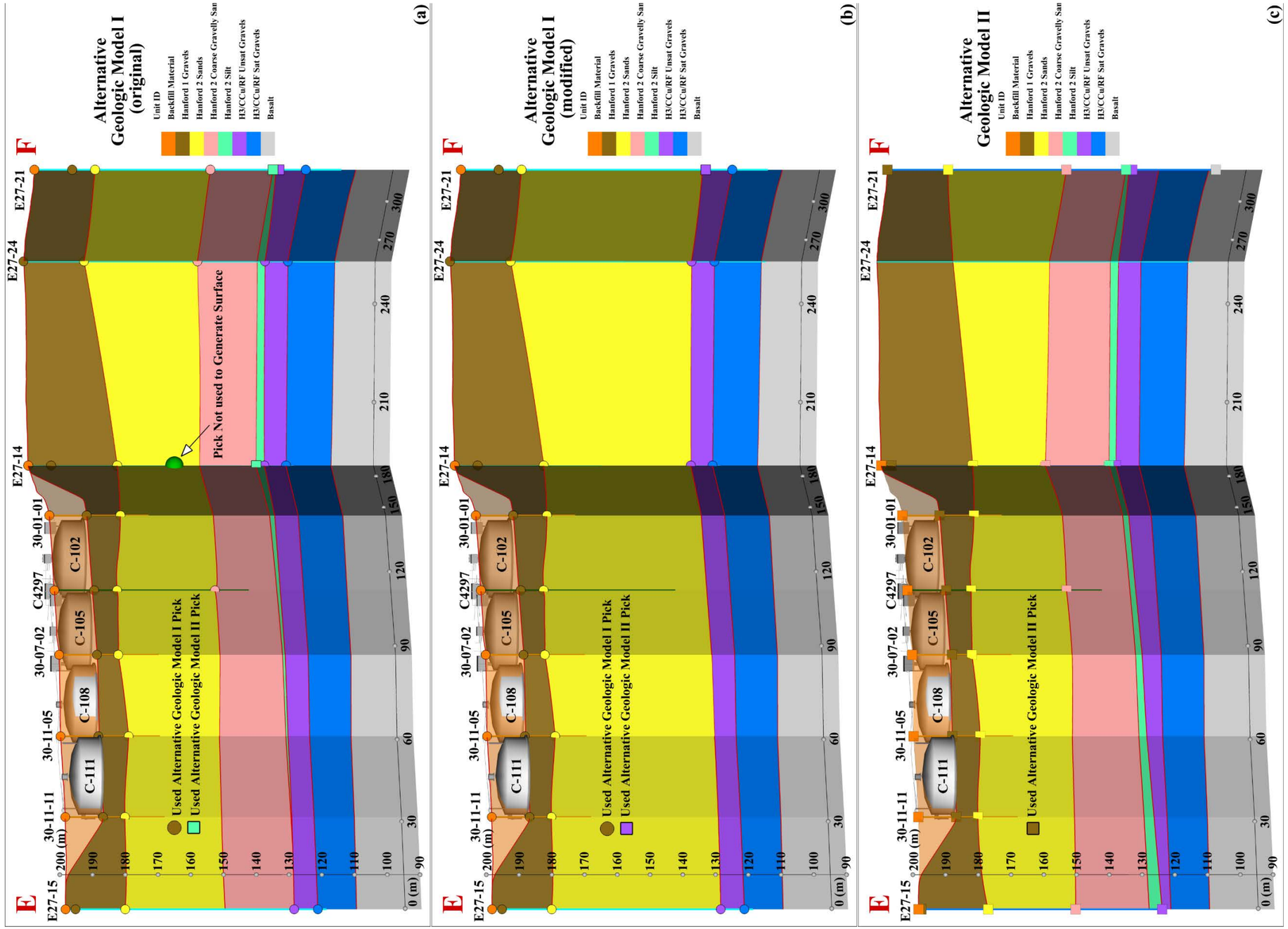

Figure 7-7. Northwest to Southeast Cross-Section E to F (red) for Different Alternative Models.

The picks for the top of each unit are given by a circle symbol at each groundwater well, dry well, direct push, and/or borehole located on the cross-section. If a well did not have a pick for the top of the unit, no circle symbol is shown. If a pick was not used in generating the surfaces, its location is shown as a green sphere on the cross-section (i.e., top of H2 Coarse Gravelly Sand unit shown at well E27-14). The contact between wells is represented by lines extracted from the surfaces. That contact is influenced by interpreted contacts at selected groundwater wells, dry wells, direct pushes, and/or boreholes that are not located on the cross-section/fence diagram, which is why the contact between wells in the cross-section is not just a straight line.

The Modified Alternative I model was used for the base case in the computer modeling for the WMA C PA. Additionally, a sensitivity case using Alternative Geologic Model II, in which the H2 unit is separated as shown in the bottom figure of the cross-section [Figures 7-4 (c) through 7-7 (c)], should be examined to evaluate the impacts of the differences the geologic unit may have on the results of the WMA C PA.

7.2 NEUTRON PROBE MOISTURE LOGGING FROM THE DIRECT PUSH DATA

One way to verify that a vadose zone groundwater model is producing correct results is to compare the model results to observed field data such as measured moisture content/matric potential in the vadose zone sediments. More often than not, these types of measurements are not available. However, because of characterization effort from the RCRA Facility investigations (DOE/ORP-2008-01, *RCRA Facility Investigation Report for Hanford Single-Shell Tank Waste Management Areas*, Appendix L and RPP-RPT-58339), moisture content data were measured at WMA C. This section presents a summary of those results which are documented in RPP-CALC-60450, *Process for Determining the Volumetric Moisture Content for the Vadose Zone Geologic Units Underlying Waste Management Area C.*

The neutron logging data came from two drywells and 63 direct push boreholes. Laboratory measured moisture content (weight % converted to volumetric moisture content) came from one groundwater well (299-E27-22) and one characterization borehole (C4297). The spacing for the neutron logging of moisture content varied from 0.05 m to 0.15 m (~0.15 ft to 0.5 ft). The spacing on the laboratory samples was greater. The locations for the moisture content measurements are shown in Figure 7-8. After duplicate measurements were removed, a total 32,912 measurements were available. The formations that were identified in the previous section were delineated in each well/borehole/direct push and a statistical analysis of volumetric moisture content data was run for each formation. Histograms showing the range of moisture content for backfill, H1, and H2 are provided in Figure 7-9. A histogram for H3 is not provided because there were not enough moisture measurements made in this formation. Table 7-1 provides the statistical analysis for each formation.

Figure 7-8. Locations and Moisture Content (% Vol) Measurements in Vadose Zone at Waste Management Area C.

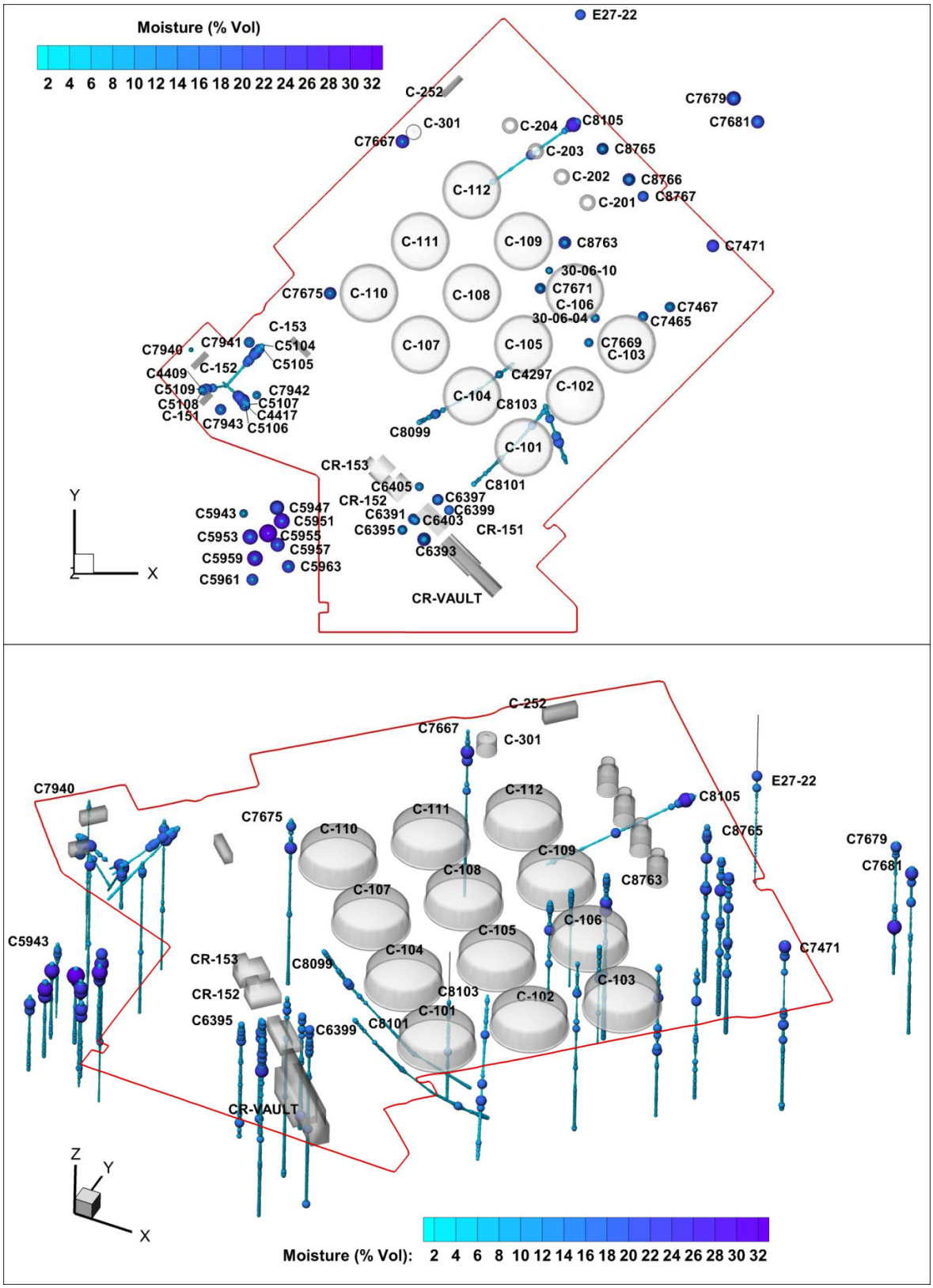

Figure 7-9. Histograms Showing the Range of Volumetric Moisture Content for the Backfill, H1, and H2 Units at Waste Management Area C.

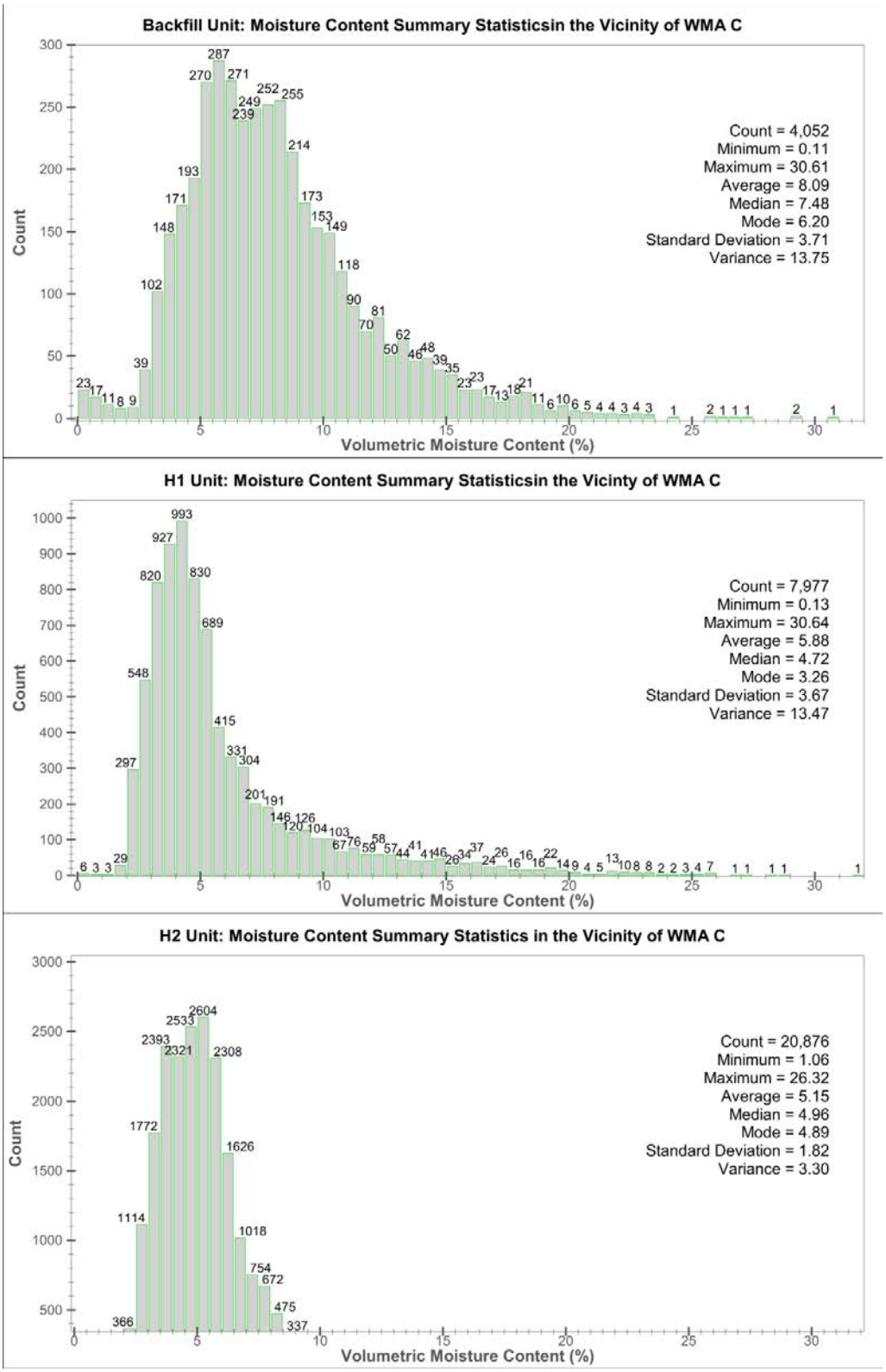

WMA = Waste Management Area

Table 7-1. Summary Statistics for Volumetric Moisture Content in the Lithologic Units Underlying Waste Management Area C.

Unit	Count of Wells	Count of Measurements	Minimum (Vol %)	Maximum (Vol %)	Average (Vol %)	Median (Vol %)	Mode (Vol %)	Standard Deviation	Variance
Backfill	52	4,052	0.11	30.61	8.09	7.48	6.20	3.71	13.75
H1	66	7,977	0.13	30.64	5.88	4.72	3.26	3.67	13.47
H2	64	20,876	1.06	26.32	5.15	4.96	4.89	1.82	3.30

Following the reduction of the field/laboratory measurements of the volumetric moisture content, the Subsurface Transport Over Multiple Phases (STOMP)©[1] vadose zone model was run with the van Genuchten parameters given in Table 4-1 of this document to compare the model results for volumetric moisture content against the values observed in the field. An average model-calculated moisture content was calculated for the three units shown in Table 7-1 over the approximate area of the tank farm as defined by the fence line shown in Figure 2-3. Table 7-2 shows the average model-calculated moisture content for those units at three different time periods; at the end of operational period, 80 years after the placement of the barrier, and 3,000 years after the placement of the barrier.

Table 7-2. Summary Statistics for Volumetric Moisture Content in the Lithologic Units Underlying Waste Management Area C Using the Hydraulic Parameters in Table 4-1.

Formation	Year	Recharge (mm/yr)	Average Moisture Content (Vol %)	Minimum Moisture Content (Vol %)	Maximum Moisture Content (Vol %)
Backfill	2020	100.0	8.0	7.3	8.6
H1	2020	100.0	12.5	10.8	13.7
H2	2020	100.0	20.9	16.0	22.1
Backfill	2100	0.5	5.0	4.8	5.7
H1	2100	0.5	8.6	7.6	9.9
H2	2100	0.5	16.0	12.9	17.7
Backfill	5020	3.5	5.1	4.9	5.5
H1	5020	3.5	8.3	7.4	9.4
H2	5020	3.5	13.4	12.1	15.8

Comparing the average moisture content values from the field data to the model-calculated average moisture content for the formations indicates that van Genuchten parameters in Table 4-1 would be appropriate for backfill unit. However, the model-calculated moisture content for the H1 and H2 formations are too high and would be inappropriate for these two units. Since the Darcy flux is divided by the aqueous moisture content, using the curves in Table 4-1 would increase travel time to the unconfined aquifer by a factor of two to three for a simplified one-dimensional representation. The hydraulic parameters in Table 4-1 are composite parameters based on measurements of pressure head (-cm) versus moisture content for samples taken in 200 West area. This led to updating the van Genuchten parameters used in the WMA C STOMP© model. The following sections provide the methodology for updating the van Genuchten parameters.

[1] Subsurface Transport Over Multiple Phases (STOMP)© is copyrighted by Battelle Memorial Institute, 1996.

7.2.1 Updated Hydraulic Properties of the Hanford H1 and H3 Gravelly Units

Other than moisture content measurements, there are no site-specific data for hydraulic properties for the H1 gravelly unit. However, as part of other Hanford Site projects, particle-size distribution, bulk density, saturated hydraulic conductivity, moisture retention, and unsaturated conductivity data have been collected for several borehole samples (Figure 7-10) at other sites in the vicinity of 241-C Tank Farm and within 200 Areas. These sites include the 218-E-12B and 218-E-10 low-level solid waste burial grounds in 200 East Area, the Environmental Restoration Disposal Facility site located in between the 200 West and 200 East Areas, and the 241-T-106 tank site located in 200 West Area. Borehole sediment samples from these sites were used as surrogates to represent the hydraulic properties for WMA C H1 and H3 gravel-dominated units.

Both H1 and H3 sediments are comprised of a significant gravel (>2-mm size) fraction. To explore the impact of gravelly sediments for the drier moisture regime, a separate study was conducted ("Variability of Gardner's α for coarse-textured sediments" [Khaleel and Relyea 2001]); a total of 79 gravelly and sandy samples were analyzed in the laboratory. The gravel fraction for 41 samples ranged from 20 to 71% (by weight); the remaining 38 samples were sandy with very little gravel fraction (Figure 7-11). A noteworthy feature of Figure 7-11 is the fact that the variability in saturated conductivity is much greater than the variability in unsaturated conductivity near saturation. Furthermore, the measured unsaturated conductivities for the gravelly samples showed less variability for the drier moisture regime, fell within a narrower range, and were well within the range of measured unsaturated conductivities for the sandy samples (see Figure 7-11). Such a generic behavior for the gravelly sediments for the drier moisture regime prompted assigning similar properties for both H1 and H3 units.

Standard laboratory and Westinghouse Hanford Company quality assurance procedures (WHC-IP-0635, *Geotechnical Engineering Procedure Manual*) were used to analyze the H1 and H3 sediment samples. The moisture retention data for the fine fraction (<2 mm) and the drainage cycle of up to -1,000 cm of pressure head were measured using "Tempe" pressure cells; the rest of the drainage data up to -15,000 cm was measured using the pressure plate extraction method ("Water Retention: Laboratory Methods" [Klute 1986]). A variation of the unit gradient method ("Hydraulic Conductivity and Diffusivity: Laboratory Methods" [Klute and Dirksen 1986]; Khaleel et al. 1995) was used to measure unsaturated hydraulic conductivities for the bulk samples. The laboratory measured data on <2 mm size fraction were corrected for the gravel fraction ("Water Content" in Methods of Soils Analysis, Part 1—Physical and Mineralogical Methods [Gardner 1986]; Khaleel and Relyea 1997). No correction was needed for the saturated and unsaturated conductivities, since these were measured on the bulk sample.

Figure 7-10. Location of Integrated Disposal Facility and Selected Boreholes in 200 Area.

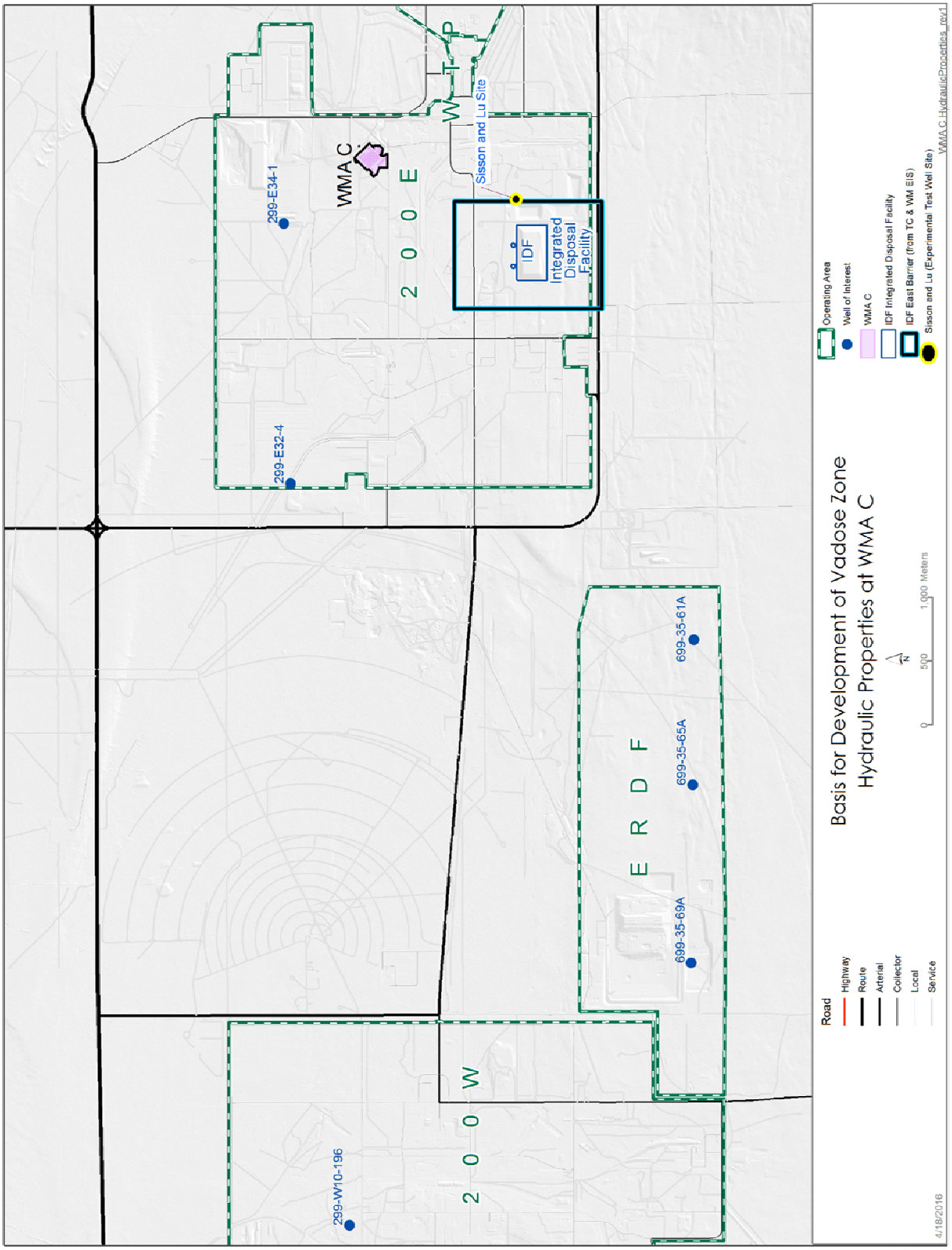

ERDF = Environmental Restoration Disposal Facility
WMA = Waste Management Area
TC & WM EIS = Tank Closure and Waste Management Environmental Impact Statement

Figure 7-11. Unsaturated Hydraulic Conductivity Measurements for Sand-dominated and Gravel-dominated Samples.

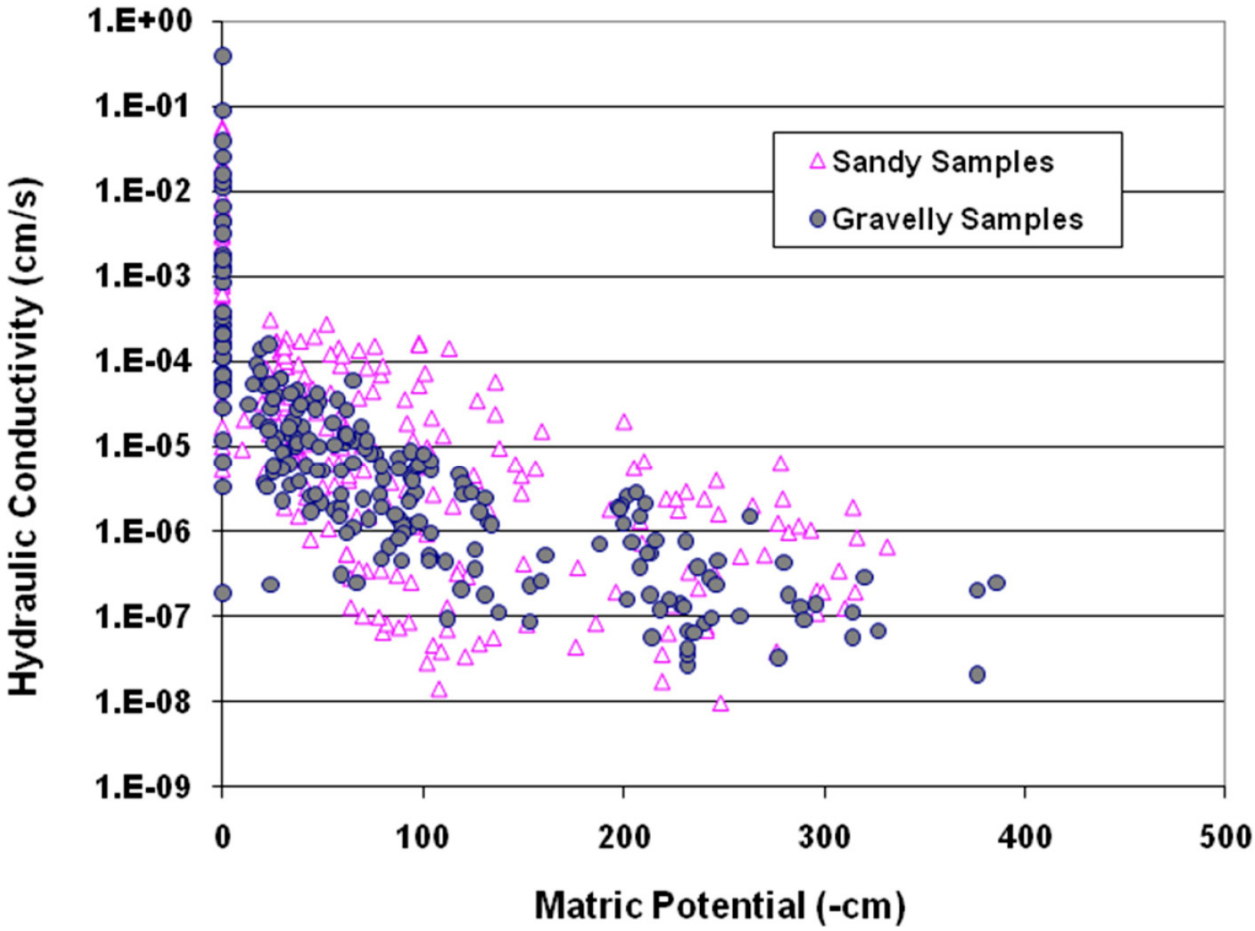

Reference: "Variability of Gardner's α for coarse-textured sediments" (Khaleel and Relyea 2001).

A simultaneous fit of both laboratory-measured moisture retention and unsaturated conductivity data was used; and all five unknown parameters (i.e., θ_r, θ_s, α, n, and K_s), with m=1-1/n (van Genuchten 1980), were fitted to the data via RETC (EPA/600/2-91/065). The pore size distribution factor, ℓ (Mualem 1976), was kept fixed at 0.5 during the simultaneous fitting. The fitted parameters, based on moisture retention and unsaturated conductivity measurements for H1 and H3 units, are shown in Table 7-3. The fitted retention and conductivity curves for H1 and H3 units are shown in Figure 7-12 and Figure 7-13, respectively.

Table 7-3. van Genuchten Parameters, Fitted Saturated Hydraulic Conductivity, and Measured Bulk Density Data for H1/H3 Units (17 Samples).

Sample	Site/Operable Unit	Borehole Number	Depth m	Percent Gravel	Θs cm^3/cm^3	Θr cm^3/cm^3	α 1/cm	n	Fitted Ks cm/s*	Bulk Density g/cm^3
5-0150	218-E-12B	299-E34-1	24.84	17	0.240	0.023	0.030	1.7077	1.47E-03	1.95
5-0157	218-E-10	299-E32-4	3.50	13	0.293	0.033	0.027	2.1675	7.77E-03	1.88
5-0152	218-E-12B	299-E34-1	65.50	26	0.280	0.025	0.044	1.3253	2.43E-03	1.85
5-0158	218-E-10	299-E32-4	71.50	44	0.214	0.013	0.008	1.4226	1.38E-04	2.15
5-0148	218-E-12B	299-E34-1	15.25	54	0.148	0.013	0.021	1.5589	2.72E-04	2.16
4-1080	ERDF	699-35-61A	93.50	43	0.178	0.000	0.007	1.3819	8.11E-06	2.00
4-0791	ERDF	699-35-65A	63.20	0	0.338	0.026	0.023	2.2565	6.81E-04	1.60
4-0792	ERDF	699-35-65A	75.40	71	0.100	0.008	0.030	1.5858	3.42E-04	2.32
4-1076	ERDF	699-35-61A	76.40	0	0.357	0.000	0.029	1.7015	1.23E-03	1.74
4-1079	ERDF	699-35-61A	90.90	61	0.163	0.000	0.014	1.3079	1.18E-04	2.06
4-1013	ERDF	699-35-69A	77.90	65	0.139	0.013	0.007	1.5656	1.06E-06	2.20
4-1012	ERDF	699-35-69A	73.90	55	0.147	0.000	0.008	1.5109	4.50E-05	2.19
3-0668	241-T-106	299-W10-196	38.90	62	0.175	0.000	0.019	1.6124	1.63E-04	2.13
3-0682	241-T-106	299-W10-196	46.10	51	0.224	0.000	0.017	1.6577	2.37E-04	2.14
3-0210	241-T-106	299-W10-196	3.10	48	0.186	0.029	0.014	1.7674	1.96E-04	2.11
3-0688	241-T-106	299-W10-196	48.50	49	0.199	0.000	0.004	1.5321	2.60E-05	2.17
3-0690	241-T-106	299-W10-196	53.7	53	0.182	0.018	0.005	1.5410	4.19E-05	2.19

*For these samples, unsaturated hydraulic conductivity values at specified moisture contents were available. The RETention Curve (RETC) code can generate the van Genuchten parameters using a simultaneous fit of unsaturated hydraulic conductivities, moisture content, and matric potential. However, when doing so, saturated hydraulic conductivity then becomes a fitting parameter.

ERDF = Environmental Restoration Disposal Facility

Figure 7-12. Moisture Retention Data for H1 and H3 Units (17 Samples). The composite curve is shown in red.

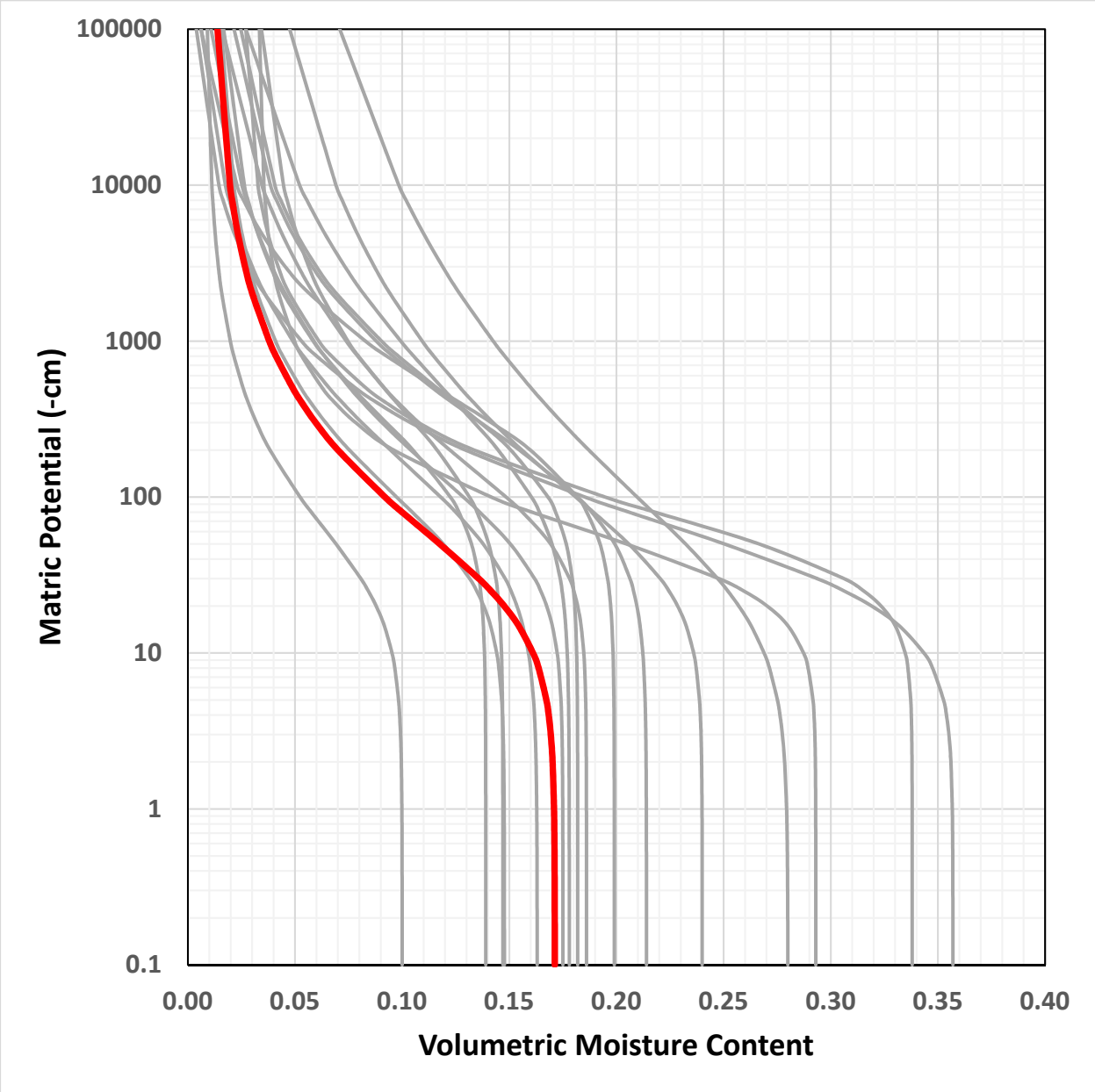

7.2.2 Updated Properties of the Hanford H2 Sand Unit

Figure 7-14 shows a representative sample of sediments associated with the Hanford H2 sand-dominated unit identified at WMA C. Because site-specific hydraulic properties data are unavailable, the available hydraulic properties database for coarse sands as well as the WMA C moisture content distribution were used to identify and characterize hydraulic properties for the Hanford H2 sand unit identified at WMA C. Using the moisture measurements as a proxy, the nearby 200 East Area IDF site (Figure 7-10) coarse sand unit correlates well with the Hanford

H2 sand unit identified at WMA C; the IDF coarse sands were thus used as surrogate for the WMA C H2 sands.

Figure 7-13. Unsaturated Hydraulic Conductivity Measurements for Sand-dominated and Gravel-dominated Samples.

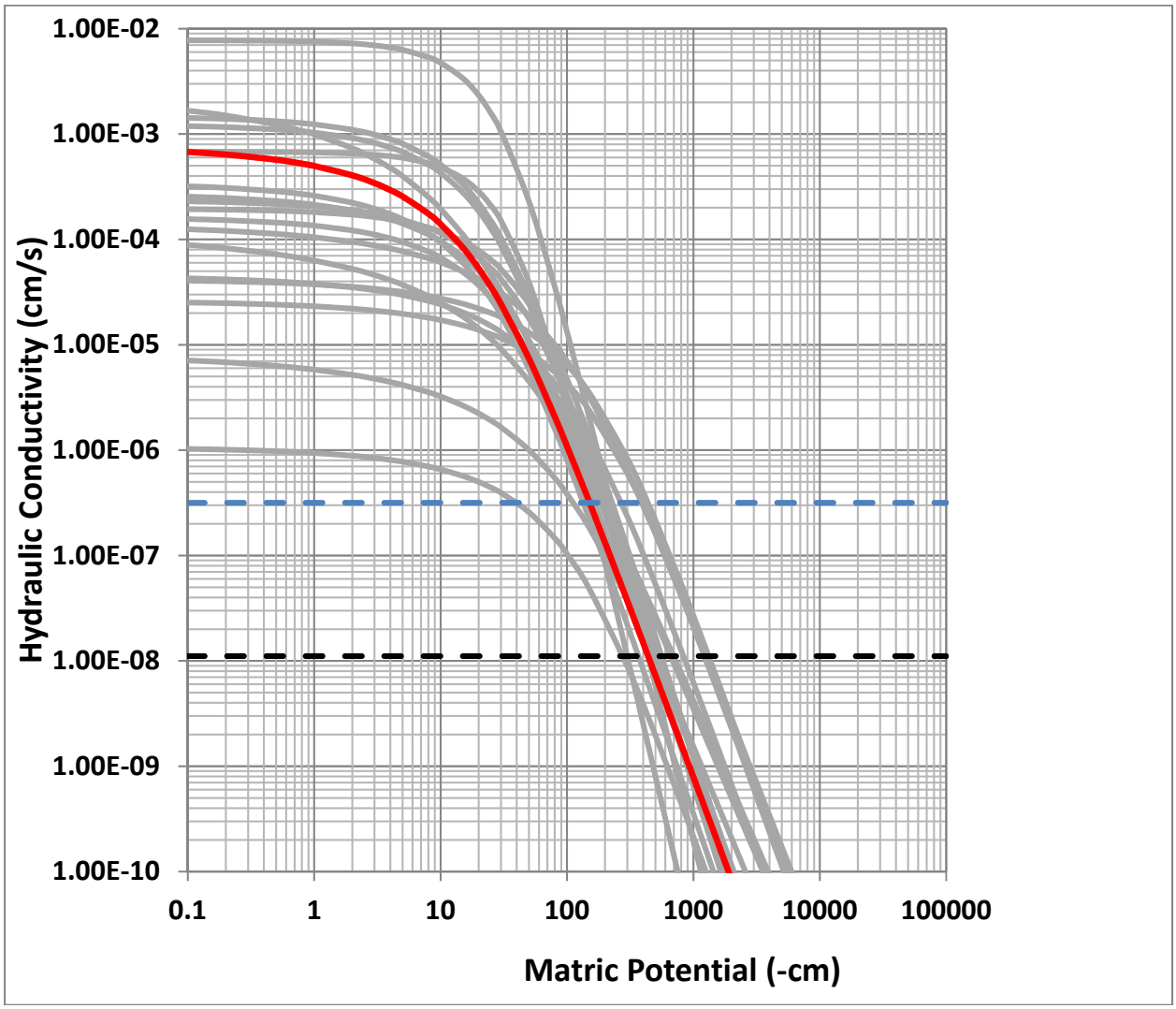

As part of site characterization for IDF, sediment samples were obtained in FY 1998, 2001 and 2002 via a borehole drilling and sampling program. The Hanford formation sandy H2 sequence identified at the IDF site is ~200 ft (~61 m) thick and, like WMA C, is the dominant facies at the site. The laboratory procedures used to analyze the IDF H2 borehole samples and analysis of samples from the three boreholes are described in appendices found in RPP-20621. RPP-20621 (Tables 1 through 3) provides the van Genuchten model parameters determined using the numerical inversion procedure and data from the multistep test. The pore-size distribution parameter ℓ (Mualem 1976) was kept fixed at 0.5. The fitted van Genuchten-Mualem parameters for the IDF H2 sandy sequence (44 samples) are reproduced in Table 7-4.

Figure 7-14. Waste Management Area C Hanford H2 Sand-Dominated Core.

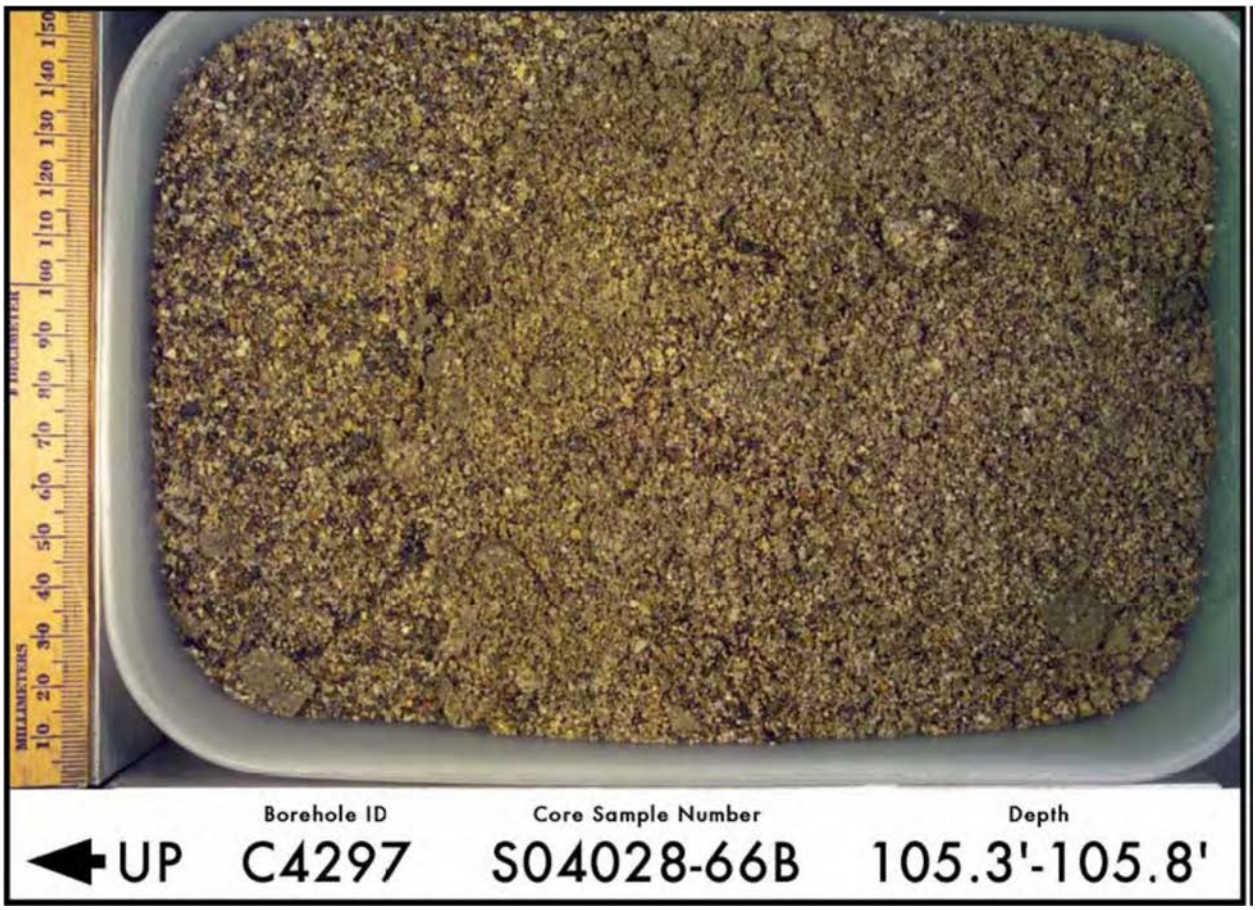

Reference: PNNL-15503, *Characterization of Vadose Zone Sediments below the C Tank Farm: Borehole C4297 and RCRA Borehole 299-E27-22*.

The IDF H2 samples contain very little gravel (>2-mm size) (RPP-20621). To account for the presence of gravel fraction for WMA C samples, the IDF H2 moisture retention data (Table 7-4) were corrected (Khaleel and Relyea 1997). Table 4.12 of PNNL-15503 suggests that the gravel fraction for the H2 unit can range from less than 1% to about 25%. Also, borehole logs (PNNL-15503) suggest the presence of a high gravel fraction, and many WMA C H2 samples are characterized as “sandy pebble gravel” and “pebbly sand.” A gravel fraction of 20% was assumed and applied to correct the IDF retention data. The fitted moisture retention curves and unsaturated conductivity curves for H2 sandy sequence as well as the WMA C H2 composite curves are shown in Figure 7-15 and Figure 7-16, respectively. To obtain the composite curves, all measurements for an EHM were pooled and the composite van Genuchten parameters were obtained via RETC code (EPA/600/2-91/065) and a simultaneous fit of both moisture retention and unsaturated conductivity data. As with individual H2 samples, the composite curves account for gravel correction.

Table 7-4. van Genuchten Parameters, Fitted Saturated Hydraulic Conductivity (44 samples), and Measured Bulk Density Data (41 samples) for Integrated Disposal Facility Borehole Samples from the H2 Sandy Sequence. (2 sheets)

Sample	θ_s (cm^3/cm^3)	θ_r (cm^3/cm^3)	α (1/cm)	n (-)	Saturated Hydraulic Conductivity (cm/s)	Bulk Density (g/cm^3)
7A[1]	0.377	0.0404	0.0290	1.825	1.04E-03	1.70
10A[1]	0.413	0.0279	0.1161	1.784	2.95E-03	1.62
12A[1]	0.363	0.0309	0.0650	1.755	2.15E-03	1.74
14A[1]	0.416	0.0324	0.0445	1.728	1.99E-03	1.58
15A[1]	0.380	0.0254	0.0487	1.844	2.09E-03	1.69
16A[1]	0.420	0.0228	0.0682	1.710	9.57E-03	1.58
17A[1]	0.423	0.0382	0.0689	1.899	1.99E-03	1.57
19A[1]	0.444	0.0279	0.2010	1.542	4.31E-03	1.52
20A[1]	0.419	0.0321	0.0305	2.081	2.54E-03	1.58
21A[1]	0.403	0.0276	0.0545	1.926	2.94E-03	1.62
22A[1]	0.352	0.0252	0.1078	1.585	5.06E-03	1.78
23A[1]	0.371	0.0411	0.0079	1.553	2.65E-04	1.72
24A[1]	0.321	0.0413	0.0130	1.684	5.69E-04	1.85
25A[1]	0.345	0.0267	0.0842	2.158	5.40E-03	1.80
27A[1]	0.377	0.0354	0.0830	1.532	8.14E-03	1.71
29A[1]	0.359	0.0317	0.0784	1.732	3.75E-03	1.76
31A[1]	0.418	0.0444	0.0058	2.012	8.21E-04	1.60
32A[1]	0.359	0.0401	0.0931	1.703	6.71E-03	1.78
34A[1]	0.316	0.0324	0.0819	2.398	1.32E-02	1.92
35A[1]	0.299	0.0428	0.0897	2.160	1.06E-02	1.98
45L[2]	0.385	0.008	0.1039	1.737	3.24E-2	1.63
45U[2]	0.385	0.005	0.088	1.664	3.24E-2	1.63
50L[2]	0.420	0.025	0.073	1.710	1.75E-3	1.54
50U[2]	0.420	0.013	0.045	1.667	1.75E-3	1.54
80L[2]	0.359	0.031	0.0403	2.368	1.05E-3	1.70
80U[2]	0.359	0.033	0.0313	2.572	1.05E-3	1.70

Table 7-4. van Genuchten Parameters, Fitted Saturated Hydraulic Conductivity (44 samples), and Measured Bulk Density Data (41 samples) for Integrated Disposal Facility Borehole Samples from the H2 Sandy Sequence. (2 sheets)

Sample	θ_s (cm^3/cm^3)	θ_r (cm^3/cm^3)	α (1/cm)	n (-)	Saturated Hydraulic Conductivity (cm/s)	Bulk Density (g/cm^3)
85L[2]	0.406	0.023	0.1074	1.697	3.84E-2	1.57
85U[2]	0.406	0.027	0.0847	1.595	3.84E-2	1.57
110L[2]	0.412	0.039	0.0362	2.328	5.16E-4	1.56
110U[2]	0.412	0.046	0.0268	3.182	5.16E-4	1.56
130L[2]	0.358	0.032	0.0940	2.003	1.97E-2	1.70
130U[2]	0.358	0.036	0.0674	1.934	1.97E-2	1.70
150L[2]	0.431	0.015	0.0992	1.547	7.48E-3	1.51
150U[2]	0.431	0.024	0.0703	1.514	7.48E-3	1.51
200L[2]	0.410	0.002	0.0995	2.162	4.93E-2	1.56
215L[2]	0.370	0.028	0.0448	1.918	2.24E-3	1.67
215U[2]	0.370	0.023	0.0333	1.815	2.24E-3	1.67
230L[2]	0.309	0.040	0.0472	1.658	3.56E-3	1.83
230U[2]	0.309	0.038	0.0400	1.658	3.56E-3	1.83
251L[2]	0.427	0.032	0.084	1.845	1.43E-2	1.57
261L[2]	0.390	0.045	0.0191	2.485	5.54E-4	1.62
C3826-171[3]	0.382	0.0226	0.0390	1.840	7.96E-3	NR
C3827-63.5[3]	0.444	0.0	0.0914	1.500	2.23E-2	NR
C3827-221[3]	0.361	0.0220	0.0660	1.770	7.30E-3	NR

Reference: RPP-20621, *Far-Field Hydrology Data Package for the Integrated Disposal Facility Performance Assessment*.

[1]Fiscal year 1998 borehole (RPP-20621).
[2]Fiscal year 2001 borehole (RPP-20621).
[3]Fiscal year 2002 borehole (RPP-20621).

NR = Not Reported

7.2.3 Alternative Geologic Model H2 Subunits Properties

For the Alternative Geologic Model II evaluation, the Hanford H2 gravel/coarse sand subunit was assumed to be more transmissive, and the Hanford H2 silty sand less transmissive, than the

Hanford H2 sand. Therefore, as an initial estimate of these properties, the hydraulic properties associated with the 5th and 95th percentile realizations of unsaturated hydraulic conductivity curves developed for the Hanford H2 sand unit were considered representative of the Hanford H2 gravel/coarse sand and the Hanford H2 silty sand subunits, respectively.

Figure 7-15. Moisture Retention Data for H2 Unit (44 Samples). The Waste Management Area C composite curve is shown in red.

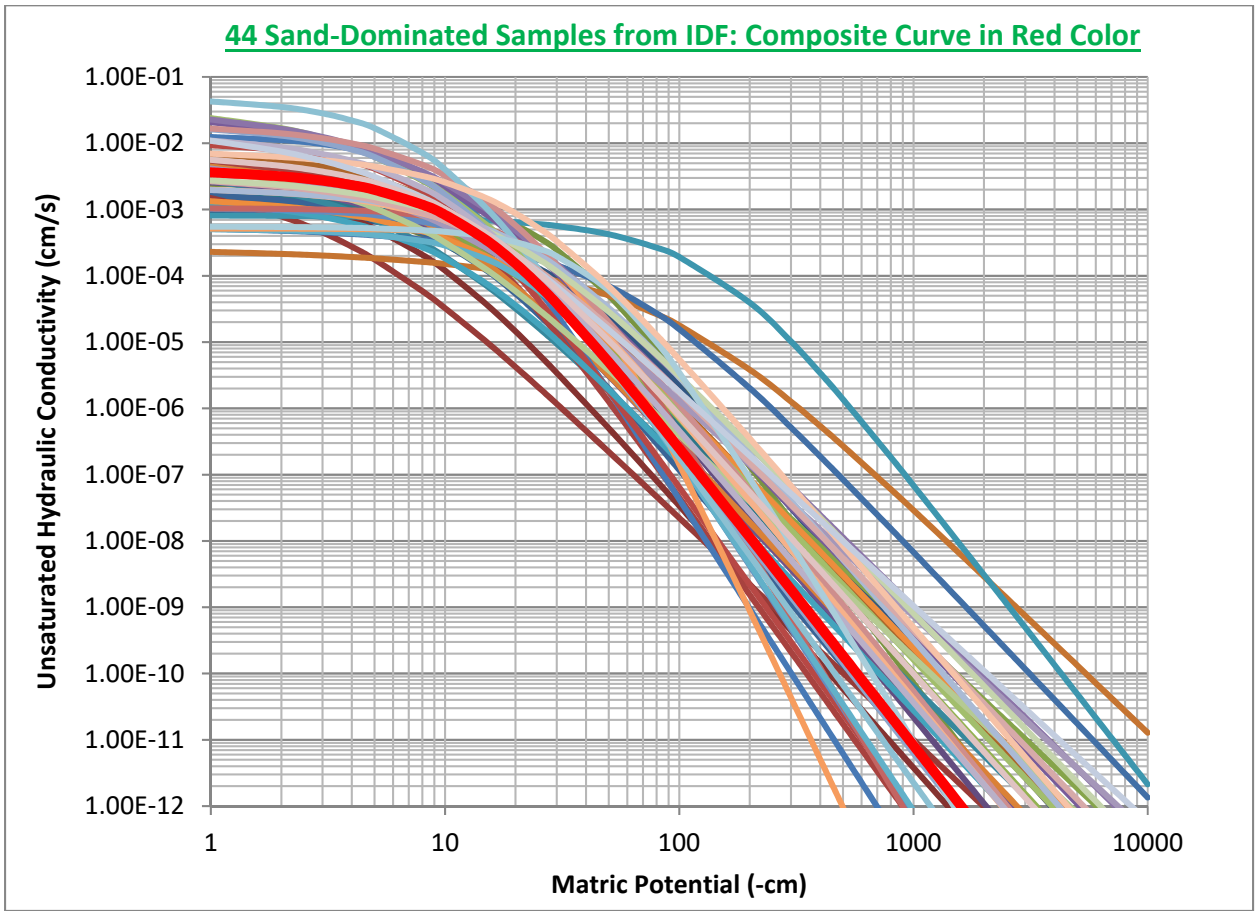

Reference: RPP-20621, *Far-Field Hydrology Data Package for the Integrated Disposal Facility Performance Assessment*.

7.2.4 Summary of Revised Hydraulic Parameters

Table 7-5 lists the upscaled composite-fitted van Genuchten-Mualem (van Genuchten 1980, Mualem 1976, EPA/600/2-91/065) base case parameters for the various strata at the WMA C site (Note: the values for backfill in this table are the same as in Table 4-1 of this document).
A stochastic model of variable moisture or tension-dependent anisotropy provides the framework for upscaling small-scale measurements to the effective (upscaled) properties for the large-scale vadose zone (Application of Stochastic Methods to Transient Flow and Transport in Heterogeneous Unsaturated Soils [Polmann 1990]). The upscaling processes factor the inherent spatial variability that occurs on different scales in heterogeneous media into the field scale parameter estimates ("Stochastic analysis of moisture plume dynamics of a field injection experiment" [Ye et al. 2005], "Estimation of effective unsaturated hydraulic conductivity tensor

using spatial moments of observed moisture plume" [Yeh et al. 2005]). Detailed discussion of the Polmann (1990) model and the derivation of the upscaled parameters are presented in RPP-CALC-60452, *Moisture Dependent Anisotropy Calculations Supporting Waste Management Area C Performance Assessment* and in Appendix B of RPP-ENV-58806, *RCRA Closure Analysis of Tank Waste Residuals Impacts at Waste Management Area C, Hanford Site, Washington*.

Figure 7-16. Unsaturated Hydraulic Conductivity Data for H2 Unit (44 Samples). The Waste Management Area C H2 composite curve is shown in red.

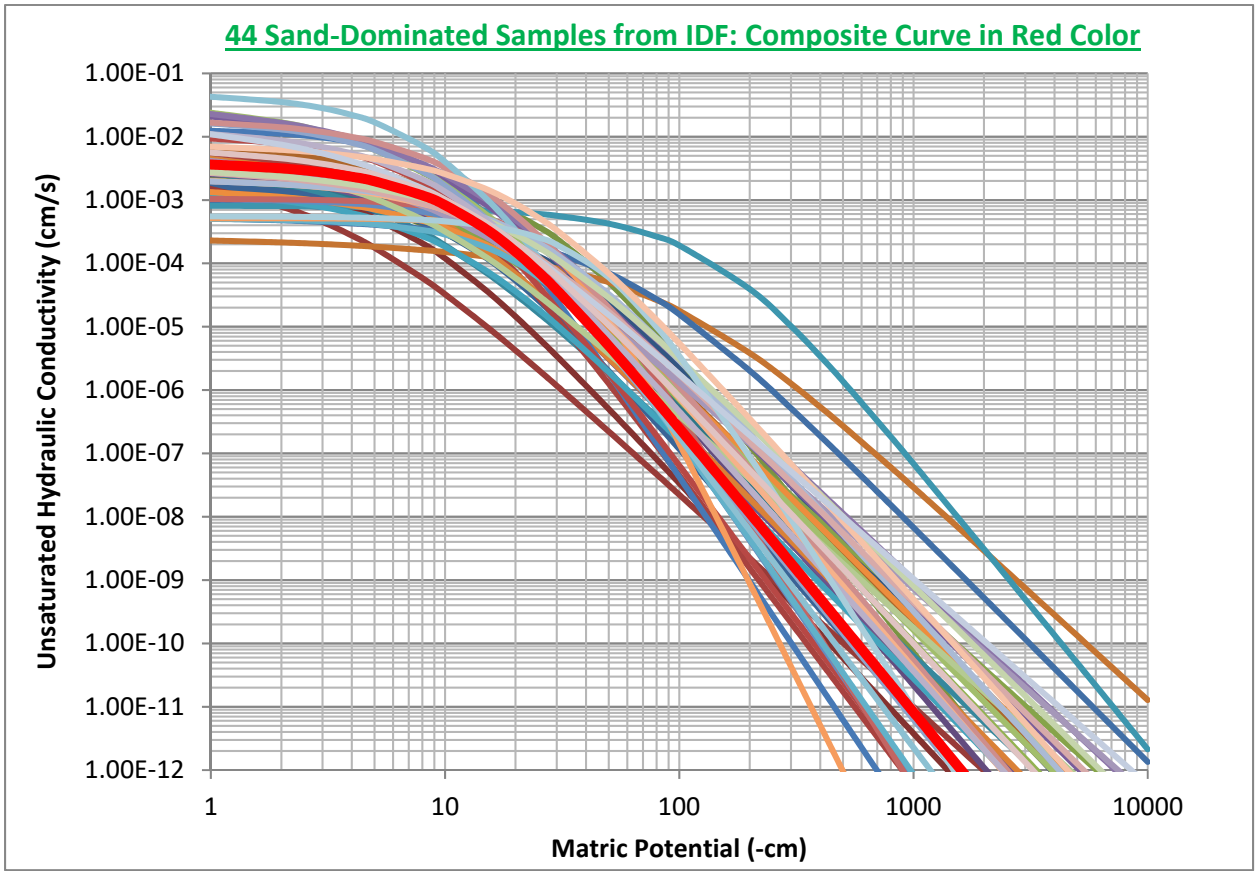

Reference: RPP-20621, *Far-Field Hydrology Data Package for the Integrated Disposal Facility Performance Assessment*.

Following the development of the new hydraulic properties, a STOMP© vadose zone model was re-run with the updated van Genuchten parameters given in Table 7-5 to compare the model results for volumetric moisture content against the values observed in the field. Table 7-6 shows the average model-calculated moisture content for those units at three different time periods; at the end of operational period, 80 years after the placement of the barrier, and 3,000 years after the placement of the barrier. Comparison of the moisture content in Table 7-6 against the observed field values in Table 7-1 shows a much better agreement between the model-calculated moisture content and field observations.

Figure 7-17 shows the vadose zone aqueous moisture content for two models at three different times. Each of those times represents a different recharge being applied in the model. The far

left plots are at the end of the operational period with a recharge of 100 mm/yr; the middle plots are at 80 years after closure with the modified RCRA C Barrier performing as designed and the recharge is 0.5 mm/yr; while the far right plots are at 3,000 years after closure and modified RCRA C barrier degrading, and the recharge for this time period is 3.5 mm/yr.

Table 7-5. Composite van Genuchten-Mualem Parameters for Various Strata at the Waste Management Area C Site Used in the Base Case Evaluations of Alternative Geologic Models I and II.

Strata	Number of Samples	θ_s	θ_r	α (1/cm)	n	ℓ^c	Fitted K_s (cm/s)[1]
Backfill (Gravelly)	10	0.138	0.010	0.021	1.374	0.5	5.60E-04
Hanford H1/H3 (Gravel-dominated)	15	0.171	0.011	0.036	1.491	0.5	7.70E-04
Hanford H2 (Sand-dominated)	44	0.315	0.039	0.063	2.047	0.5	4.15E-03
Hanford H2 –Gravel/coarse sand subunit*	not applicable	0.265	0.002	0.108	1.724	0.5	1.68E-02
Hanford H2 – Silty-sand subunit[2]	not applicable	0.354	0.029	0.040	1.633	0.5	1.79E-03

[1] For these samples, unsaturated hydraulic conductivity values at specified moisture contents were available. The RETention Curve (RETC) code can generate the van Genuchten parameters using a simultaneous fit of unsaturated hydraulic conductivities, moisture content, and matric potential. However, when doing so, saturated hydraulic conductivity then becomes a fitting parameter.

[2] Hydraulic properties of these units are only used in numerical model simulation of Alternative Geologic Model II. As an initial estimate of these properties, the hydraulic properties associated with the 5th and 95th percentile realizations of unsaturated hydraulic conductivity curves developed in the Uncertainty and Sensitivity Analysis for the Hanford H2 sand unit were considered to be representative of the Hanford H2 silty sand and the Hanford H2 gravel/coarse sand subunits, respectively.

For the upper row of results, the model used the van Genuchten parameters in Table 4-1 of this document; while for the bottom row of results, the model used the updated van Genuchten parameters (Table 7-5). It is clearly shown in these plots that the aqueous moisture content is 1.5 to 3 times higher in the upper plots than in the lower plots. Comparing the model-calculated results for vadose zone aqueous moisture content against the field observations leads to the conclusion that the revised van Genuchten parameters should be used for the model, rather than the values in Table 4-1 of this document.

The Darcy flux in the model is divided by the aqueous moisture content to calculate the pore water velocity and hence the travel time through the vadose zone. High aqueous moisture content means a longer travel time through the vadose zone. This is illustrated by Figure 7-18 which shows the vadose zone pore water velocity for the same three times in Figure 7-17. These plots are one cross-section through tank row C-102, C-105, C-108, and C-111. Again, for the upper row of plots the model used the van Genuchten parameters in Table 4-1 of this document; while for the bottom row of results, the model used the updated van Genuchten parameters (Table 7-5). The vadose zone pore water velocities are much higher in the lower plots.

Table 7-6. Summary Statistics for Volumetric Moisture Content in the Lithologic Units Underlying Waste Management Area C Using Updated van Genuchten Parameters.

Formation	Year	Recharge (mm/yr)	Average Moisture Content (Vol %)	Minimum Moisture Content (Vol %)	Maximum Moisture Content (Vol %)
Backfill	2020	100.0	8.2	7.8	9.1
H1	2020	100.0	7.7	5.8	8.7
H2	2020	100.0	8.1	6.1	9.1
Backfill	2100	0.5	5.6	5.0	7.6
H1	2100	0.5	5.2	4.2	6.5
H2	2100	0.5	6.2	5.1	7.1
Backfill	5020	3.5	6.0	5.7	7.9
H1	5020	3.5	5.3	4.6	6.8
H2	5020	3.5	5.9	5.3	6.7

To quantify the decrease in travel time, streamlines with time markers have been added to each plot. The streamline shows the path a particle will take from the bottom of the backfill to the unconfined aquifer. The time markers show the distance it travels between the time markers for a specified time. The time markers for the left column of plots are every 20 years, the middle column has time markers every 300 years, while the right column has time markers every 500 years. Table 7-7 provides the distance a particle would take to reach a time marker at a specified time, as well as the approximate time it would take a particle to reach the vadose zone. It should be noted that the plots on the left and right are approximately steady-state; however, the plot in the middle is not. The higher recharge from the operation period is still draining at the bottom of the plot, but the upper portion of the plot is experiencing the drastic decrease in recharge after the modified RCRA C barrier has been placed over WMA C. The distance a particle would travel over the same time period is approximately 2 to 3.5 times higher with the revised van Genuchten parameters. Comparing the model-calculated results for vadose zone aqueous moisture content against the field observations leads to the conclusion that the revised van Genuchten parameters should be used for the model, rather than the values in Table 4-1 of this document. This conclusion is further buttressed by the observation that contamination in the monitoring wells around WMA C was first observed between the years 2000 to 2005 approximately 30 to 40 years after known unplanned releases. The model-calculated travel time is approximately 50 years using the revised van Genuchten parameters under operational conditions, while it is approximately 140 years using the parameters in Table 4-1, which suggests that the bulk of the contamination is still in the vadose zone and it should not be observed in the monitoring wells.

7.2.5 Alternative Heterogenous Model

The recent availability of the moisture content data collected at WMA C allowed the development of an alternative heterogeneous model based on the moisture content data. The

heterogeneous model is briefly summarized here, but fully documented in RPP-CALC-60345, *Heterogeneous Media Model for Waste Management Area C Performance Assessment* and Appendix F of RPP-ENV-58806.

For this model, a 3D model of the distribution of moisture content has been developed based on a geostatistical evaluation of soil moisture data collected at WMA C. An extensive set of moisture content data and information exists at WMA C from neutron moisture logging of direct push borehole and dry well locations. These moisture content data have been collected long after the occurrence of past leaks and discharges at the farm (RPP-CALC-60345), and therefore are regarded as representing the vadose zone at equilibrium with natural recharge. A geostatistical analysis of the moisture content data yielded vertical as well as horizontal correlation length scales for moisture content. The experimental variograms for moisture content used in the geostatistical analysis were fit with an exponential model having a vertical correlation length of ~15 m and a horizontal correlation length of ~85 m. Subsequent kriging yielded a heterogeneous moisture distribution, which, unlike the EHM approximation, captures a higher level of spatial variability of moisture content and associated variability in hydraulic properties (RPP-CALC-60345). Figure 7-19 represents the plan view of 3D WMA C PA/RCRA Closure Analysis model domain and krigged moisture content based on the level of discretization of the model domain. Figure 7-20 (RPP-CALC-60345) presents the location of the different cross sections of the model; Figure 7-21 and Figure 7-22 show the two-dimensional (2D) cross sections of the model.

7.2.5.1 Development of Two-Dimensional STOMP©-Based Models from Three-Dimensional Models

7.2.5.1.1 Base Case Two-Dimensional Model. From the 3D base case model, 2D models were extracted for three different cross sections. Figure 7-23 shows the location of the selected cross sections. These cross sections were selected to be in the same locations as the cross section B-B’ and cross section C-C’ shown in Figure 7-20. Two orthogonal directions were chosen to represent behavior in different directions. Cross section 1 cuts through the tanks while cross section 2 does not.

Figure 7-17. Plots of Model-Calculated Aqueous Moisture Content for Three Time Periods. Upper Row of Plots Uses the van Genuchten Parameters in Table 4-1, while the Lower Row of Plots Uses the Updated van Genuchten Parameters.

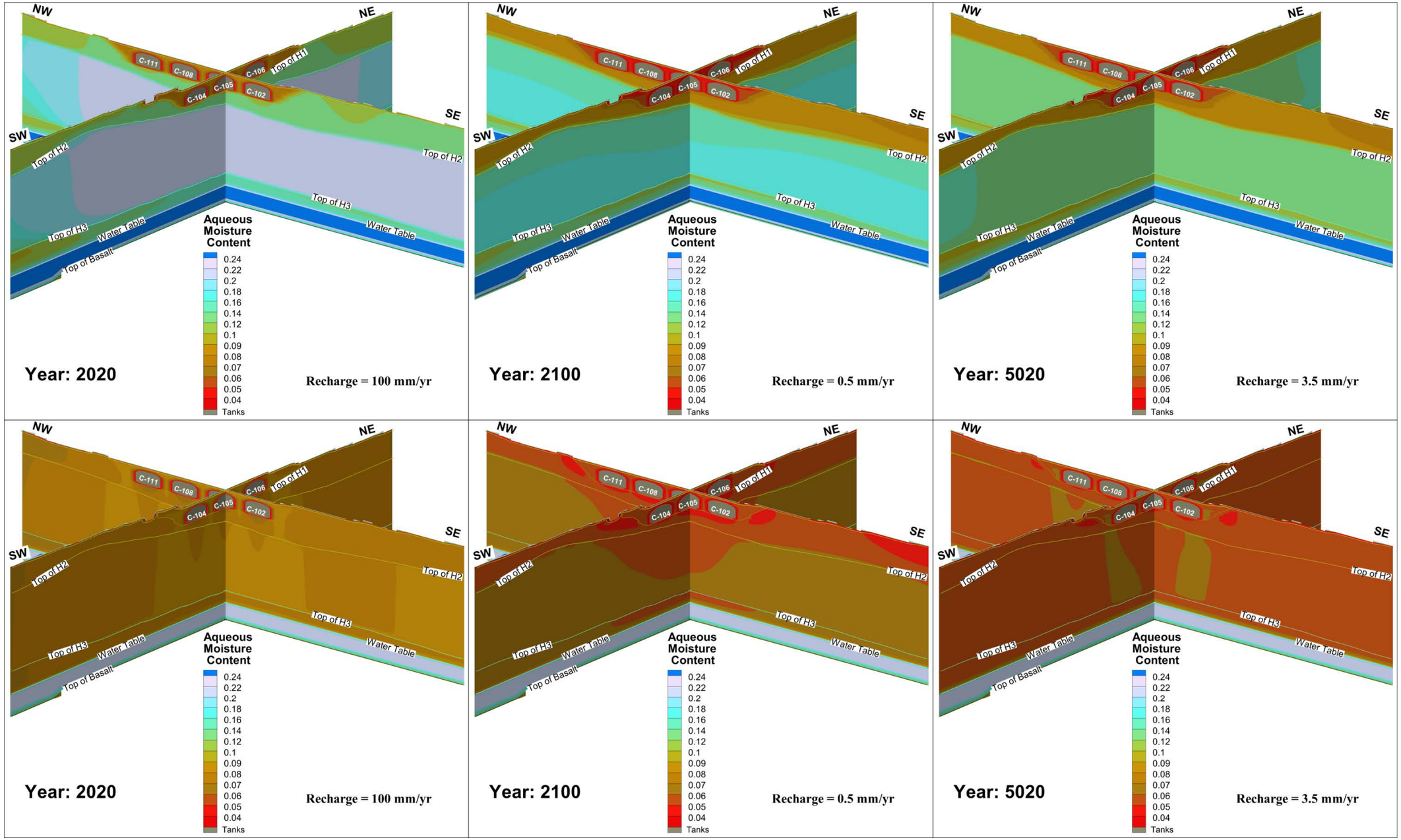

Figure 7-18. Plots of Model-Calculated Vadose Zone Pore Water Velocity along with Streamlines and Time Markers for Three Time Periods along a Cross-Section of the Model going through Tanks 241-C-102, 241-C-105, 241-C-108 and 241-C-111. Upper Row of Plots Uses the van Genuchten Parameters in Table 4-1, while the Lower Row of Plots Uses the Updated van Genuchten Parameters.

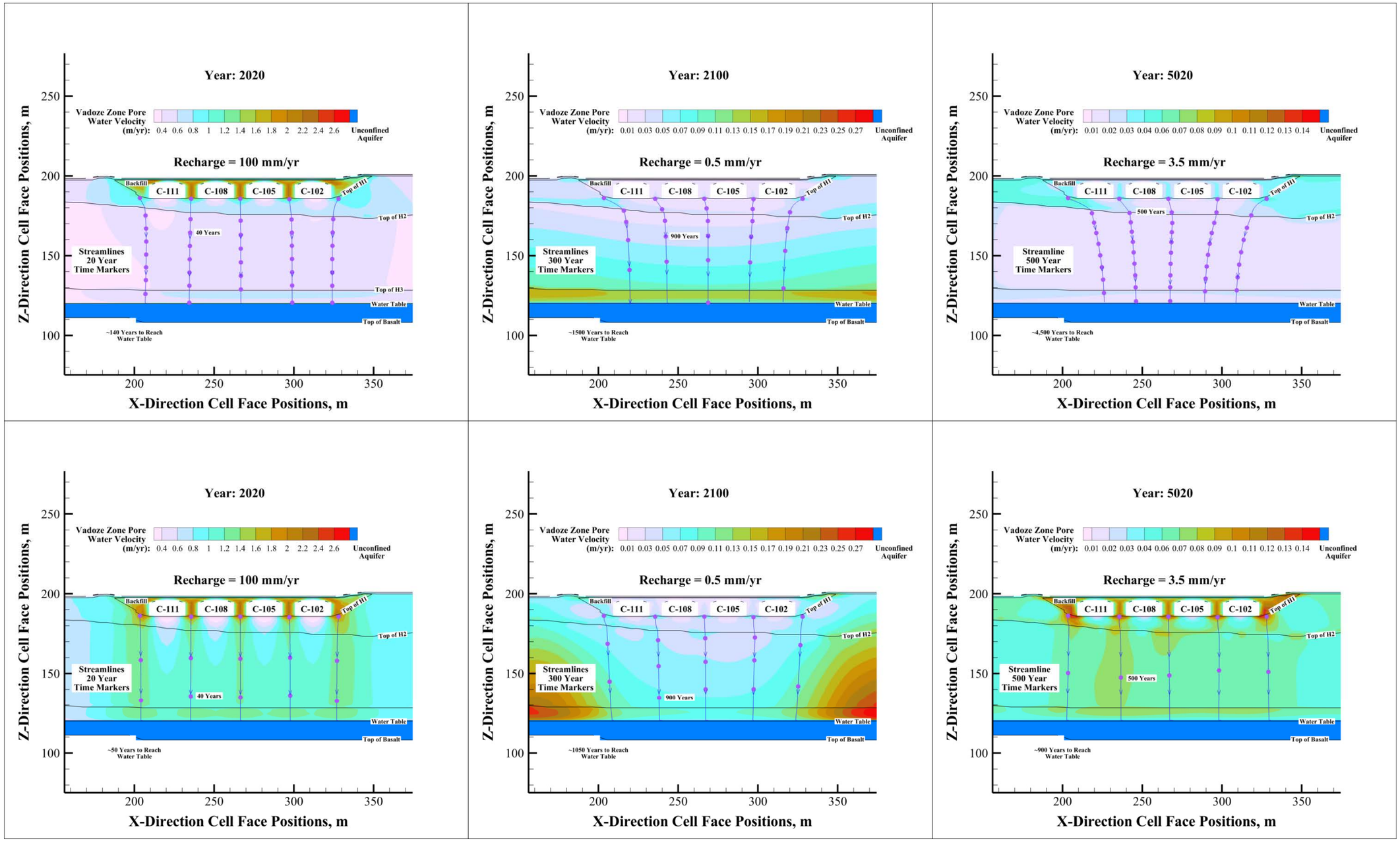

Table 7-7. Travel Time Calculations Using the Original and Updated van Genuchten Parameters.

Figure 7-18 Plot	Van Genuchten Hydraulic Properties	Time (year)	Time Mark (years)	Distance Travel to Reach Time Mark (m)	Approximate Time to Water Table (years)
Upper Left	Original	2020	40	21.27	50
Lower Left	Updated	2020	40	50.08	140
Upper Middle	Original	2100	900	25.07	1,500
Lower Middle	Updated	2100	900	51.22	1,050
Upper Right	Original	5020	500	10.86	4,500
Lower Right	Updated	5020	500	38.06	900

Figure 7-19. Plan View of Waste Management Area C Performance Assessment Model and Moisture Content-Based Model.

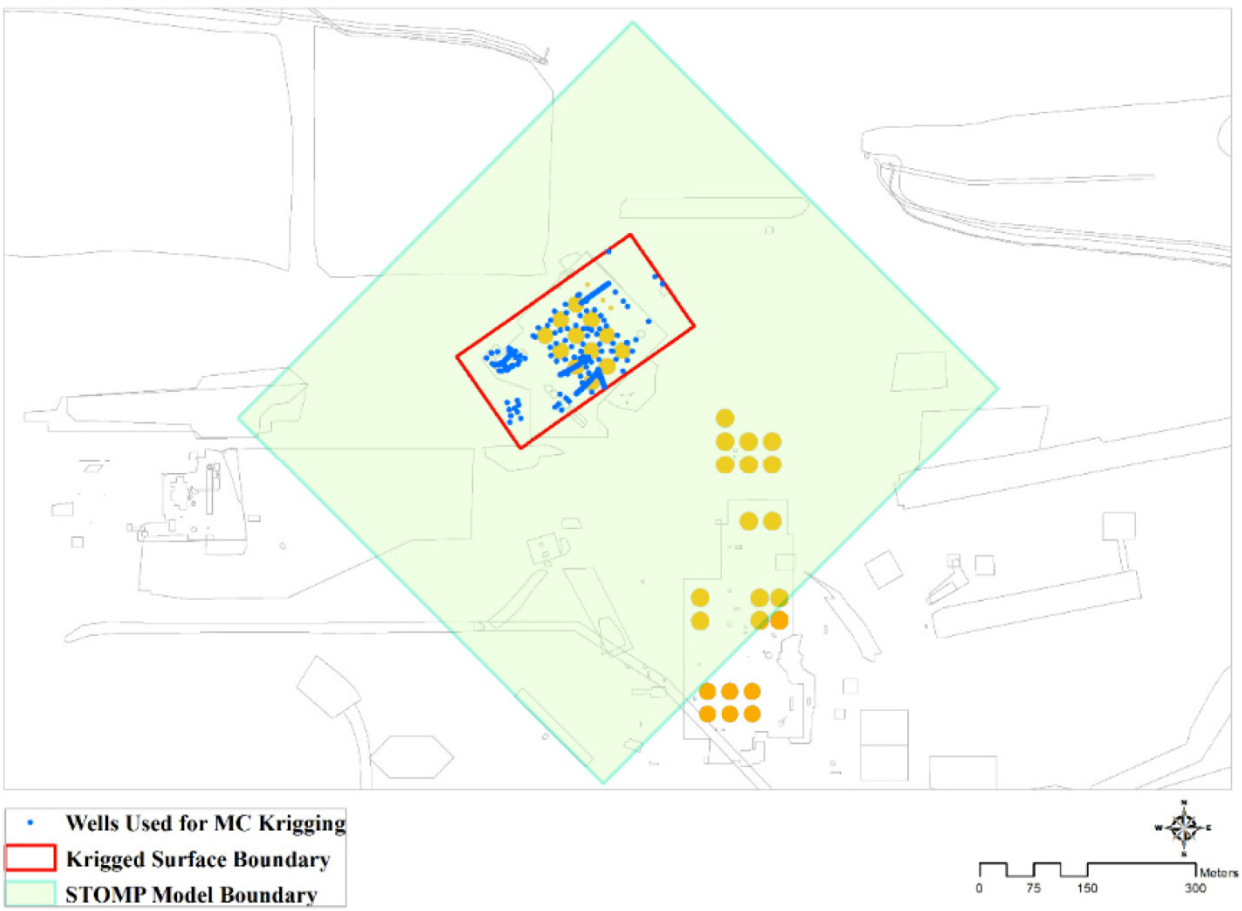

Subsurface Transport Over Multiple Phases (STOMP)© is copyrighted by Battelle Memorial Institute, 1996.

Figure 7-20. Waste Management Area C Basemap with Moisture Content (vol %) Data Locations.

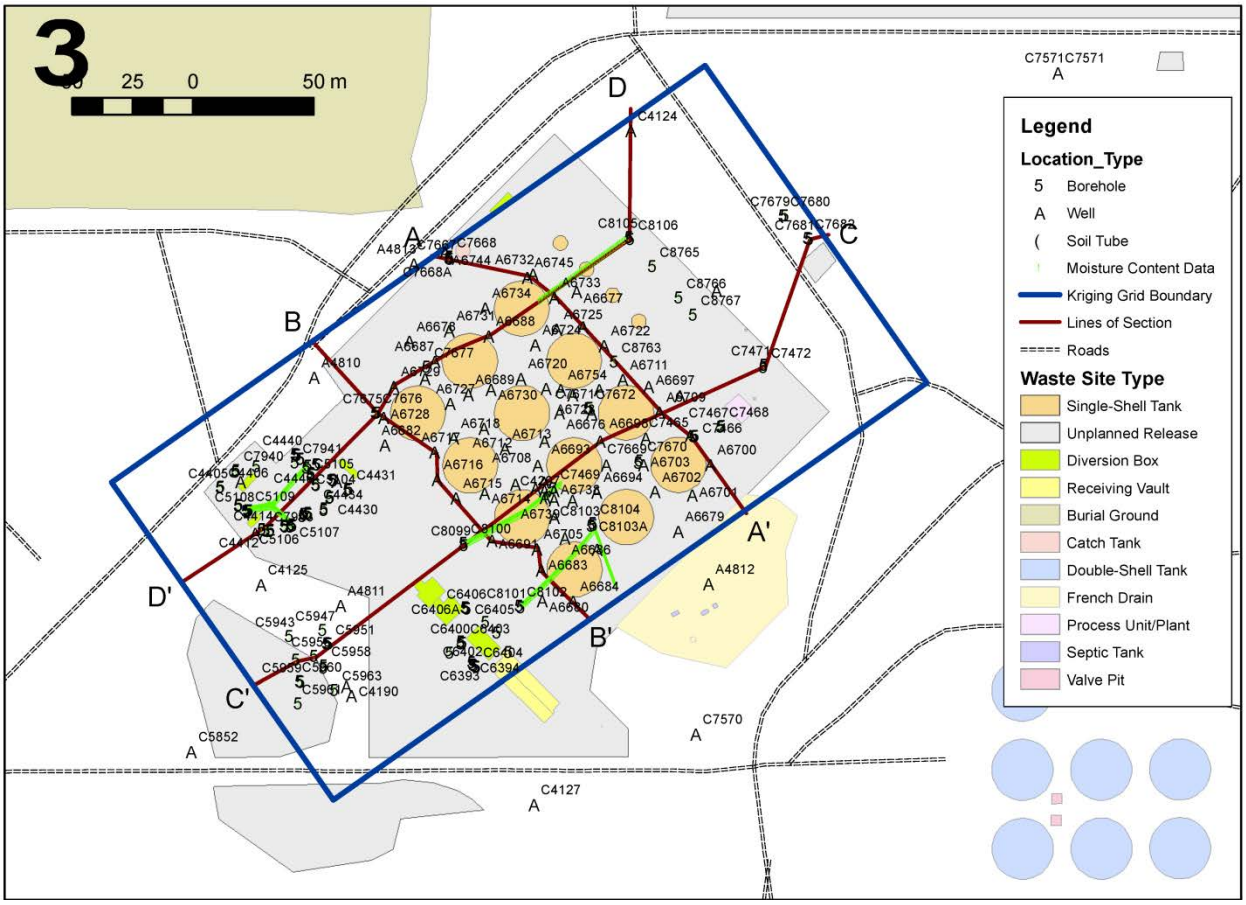

Reference: RPP-CALC-60345, *Heterogeneous Media Model for Waste Management Area C Performance Assessment*.

The steps to develop the 2D model are:

1. Export the 3D STOMP© model grid into TecPlot 360®[2] software for selection of 2D cross section models.

2. For cross section 1, J = 46 (Y direction index for STOMP© Model) has been selected to create an X-Z model grid. The geologic properties and the flow and transport properties were kept the same as they were in the original 3D model.

3. The same steps were followed for cross section 2, J = 33 (Y direction node index for STOMP© Model).

4. For cross section 3, I = 46 (X direction node index for STOMP©) was selected to create a Y-Z model grid.

[2] Tecplot 360® is a registered trademark of Tecplot, Inc., 3535 Factoria Blvd. SE, Bellevue, Washington.

Figure 7-21. Cross Section B-B' with Continuous Contours for Moisture Content (vol %) Interpolation.

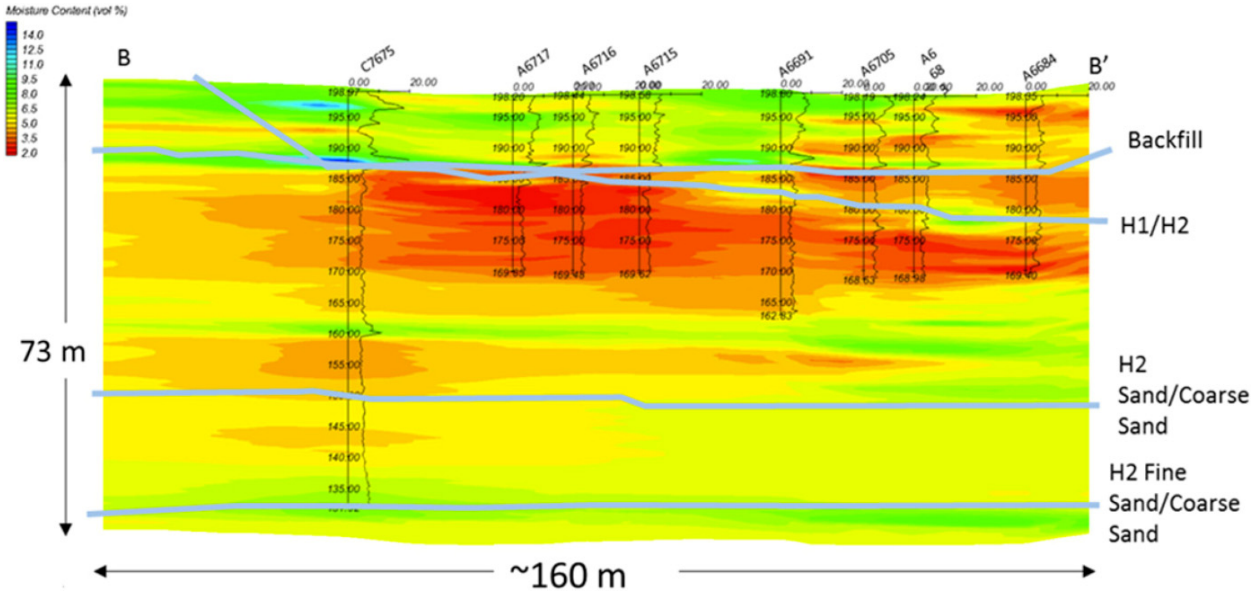

Reference: RPP-CALC-60345, *Heterogeneous Media Model for Waste Management Area C Performance Assessment*.

Figure 7-22. Cross Section C-C' with Continuous Contours for Moisture Content (vol %) Interpolation.

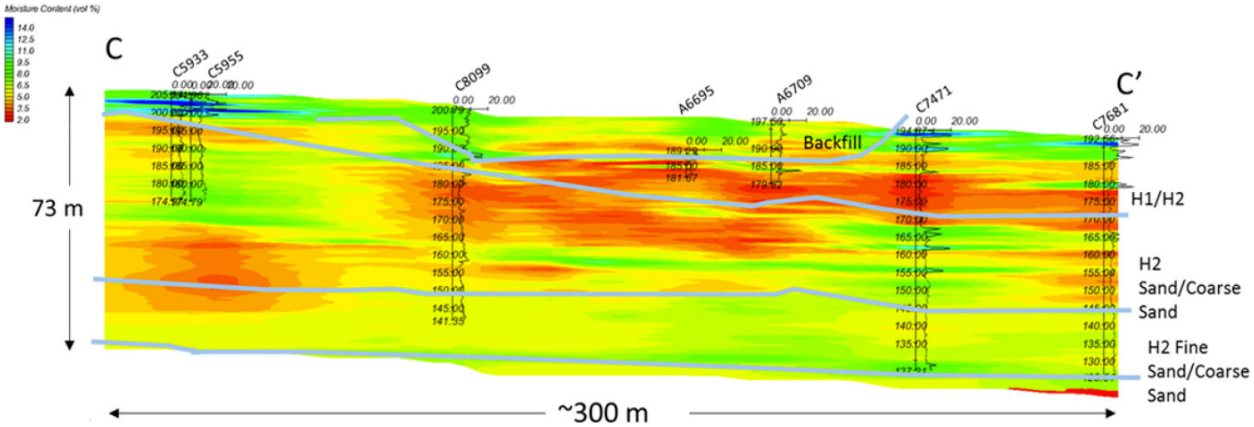

Reference: RPP-CALC-60345, *Heterogeneous Media Model for Waste Management Area C Performance Assessment*.

7.2.5.1.2 Development of Heterogeneous Model. In the WMA C PA Base Case Model, the major H2 Sand unit was considered a single homogeneous unit, but here the plan was to introduce heterogeneity based on the 3D moisture model.

Figure 7-23. Location of Selected Cross Sections for the Two-Dimensional Models.

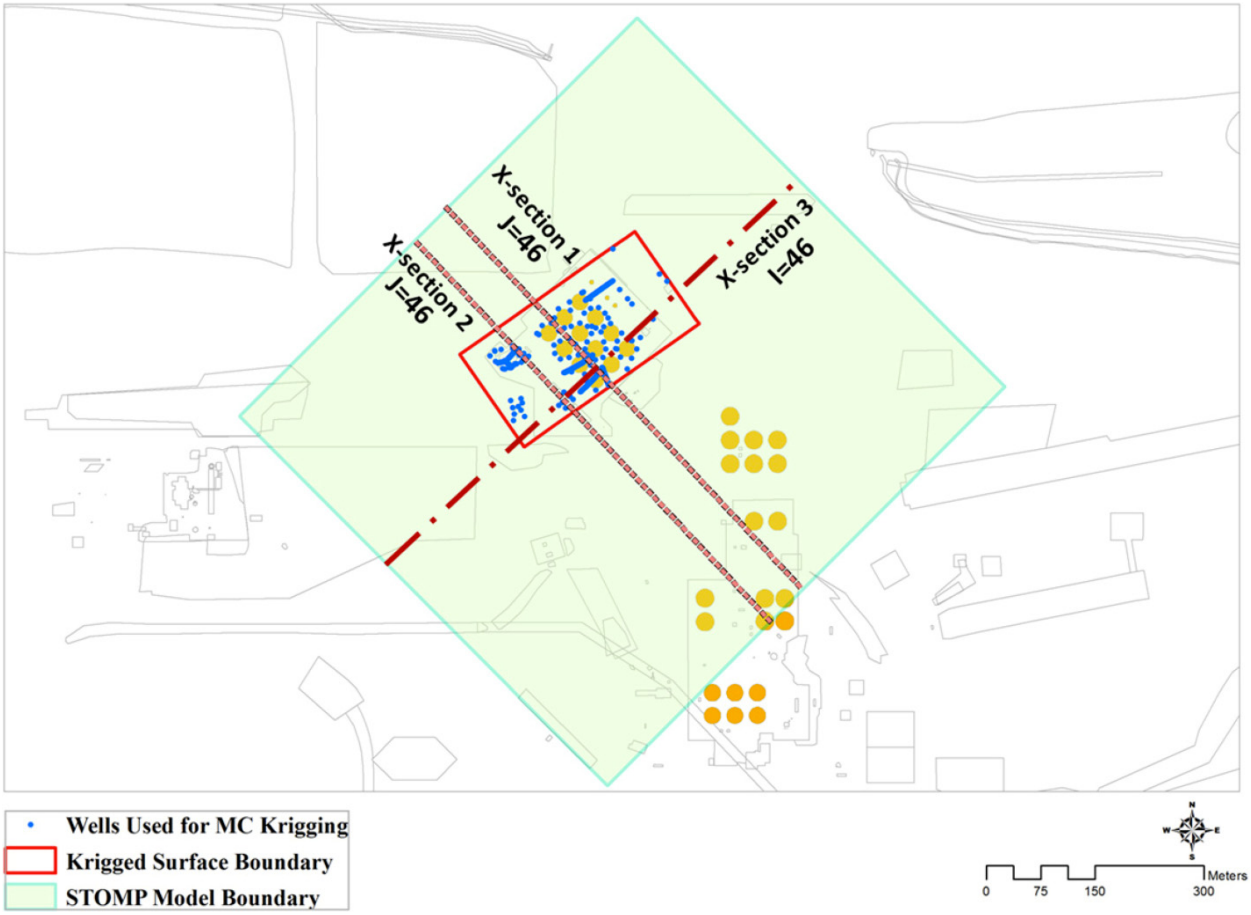

Subsurface Transport Over Multiple Phases (STOMP)© is copyrighted by Battelle Memorial Institute, 1996.

7.2.5.1.2.1 Interpretation of the Three-Dimensional Moisture Model. The following steps were followed to develop the geology of the heterogeneous model from the moisture content model.

1. Four different moisture content bands were used to define the heterogeneous layers in the H1 and H2 units based on the histogram of the observed moisture content data reported in RPP-CALC-60345. These moisture content bands qualitatively correlate with the sand/silt content of the sediments as inferred from the characterization of vadose zone sediments within WMA C (PNNL-15503). Typically, increasing volumetric moisture content from 6% to >10% reflects increasing silt content in the sediments. Based on the characterization of vadose zone sediments in WMA C (PNNL-15503), it is observed that <6% moisture content is associated with sediments with no, or negligible, silt content (primarily sand or gravelly sand), while sediment with >10% volumetric moisture content is silt-dominated. For volumetric moisture contents, within 6% and 10% of the increasing moisture content is understood to reflect increasing silt content. To define the moisture content bands for the purpose of model parameterization, two additional classes

are introduced, one with 6% to 8% and other with 8% to 10% volumetric moisture content. The four moisture content bands are summarized below:

- 2% to 6% – correlates to sand with some gravel fraction
- 6% to 8% – correlates to sandy units with minor silt fraction
- 8% to 10% – correlates to sandy-silty sand units
- >10% – correlates to predominantly silty units.

2. Using the Tecplot 360® linear interpolation technique, the moisture content values from the moisture model were interpolated in the STOMP© Model grid.

3. The STOMP© Model zonation number for each of the model grid blocks was printed out along with the moisture content values.

4. The original STOMP© model has five different hydrostratigraphic units defined as implemented in STOMP© as rock/soil zones:

   - Backfill: gravel-dominated
   - H1: gravel-dominated unit
   - H2: sand-dominated unit
   - H3: gravel-dominated unit
   - Aquifer.

5. Four additional rock/soil zones are introduced corresponding to the four moisture content bands by altering the original zones. These four zones are added within the WMA C model domain defined by the kriged area in Figure 7-23 (red rectangular box). For areas outside this box, the original five rock/soil zones are retained, thus leading to total of nine different rock/zones.

7.2.5.1.2.2 Vadose Zone Hydraulic Properties for Different Units. Table 7-5 shows the vadose zone hydraulic properties for the hydrostratigraphic units defined in the base case model. For the heterogeneous case, we have selected hydraulic properties for four additional zones/layers that compare favorably with the moisture content data under current recharge conditions.

The hydraulic properties for the new zones/layers have been selected by analyzing 44 IDF sandy samples as presented in Section 7.2.2. Figures 7-16 and 7-17 show the moisture retention curves and unsaturated hydraulic conductivity curves for the 44 IDF samples. Four samples out of the 44 samples were selected to represent the new moisture content-based units. The four samples were chosen such that the resulting moisture content distribution at unit gradient condition corresponds to the moisture content bands represented by the samples. Figure 7-24 shows the moisture retention curves and unsaturated hydraulic conductivity curves for the four new units that correlate with the four zones based on moisture content. Table 7-8 summarizes the properties for all the new units.

Figure 7-24. Moisture Retention Curves and Unsaturated Hydraulic Conductivity Curves for the Four New Units.

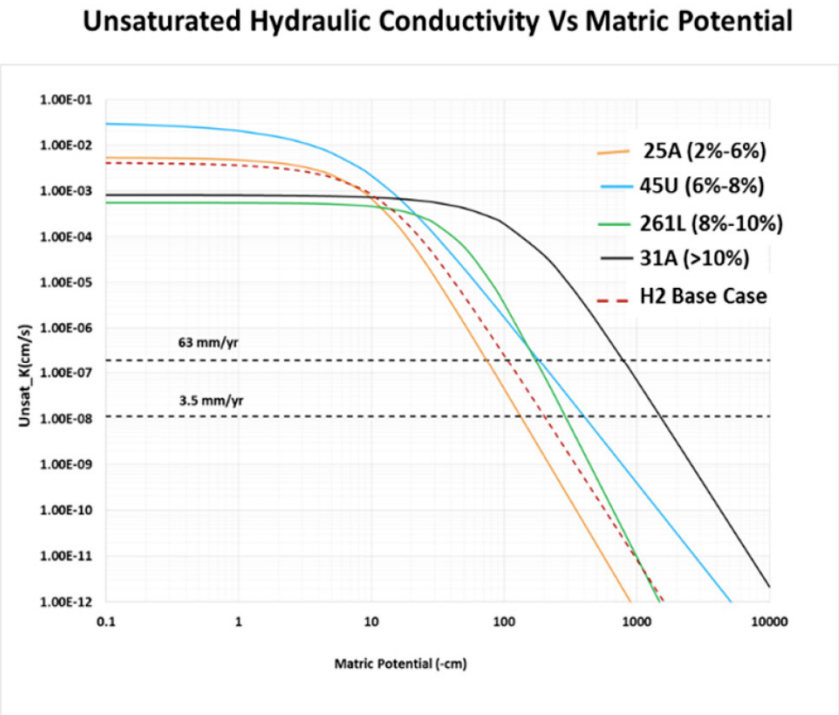

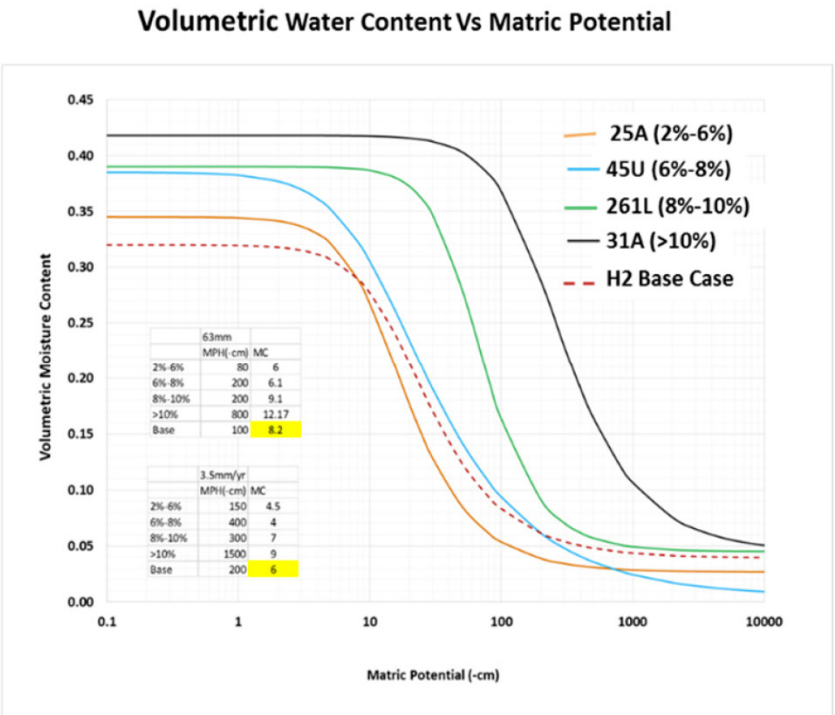

Table 7-8. Summary of Vadose Zone Hydraulic Properties for the New Units.

Samples (Moisture Content Zones)	θ_s	θ_r	α (1/cm)	n	ℓ	Fitted K_s (cm/s)*
25A (2%-6%)	0.345	0.0267	0.0842	2.158	0.5	5.40E-03
45U (6%-8%)	0.385	0.0050	0.0880	1.664	0.5	3.24E-02
261L (8%-10%)	0.390	0.0450	0.0191	2.485	0.5	5.54E-04
31A (>10%)	0.418	0.0444	0.0058	2.012	0.5	8.21E-04

*For these samples, unsaturated hydraulic conductivity values at specified moisture contents were available. The RETention Curve (RETC) code can generate the van Genuchten parameters using a simultaneous fit of unsaturated hydraulic conductivities, moisture content, and matric potential. However, when doing so, saturated hydraulic conductivity then becomes a fitting parameter.

Moisture-dependent anisotropy was applied to the 2D cross section model derived from the 3D base case model to be consistent with the upscaling methodology used for EHM-based models, but was not needed for the heterogeneous case due to additional rock/soil zones.

7.3 UPDATED TRANSPORT PROPERTIES FOR THE VADOSE ZONE SEDIMENTS

The updated effective transport parameters (i.e., bulk density, bulk distribution coefficient (K_d) and macrodispersivity) estimates used in the base case and sensitivity cases are described in this section. Because of natural variability, the transport parameters are all spatially variable. The purpose is similar to the upscaled flow parameters, to evaluate the effect of such variability on the large-scale transport process.

7.3.1 Bulk Density

Effective bulk density (ρ_b) estimates are needed to calculate retardation factors for different species. The average ρ_b, E[ρ_b] estimates for various strata at WMA C are presented in Table 7-9. These estimates are the average of the bulk density sample values listed in Table 7-3 and Table 7-4.

7.3.2 Bulk Distribution Coefficient (K_d)

The geochemistry conceptual model component involves the technical basis and rationale for the specific radionuclide partitioning behavior or sorption characteristics regarding release, retardation, and attenuation mechanisms, and any simplifying assumptions. The key aspects of this geochemistry conceptual model include the following, which are discussed in detail in DOE/RL-2011-50, *Regulatory Basis and Implementation of a Graded Approach to Evaluation of Groundwater Protection*:

- The rationale for the simplifying assumption that the use of a linear K_d isotherm is a reasonable conservative description for the release and attenuation of radionuclides in the context of providing an upper-bounding condition

- The rationale and source(s) of the data used in the selection of radionuclide K_d values
- The rationale for the use of a single K_d in the vadose zone units.

Table 7-9. Updated Effective Bulk Density ($E[\rho_b]$, g/cm^3) Estimates for Various Strata at Waste Management Area C Used in the Base Case Evaluations of Alternative Geologic Models I and II.

Strata	$E[\rho_b]$
Backfill (Table 4-5)	2.13
Hanford H1/H3 (Gravel-dominated)[1]	2.05
Hanford H2 (Sand-dominated)[2]	1.71
Hanford H2 – Gravel/coarse sand subunit[3]	1.83
Hanford H2 – Silty-sand subunit[3]	1.61

[1] Average of bulk densities in Table 7-3.

[2] Average of bulk densities in Table 7-4.

[3] Effective bulk densities of these units are only used in numerical model simulation of Alternative Geologic Model II. These bulk densities were calculated by calculating a particle density (2.49g/cc) for the H2 sand (porosity = 0.315) and using that particle density and adjusting for the porosity for the H2 Coarse (0.265) and H2 Silty (0.354)

The geochemistry conceptual models for the Hanford Site are based on extensive laboratory studies, testing, and measurements of adsorption and desorption coefficients under saturated and unsaturated conditions involving Hanford Site-specific sediments, contaminants, and conditions (DOE/RL-2011-50, PNNL-13895). The recommended K_d values in Table 7-10 are used in the PA/RCRA Closure Analysis, rather than binning of K_ds as described in Section 4.5.3. The references which supplied the basis and rationale for the K_d values used to approximate the transport of the contaminants and radionuclides are also given in Table 7-10. Along with the recommended K_d values, are the gravel-corrected values. The gravel correction lowers the K_d value to account for the gravel content per the procedure described in PNNL-17154, *Geochemical Characterization Data Package for the Vadose Zone in the Single-Shell Tank Waste Management Areas at the Hanford Site*. PNNL-17154 indicates that K_d values are typically lower for materials that contain significant amounts of gravel (notably Backfill, Hanford H1, and Hanford H3) than those determined with <2 mm size material. The gravel corrected values are not included in the table for the contaminants and radionuclides that the 3D screening evaluation indicated would not arrive at the water table within 10,000 years.

Table 7-10. Distribution Coefficients (K_d) Values Used to Approximate the Transport of the Radionuclides in the Base Case. (2 sheets)

Element or Contaminant	Base Case K_d (mL/g)				
	< 2 mm Material	Backfill	Hanford H1/H3	Hanford H2	Reference
Ac	350	NM	NM	NM	PNNL-16663
Al	1,500	NM	NM	NM	Table 4-8
Am	600	NM	NM	NM	PNNL-17154
B	3	NM	NM	NM	Table 4-8
C	1	0.46	0.58	0.8	PNNL-17154
Cm	350	NM	NM	NM	PNNL-16663
CN	0	NM	NM	NM	Table 4-8
Co	0	0	0	0	PNNL-17154
Cr	0	0	0	0	PNNL-17154
Cs	100	NM	NM	NM	PNNL-17154
Eu	10	NM	NM	NM	PNNL-17154
F	0	0	0	0	PNNL-17154
Fe	25	NM	NM	NM	Table 4-8
H	0	0	0	0	PNNL-17154
Hg	52	NM	NM	NM	Table 4-8
I	0.2	0.09	0.12	0.16	PNNL-17154
Mn	65	NM	NM	NM	Table 4-8
Nb	0	0	0	0	PNNL-16663
Ni	3	1.4	1.7	2.4	PNNL-17154
NO_2	0	0	0	0	PNNL-17154
NO_3	0	0	0	0	PNNL-17154
Np	10	NM	NM	NM	PNNL-17154
Pa	300	NM	NM	NM	PNNL-17154
Pb	10	NM	NM	NM	PNNL-17154
Pu	600	NM	NM	NM	PNNL-17154
Ra	10	NM	NM	NM	PNNL-17154
Rn	0	0	0	0	No relevant information available
Se	0.1	0.05	0.06	0.08	PNNL-17154
Sm	10	NM	NM	NM	PNNL-17154

Table 7-10. Distribution Coefficients (K_d) Values Used to Approximate the Transport of the Radionuclides in the Base Case. (2 sheets)

Element or Contaminant	Base Case K_d (mL/g)				
	< 2 mm Material	Backfill	Hanford H1/H3	Hanford H2	Reference
Sn	0.5	0.23	0.29	0.4	PNNL-17154
Sr	10	NM	NM	NM	PNNL-17154
TBP	1.89	NM	NM	NM	Table 4-8
Tc	0	0	0	0	PNNL-16663
Th	300	NM	NM	NM	PNNL-16663
U	0.6	0.28	0.35	0.48	Table 4-8
Zr	300	NM	NM	NM	PNNL-16663

NM = not included in the 3D modeling because the results of screening indicated the element or contaminant does not arrive at the water table within 10,000 years.

References:
PNNL-16663, *Geochemical Processes Data Package for the Vadose Zone in the Single-Shell Tank Waste Management Areas at the Hanford Site*.
PNNL-17154, *Geochemical Characterization Data Package for the Vadose Zone in the Single-Shell Tank Waste Management Areas at the Hanford Site*.
RPP-RPT-46088, *Flow and Transport in the Natural System at Waste Management Area C.*

7.3.3 Updated Macrodispersivity Estimates

Field observations indicate that the dispersion coefficients required to describe the large-scale transport processes, at field scales of tens or hundreds of meters, are much different from those observed in small-scale laboratory experiments (Gelhar 1993). In fact, field-scale dispersivities (i.e., macrodispersivities) may often be orders of magnitude larger than those observed in the laboratory. While there is general agreement in hydrology literature that hydraulic conductivity variations induced by field-scale heterogeneities play an important role in field-scale transport processes, there does not appear to be a clear consensus about how best to describe such processes quantitatively (Gelhar 1993).

Dispersivities are a function of matric potential (or soil moisture content) in unsaturated media ("Stochastic Modeling of Large-Scale Transient Unsaturated Flow Systems" [Mantoglou and Gelhar 1987]). As with saturated media, heterogeneities that exist at various length scales result also in a scale dependence of macrodispersivities in unsaturated media (Gelhar et al. 1992). Dispersivities increase with time, or equivalently with distance, until they tend to converge on their unique asymptotic (large-time) values. The use of a constant (asymptotic) macrodispersivity is thus considered appropriate in PA simulations (NUREG/CR-6114; NUREG/CR-5965, *Modeling Field Scale Unsaturated Flow and Transport Processes*).

Note that unsaturated media macrodispersivity estimates for the relatively dry moisture regime found at Hanford are expected to be smaller than estimates of macrodispersivity for saturated

media. A range of estimates of macrodispersivity is provided in RPP-ENV-58806, Appendix B, Table B-11. These estimates are based on numerical simulations, stochastic, theory, and experimental data. The recommended values used in PA modeling are given in Table 7-11. Note that the values given in Table 7-11 are on the lower end of the range provided in RPP-ENV-58806, Appendix B, Table B-11 and are also lower than given in Table 4-6 of this document. The lower macrodispersivity leads to less dispersion, a high peak concentration, and a sharper peak.

Table 7-11. Macrodispersivity Estimates for Various Strata at Waste Management Area C Used in the Base Case Evaluations of Alternative Geologic Models I and II.

Strata	A_L (cm)	A_T (cm)
Backfill (Gravelly)	~20	2.0
Hanford H1/H3 (Gravel-dominated)	~20	2.0
Hanford H2 (Sand-dominated)	~25	2.5
Hanford H2 –Gravel/coarse sand subunit*	~25	2.5
Hanford H2 – Silty-sand subunit*	~25	2.5

*Macrodispersivities of these units are only used in numerical model simulation of Alternative Geologic Model II.

7.4 UPDATED UNCONFINED AQUIFER PROPERTY ESTIMATES

The groundwater conceptual model for WMA C includes the uppermost unconfined aquifer system that exists within a channel eroded by the cataclysmic floods of the Pleistocene. The base of the aquifer is the underlying basalt surface. The undifferentiated lower sands and gravels associated with the Hanford formation, CCU, and the Ringold Formation (Unit A) that comprise the aquifer sediments are simply categorized as saturated Hanford H3 sediments in the model. The thickness of the uppermost aquifer beneath WMA C is ~12 m (39 ft). The model results provided represent concentrations in the upper 5 m (16.4 ft) of the aquifer. The 5-m vertical interval corresponds to the well screen length of a conceptual groundwater monitoring well, and is also depth interval used in WAC 173-340-747, “Deriving Soil Concentrations for Groundwater Protection,” Equation 747-4 to calculated volume of groundwater flow.

Groundwater flow beneath WMA C has been historically difficult to measure because the hydraulic gradient is very small and the hydraulic conductivity is very large in this region of the Hanford Site. In addition, the water table continues to recover from the operational liquid discharges at 216-B-3 Pond system and other large discharge sites in 200 East Area Figure 7-25a-c. The projected equilibrium state is expected to be similar to its pre-Hanford behavior (Figure 7-25a).

The hydraulic heads around WMA C are expected to continue declining slowly until they stabilize around year 2030 at 119.5 m (392 ft) (CP-47631, *Model Package Report: Central Plateau Groundwater Model Version 3.3*). The gradient is generally expected to slope from

northwest to southeast with a value of about 0.00002 m/m, which is close to the one observed prior to start of Hanford operations (Figure 7-25a). Changes in hydraulic gradient are only expected to occur within the first 10 to 50 years of the post-closure simulation period. As a result, the post-closure position of the water table and associated hydraulic gradient can only be evaluated through modeling. Consequently, the groundwater flux in the aquifer beneath WMA C is calculated on the basis of the aquifer hydraulic properties, and the hydraulic gradient projected to exist in the future.

7.4.1 Unconfined Aquifer Hydraulic Properties

7.4.1.1 Hydraulic Conductivity Estimate. At the field scale, assigning identifying appropriate permeabilities is best conducted using inverse modeling conditioned by available data, using appropriate boundary conditions ("An Analysis Platform for Multiscale Hydrogeologic Modeling with Emphasis on Hybrid Multiscale Methods" [Scheibe et al. 2015]; MASSFLUX-1, *Use and Measurement of Mass Flux and Mass Discharge*). In-situ measures of aquifer flow and hydraulic properties inferred from hydraulic testing represent relatively small areas compared to the overall scale and dimensions of the model domain, and therefore do not provide representative results for the field scale. Similarly, individual well-based slug and pump tests provide information at a relatively small scale, albeit larger than permeameter tests. Permeameter, slug, and pump tests are also limited in their ability to quantify spatial averages or trends, and are less likely to produce central measures of flow magnitudes than a regional model (MASSFLUX-1). Field estimates for saturated hydraulic conductivity based on slug tests, for example, provide estimates of hydraulic representation at a scale of meters and are not considered generally appropriate to be used directly in the modeling, even though slug and pumping test data are important input for model calibration.

Consequently, in evaluating available information for the aquifer at WMA C, hydraulic conductivities derived from a calibrated model are regarded as more reliable than direct measurements by permeameter, slug, or pump tests. This distinction is important because substantially different values for hydraulic conductivity have been estimated by various investigators using different methods (RPP-ENV-58806 Appendix C).

To date, the Central Plateau Groundwater Model (CPGWM, CP-47631) appears to be the most appropriate and applicable calibrated model to provide that parameterization. The CPGWM provides calibrated hydraulic conductivity estimates for the model layers and hydrostratigraphic units present within the aquifer in the vicinity of WMA C. The calibrated CPGWM produces a relatively high hydraulic conductivity estimate (11,000 m/day) for the ancestral Columbia River Channel deposits (undifferentiated gravel). This is also the recommended value to be used in the PA/RCRA Closure Analysis modeling along with sensitivity analysis (Section 7.4.3). The CPGWM estimate of vertical anisotropy ratio of 0.1 is also incorporated in the WMA C base case. Table 7-12 presents a summary of the updated aquifer hydraulic parameters for the Hanford H3 – aquifer. The aquifer, identified as Hanford H3 – aquifer, is separated from that portion of the Hanford H3 above the water table, reflecting the distinctly different saturation conditions.

Figure 7-25a. Hind Cast Water Table Map of the Hanford Site, January 1944.

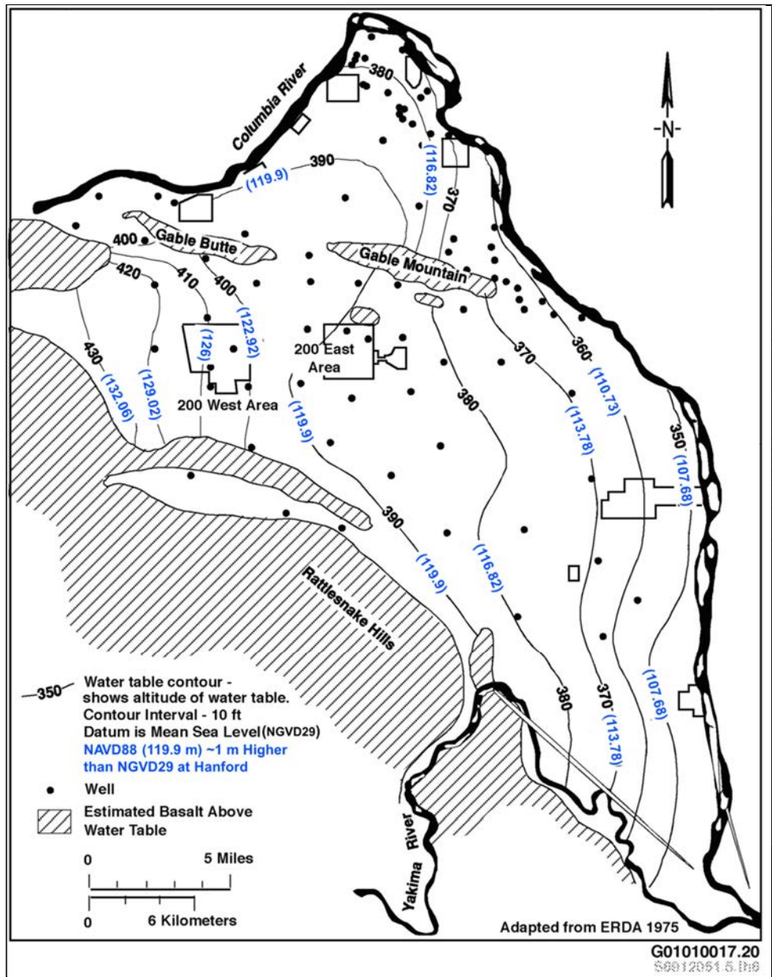

ERDA 1975 refers to ERDA-1538, *Final Environmental Impact Statement, Waste Management Operations, Hanford Reservation, Richland, Washington.*

Figure 7-25b. Water Table Elevations for June 1987.

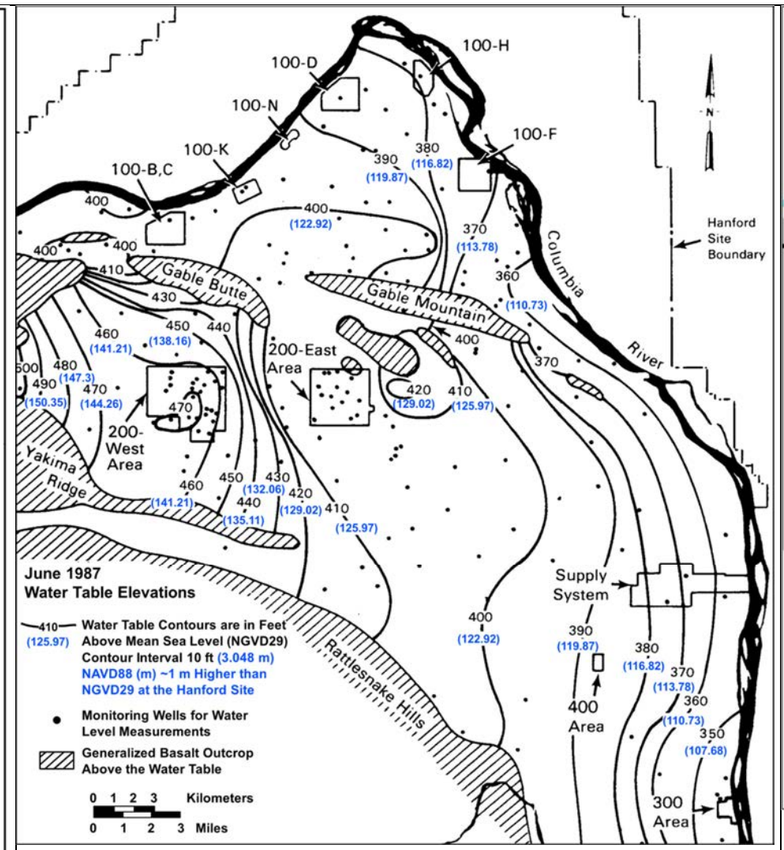

Reference: PNL-6464, *Environmental Monitoring at Hanford for 1987.*

Figure 7-25c. Water Table Elevations for 2013.

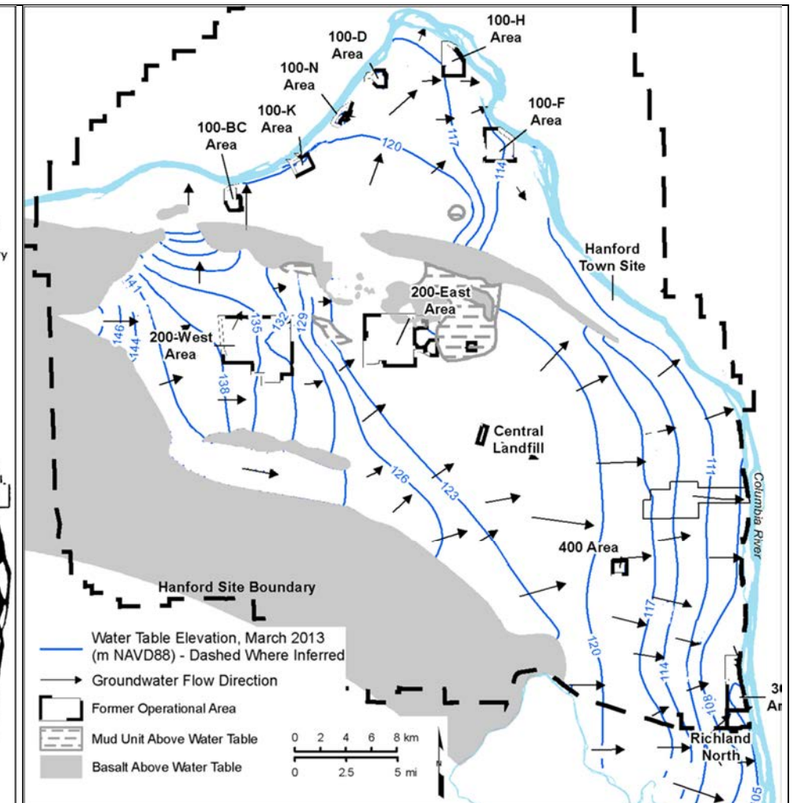

Modified from: DOE/RL-2014-32, *Hanford Site Groundwater Monitoring Report for 2013.*

Table 7-12. Updated Hydraulic Properties for Aquifer Soil Type at Waste Management Area C.

Aquifer Soil Type	Total Porosity	Saturated Moisture Content	Horizontal Saturated Hydraulic Conductivity[a] (m/day)	Longitudinal Dispersivity[b] (m)	Aquifer Hydraulic Gradient (m/m)
Hanford H3 (aquifer)	0.20	0.20	11,000	10.5	0.00002

[a] Vertical Saturated Hydraulic Conductivity assumed equal to 1/10 of the Horizontal Saturated Hydraulic Conductivity.
[b] Transverse dispersivity assumed to be equal to 1/10 of the longitudinal dispersivity.

7.4.1.2 Hydraulic Gradient. The hydraulic gradient estimate (Table 7-12) is based on the CPGWM estimates of future conditions within the Central Plateau. Water levels in the 200 East Area continue to decline, and evaluation of current flow direction and rate of groundwater flow at WMA C is difficult due to the very low hydraulic gradient. However, no appreciable change in hydraulic gradient is expected to occur after about 100 years after closure of WMA C, once the remedial actions in the nearby operable units are completed and the water table is at or near steady state. It is expected that by the time the contaminants are released from WMA C and reach the water table, several hundred years would have passed and the water table would be at a steady-state condition. These conditions justify the use of a single value of hydraulic gradient for the water table, even though it is known to have changed substantially in the past owing to operational releases.

7.4.2 Updated Transport Properties for the Unconfined Aquifer

7.4.2.1 Porosity. A value of 0.20 was chosen for the porosity in the STOMP© EHM. This value is consistent the aquifer test results from well 699-55-50 presented in HW-60601, *Aquifer Characteristics and Ground-Water Movement at Hanford*. According to RPP-14430, porosity is generally estimated to be about 30% for unconsolidated coarse-grained sediments, but a value closer to 20% may be more appropriate where boulders and cobbles are present and mixed with sand and gravels, such as at WMA C. The porosity value is also within the range of other estimated values: 0.06 determined from an aquifer pumping test at a well (699-62-43) screened within the Hanford gravel sequence similar to that at WMA C (HW-60601); and 0.1 derived from laboratory tests of Hanford gravels discussed in PNNL-19277, *Conceptual Models for Migration of Key Groundwater Contaminants Through the Vadose Zone and Into the Unconfined Aquifer Below the B-Complex*, and 0.25 in Section 5 of this document.

7.4.2.2 Macrodispersivity. The longitudinal and transverse macrodispersivity estimates in the saturated zone are based on a review of three general relationships ("Universal Scaling of Hydraulic Conductivities and Dispersivities in Geologic Media" [Neuman 1990]; "Longitudinal Dispersivity Data and Implications for Scaling Behavior" [Schulze-Makuch 2005]; and "Use of Weighted Least-Squares Method in Evaluation of the Relationship Between Dispersivity and Filed Scale" [Xu and Eckstein 1995]) that quantify the dependence of this parameter on measurement scale (L_s). The calculated values fall within the range of 1 to 20 m (RPP-ENV-58806, Table C-3) for 100 m, which is the approximate distance of travel to the

compliance well located in the saturated zone. Thus, a value of 10.5 m is considered representative of the range of values.

The ratio of longitudinal to transverse macrodispersivity is chosen to be 10 based on RPP-17209 and "Field Study of a Long and Very Narrow Contaminant Plume" (van der Kamp et al. 1994).

7.5 DISPOSITION OF PROPOSED SENSITIVITY ANALYSES FROM SCOPING

The range of sensitivity analyses identified during scoping was proposed to evaluate changes in calculated groundwater impacts that result from changes in input parameter estimates. Parameter value ranges used in these analyses were selected by one of several methods. As discussed in Section 1 of the WMA C PA, as part of the scoping process leading up to the implementation of the PA, stakeholders expressed specific interest in seeing the results of specific sets of input parameters. In addition to these agreed sets of sensitivity analyses, additional sensitivity cases were identified during the implementation of the PA to evaluate the importance of specific safety functions on the behavior of the disposal system. The result is a set of sensitivity analyses intended to represent the effects of changing a broad set of input assumptions. It is also emphasized that these sensitivity analyses have been augmented by probabilistic uncertainty analyses of the WMA C PA (see Section 8.1 of RPP-ENV-58782, *Performance Assessment of Waste Management Area C, Hanford Site, Washington*), which specifically evaluate parameter uncertainties. By contrast, the sensitivity analyses are generally intended to evaluate changes in parameters and modeling assumptions, to demonstrate the effect that alternatives have on the groundwater concentrations at the point of calculation.

Tables 7-13 and 7-14 provide a summary of the final disposition of sensitivity analysis proposed during scoping along with additional cases that were identified and evaluated as a part of the PA and RCRA Closure Analysis implementation in the specific areas of alternative conceptual models and vadose zone properties, and aquifer properties.

The parameters that determine the groundwater flux and the amount of dilution that occurs in the aquifer are the hydraulic conductivity and hydraulic gradient. In a natural system, the two parameters offset one another. If the groundwater flux through an aquifer volume remains constant, then in areas with high hydraulic conductivity, the hydraulic gradient will be less, and vice versa. They are considered to be coupled parameters because changes to the flux term caused by changes made to one term are inseparable from changes made to the other term. These parameters act inversely proportional to one another, and the same change in the flux can be made by making the same proportional change to either parameter. Therefore, only one of the parameters, e.g., hydraulic conductivity, needs to be varied to produce the variability in the flux necessary to conduct the sensitivity analysis. For this sensitivity evaluation, the hydraulic conductivity is varied. The sensitivity analysis includes two values of hydraulic conductivity, the 5th percentile value (4,200 m/day [13,800 ft/day]) and the 95th percentile value (17,800 m/day [58,400 ft/day]).

Table 7-13. Summary of Disposition of Alternative Conceptual Models and Vadose Zone Related Sensitivity Analysis Proposed during Scoping. (5 sheets)

Category of Sensitivity Cases	Scoping Sensitivity Case Designation	Explanation of the Sensitivity Case	Disposition of Performance Assessment	Performance Assessment Sensitivity Case Designation
Vadose Zone Conceptual Model	Alternative model based on consideration of characterization data from Phase 1.	Unsaturated hydraulic conductivity of the vadose zone units from Table 4-1 of RPP-RPT-46088 with denominator case for recharge (Table 4-13 in RPP-RPT-44042 Rev. A), known sources of waste losses/leaks (Table 6-1 in RPP-RPT-42294, Rev. 0) and effects of prescribed sloping beds with breaks.	Superseded by updated data analyses, conceptual models and parameters for vadose zone (VZ). Alternative Models I and II (see RPP-RPT-56356), new work on facies-based representations of spatial heterogeneity (see RPP-ENV-58782 Appendix F and RPP-ENV-58806 Appendix F). Global effects of VZ evaluated as part of Safety Functions and Barrier Analyses (see RPP-ENV-58782 Appendix F and RPP-ENV-58806 Appendix F).	Incorporated in both DOE O 435.1 and RCRA Closure analysis; Sensitivity cases: **vzp01, vzp02, vzp03**, and **vzp04** (see Section 8.2.1 of RPP-ENV-58782 and Section 9.3 of RPP-ENV-58806).
	Alternative Model based on consideration of hydraulic effects of: • clastic dike(s) • unsealed dry well • unsealed groundwater well.	Unsaturated hydraulic conductivity of the vadose zone units from Tables 4-1 and 4-3 of RPP-RPT-46088 with denominator case for recharge (Table 4-13 in RPP-RPT-44042 Rev. A), known sources of waste losses/leaks (Table 6-1 in RPP-RPT-42294, Rev. 0) and effects of: • Natural preferred pathways (prescribed clastic dike) (see sample results in Table 4-3 of RPP-RPT-46088) • Man-made preferred pathways (prescribed unsealed dry well, groundwater well or borehole).	Superseded by updated data analyses, conceptual models and parameters for VZ. Alternative Models I and II (see RPP-RPT-56356), new work on facies-based representations of spatial heterogeneity (see RPP-ENV-58782 Appendix F and RPP-ENV-58806 Appendix F). Global effects of VZ evaluated as part of Safety Functions and Barrier Analyses (see RPP-ENV-58782 Appendix F and RPP-ENV-58806 Appendix F).	Incorporated in both DOE O 435.1 and RCRA Closure analysis; Sensitivity case: **vzp04** (see Section 8.2.1 of RPP-ENV-58782 and Section 9.3 of RPP-ENV-58806).

Table 7-13. Summary of Disposition of Alternative Conceptual Models and Vadose Zone Related Sensitivity Analysis Proposed during Scoping. (5 sheets)

Category of Sensitivity Cases	Scoping Sensitivity Case Designation	Explanation of the Sensitivity Case	Disposition of Performance Assessment	Performance Assessment Sensitivity Case Designation
Vadose Zone Conceptual Model (continued)	Higher values case of saturated hydraulic conductivity of the vadose zone units.	Saturated hydraulic conductivity of the vadose zone units from Table 6-3 of RPP-RPT-46088 of 500 m/d with recommended parameters for moisture-dependent anisotropy (see Table 4-4 of RPP-RPT-46088).	Clastic dike sensitivity case included in performance assessment (PA). Unsealed well case evaluated for analyses of past leaks.	Incorporated in both DOE O 435.1 and RCRA Closure analysis; Sensitivity case: **vzp05** (see Section 8.2.1 of RPP-ENV-58782 and Section 9.3 of RPP-ENV-58806). The clastic dike and unsealed borehole cases within the analysis of past leaks (RPP-RPT-59197, Rev. 0) are scoping cases 4e and 4f.
	Lower values case of saturated hydraulic conductivity of the vadose zone units.	Saturated hydraulic conductivity of individual units from Table 6-3 of RPP-RPT-46088 of 0.1 m/day with recommended parameters for moisture-dependent anisotropy (see Table 4-4 of RPP-RPT-46088).	Wide range of VZ parameters included in probabilistic uncertainty analyses including these conditions.	Incorporated in both DOE O 435.1 and RCRA Closure analysis; Sensitivity cases: **vzp02** and **vzp03** (see Section 8.2.1 of RPP-ENV-58782 and Section 9.3 of RPP-ENV-58806)
	Homogeneous conditions (1).	Unsaturated hydraulic properties of the vadose zone units containing primarily sand (H2 sands unit) from Table 4-1 of RPP-RPT-46088 with recommended parameters for moisture-dependent anisotropy (see Table 4-4 of this report).	Wide range of VZ parameters included in uncertainty analyses including these conditions.	Incorporated in both DOE O 435.1 and RCRA Closure analysis; Sensitivity cases: **vzp01** (see Section 8.2.1 of RPP-ENV-58782 and Section 9.3 of RPP-ENV-58806).
	Homogeneous conditions (2).	Unsaturated hydraulic properties of the vadose zone units containing primarily gravel (H1 gravelly sand unit) from Table 4-1 of RPP-RPT-46088 with recommended parameters for moisture-dependent anisotropy (see Table 4-4 of this report).	Superseded by updated data analyses, conceptual models and parameters for VZ. Alternative Models I and II, new work on facies-based representations of spatial heterogeneity.	Incorporated in DOE O 435.1 analysis, identify nominal and 95% VZ parameters.

Table 7-13. Summary of Disposition of Alternative Conceptual Models and Vadose Zone Related Sensitivity Analysis Proposed during Scoping. (5 sheets)

Category of Sensitivity Cases	Scoping Sensitivity Case Designation	Explanation of the Sensitivity Case	Disposition of Performance Assessment	Performance Assessment Sensitivity Case Designation
Vadose Zone Conceptual Model (continued)	Homogeneous conditions (3)	Unsaturated hydraulic properties of the vadose zone units containing primarily sand (H2 sands unit) from Table 4-1 of RPP-RPT-46088 with assumed parameters to represent isotropic conditions.	Superseded by updated data analyses, conceptual models and parameters for VZ. Alternative Models I and II, new work on facies-based representations of spatial heterogeneity.	Incorporated in both DOE O 435.1 and RCRA Closure analysis; Sensitivity cases: **vzp01, vzp02, vzp03,** and **vzp04** (see Section 8.2.1 of RPP-ENV-58782 and Section 9.3 of RPP-ENV-58806).
	Homogeneous conditions (4)	Unsaturated hydraulic properties of the vadose zone units containing primarily gravel (H1 gravelly sand unit) from Table 4-1 of RPP-RPT-46088 with assumed parameters to represent isotropic conditions.	Superseded by updated data analyses, conceptual models and parameters for VZ. Alternative Models I and II, new work on facies-based representations of spatial heterogeneity.	Incorporated in both DOE O 435.1 and RCRA Closure analysis; Sensitivity cases: **vzp01, vzp02, vzp03,** and **vzp04** (see Section 8.2.1 of RPP-ENV-58782 and Section 9.3 of RPP-ENV-58806).
	Heterogeneous Case (to be determined).	A random field of hydraulic conductivity generated for available data on moisture content and grain size to approximate the effect of fine-scale heterogeneity on flow and transport (Note: this case will be developed using similar techniques described in "Development of a Conceptual Model for Vadose Zone Transport of Technetium-99 at Hanford's BC Cribs and the Screening of Remedial Alternatives" [Ward et al. 2009]).	Superseded by updated data analyses, conceptual models and parameters for VZ. Alternative Models I and II, new work on facies-based representations of spatial heterogeneity.	Incorporated in both DOE O 435.1 and RCRA Closure analysis; Sensitivity cases: **vzp01, vzp02, vzp03,** and **vzp04** (see Section 8.2.1 of RPP-ENV-58782 and Section 9.3 of RPP-ENV-58806).

Table 7-13. Summary of Disposition of Alternative Conceptual Models and Vadose Zone Related Sensitivity Analysis Proposed during Scoping. (5 sheets)

Category of Sensitivity Cases	Scoping Sensitivity Case Designation	Explanation of the Sensitivity Case	Disposition of Performance Assessment	Performance Assessment Sensitivity Case Designation
Contaminant Transport Properties Vadose Zone (porosity, bulk density etc.)	No change.	—	A heterogeneous case based on water content information was developed as part of the PA effort. Alternative conceptual models of heterogeneity developed by Pacific Northwest National Laboratory (PNNL) using both facies-based and water content-based approaches.	Incorporated in both DOE O 435.1 and RCRA Closure analysis, relevant alternative conceptual and numerical model is provided in Appendix F of both RPP-ENV-58782 and RPP-ENV-58806. Results of evaluations of tank residual and past impacts using the facies-based and water content-based heterogeneous models of Waste Management Area C developed by PNNL will be published in a separate PNNL technical report in Fall of 2016.
Geochemical Parameters (Bulk Distribution Coefficient K_d) for the Vadose Zone	Uranium (0.2 and 2.0 mL/g).	See Table 6-3 in RPP-RPT-46088, Rev. 1.	Addressed in probabilistic uncertainty analysis.	Incorporated in DOE O 435.1 analysis, discussion of uncertainty of this parameter is provided in Section 8.1.3.5 of RPP-ENV-58782.
	Iodine-129 (0.2 mL/g).	See Table 6-3 in RPP-RPT-46088, Rev. 1.	Addressed in probabilistic uncertainty analysis.	Incorporated in DOE O 435.1 analysis, discussion of uncertainty of this parameter is provided in Section 8.1.3.5 of RPP-ENV-58782.

Table 7-13. Summary of Disposition of Alternative Conceptual Models and Vadose Zone Related Sensitivity Analysis Proposed during Scoping. (5 sheets)

Category of Sensitivity Cases	Scoping Sensitivity Case Designation	Explanation of the Sensitivity Case	Disposition of Performance Assessment	Performance Assessment Sensitivity Case Designation
Geochemical Parameters (Bulk Distribution Coefficient K_d) for the Vadose Zone (continued)	Technetium-99 (0.1 mL/g).	See Table 6-3 in RPP-RPT-46088, Rev. 1.	Addressed in probabilistic uncertainty analysis.	Incorporated in DOE O 435.1 analysis, discussion of uncertainty of this parameter is provided in Section 8.1.3.5 of RPP-ENV-58782.
	Chromium (0.3 mL/g).	See Table 6-3 in RPP-RPT-46088, Rev. 1.	Included for RCRA Closure analysis.	Incorporated in DOE O 435.1 analysis, discussion of uncertainty of this parameter is provided in Section 8.1.3.5 of RPP-ENV-58782.
	Non-linear adsorption isotherm with selected constituents (to be determined).	Fruenlich and Langmuir Isotherms.	Fruenlich and Langmuir Isotherms not specific run in current PA.	—

RCRA = *Resource Conservation and Recovery Act of 1976*, Public Law 94-580, 90 Stat. 2795, 42 USC 901, et seq.

References:

DOE O 435.1, 2001, *Radioactive Waste Management*.
RPP-ENV-58782, *Performance Assessment of Waste Management Area C, Hanford Site, Washington*.
RPP-ENV-58806, *RCRA Closure Analysis of Tank Waste Residuals Impacts at Waste Management Area C, Hanford Site, Washington*.
RPP-RPT-44042, *Recharge and Waste Release within Engineered System in Waste Management Area C*.
RPP-RPT-46088, *Flow and Transport in the Natural System at Waste Management Area C*.
RPP-RPT-59197, *Analysis of Past Tank Waste Leaks and Losses in the Vicinity of Waste Management Area C at the Hanford Site, Southeast Washington*.

Table 7-14. Summary of Disposition of Alternative Conceptual Models and Vadose Zone Related Sensitivity Analysis Proposed during Scoping. (2 sheets)

Category of Sensitivity Cases	Scoping Sensitivity Case Designation	Explanation of the Sensitivity Case	Disposition of Performance Assessment	Performance Assessment Sensitivity Case Designation
Groundwater Hydraulic Properties	Saturated Hydraulic conductivity (m/day) = 100 to 7,000	See Table 6-4 in RPP-RPT-46088, Rev. 1	Addressed in probabilistic uncertainty analysis. Partly superseded by new information from Central Plateau groundwater model (CP-47631 and CP-57037) and the use of groundwater flux as a bulk representation of hydraulic properties, hydraulic gradient, and saturated thickness (see RPP-ENV-58782 Appendix C and RPP-ENV-58806 Appendix C).	Incorporated in both DOE O 435.1 and RCRA Closure analysis; Sensitivity cases: **gwp01** and **gwp03** (see Section 8.2.2 of RPP-ENV-58782 and RPP-ENV-58806 Section 9.1). Uncertainty discussion of these groundwater-related parameters is provided in Section 8.1.3 of RPP-ENV-58782.
	Depth to Water Table (71 to 97 m)	See Table 6-4 in RPP-RPT-46088, Rev. 1	Addressed in probabilistic uncertainty analysis. Partly superseded by new information from Central Plateau groundwater model and the use of groundwater flux as a bulk representation of hydraulic properties, hydraulic gradient, and saturated thickness.	Based on DOE O 435.1 analysis, relevant sensitivity cases are **gwp01** and **gwp03** (see Section 8.2.2 of RPP-ENV-58782 and RPP-ENV-58806 Section 9.1). Uncertainty discussion of these groundwater-related parameters is provided in Section 8.1.3 of RPP-ENV-58782.
	Hydraulic Gradient (1E-04 to 2E-05)	See Table 6-4 in RPP-RPT-46088, Rev. 1	Addressed in probabilistic uncertainty analysis. Partly superseded by new information from Central Plateau groundwater model and the use of groundwater flux as a bulk representation of hydraulic properties, hydraulic gradient, and saturated thickness.	Based on DOE O 435.1 analysis, relevant sensitivity cases are **gwp01** and **gwp03** (see Section 8.2.2 of RPP-ENV-58782 and RPP-ENV-58806 Section 9.1). Uncertainty discussion of these groundwater-related parameters is provided in Section 8.1.3 of RPP-ENV-58782.
Contaminant Transport Properties for Groundwater (porosity, bulk density etc.)	—	—	Addressed in probabilistic uncertainty analysis.	Based on DOE O 435.1 analysis, discussion of uncertainty of this parameter is provided in Section 8.1.3 of RPP-ENV-58782.

Table 7-14. Summary of Disposition of Alternative Conceptual Models and Vadose Zone Related Sensitivity Analysis Proposed during Scoping. (2 sheets)

Category of Sensitivity Cases	Scoping Sensitivity Case Designation	Explanation of the Sensitivity Case	Disposition of Performance Assessment	Performance Assessment Sensitivity Case Designation
Geochemical Parameters (Bulk Distribution Coefficient K_d) for Groundwater	Uranium (0.2 and 2.0 mL/g)	See Table 6-3 in RPP-RPT-46088, Rev. 1	Addressed in probabilistic uncertainty analysis.	Based on DOE O 435.1 analysis, discussion of uncertainty of this parameter is provided in Section 8.1.3.5 of RPP-ENV-58782.
	Iodine-129 (0.2 mL/g)	See Table 6-3 in RPP-RPT-46088, Rev. 1	Addressed in probabilistic uncertainty analysis.	Based on DOE O 435.1 analysis, discussion of uncertainty of this parameter is provided in Section 8.1.3.5 of RPP-ENV-58782.
	Technetium-99 (0.1 mL/g)	See Table 6-3 in RPP-RPT-46088, Rev. 1	Addressed in probabilistic uncertainty analysis.	Based on DOE O 435.1 analysis, discussion of uncertainty of this parameter is provided in Section 8.1.3.5 of RPP-ENV-58782.
	Chromium (0.3 mL/g)	See Table 6-3 in RPP-RPT-46088, Rev. 1	This specific case not run. Bounded by use of K_d=0 for Cr in RCRA Closure analysis.	Not applicable.

RCRA = *Resource Conservation and Recovery Act of 1976*, Public Law 94-580, 90 Stat. 2795, 42 USC 901, et seq.

References:

CP-47631, *Model Package Report: Central Plateau Groundwater Model Version 3.4.*
CP-57037, *Model Package Report: Plateau to River Groundwater Transport Model Version 7.1.*
DOE O 435.1, 2001, *Radioactive Waste Management.*
RPP-ENV-58782, *Performance Assessment of Waste Management Area C, Hanford Site, Washington.*
RPP-ENV-58806, *RCRA Closure Analysis of Tank Waste Residuals Impacts at Waste Management Area C, Hanford Site, Washington.*
RPP-RPT-46088, *Flow and Transport in the Natural System at Waste Management Area C.*

This page intentionally left blank.

8.0 REFERENCES

ARH-LD-127, 1976, *Geology of the 241-A Tank Farm*, Atlantic Richfield Hanford Company, Richland, Washington.

ARH-LD-128, 1976, *Geology of the 241-AX Tank Farm*, Atlantic Richfield Hanford Company, Richland, Washington.

ARH-LD-132, 1976, *Geology of the 241-C Tank Farm*, Atlantic Richfield Hanford Company, Richland, Washington.

Atomic Energy Act of 1954, 42 USC 2011, et seq.

Baker V. R., B. N. Bjornstad, A. J. Busacca, K. R. Fecht, E. P. Kiver, U. L. Moddy, J. G. Rigby, D. F. Stradling, and A. M. Tallman, 1991, "Quaternary Geology of the Columbia Plateau," *The Geology of North America, Quaternary Nonglacial Geology: Conterminous U.S.*, Vol. K-2, Chapter 8, pp. 215-250.

Bedient, P. B., H. S. Rifai, and C. J. Newell, 1994, Ground Water Contamination – Transport and Remediation, PTR Prentice Hall, Englewood Cliffs, New Jersey.

BHI-00184, 1995, *Miocene- to Pliocene-Aged Suprabasalt Sediments of the Hanford Site, South-Central Washington*, Rev. 00, Bechtel Hanford, Inc., Richland, Washington.

BHI-01103, 1999, *Clastic Injection Dikes of the Pasco Basin and Vicinity: Geologic Atlas Series*, Rev. 0, Bechtel Hanford, Inc., Richland, Washington.

BNWL-B-360, 1974, *Selected Water Table Contour Maps and Well Hydrographs for the Hanford Reservation, 1944-1973*, Pacific Northwest Laboratories, Richland, Washington.

BNWL-243, 1966, *Soil Survey Hanford Project in Benton County Washington*, Pacific Northwest Laboratory, Richland, Washington.

Campbell, N. P, 1989, "Structural and Stratigraphic Interpretation of Rocks under the Yakima Fold Belt, Columbia Basin, Based on Recent Surface Mapping and Well Data," in *Volcanism and Tectonism on the Columbia River Flood-Basalt Province*, Geological Society of America, Special Paper 239.

Comprehensive Environmental Response, Compensation, and Liability Act of 1980, 42 USC 9601 et seq., as amended

CP-47631, 2011, *Model Package Report: Central Plateau Groundwater Model Version 3.3*, Rev. 0, CH2M HILL Plateau Remediation Company, Richland, Washington.

CP-47631, 2013, *Model Package Report: Central Plateau Groundwater Model Version 3.4*, Rev. 1, CH2M HILL Plateau Remediation Company, Richland, Washington.

CP-57037, 2015, *Model Package Report: Plateau to River Groundwater Transport Model Version 7.1*, Rev. 0, CH2M HILL Plateau Remediation Company, Richland, Washington.

De Smedt, F. and P. J. Wierenga, 1984, "Solute Transfer through Columns of Glass Beads," *Water Resources Research*, Vol. 20, No. 2, pp. 225–232.

DOE/EIS-0391, 2009, *Draft Tank Closure and Waste Management Environmental Impact Statement for the Hanford Site, Richland, Washington*, U.S. Department of Energy, Richland, Washington.

DOE/ORP-2000-24, 2001, *Hanford Immobilized Low-Activity Tank Waste Performance Assessment: 2001 Version*, Rev. 0, U.S. Department of Energy, Office of River Protection, Richland, Washington.

DOE/ORP-2005-01, 2005, *Initial Single-Shell Tank System Performance Assessment for the Hanford Site*, Rev. 0, U.S. Department of Energy, Office of River Protection, Richland, Washington.

DOE/ORP-2008-01, 2010, *RCRA Facility Investigation Report for Hanford Single-Shell Tank Waste Management Areas*, Rev. 1, U.S. Department of Energy, Office of River Protection, Richland, Washington.

DOE/RL-92-05, 1993, *B Plant Source Aggregate Area Management Study Report*, Rev. 0, U.S. Department of Energy, Richland, Washington.

DOE/RL-92-23, 1992, *Hanford Site Groundwater Background*, U.S. Department of Energy, Richland, Washington.

DOE/RL-96-17, 2009, *Remedial Design Report/Remedial Action Work Plan for the 100 Area*, Rev. 6, U.S. Department of Energy, Richland Operations Office, Richland, Washington.

DOE/RL-96-61, 1997, *Hanford Site Background: Part 3, Groundwater Background*, Rev. 0, U.S. Department of Energy, Richland, Washington.

DOE/RL-98-72, 1999, *Retrieval Performance Evaluation Methodology for the AX Tank Farm*, U.S. Department of Energy, Richland Operations Office, Richland, Washington.

DOE/RL-2002-39, 2002, *Standardized Stratigraphic Nomenclature for Post-Ringold-Formation Sediments Within the Central Pasco Basin*, Rev. 0, U.S. Department of Energy, Richland Operations Office, Richland, Washington.

DOE/RL-2008-66, 2009, *Hanford Site Groundwater Monitoring for Fiscal Year 2008*, CH2M Hill Plateau Remediation Contractor, Richland, Washington.

DOE/RL-2011-50, 2012, *Regulatory Basis and Implementation of a Graded Approach to Evaluation of Groundwater Protection*, Rev. 1, U.S. Department of Energy, Richland Operations Office, Richland, Washington.

DOE/RL-2014-32, 2014, *Hanford Site Groundwater Monitoring Report for 2013*, Rev. 0, U.S. Department of Energy, Richland Operations Office, Richland, Washington.

DOE/RW-0164, 1988, *Consultation Draft Site Characterization Plan. Reference Repository Location, Hanford Site, Washington*, U.S. Department of Energy, Office of Civilian Radioactive Waste Management, Washington, D.C.

Ecology, EPA, and DOE, 1989, *Hanford Federal Facility Agreement and Consent Order – Tri-Party Agreement*, 2 vols., as amended, State of Washington Department of Ecology, U.S. Environmental Protection Agency, and U.S. Department of Energy, Olympia, Washington.

Ecology Publication No. 94-145, 1994, *Model Toxics Control Act Cleanup Levels & Risk Calculations (CLARC) Version 3.1*, Washington State Department of Ecology Toxics Clean-up Program, Olympia, Washington.

EDF-ER-275, 2004, *Engineering Design File – Fate and Transport Modeling Results and Summary Report*, Rev. 3, Idaho National Engineering and Environmental Laboratory, Idaho Falls, Idaho.

EM-ER-01-115, 2001, "K_d Values for INTEC Groundwater Modeling" (letter from T. Jenkins to M. Doornbos, BBWI, dated July 3), U.S. Department of Energy, Idaho Operations Office Idaho Falls, Idaho.

EPA 402-R-99-004A, 1999, *Understanding Variation in Partition Coefficient, Kd, Values*, U.S. Environmental Protection Agency, Washington, D.C.

EPA/540/R-95/128, 1996, *Soil Screening Guidance: Technical Background Document*, Second Edition, U.S. Environmental Protection Agency, Washington, D.C.

EPA/600/2-91/065, 1991, *The RETC Code for Quantifying the Hydraulic Functions of Unsaturated Soils*, U.S. Environmental Protection Agency, Washington, D.C.

ERDA-1538, 1975, *Final Environmental Impact Statement, Waste Management Operations, Hanford Reservation, Richland, Washington*, U.S. Energy Research and Development Administration, Richland, Washington.

Fecht, K. R., S. P. Reidel, and A. M. Tallman, 1987, "Paleodrainage of the Columbia River System on the Columbia Plateau of Washington State – A Summary," *Selected Papers on the Geology of Washington*, Washington Division of Geology and Earth Resources, Bulletin 77, pp. 219–248.

Flury, M., J. B. Mathison, and J. B. Harsh, 2002, "In Situ Mobilization of Colloids and Transport of Cesium in Hanford Sediments," *Environmental Science & Technology*, Vol. 36, No. 24, pp. 5335–5341.

Freeze, R. A. and J. A. Cherry, 1979, Groundwater, Prentice-Hall, Inc., Englewood Cliffs, New Jersey.

FS-NW-LT-5367, 2010, "Submittal of C Farm Geology/Geophyics Review, Task 26" (letter report from K. D. Reynolds to M. Connelly, Washington River Protection Solutions, June 18), Energy*Solutions*, Richland, Washington.

Gardner, W. H., 1986, "Water Content," in Methods of Soils Analysis, Part 1—Physical and Mineralogical Methods, pp. 493–544, *American Society of Agronomy-Soil Science Society of America*, Madison, Wisconsin.

Gee, G. W., M. J. Fayer, M. L. Rockhold, and M. D. Campbell, 1992, "Variations in Recharge at the Hanford Site," *Northwest Science*, Vol. 66, pp. 237–250.

Gelhar, L. W., 1993, Stochastic Subsurface Hydrology, Prentice Hall, New York, New York.

Gelhar, L. W., C. Welty, and K. R. Rehfeldt, 1992, "A Critical Review of Data on Field Scale Dispersion in Aquifers," *Water Resources Research*, Vol. 28, pp. 1955–1974.

HNF-2603, 1998, *A Summary and Evaluation of Hanford Site Tank Farm Subsurface Contamination*, Rev. 0, Lockheed Martin Hanford Corporation, Richland, Washington.

HNF-4936, 1999, *Subsurface Physical Conditions Description of the S-SX Waste Management Area*, Rev. 0, Lockheed Martin Hanford Corporation, Richland, Washington.

HNF-5507, 2000, *Subsurface Conditions Description of the B-BX-BY Waste Management Area*, Rev. 0A, CH2M HILL Hanford Group, Inc, Richland, Washington.

HNF-EP-0182, 2009, *Waste Tank Summary Report for Month Ending April 30, 2009*, Rev. 253, Washington River Protection Solutions LLC, Richland, Washington.

Honeyman, B. D., 1984, Cation and Anion Adsorption at the Oxide/Solution Interface in Systems Containing Binary Mixtures of Adsorbents: An Investigation of the Concept of Adsorptive Additivity, Ph.D. Thesis, Stanford University, Stanford, California.

HW-40469, 1955, *Changes in the Hanford Ground Water Table 1944-1955*, Hanford Atomic Products Operation, Richland, Washington.

HW-60601, 1959, *Aquifer Characteristics and Ground-Water Movement at Hanford*, General Electric Company, Hanford Atomic Products Operation, Richland, Washington.

HW-61780, 1959, *Subsurface Geology of the Hanford Separation Areas*, Hanford Atomic Products Operation, General Electric Company, Richland, Washington.

Kersting, A. B., D. W. Efurd, D. L. Finnegan, D. J. Rokop, D. K. Smith, and J. L. Thompson, 1999, "Migration of Plutonium in Ground Water at the Nevada Test Site," *Nature*, Vol. 397, Issue 6714, pp. 56–59.

Khaleel, R. and J. F. Relyea, 1997, "Correcting Laboratory-Measured Moisture Retention Data for Gravels," *Water Resources Research*, Vol. 33, Issue 8, pp. 1875–1878.

Khaleel, R. and J. F. Relyea, 2001, "Variability of Gardner's α for coarse-textured sediments," *Water Resources Research*, Vol. 37, No. 6, pp. 1567–1575.

Khaleel, R., J. F. Relyea, and J. L. Conca, 1995, "Evaluation of van Genuchten-Mualem relationships to estimate hydraulic conductivity at low water contents," *Water Resources Research*, Vol. 31, Issue 11, pp. 2659–2668.

Klute, A., 1986, "Water Retention: Laboratory Methods," in Methods of Soil Analysis, Part 1—Physical and Mineralogical Methods, pp. 635–660, *American Society of Agronomy-Soil Science Society of America*, Madison, Wisconsin.

Klute, A. and C. Dirksen, 1986, "Hydraulic Conductivity and Diffusivity: Laboratory Methods," in Methods of Soil Analysis, Part 1—Physical and Mineralogical Methods, pp. 687–734, *American Society of Agronomy-Soil Science Society of America*, Madison, Wisconsin.

Lindsey, K. A., S. P. Reidel, K. R. Fecht, J. L. Slate, A. G. Law, and A. M. Tallman, 1994, "Geohydrologic Setting of the Hanford Site, South-Central Washington," *Geologic Field Trips in the Pacific Northwest*, 1994 Geological Society of America Annual Meeting, Vol. 1, Chap. 1C, pp. 1–16.

Mantoglou, A. and L. W. Gelhar, 1987, "Stochastic Modeling of Large-Scale Transient Unsaturated Flow Systems," *Water Resources Research*, Vol. 23, No. 1, pp. 37–46.

MASSFLUX-1, 2010, *Use and Measurement of Mass Flux and Mass Discharge*, The Interstate Technology & Regulatory Council, Integrated DNAPL Site Strategy Team, Washington, D.C.

McCaffrey, R., A. I. Qamar, R. W. King, R. Wells, G. Khazaradze, C. A. Williams, C. W. Stevens, J. J. Vollick and P. C. Zwick, 2007, "Fault locking, block rotation and crustal deformation in the Pacific Northwest," *Geophysical Journal International*, Vol. 169, Issue 3, pp. 1315–1340.

McCarthy, J. F. and J. M. Zachara, 1989, "Subsurface Transport of Contaminants," *Environmental Science & Technology*, Vol. 23, No. 5, pp. 496–502.

Millington, R. J. and J. P. Quirk, 1961, "Permeability of Porous Solids," *Transactions of the Faraday Society*, Vol. 57, pp. 1200–1207.

Mualem, Y., 1976, "A New Model for Predicting the Hydraulic Conductivity of Unsaturated Porous Media," *Water Resources Research*, Vol. 12, No. 3, pp. 513–522.

Murray, C. J., A. L. Ward, and J. Wilson, 2007, "Influence of Clastic Dikes on Vertical Migration of Contaminants at the Hanford Site," *Vadose Zone Journal*, Vol. 6, No. 4, pp. 959–970.

Newcomb, R. C., 1958, "Ringold Formation of Pleistocene Age in Type Locality, the White Bluffs, Washington," *American Journal of Science*, Vol. 256, pp. 328–340.

Neuman, S. P., 1990, "Universal Scaling of Hydraulic Conductivities and Dispersivities in Geologic Media," *Water Resources Research*, Vol. 26, No. 8, pp. 1749–1758.

Nkedi-Kizza, P., J. W. Biggar, M. T. van Genuchten, P. J. Wierenga, H. M. Selim, J. M. Davidson, and D. R. Nielsen, 1983, "Modeling Tritium and Chloride 36 Transport Through an Aggregated Oxisol," *Water Resources Research*, Vol. 19, Issue 3, pp. 691–700.

NUREG/CR-5965, 1994, *Modeling Field Scale Unsaturated Flow and Transport Processes*, Nuclear Regulatory Commission, Washington, D.C.

NUREG/CR-6114, 1994, *Auxiliary Analyses in Support of Performance Assessment of a Hypothetical Low-Level Waste Facility: Groundwater Flow and Transport Simulation*, Vol. 3, U.S. Nuclear Regulatory Commission, Washington, D.C.

Open File Report 94-8, 1994, *Geologic Map of the Richland 1:100,000 Quadrangle, Washington*, Washington State Department of Natural Resources, Olympia, Washington.

Pace, M. N., M. A. Hayes, P. M. Jardine, T. L. Mehlhorn, J. M. Zachara, B. N. Bjornstad, 2003, "Quantifying the Effects of Small-Scale Heterogeneities on Flow and Transport in Undisturbed Cores from the Hanford Formation," *Vadose Zone Journal*, Vol. 2, pp. 664–676.

Pluhar, C. J., 2003, "Paleomagnetic and Geochemical Applications to Tectonics and Quaternary Geology: Studies at Coso Volcanic Field, CA and the Channeled Scabland, WA," University of California, Santa Cruz, California.

Pluhar, C. J., B. N. Bjornstad, S. P. Reidel, R. S. Coe, and P. B. Nelson, 2006, "Magnetostratiphic Evidence from the Cold Creek Bar for Onset of Ice-Age Cataclysmic Floods in Eastern Washington During the Early Pleistocene," *Quaternary Research*, Vol. 65, pp. 123–135.

PNL-2899, 1979, *Radiological Status of the Ground-Water Beneath the Hanford Project January – December 1978*, Pacific Northwest Laboratory, Richland, Washington.

PNL-6415, 1996, *Hanford Site National Environmental Policy Act (NEPA) Characterization*, Rev. 8, Pacific Northwest National Laboratory, Richland, Washington.

PNL-6464, 1988, *Environmental Monitoring at Hanford for 1987*, Pacific Northwest Laboratory, Richland, Washington.

PNL-6820, 1989, *Hydrogeology of the 200 Areas Low-Level Burial Grounds – An Interim Report*, Volumes 1 and 2, Pacific Northwest National Laboratory, Richland, Washington.

PNL-8337, 1992, *Summary and Evaluation of Available Hydraulic Property Data for the Hanford Site Unconfined Aquifer System*, Pacific Northwest Laboratory, Richland, Washington.

PNL-8971, 1993, *Three-Dimensional Conceptual Model for the Hanford Site Unconfined Aquifer System, FY 1993 Status Report*, Pacific Northwest Laboratory, Richland, Washington.

PNL-10285, 1995, *Estimated Recharge Rates at the Hanford Site*, Pacific Northwest Laboratory, Richland, Washington.

PNL-10886, 1995, *Development of a Three-Dimensional Ground-Water Model of the Hanford Site Unconfined Aquifer System: FY 1995 Status Report*, Pacific Northwest National Laboratory, Richland, Washington.

PNNL-12261, 2000, *Revised Hydrogeology for the Suprabasalt Aquifer System, 200-East Area and Vicinity, Hanford Site, Washington*, Pacific Northwest National Laboratory, Richland, Washington.

PNNL-13023, 2001, *RCRA Groundwater Monitoring Plan for Single-Shell Tank Waste Management Area A-AX at the Hanford Site*, Pacific Northwest National Laboratory, Richland, Washington.

PNNL-13024, 2001, *RCRA Groundwater Monitoring Plan for Single-Shell Tank Waste Management Area C at the Hanford Site*, Pacific Northwest National Laboratory, Richland, Washington.

PNNL-13037, 2004, *Geochemical Data Package for the 2005 Hanford Integrated Disposal Facility Performance Assessment*, Rev. 2, Pacific Northwest National Laboratory, Richland, Washington.

PNNL-13080, 2000, *Hanford Site Groundwater Monitoring: Setting, Sources, and Methods*, Pacific Northwest National Laboratory, Richland, Washington.

PNNL-13378, 2001, *Results of Detailed Hydrologic Characterization Tests – Fiscal Year 1999*, Pacific Northwest National Laboratory, Richland, Washington.

PNNL-13400, 2000, *Groundwater Flow and Transport Calculations Supporting the Immobilized Low-Activity Waste Disposal Facility Performance Assessment*, Pacific Northwest National Laboratory, Richland, Washington.

PNNL-13404, 2001, *Hanford Site Groundwater Monitoring for Fiscal Year 2000*, Pacific Northwest National Laboratory, Richland, Washington.

PNNL-13447, 2001, *Transient Inverse Calibration of Hanford Site-Wide Groundwater Model to Hanford Operational Impacts – 1943 to 1996*, Pacific Northwest National Laboratory, Richland, Washington.

PNNL-13514, 2001, *Results of Detailed Hydrologic Characterization Tests – Fiscal Year 2000*, Pacific Northwest National Laboratory, Richland, Washington.

PNNL-13672, 2001, *A Catalog of Vadose Zone Hydraulic Properties for the Hanford Site*, Pacific Northwest National Laboratory, Richland, Washington.

PNNL-13672, 2002, *A Catalog of Vadose Zone Hydraulic Properties for the Hanford Site*, Rev. 1, Pacific Northwest National Laboratory, Richland, Washington.

PNNL-13801, 2002, *Groundwater Quality Assessment Report for Waste Management Area S-SX (April 2000 through December 2001)*, Pacific Northwest National Laboratory, Richland Washington.

PNNL-13858, 2002, *Revised Hydrogeology for the Suprabasalt Aquifer System, 200-West Area and Vicinity, Hanford, Washington*, Pacific Northwest National Laboratory, Richland, Washington.

PNNL-13895, 2002, *Hanford Contaminant Distribution Coefficient Database and Users Guide*, Pacific Northwest National Laboratory, Richland, Washington.

PNNL-13895, 2003, *Hanford Contaminant Distribution Coefficient Database and Users Guide*, Rev. 1, Pacific Northwest National Laboratory, Richland, Washington.

PNNL-14186, 2003, *Results of Detailed Hydrologic Characterization Tests – Fiscal Year 2002*, Pacific Northwest National Laboratory, Richland, Washington.

PNNL-14286, 2003, *STOMP Subsurface Transport Over Multiple Phases Version 3.0 User's Guide*, Pacific Northwest National Laboratory, Richland, Washington.

PNNL-14538, 2003, *Borehole Data Package for R.C.R.A. Wells 299-E25-93 and 299-E24-22 at Single-Shell Tank Waste Management Area A-AX, Hanford Site, Washington*, Pacific Northwest National Laboratory, Richland, Washington.

PNNL-14594, 2004, *Characterization of Vadose Zone Sediments Below the TX Tank Farm: Boreholes C3830, C3831, C3832 and RCRA Borehole 299-W10-27*, Pacific Northwest National Laboratory, Richland, Washington.

PNNL-14656, 2004, *Borehole Data Package for Four CY 2003 RCRA Wells 299-E27-4, 299-E27-21, 299-E27-22, and 299-E27-23 at Single-Shell Tank, Waste Management Area C, Hanford Site, Washington*, Pacific Northwest National Laboratory, Richland, Washington.

PNNL-14702, 2006, *Vadose Zone Hydrogeology Data Package for Hanford Assessments*, Rev. 1, Pacific Northwest National Laboratory, Richland, Washington.

PNNL-14804, 2004, *Results of Detailed Hydrologic Characterization Tests – Fiscal Year 2003*, Pacific Northwest National Laboratory, Richland, Washington.

PNNL-14849, 2004, *Characterization of Vadose Zone Sediments Below the T Tank Farm: Boreholes C4104, C4105, 299-W10-196, and RCRA Borehole 299-W11-39*, Pacific Northwest National Laboratory, Richland, Washington.

PNNL-15301, 2006, *RCRA Assessment Plan for Single-Shell Tank Waste Management Area T*, Pacific Northwest National Laboratory, Richland, Washington.

PNNL-15503, 2008, *Characterization of Vadose Zone Sediments Below the C Tank Farm: Borehole C4297 and RCRA Borehole 299-E27-22*, Rev. 1, Pacific Northwest National Laboratory, Richland, Washington.

PNNL-15617, 2008, *Characterization of Vadose Zone Sediments from C Waste Management Area: Investigation of the C-152 Transfer Line Leak*, Rev. 1, Pacific Northwest National Laboratory, Richland, Washington.

PNNL-15670, 2006, *Hanford Site Groundwater Monitoring for Fiscal Year 2005*, Pacific Northwest National Laboratory, Richland, Washington.

PNNL-15670, 2006, *Hanford Site Groundwater Monitoring for Fiscal Year 2005*, Chapter 2.10, "200-BP-5 Operable Unit," Pacific Northwest National Laboratory, Richland, Washington.

PNNL-15837, 2007, *Data Package for Past and Current Groundwater Flow and Contamination Beneath Single-Shell Tank Waste Management Areas*, Pacific Northwest National Laboratory, Richland, Washington.

PNNL-15955, 2007, *Geology Data Package for the Single-Shell Tank Waste Management Areas at the Hanford Site*, Pacific Northwest National Laboratory, Richland, Washington.

PNNL-16407, 2007, *Geology of the Waste Treatment Plant Seismic Boreholes*, Rev. 1, Pacific Northwest National Laboratory, Richland, Washington.

PNNL-16663, 2007, *Geochemical Processes Data Package for the Vadose Zone in the Single-Shell Tank Waste Management Areas at the Hanford Site*, Pacific Northwest National Laboratory, Richland, Washington.

PNNL-17154, 2008, *Geochemical Characterization Data Package for the Vadose Zone in the Single-Shell Tank Waste Management Areas at the Hanford Site*, Pacific Northwest National Laboratory, Richland, Washington.

PNNL-19071, 2009, *Annual Hanford Seismic Report for Fiscal Year 2009*, Pacific Northwest National Laboratory, Richland, Washington.

PNNL-19277, 2010, *Conceptual Models for Migration of Key Groundwater Contaminants Through the Vadose Zone and Into the Unconfined Aquifer Below the B-Complex*, Rev. 0, Pacific Northwest National Laboratory, Richland, Washington.

Polmann, D. J., 1990, Application of Stochastic Methods to Transient Flow and Transport in Heterogeneous Unsaturated Soils, Ph.D. Thesis, Massachusetts Institute of Technology, Cambridge, Massachusetts.

PSPL, 1981, *Skagit/Hanford Nuclear Project, Preliminary Safety Analysis Report*, Vol. 1, Puget Sound Power and Light Company, Seattle, Washington.

Reidel, S. P., N. P. Campbell, K. R. Fecht, and K. A. Lindsey, 1994, "Late Cenozoic Structure and Stratigraphy of South-Central Washington," *Regional Geology of Washington State*, Washington Division of Geology and Earth Resources, Bulletin 80, pp. 159–180.

Reidel, S. P. and T. L. Tolan, 2009, "Landscape Evolution in a Flood-Basalt Province: an Example from the Pacific Northwest," Paper No. 6-2 in Session No. 6, The Evolution of Basaltic Landscapes: Time and the River and Lava Flowing, 2009 Portland GSA Annual Meeting (18-21 October 2009), Portland, Oregon.

Reidel, S. P., T. L. Tolan, P. R. Hooper, M. H. Beeson, K. R. Fecht, R. D. Bentley, and J. L. Anderson, 1989, "The Grande Ronde Basalt, Columbia River Basalt Group; Stratigraphic Descriptions and Correlations in Washington, Oregon, and Idaho," in *Volcanism and Tectonism in the Columbia River Flood-Basalt Province*, Geological Society of America, Special Paper 239, pp. 21–53.

Resource Conservation and Recovery Act of 1976, 42 USC 6901 et seq.

RHO-BWI-ST-4, 1979, *Geologic Studies of the Columbia Plateau – A Status Report: October 1979*, Rockwell Hanford Operations, Richland, Washington.

RHO-BWI-ST-14, 1981, *Subsurface Geology of the Cold Creek Syncline*, "Chapter 3 – Wanapum and Saddle Mountains Basalts of the Cold Creek Syncline Area," Rockwell Hanford Operations, Richland, Washington.

RHO-ST-23, 1979, *Geology of the Separation Areas, Hanford Site, South-Central Washington*, Rockwell Hanford Operations, Richland, Washington.

Risk Assessment Information System, Queried 04/2010, http://rais.ornl.gov/.

Roy, S. B., and D. A. Dzombak, 1997, "Chemical Factors Influencing Colloid-Facilitated Transport of Contaminants in Porous Media," *Environmental Science & Technology*, Vol. 31, No. 3, pp. 656–664.

RPP-6296, 2000, *Modeling Data Package for S-SX Field Investigation Report (FIR)*, Rev. 0, CH2M HILL Hanford Group, Inc., Richland, Washington.

RPP-7884, 2002, *Field Investigation Report for Waste Management Area S-SX*, Rev. 0, CH2M HILL Hanford Group, Inc., Richland, Washington.

RPP-8531, 2001, *Vadose Zone Geology of Boreholes 299-W10-27 and 299-W11-39 T-TX-TY Waste Management Area Hanford Site, South-Central Washington*, Rev. 0, CH2M HILL Hanford Group, Inc., Richland, Washington.

RPP-8681, 2001, *Vadose Zone Geology of Boreholes 299-E33-45 and 299-E33-46 B-BX-BY Waste Management Area Hanford Site, South-Central Washington*, Rev. 0, CH2M HILL Hanford Group, Inc., Richland, Washington.

RPP-9223, 2001, *Modeling Data Package for B-BX-BY Field Investigation Report (FIR)*, Rev. 0, CH2M HILL Hanford Group, Inc., Richland, Washington.

RPP-13310, 2006, *Modeling Data Package for an Initial Assessment of Closure of the C Tank Farm*, Rev. 1, CH2M HILL Hanford Group, Inc.

RPP-14430, 2003, *Subsurface Conditions Description of the C and A-AX Waste Management Area*, Rev. 0, CH2M HILL Hanford Group, Inc., Richland, Washington.

RPP-15808, 2003, *Subsurface Conditions Description of the U Waste Management Area*, Rev. 0, CH2M Hill Hanford Group, Inc., Richland, Washington.

RPP-17209, 2006, *Modeling Data Package for an Initial Assessment of Closure of the S and SX Tank Farms*, Rev. 1, CH2M HILL Hanford Group, Inc., Richland, Washington.

RPP-20621, 2004, *Far-Field Hydrology Data Package for the Integrated Disposal Facility Performance Assessment*, Rev. 0, "Appendix F. Physical and Hydraulic Measurements of FY1998 Clastic Dike Samples," CH2M HILL Hanford Group, Inc., Richland, Washington.

RPP-23748, 2006, *Geology, Hydrogeology, Geochemistry, and Mineralogy Data Package for the Single-Shell Tank Waste Management Areas at the Hanford Site*, Rev. 0, CH2M HILL Hanford Group, Inc., Richland, Washington.

RPP-35484, 2008, *Field Investigation Report for Waste Management Areas C and A-AX*, Rev. 1, CH2M HILL Hanford Group, Inc., Richland, Washington.

RPP-CALC-60345, 2016, *Heterogeneous Media Model for Waste Management Area C Performance Assessment*, Rev. 0, INTERA, Inc./Washington River Protection Solutions, LLC, Inc., Richland, Washington.

RPP-CALC-60450, 2016, *Process for Determining the Volumetric Moisture Content for the Vadose Zone Geologic Units Underlying Waste Management Area C*, Rev. 0, Washington River Protection Solutions, LLC, Inc., Richland, Washington.

RPP-CALC-60452, 2016, *Moisture Dependent Anisotropy Calculations Supporting Waste Management Area C Performance Assessment*, Rev. 0, Washington River Protection Solutions, LLC, Inc., Richland, Washington.

RPP-ENV-58806, 2016, *RCRA Closure Analysis of Tank Waste Residuals Impacts at Waste Management Area C, Hanford Site, Washington*, Rev. 0, Washington River Protection Solutions, LLC, Richland, Washington.

RPP-ENV-58782, 2016, *Performance Assessment of Waste Management Area C, Hanford Site, Washington*, INTERA, Inc./CH2M HILL Plateau Remediation Company/Ramboll Environ, Inc./Washington River Protection Solutions, LLC/TecGeo, Inc., Richland, Washington.

RPP-PLAN-39114, 2009, *Phase 2 RCRA Facility Investigation/Corrective Measures Study Work Plan for Waste Management Area C*, Rev. 1, Washington River Protection Solutions LLC, Inc., Richland, Washington.

RPP-RPT-35222, 2007, *Far-Field Hydrology Data Package for the RCRA Facility Investigation (RFI) Report*, CH2M HILL Hanford Group, Inc., Richland, Washington.

RPP-RPT-38152, 2008, *Data Quality Objectives Report Phase 2 Characterization for Waste Management Area C RCRA Field Investigation/Corrective Measures Study*, Rev. 0, Cenibark International, Inc., Richland, Washington.

RPP-RPT-41918, 2010, *Assessment Context for Performance Assessment for Waste in C Tank Farm Facilities after Closure*, Rev. 0, Washington River Protection Solutions LLC, Inc., Richland, Washington.

RPP-RPT-42294, 2009, *Hanford Waste Management Area C Soil Contamination Inventory Estimates*, Rev. 0, Washington River Protection Solutions LLC, Richland, Washington.

RPP-RPT-44042, 2009, *Recharge and Waste Release within Engineered System in Waste Management Area C*, Rev. A, Washington River Protection Solutions LLC, Richland, Washington.

RPP-RPT-46088, 2010, *Flow and Transport in the Natural System at Waste Management Area C*, Rev. 1, Washington River Protection Solutions, LLC/GSI Water Solutions, Inc., Richland, Washington.

RPP-RPT-56356, 2014, *Development of Alternative Digital Geologic Models of Waste Management Area C*, Rev. 0, Freestone Environmental Services Inc./Washington River Protection Solutions, LLC, Richland, Washington.

RPP-RPT-56356, 2020, *Development of Alternative Digital Geologic Models of Waste Management Area C*, Rev. 1, Freestone Environmental Services Inc./Washington River Protection Solutions, LLC, Richland, Washington.

RPP-RPT-58339, 2014, *Phase 2 RCRA Facility Investigation Report for Waste Management Area C*, Draft A, Washington River Protection Solutions, LLC, Richland, Washington.

RPP-RPT-59197, 2016, *Analysis of Past Tank Waste Leaks and Losses in the Vicinity of Waste Management Area C at the Hanford Site, Southeast Washington*, Rev. 0, Washington River Protection Solutions LLC, Richland, Washington.

Scheibe, T. D., E. M. Murphy, X. Chen, A. K. Rice, K. C. Carroll, B. J. Palmer, A. M. Tartakovsky, I. Battiato, and B. D. Wood, 2015, "An Analysis Platform for Multiscale Hydrogeologic Modeling with Emphasis on Hybrid Multiscale Methods," *Groundwater*, Vol. 53, No. 1, pp. 38–56.

Schulze-Makuch, D., 2005, "Longitudinal Dispersivity Data and Implications for Scaling Behavior," *Ground Water*, Vol. 43, No. 3, pp. 443–456.

Sen, T. K. and K. C. Khilar, 2006, "Review on Subsurface Colloids and Colloid-Associated Contaminant Transport in Saturated Porous Media," *Advances in Colloid and Interface Science*, Vol. 119, pp. 71–96.

Sobczyk, S., 2014-03-10, "WMA C geology" (e-mail to M. P. Bergeron, Washington River Protection Solutions, LLC), Environmental Restoration & Waste Management Program, Nez Perce Tribe, Lapwai, Idaho.

Spitz, K. and J. Moreno, 1996, A Practical Guide to Groundwater and Solute Transport Modeling, John Wiley and Sons, Inc., New York, New York.

Stiff, H. A. Jr., 1983, "The Interpretation of Chemical Water Analysis by Means of Patterns," in Chemical Hydrology, W. Back and R. A. Freeze (eds.), Benchmark Papers in Geology, Volume 73, Hutchinson Ross Publishing Company, Stroudsburg, Pennsylvania

"Technical Guidance Document for Tank Closure Environmental Impact Statement Vadose Zone and Groundwater Revised Analyses" (http://www.hanford.gov/orp/uploadfiles/TCEIS-Vadose.pdf).

Tolan, T. L., Martin, B. S., Reidel, S. P., Anderson, J. L., Lindsey, K. A., Burt, W. C., 2009, "An introduction to the stratigraphy, structural geology, and hydrogeology of the Columbia River Flood-Basalt Province: A primer for the GSA Columbia River Basalt Group field trips," *Volcanoes to Vineyards: Geologic Field Trips through the Dynamic Landscape of the Pacific Northwest*, Geological Society of America Field Guide 15, pp. 599–643.

USGS Bulletin 1457-G, 1979, *Revisions in stratigraphic nomenclature of the Columbia River Basalt Group*, U.S. Geological Survey, Washington, D.C.

USGS-W-P-7, 1949, *Geologic and Hydrologic Features of the Richland Area, Washington, Relevant to the Disposal of Waste at the Hanford Operations of the Atomic Energy Commission; Interim Report No. 1*, U.S. Geological Survey, Department of Interior, Portland Oregon.

van der Kamp, G., L. D. Luba, J. A. Cherry, and H. Maathuis, 1994, "Field Study of a Long and Very Narrow Contaminant Plume," *Ground Water*, Vol. 32, No. 6, pp. 1008–1016.

van Genuchten, M, Th. 1980, "A Closed-form Equation for Predicting the Hydraulic Conductivity of Unsaturated Soils," *Soil Science Society of America Journal*, Vol. 44, pp. 892–989.

WAC 173-160, "Minimum Standards for the Construction and Maintenance of Wells," *Washington Administrative Code*, as amended.

WAC 173-340, "Model Toxics Control Act – Cleanup," *Washington Administrative Code*, as amended.

WAC 173-340-747, "Deriving Soil Concentrations for Groundwater Protection," *Washington Administrative Code*, as amended.

Wan, J. M., T. K. Tokunaga, E. Saiz, J. T. Larsen, Z. P. Zheng, and R. A. Couture, 2004a, "Colloid Formation at Waste Plume Fronts," *Environmental Science & Technology*, Vol. 38, No. 22, pp. 6066–6073.

Wan, J. M., T. K. Tokunaga, J. T. Larsen, and R. J. Serne, 2004b, "Geochemical Evolution of Highly Alkaline and Saline Tank Waste Plumes during Seepage through Vadose Zone Sediments," *Geochimica et Cosmochimica Acta*, Vol. 68, No. 3, pp. 491–502.

Ward, A. L., R. J. Serne, and M. W. Benecke, 2009, "Development of a Conceptual Model for Vadose Zone Transport of Tc-99 at Hanford's BC Cribs and the Screening of Remedial Alternatives," Paper 9458, in *Proceedings of the 35th International Waste Management Conference (WM'09)*, Phoenix, Arizona.

Waters, A. C., 1961, "Stratigraphic and Lithologic Variations in the Columbia River Basalt," *American Journal of Science*, Vol. 259, pp. 583–611.

WHC-EP-0883, 1995, *Variability and Scaling of Hydraulic Properties of 200 Area Soils, Hanford Site*, Westinghouse Hanford Company, Richland, Washington.

WHC-IP-0635, 1991, *Geotechnical Engineering Procedure Manual*, Vols. 1 and 2, Westinghouse Hanford Company, Richland, Washington.

WHC-MR-0391, 1992, *Field Trip Guide to the Hanford Site*, Westinghouse Hanford Company, Richland, Washington.

WHC-SD-EN-EE-004, 1991, *Revised Stratigraphy for the Ringold Formation, Hanford Site, South-Central Washington*, Rev. 0, Westinghouse Hanford Company, Richland, Washington.

WHC-SD-EN-TI-012, 1992, *Geologic Setting of the 200 East Area: An Update*, Rev. 0, Westinghouse Hanford Company, Richland, Washington.

WHC-SD-EN-TI-147, 1993, *Hydrologic Testing at the Single-Shell Tanks, 1989*, Rev. 0, Westinghouse Hanford Company, Richland, Washington.

WHC-SD-W236A-TI-002, 1996, *Probabilistic Seismic Hazard Analysis, DOE Hanford Site, Washington*, Rev. 1A, Westinghouse Hanford Company, Richland, Washington.

WHC-SD-WM-EE-004, 1995, *Performance Assessment of Grouted Double-Shell Tank Waste Disposal at Hanford*, Rev. 1, Westinghouse Hanford Company, Richland, Washington.

Wicks, C. W., J. S. Gomberg, and C. S. Weaver, 2009, "InSAR measurement of surface deformation at the Hanford Reservation associated with the 2009 Wooded Island earthquake swarm (Invited)," in *American Geophysical Union, Fall Meeting 2009*, San Francisco, California.

WMP-17524, 2003, *Vadose Zone Hydraulic Property Letter Reports*, Rev. 0, Fluor Hanford, Richland, Washington.

WMP-22817, 2004, *Geologic Contacts Database for the 200 Areas of the Hanford Site*, Rev. 0, Fluor Hanford, Inc., Richland, Washington.

Xu, M. and Y. Eckstein, 1995, "Use of Weighted Least-Squares Method in Evaluation of the Relationship Between Dispersivity and Filed Scale," *Ground Water*, Vol. 33, No. 6, pp. 905–908.

Ye, M., R. Khaleel, and T.-C. J. Yeh, 2005, "Stochastic analysis of moisture plume dynamics of a field injection experiment," *Water Resources Research*, Vol. 41, W03013, pp. 1–13.

Yeh, T.-C. J., M. Ye, and R. Khaleel, 2005, "Estimation of effective unsaturated hydraulic conductivity tensor using spatial moments of observed moisture plume," *Water Resources Research*, Vol. 41, W03014, pp. 1–12.

Zachara, J. M., R. J. Serne, M. D. Freshley, F. M. Mann, F. J. Anderson, M. I. Wood, T. E. Jones, and D. A. Myers, 2007, "Geochemical Processes Controlling Migration of Tank Wastes in Hanford's Vadose Zone," *Vadose Zone Journal*, Vol. 6, No. 4, pp. 985–1003.